IN VITRO AND *IN VIVO* EFFECT OF *ASPALATHUS LINEARIS* AND ITS MAJOR POLYPHENOLS ON CARBOHYDRATE AND LIPID METABOLISM IN INSULIN RESISTANT MODELS

Sithandiwe Eunice Mazibuko

Student number: 20022468

A thesis submitted in fulfilment of the requirements for the degree of Doctor of Philosophy in Biochemistry at the Faculty of Biochemistry and Microbiology, University of Zululand

Supervisor: Dr Christo Muller

Co-supervisor: Prof Andy Opoku and Prof Elizabeth Joubert

April 2014

Declaration

I,……, hereby declare that the work on which this thesis is based is my original work (except where acknowledgements indicate otherwise), and that neither the whole work or part of it has been, is being, or is to be submitted for another degree in this or any other university.

I empower the University of Zululand to reproduce for the purpose of research either the whole or any portion of the contents in any manner whatsoever.

Signature: …….. Date: …….

Sithandiwe Eunice Mazibuko (student number: 20022468)

ABSTRACT

Introduction

High levels of saturated fatty acids (SFAs), such as palmitate, are associated with insulin resistance of muscle, fat and liver. Skeletal muscle, which accounts for up to 80% of peripheral glucose disposal, is particularly vulnerable to increased levels of SFAs. Rooibos (*Aspalathus linearis*) and its unique dihydrochalcone *C*-glucoside, aspalathin, shown to reduce hyperglycemia in diabetic rats, could play a role in preventing or ameliorating the development of insulin resistance. This study aims to establish whether rooibos and its major phenolic compounds (aspalathin, orientin, isoorientin and rutin) can ameliorate palmitate-induced insulin-resistance in C2C12 skeletal muscle cells, 3T3-L1 adipocytes and in C3A liver cells. The efficacy of rooibos will also be assessed in an obese insulin-resistant (OB/IR) rat model.

Methods

C2C12 myotubules, 3T3-L1 adipocytes and C3A liver cells were made insulin-resistant by culturing them with 0.75 mM palmitate for 16 h under standard culture conditions. Thereafter the muscle, fat and liver cells were cultured for 3 h in DMEM with or without 0.75 mM palmitate and insulin (1 µM) supplemented with either an aqueous fermented rooibos extract (FRE), organic solvent-based aspalathin-enriched unfermented rooibos extract (GRE) or the compounds aspalathin, orientin, isoorientin or rutin, respectively. The extracts were used at a concentration of 10 µg/mL and the compounds at 10 µM. Glucose uptake, palmitate uptake, mitochondrial activity and adenosine triphosphate (ATP) concentrations were determined. Messenger RNA and protein expression of effector proteins relevant to insulin-signalling, 5’ adenosine monophosphate activated protein kinase (AMPK), lipid metabolism and palmitate-induced inflammatory pathways, were investigated by RT-PCR and Western blot analyses. To confirm the *in vitro* findings OB/IR rats were treated at various doses (32, 97 and 195 mg/kg BW) of GRE for 12 weeks. Body weights and blood glucose

concentrations were monitored weekly and fasting insulin concentrations were assessed after 12 weeks treatment. Gene and proteins relevant to insulin resistance, insulin transduction and AMPK expression were performed on the skeletal muscle and liver.

Results

High-performance liquid chromatography with diode-array detection (HPLC-DAD) analysis showed that GRE, apart from aspalathin, had significantly higher levels of the other major phenolic compounds than were present in FRE. After 16 h culture with palmitate (0.75 mM) insulin resistance was confirmed in all three cell lines by a reduction in insulin-stimulated glucose uptake. Treating the cells for 3 h with FRE and GRE reversed the inhibitory effects of palmitate on insulin-stimulated glucose uptake, mitochondrial activity and ATP concentrations. The phenolic compounds tested were shown to have similar effects. Gene and protein studies were conducted on cells treated with GRE and aspalathin, respectively, to further elucidate the mechanism(s) of action. At a mechanistic level both GRE and aspalathin down-regulated protein kinase C theta (PKCθ) activation in C2C12 muscle cells and nuclear factor kappa beta (NF-κB) activation in 3T3-L1 adipocytes. PKCθ and NF-κB are known to be activated by palmitate and are involved in insulin resistance. GRE and aspalathin also increased the activation of the key regulatory proteins threonine kinase B (AKT) and AMPK, which are involved in insulin and non-insulin regulated signalling pathways of glucose and lipid metabolism. Protein expression of glucose transporter 4 (GLUT4), the insulin responsive glucose transporter, was also increased in C2C12 muscle and 3T3-L1 adipocytes, while glucose transporter 2 (GLUT2) expression was increased in C3A liver cells. GRE and aspalathin also increased the expression of peroxisome proliferator-activated receptor gamma (PPARγ) and carnitine palmitoyltransferase one (CPT1) that regulate lipid metabolism in 3T3-L1 adipocytes and C3A liver cells. Malonyl CoA, the rate-limiting substrate for lipid oxidation was also reduced in 3T3-L1 adipocytes and C3A liver cells. In the OB/IR rat model GRE lowered elevated insulin concentrations and improved insulin sensitivity as calculated by

homeostasis model assessment-estimated insulin resistance (HOMA-IR). At a genetic level, results showed that GRE increased insulin receptor (Insr), phosphatidylinositol 3-kinase (Pi3k), Ampk and Glut4 in muscle and Insr, insulin receptor substrate 1 and 2 (Irs1 and 2), Pi3k and Ampk mRNA expression in liver. The activation of AMPK was also enhanced. The findings in the OB/IR rat model are strongly supported by the *in vitro* results whereby GRE enhanced insulin signalling via PI3K. Activation of AMPK by GRE is another important pathway that could further ameliorate palmitate-induced insulin resistance. The inhibition of PKCθ in muscle cells and NF-κB activation in adipocytes suggest that GRE also supressed the palmitate-induced inflammatory pathway. The similar mechanistic effects induced by aspalathin *in vitro* suggest that aspalathin could contribute significantly to the effects observed for GRE. Activation of AKT and AMPK, along with the suppression of PKCθ and NF-κB offer a plausible mechanistic explanation for this ameliorative effect on insulin-resistance.

ACKNOWLEDGEMENTS

I wish to express my gratitude to all the people who that helped and supported me during this study.

To my supervisor, Dr C Muller for personal guidance, support and for taking time out to explain to me what science means. Even though you had a busy schedule you always managed to be available when I needed your help. Without your support I wouldn't have made it, thank you.

To my co-supervisors, Professor A Opoku and Professor E Joubert for providing their scientific assistance and guidance throughout the project. Thank you for the support.

The Diabetes Discovery Platform (DDP) Director, Dr J Louw, thank you for giving me the opportunity to study at DDP. I appreciate your support and your belief in me.

I would also like to thank my colleagues at DDP:

Dr M Sanderson and Ms O Patel, for technical support in the tissue culture laboratory, for support and words of encouragement,

Mr PV Dludla, thank you for your help in preparing the thesis and also for your emotional support,

Mr Linden and Mrs Rossler your technical assistance is highly appreciated,

Mrs C Roux your support with the animal studies is much appreciated,

Dr R Johnson, thank for your support with the Western blots and interpretation thereof,

Ms Ghoor thank you for training me and helping me with my mRNA studies,

To all my other colleagues at DDP thank you for your support.

A special thank you to my husband, Mduduzi Mbeje, who is also my friend, thank you for understanding when I had to work late and on weekends, thank you for the

support. Thank you so much my love for taking care of our sons and the housework so that I could focus on my study. You are such an amazing husband.

My sons Lwandle and Sethu, for understanding when mommy had to work late. I promise to spend more time with you now.

To my family, my mother and my grandmother, thank you for your constant encouragement, support and prayers throughout this study.

To my in-laws, thank you for your support, and understanding when I was unavailable to perform the “makoti” duties due to my studies.

To all my friends, thank you for the support.

To my best friend Dr Samke Mdladla, thank for the sisterly love you gave me.

To my cousin Londie Sikhakhane and Nonto Mbeje for playing a mothers role in my absence at home, thank you ladies.

Most of all I would like to thank God almighty for the strength He gave me to finish this project.

The financial support for this study was provided by the Diabetes Discovery Platform of the South African Medical Research Council, National Research foundation (Thuthuka grant number TTK20110905000026748) and the University of Zululand.

TABLE OF CONTENTS

APPENDIX 5

List of figures

List of tables

ABBREVIATIONS

ω-3	Omega 3 fatty acids
ω-6	Omega 6 fatty acids
β-cells	Pancreatic beta cells
ACC	Acetyl-CoA
Act B	Beta actin
ADP	Adenosine-5-diphosphate
AICAR	5-Aminoimidazole-4-carboxamide-1-β-D-ribofuranoside
Akt	Threonine kinase B
AMP	Activated protein kinase
AMPK	Adenosine monophosphate-activated protein kinase
ANOVA	Analysis of variance
AQ	Absolute quantification
ASP	Aspalathin
ATCC	American type culture collection
ATGL	Adipose triglyceride lipase
ATP	Adenosine-5-triphosphate
BSA	Bovine serum albumin
BW	Body weight
C/EBPs	CCAAT- enhancer-binding proteins
C/EBPα	CCAAT-enhancer-binding proteins alpha
C/EBPβ	CCAAT-enhancer-binding proteins beta
CaMKK	Calmodulin-dependent protein kinase kinase
CD36/FAT	Fatty acid translocase
cDNA	Complementary deoxyribonucleic acid
CO_2	Carbon dioxide
CPM	Counts per minute
CPTI	Carnitine palmitoyltransferase one
Ct	Threshold cycle
CVD	Cardiovascular disease

DAG	Diacylglycerol
DMEM	Dulbecco’s modified eagle’s medium
DMSO	Dimethyl sulfoxide
dNTPs	Deoxynucleotide triphosphates
DOG	2-Deoxy-[^{3}H]-D-glucose
DPBS	Dulbecco’s phosphate buffered saline
DPM	Disintegrations per minute
ECRA	Ethical consumer research association
EFFAs	Essential free fatty acids
ELISA	Enzyme-linked immunosorbant assay
EMEM	Eagle’s minimum essential medium
EtOH	Ethanol
F6P	Fructose-6-phosphate
FABP	Fatty acid binding protein
FABPc	Cytoplasmic fatty acid binding protein
FABPpm	Plasma membrane fatty acid binding protein
$FADH_2$	Flavin adenine dinucleotide
FATP	Fatty acid transporter protein
FATP1	Fatty acid transporter one
FBP	Fructose-1,6-biphosphate
FBS	Fetal bovine serum
FCS	Fetal calf serum
FFA	Free fatty acid
fINS	Fasting serum insulin concentrations
FOXO1	Forkhead box protein O1
fPG	Fasting plasma glucose concentrations
FRE	Aqueous fermented rooibos extract
G3PDH	Glyceraldehyde 3-phosphate dehydrogenase
G6P	Glucose-6-phosphate
G6Pase	Glucose-6-phosphatase
G6PD	Glucose-6-phosphate dehydrogenase

GAPDH	Glyceraldehyde-3-phosphate dehydrogenase
GI	Glycemic index
GLUT	Glucose transporter
GLUT1, 2, 3 and 4	Glucose transporter one, two, three and four
GPAT	Glycerolphosphate acyltransferase
GRE	Organic solvent-based aspalathin-enriched unfermented (green) rooibos extract
GSK3	Glycogen synthase kinase three
Gsy	Glycogen synthase
H	Hour
HDL	High density lipoprotein
HMG-CoA	3-hydroxy-3-methylglutaryl-coenzyme
HOMA-IR	Homeostasis model assessment-estimated insulin resistance
HPLC-DAD	High-performance liquid chromatography with diode-array detection
HRP	Horseradish peroxidase
HS	Horse serum
HSL	Hormone sensitive lipase
IBMX	3-Isobutyl-1-methylxanthine
IDDM	Insulin-dependent diabetes mellitus
INSR	Insulin receptor
IR	Insulin resistance
IRS	Insulin receptor substrate
IRS1 and 2	Insulin receptor substrate one and two
ISO	Isoorientin
JNK	c-Jun N-terminal kinases
LCFA	Long chain fatty acids
LPL	Lipoprotein lipase
LKB 1	Liver kinase B1
MAPK	Mitogen-activated protein kinase

MEF	Myocyte enhancer factor
MGB	Minor groove binder
MRF	Myogenic regulatory factors
mRNA	Messenger ribonucleic acid
MTT	3-(4,5-dimethylthiazol-2-yl)-2,5-diphenyltetrazolium bromide
MUFFAs	Monounsaturated free fatty acids
Myf5	Myogenic factor 5
MyoD	Myogenic determination
Na_3VO_4	Sodium tetraoxovanadate (V)
NADH	Nicotinamide adenine dinucleotide
NaF	Sodium fluoride
$NaHCO_3$	Sodium bicarbonate
NaOH	Sodium hydroxide
NFQ	Non-fluorescent quencher
NF-κB	Nuclear factor kappa beta
NIDDM	Noninsulin-dependent diabetes mellitus
NMR	Nuclear magnetic resonance
NP40	Nonyl phenoxypolyethoxylethanol
Nrf2	Nuclear factor erythroid-derived 2-like 2
NTC	No template control
OB/IR	Obesity insulin resistance
OD	Optical density
OGTT	Oral glucose tolerance test
NQO1	NAD(P)H:quinone acceptor oxidoreductase 1
ORE	Orientin
PABPpm	Plasma membrane-bound fatty acid binding protein
PBS	Phosphate buffered saline
PCA	Perchloric acid
PCR	Polymerase chain reaction
PDK1	Pyruvate dehydrogenase kinase, isozyme 1

PEP	Phosphoenolpyruvate
PEPCK	Phosphoenolpyruvate carboxykinase
PFK	Phosphofructokinase
PI3K	Phosphatidylinositol 3-kinase
PIP_3	Phosphatidylinositol (3, 4, 5)-triphosphate
PKC	Protein kinase C
PKCθ	Protein kinase C theta
PKCε	Protein kinase C epilson
PKCζ	Protein kinase C zeta
PMSF	Phenylmethylsulfonyl fluoride
PPAG	Phenylpyruvic acid glucoside
PPARs	Peroxisome proliferator-activated receptors
PUFs	Polyunsaturated fatty acid
PVDF	Polyvinylidene difluoride
qRT-PCR	Quantitative real-time polymerase chain reaction
RIA	Radioimmunoassay
RT	Reverse transcription
RUT	Rutin
SDS	Sodium dodecyl sulphate
SDS-Page	Sodium dodecyl sulfate poly-acrylamide gel electrophoresis
SFAs	Saturated fatty acids
SGLT	Sodium glucose co-transporters
SGLT1 and 2	Sodium glucose co-transporters one and two
SH2	Src homology 2 domain
SHC	Src homologous and collagen protein
SNP	Single nucleotide polymorphisms
SOCS3	Suppressor of cytokine signalling 3
SOP	Standard operating procedures
SREBP	Sterol regulatory element-binding protein
STZ	Streptozotocin

T1D	Type 1 diabetes
T2D	Type 2 diabetes
TBST	Tris-buffered saline and Tween 20
TCA	Tricarboxylic citric acid
TG	Triglycerides
TMB	3, 3′, 5, 5′-Tetramethylbenzidine
TNF-α	Tumor necrosis factor alpha
UFFAs	Unsaturated free fatty acids
VLDL	Very low density lipoproteins
WHO	World Health Organisation

Outputs

Conference presentations

SE Mazibuko, CJF Muller, E. Joubert, R Johnson, D de Beer, A Opoku and J Louw. Aspalathin-enriched green Rooibos ameliorates peripheral insulin resistance in muscle cells: The role of major phenolic compounds. World International Diabetes Federation Congress, Melbourne, Australia 2-6 December 2013.

SE Mazibuko, CJF Muller, E. Joubert, R Johnson, D de Beer, A Opoku and J Louw. Amelioration of insulin resistance in C2C12 cells by rooibos *(Aspalathus linearis).* MRC Early Career Scientist Conference, Cape Town 24-25 October 2012.

SE Mazibuko, CJF Muller, E. Joubert, R Johnson, D de Beer, A Opoku and J Louw. Amelioration of insulin resistance in C2C12 cells by rooibos *(Aspalathus linearis).* 40th Conference of the Physiology Society of Southern Africa. University of Stellenbosch, Cape Town 10-13 September 2012.

Publications

S.E. Mazibuko, C.J.F. Muller, E. Joubert, D de Beer, R Johnson, A. Opoku and J Louw. Amelioration of palmitate-induced insulin resistance in C2C12 muscle cells by rooibos (*Aspalathus linearis*). Phytomedicine 2013, 20 (10), 813–819).

Press release

More scientific evidence for the anti-diabetic potential of Rooibos. http://www.sarooibos.co.za/press-releases/176-more-scientific-evidence-for-the-anti-diabetic-potential-of-rooibos

Rooibos may be beneficial in countering diabetes.

http://www.all4women.co.za/health/health-news/rooibos-may-be-beneficial-in-countering-diabetes

Chapter 1

Introduction to the present study

Insulin resistance is a characteristic feature for many metabolic abnormalities. It has been proposed to be the strongest risk factor for the development of obesity and type 2 diabetes (T2D). An unhealthy lifestyle and diet high in fat content, refined carbohydrates and sugars are associated with an increased risk for developing metabolic diseases including obesity and T2D (Daudon *et al.,* 2006; Weickert, 2012; Li *et al.,* 2013). Traditionally T2D was considered a disease of developed nations, however, the prevalence of T2D is increasing at an alarming rate in developing countries. In sub-Saharan Africa, the prevalence of T2D is estimated at 10.8 million and expected to rise to 18.7 million by 2025 (Ayah *et al.*, 2013). Reasons for the high incidence of T2D in the developing world includes, amongst others, increased prosperity, urbanisation and a shift towards a "Westernised lifestyle" (Wild *et al.*, 2004).

Studies have revealed that insulin resistance is exacerbated by weight gain, inactivity and poor diet. Diets rich in carbohydrates particularly those with a high glycemic index (GI) contribute to weight gain which has been shown to increase postprandial glucose and insulin levels. This impairs fat oxidation and glucose metabolism (Riccardi and Rivellese, 2000). The excessive intake of saturated fatty acids (SFAs) has been shown to exacerbate insulin resistance. Changes in lifestyle (dietary and physical activity) has been reported to have positive effects on insulin sensitivity and insulin resistance (McAuley *et al.*, 2002; Corcoran *et al.*, 2007; Colberg *et al.*, 2010,). Several studies have reported that substituting SFA with polyunsaturated fatty acids (PUFAs) including omega 3 (ω-3) and omega 6 (ω-6) fatty acids improved insulin sensitivity. Substituting your SFAs with monounsaturated fatty acids (MUFAs) such as oleic acid could also help to ameliorate insulin resistance (Ghafoorunissa *et al.*, 2005; Rasmussen *et al.*, 2006; De Santa Olalla *et al*., 2009; Kurotani *et al.*, 2013). Research has also shown that consumption of less refined carbohydrates with lower glycemic indices (GI) could improve insulin resistance in patients with T2D (Willett *et al.*, 2002; Anderson *et al.*,

2009). A high dietary fibre intake has also been reported to have a beneficial effect by reducing postprandial glucose (Jenkins *et al.*, 2003; Weickert *et al.*, 2008).

Polyphenols have become a popular area of research mainly due to their perceived health benefits. Increasing the phenolic content of a diet, apart from its antioxidant benefit, has an effect on essential signalling molecules involved in carbohydrate and lipid metabolism (Hanhineva *et al.,* 2010; Lobo *et al.,* 2010; Skrobuk, 2012; Bahadoran *et al.*, 2013). These effects could potentially protect against metabolic disease and the harmful effects of insulin resistance, thereby slowing or preventing downstream metabolic deterioration and progression towards serious disease such as obesity and the development of T2D (Hanhineva *et al.*, 2010; Shao *et al.*, 2012). This study aims to demonstrate that *Aspalathus linearis* (rooibos) and its major phenolic compounds could protect against insulin resistance and elucidate the mechanisms involved.

The objects of this study are to assess the efficacy of rooibos and its major phenolic compounds, the dihydrochalcone *C*-glycoside, aspalathin, a novel rooibos compound, and its flavone oxidation products orientin and isoorientin, as well as one of its flavonol *O*-glycosides, rutin for the prevention and/or reversal of experimentally-induced insulin resistance by palmitate in C2C12 muscle, 3T3-L1 adipocytes and C3A liver cells and to elucidate the biological mechanism/s involved. Furthermore, the *in vivo* metabolic and cell signalling effects of rooibos in a diet-induced obese insulin resistant (OB/IR) Wistar rat model will be assessed.

Initially, a dose study will be performed on the C2C12 muscle, 3T3-L1 adipocytes and C3A liver cells using log dilutions at six concentrations to determine the optimal concentration to be used for further *in vitro* study. For the *in vitro* study, the effect of an aqueous fermented rooibos extract (FRE), a solvent-based aspalathin-enriched unfermented green rooibos extract (GRE) and the selected flavonoids (aspalathin, orientin, isoorientin and rutin) will be assessed in the respective palmitate-induced insulin resistant cells.

Insulin resistance will be induced by adding 0.75 mM palmitate to the culture media of C2C12 skeletal muscle, 3T3-L1 adipocytes and C3A liver cells for 16 h. These insulin resistant cells will then be treated with FRE, GRE and the flavonoids aspalathin,

orientin, isoorientin and rutin for 3 h. The effects of the extracts and compounds on basal and insulin-stimulated glucose and lipid metabolism will be assessed. The effect on mRNA and proteins relevant to insulin transduction and other relevant pathways will be determined to elucidate the molecular mechanism(s) of action.

Chapter 2

Literature review

2.1. Insulin

Insulin is a peptide hormone produced by pancreatic beta cells located in the islets of Langerhans. In humans insulin has a molecular weight of 5808 Da and consists of an A chain which has 21 amino acids and a B chain with 30 amino acids. It is a potent anabolic hormone that is important for regulating glucose, lipid and protein metabolism (Chang *et al.,* 2004). Insulin maintains glucose homeostasis by stimulating the uptake, utilisation and storage of glucose in muscle and adipose tissue, and inhibits hepatic glucose production (Pessin and Saltiel, 2000; Chang *et al.,* 2004; Skrobuk, 2012). In the liver and muscle insulin stimulates the storage of glucose in the form of glycogen (Wilcox, 2005; DeFronzo and Tripathy, 2009; Olson, 2012). Insulin is also important for lipid metabolism where it promotes synthesis of fatty acid in the liver, and inhibits breakdown of fat (lipolysis) in fat cells or adipocytes. A lack of insulin, or an inability of cells to adequately respond to insulin, leads to the development of diabetes mellitus (DM) (Lebovitz, 1999; Saltiel and Kahn, 2001).

2.2. Insulin receptor (INSR)

When insulin binds to the insulin receptor (INSR), the receptor initiates a well-defined transduction cascade culminating in the translocation of the insulin responsive glucose transporter isoform 4 (GLUT4) to the cell surface of insulin sensitive tissues such as muscle and adipose tissue thereby regulating glucose uptake (Chang *et al.,* 2004; Suryawan *et al.,* 2003). In addition, insulin transduction initiates and regulates its various other cellular responses, including lipid and protein metabolism (Rhodes and White, 2002). The INSR is a glycoprotein transmembrane, tetrameric enzyme complex consisting of two α- and two β-subunits. When insulin binds to the receptor binding sites on the extracellular α-subunit, tyrosine kinase activity in the β-unit is increased and phosphorylation of the cytoplasmic β-subunit is initiated. Initially, the first β-subunit activates the second unit by transphosphorylation which increases tyrosine catalytic

activity and results in autophosphorylation of the intracellular tail portions as well as the juxtamembrane regions of the receptor (Kahn and White, 1988; Li *et al.,* 2001). Once phosphorylated, the cytoplasmic and membrane portion of the subunit phosphorylates the insulin receptor substrate (IRS) on its tyrosine residues thereby initiating the activation of a series of membrane-bound and cytoplasmic effector and adaptor molecules (Kasuga *et al.,* 1990; Kahn and Saad, 1992).

2.2.1. Insulin receptor signal transduction

Several intracellular proteins have been identified as phosphorylation substrates for the insulin receptor. These substrates include insulin receptor substrates 1 and 2 (IRS1, IRS2) and src homology and collagen protein (SHC). The best-studied of these proteins are IRS1. IRS1 is mainly responsible for perpetuating the insulin signal in muscle and adipose tissue, while IRS2 is the major substrate in the liver cells (White, 1997; Draznin, 2006; DeFronzo and Tripathy, 2009). The activation and membrane docking of phosphatidylinositol 3 kinase (PI3K), following binding of the phosphorylated IRS to the p85 regulatory subunit of PI3K, is a crucial and pivotal step in downstream insulin signalling. This releases the inhibitory effect of the “regulatory” p85 subunit on the p110 catalytic subunit of PI3K and activates PI3K. Once activated, the membrane-bound PI3K phosphorylates phosphatidylinositol-(4,5)-biphosphate (PI-4,5-P2) to form phosphatidylinositol-3,4,5-triphosphate (PIP3) (Gruzman *et al*., 2009). Active PIP3 interacts with phosphosinsositide-dependent kinase 1 (PDK1) which recruits and phosphorylates AKT (also known as protein kinase B) and protein kinase C ζ (PKCζ) (Giri *et al.,* 2004). Activation of AKT promotes cell survival through activation of metabolic processes and protein kinase C (PKC) is involved in a wide array of cellular processes such as cell proliferation, differentiation and apoptosis (Anhê *et al*., 2006). The activation of AKT and PKCζ results in the translocation of GLUT4 via exocytosis from intracellular vesicles to the plasma membrane (Wang *et al.,* 1999). In muscle and fat cells this causes a surge in glucose uptake as a response to insulin binding to the receptor.

2.3. Glucose transporters

Glucose transporters (GLUTs) are integral membrane proteins that transport glucose and related hexoses across the lipid plasma membrane, either from the extracellular space into the cytoplasm or from within the cell to the extracellular space (Ludewig and Frommer, 2002; Shi, 2013). Binding of glucose to the glucose transporter provokes a conformational change initiating transport and the release of glucose across the membrane. Each glucose transporter isoform plays a specific role in glucose transport determined by its tissue distribution, substrate specificity, transport kinetics, and regulated expression in different physiological conditions (Thorens and Mueckler). Glucose transporter isoform 1 (GLUT1) is present in all cells and is largely responsible for regulating basal glucose and ensuring a steady influx of glucose into cells. It also plays a role in transporting glucose across epithelial and endothelial barrier tissues. Makni *et al.* (2008) reported that GLUT1 polymorphisms are associated with T2D in the Tunisian population. Glucose transporter protein isoform 4 (GLUT4) is expressed exclusively in fat and muscle. It is responsible for increased glucose disposal into these tissues postprandially, thereby maintaining normoglycemia. Insulin stimulation results in GLUT4 translocation from intracellular vesicles within a cell to the plasma membrane and thereby increases glucose uptake. When insulin levels decrease in the blood and insulin receptors are no longer occupied, the glucose transporters are recycled back into the cytoplasm. Failure of GLUT4 to translocate to the plasma membrane results in insulin resistance and T2D (Funaki *et al.,* 2004). The glucose transporter isoform 2 (GLUT2) is a high-Km glucose transporter expressed in hepatocytes, pancreatic beta cells, and the basolateral membranes of intestinal and renal epithelial cells. GLUT2, in contrast to the other transporters, facilitates bidirectional glucose transport into and out of the cell (Thorens and Mueckler, 2010). In enterocytes it facilitates glucose uptake from the gut. In the kidney, proximal convoluted tubule epithelial cells transport of reabsorbed glucose back into the circulation is facilitated via GLUT2 (Stümpel *et al.,* 2001; DeFronzo and Davidson, 2012). In pancreatic β-cells GLUT2 is involved in sensing circulating glucose levels and thereby regulation of insulin secretion. In the liver, insulin regulates GLUT2 glucose uptake and the release of hepatic neogenic glucose back into the circulation. Single nucleotide polymorphisms (SNPs) in the GLUT2 gene of Finish subjects with

impaired glucose tolerance were associated with a threefold risk for developing T2D (Laukkanen *et al.,* 2005). In addition to the facilitative glucose transporters, described above, sodium dependent glucose transporters (SGLTs) contribute to glucose absorption, reabsorption and uptake into the cell. On the apical (luminal) membrane of the proximal convoluted tubule epithelial cell, SGLT 2 accounts for about 90% of glucose reabsorption from the glomerular filtrate (Su, 2009, DeFronzo and Davidson, 2012; Dokken, 2012). SGLT 2 inhibitors have become an important drug target for the treatment of T2D (Valentine, 2012). SGLT 2 is also implicated in the transport of flavonoids across the cell membrane (Walgren *et al.,* 2000; Kottra and Daniel, 2007).

2.4. Glucose metabolism

Glucose is a major source of energy in all living organisms. To facilitate uptake into the cell, glucose is actively transported across the cell membrane into the cytosol. After entering the cell, glucose is converted to ATP, glycogen or fatty acids (Da Poian *et al.,* 2010). The fate of glucose in the cell is tightly regulated and is dependent on a number of factors such as the concentrations of ATP, glycogen and fat energy stores. Glycolysis is a catabolic pathway in which glucose is broken down to pyruvate in the cytoplasm. It involves several steps such as the phosphorylation of glucose to glucose-6-phosphate (G6P) by hexokinase (Blin, 1999; Buchakjian and Kornbluth, 2010). G6P can be converted to glycogen during glycogenesis or it can be utilized as an energy source during glycolysis (O'Boyle and Beamish, 1977; Berg *et al.,* 2002). The final product of glycolysis is pyruvate. The enzyme pyruvate dehydrogenase converts pyruvate to oxaloacetic acid and acetyl-CoA. Acetyl-CoA and oxaloacetic acid enters the TCA cycle where it is fully oxidised to CO_2 yielding 12 molecules of ATP and water (Fig. 2.1).

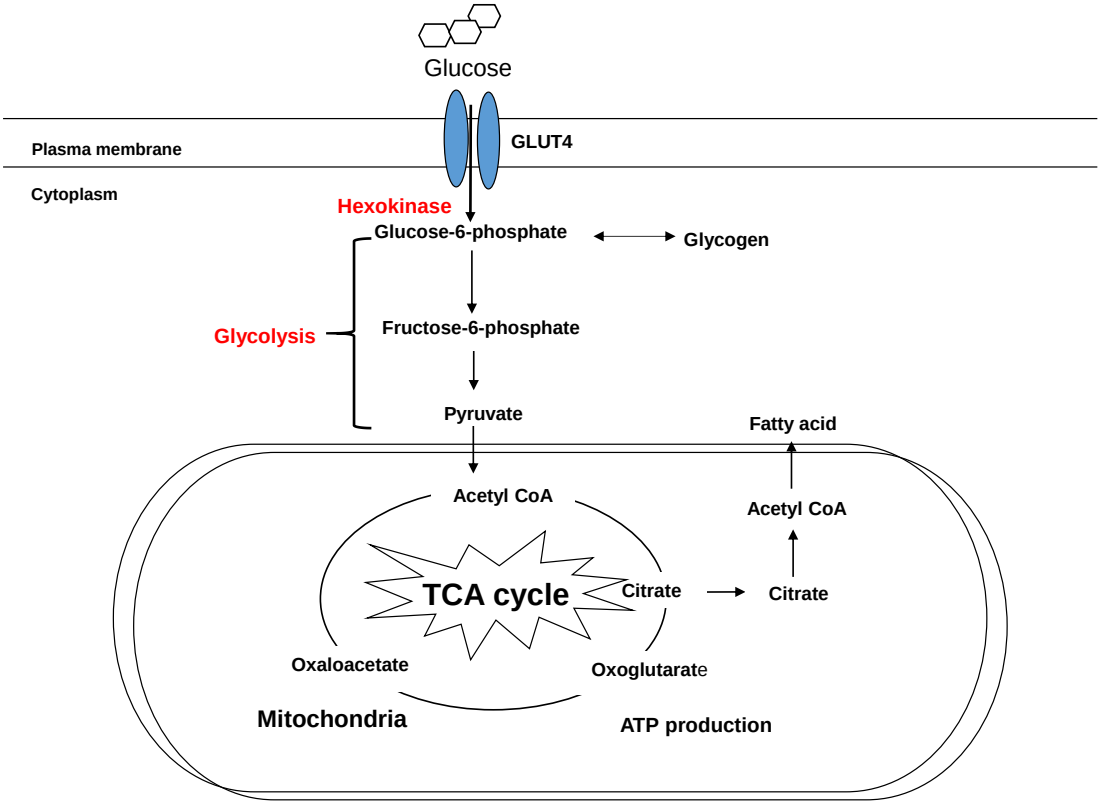

Figure 2.1 A schematic diagram of glycolysis and the tricarboxylic acid cycle. During glycolysis, glucose is broken down in the cytoplasm to pyruvate which enters the mitochondrion and is converted to acetyl-CoA. Acetyl-CoA is either converted to ATP via the tricarboxylic acid cycle (TCA) or is transported back to the cytoplasm as citrate for lipid synthesis

2.5. Fatty acids

Fatty acids are elongated hydrocarbon chains with a terminal carboxylate group. Apart from being a source of fuel, fatty acids have various other functions. Fatty acids serve as building blocks for phospholipids, glycolipids and act as hormones or intracellular messengers (Dutta-Roy, 2000; Berg *et al.,* 2002; Kalish *et al.*, 2012). They can be categorised into four major classes. Saturated fatty acids (SFAs) which lack double bonds in the hydrocarbon chain and therefore are saturated with hydrogen atoms (Marcel and Suzue, 1972). SFAs, especially long-chain fatty acids are generally regarded as unhealthy (Belfort *et al.,* 2005). Unsaturated fatty acids (UFAs) have at least one double bond on the hydrocarbon chain and are regarded to be healthier than saturated fats (Risérus, 2008; Gao *et al.,* 2009; Montel-Hagen *et al.,* 2009). Palmitate (C16:0), a saturated fatty acid commonly found in plants and animals, is associated with the development of insulin resistance, while unsaturated fatty acids such as oleic (C18:1) acids have been demonstrated to have insulin sensitising effects, thus considered to be more healthy (Mozaffarian *et al.*, 2004; Risérus, 2008). Essential fatty acids or PUFAs such as omega 3 (18:3) and omega 6 fatty acids (18:2) with more than one double bond are an integral component of cell membranes. Diets rich in essential fatty acids increase the cell membrane PUFA content, fluidity and enhances insulin receptor activity (Haag and Dippenaar*,* 2005; Risérus, 2008; De Santa Olalla *et al.,* 2009; Siriwardhana *et al.,* 2012).

2.5.1. Fatty acid transport

Lipids are hydrophobic in nature, therefore could passively diffuse across the lipophilic cell membrane, evidence suggests that the majority of free fatty acid uptake into the cell occurs through active transport facilitated by membrane associated proteins. These proteins include the peripheral membrane protein ($PABP_{pm}$), the transmembrane protein, fatty acid translocase or CD 36 and the fatty acid transport proteins 1-6 (FATP 1-6) (Dutta-Roy, 2000; Glatz *et al.,* 2010). Studies have shown that $FABP_{pm}$ and CD 36 co-transport free fatty acid, especially very long-chain fatty acids. In skeletal muscle CD 36 plays a major role in transporting palmitate into the cell (Pelsers *et al.,* 2008; Sebastián *et al.,* 2009). In skeletal muscle and adipocytes,

translocation of GLUT4 and CD 36 coordinate insulin-stimulated postprandial glucose and lipid uptake (Corcoran *et al.,* 2007; Sebastián *et al.,* 2009). The FATPs are tissue specific with FATP 1, 4 and 6 expressed in skeletal muscle, while FATP 1 is mainly expressed in adipose tissue, and FATP 2, 3, 4 and 5 are expressed in the liver. (Frayn *et al.,* 2006; Wu *et al.,* 2006; Karpe *et al.,* 2011; Li *et al.,* 2013). In 3T3-L1 adipocytes FATP 1 was found to affect basal lipid uptake. In rat skeletal muscle both FATP 1 and FATP 4 were involved in lipid uptake, however it appears that FATP 4 is the more effective transporter. It further appears that the FATPs are fatty acid specific with FATP 1, 4 and 6 being involved in palmitate transport (Glatz *et al.,* 2010). Although the precise role of caveolins in FA transport is still controversial it appears that at least for HepG2 and 3T3-L1 adipocytes, caveolin 1 and CD 36 coordinate and facilitate endocytotic fatty acid uptake (Pohl *et al.,* 2002; Pohl *et al.,* 2004). In muscle, caveolin 3 is co-localised with CD 36 indicating some collaboration during fatty acid uptake (Keizer *et al.,* 2004). Esterification of fatty acids by acetyl-CoA synthetase provides a concentration gradient to drive fatty acid transport across the plasma membrane. Dissociation of the fatty acids from the lipophilic plasma membrane to the hydrophilic cytosol is facilitated by binding of the transported fatty acids to $FABP_C$ (Glatz *et al.*, 2010).

2.5.2. Fatty acid metabolism and β-oxidation

For lipid oxidation, long-chain fatty acyl CoA has to be transported across the mitochondrial membranes by the carnitine shuttle system (Koonen *et al.,* 2005; García-Martínez *et al.,* 2005). This shuttle system consists of malonyl-CoA sensitive carnitine palmitoyltransferase 1 (CPT I) that resides on the mitochondrial outer membrane and transesterifies long-chain acyl CoA to long-chain acylcarnitine. Long-chain acylcarnitine is translocated to the inner mitochondrial membrane by carnitine: acylcarnitine translocase were carnitine palmitoyltransferase II (CPT II) located on the inner membrane converts the long-chain acylcarnitine back to long chain acyl-CoA. In the mitochondrial matrix long-chain acyl CoA is converted to acetyl-CoA by β-oxidation. The acetyl-CoA produced enters the TCA cycle. The final product produced by β oxidation in the TCA cycle is NADH and $FADH_2$ which is used by the electron transport chain to produce ATP (Berg, 2002) (Fig. 2.2). Malonyl-CoA concentrations inhibit CPT-1 activity thereby regulating fatty acid oxidation depending on cellular

energy demand (Kerner and Hoppel, 2000; Koonen *et al.,* 2005; Frayn *et al.*, 2006; Glatz *et al.,* 2010) (Fig. 2.2). In addition to CPT-1, fatty acid transporters such as CD 36 and FABPpm, but mainly CD 36, also present in the mitochondrial membrane. Mitochondrial CD 36 is involved with regulation of fatty acid oxidation in skeletal muscle during periods of increased energy demand such as exercise (Holloway *et al.*, 2007).

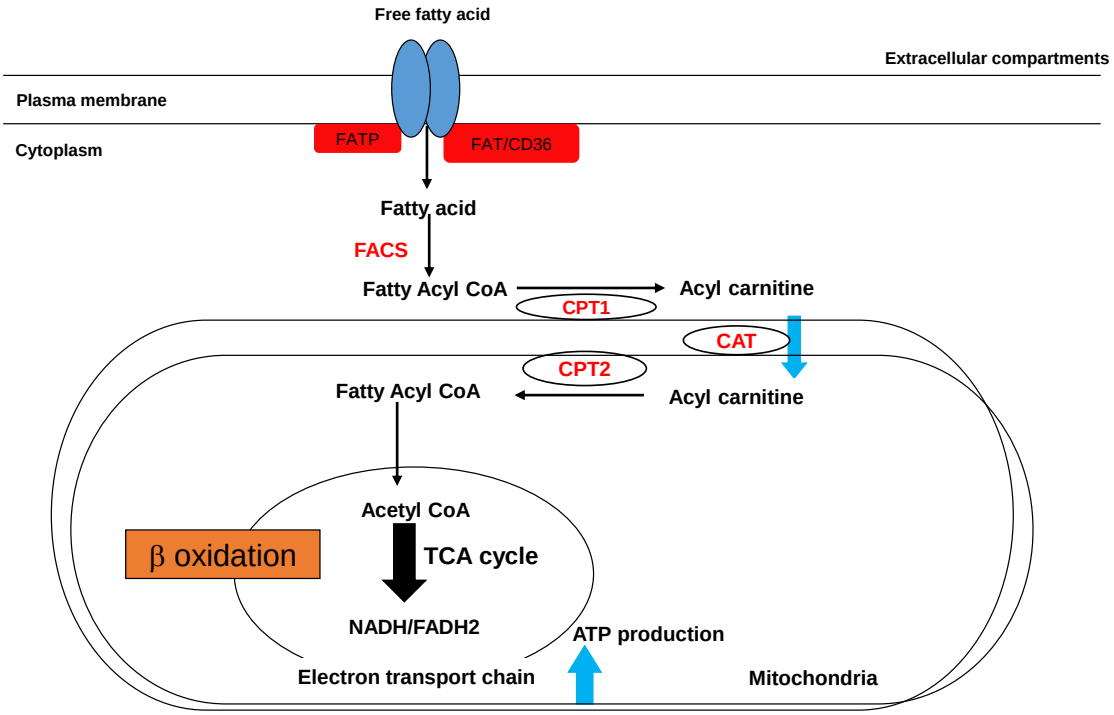

Figure 2.2. An illustration on fatty acid oxidation. Fatty acids are transported by fatty acid transporters from outside the cell into the cell. Once inside the cell fatty acids are converted to fatty acyl CoA by fatty acyl-CoA synthase (FACS) and carnitine palmitoyltransferase 1 (CPT1) convert the fatty acyl CoA to Acyl carnitine where is it transported by carnitine translocase into the mitochondria once inside the mitochondria palmitoyltransferase 2 (CPT2) converts the Acyl carnitine back to fatty acyl CoA where it enters the TCA cycle as acetyl CoA for β-oxidation. Illustration adapted from Fillmore *et al.,* (2011).

2.6. Insulin stimulated glucose uptake and metabolism

Skeletal muscle accounts for approximately 70-80% of peripheral glucose disposal and therefore plays a major part in maintaining normoglycemia. Skeletal muscle uses both glucose and free fatty acids (FFAs) as fuel sources for energy (Corcoran *et al.,* 2007). In the fasting state, circulating plasma glucose concentrations decrease while the plasma fatty acids become more readily available, in this situation the muscle switches to using fatty acids as its primary source of fuel (Abdul-Ghani and DeFronzo, 2010). Postprandially, plasma glucose levels increase, stimulating the release of insulin from the pancreatic β-cells (Kim *et al.,* 2008). When insulin binds to the insulin receptor, present on the cell membranes of most cells including skeletal muscle, liver, fat and kidney cells, the insulin receptor is phosphorylated. This activates a complex signalling cascade of protein kinases and transcriptional proteins, culminating in the translocation of GLUT4 from the intracellular compartment into the cell membrane in muscle and fat cells. In addition insulin stimulates the biosynthesis of glucose transporters including GLUT1, GLUT2 and GLUT4 thereby increases glucose uptake capacity in various cells (Abdul-Ghani and DeFronzo, 2010). Once glucose enters the cell it is phosphorylated by hexokinase, converting glucose to G6P which is either catalyzed by glycolysis and oxidation to pyruvate and ATP when energy is required or stored as glycogen and lipid when glucose levels are increased (Dimitriadis *et al.,* 2011; Von Wilamowitz-Moellendorff *et al.,* 2013).

2.7. Alternative pathways involved in glucose uptake and metabolism

2.7.1. AMP-activated protein kinase (AMPK)

Alternative non-insulin-dependent pathways linked to glucose uptake and metabolism are regulated by adenosine monophosphate-activated protein kinase (AMPK). AMPK, a heterotrimeric serine/threonine protein kinase protein is responsible for maintaining cellular energy levels and controls glucose and lipid metabolism in various organs, especially in skeletal muscle and liver (Gruzman *et al.,* 2009). Cellular energy consuming events such as periods of starvation, exercise and hypoxia decrease

cellular ATP content, with concomitant increases in AMP and ADP levels. AMP and/or ADP allosterically bind to the γ-subunit of AMPK causing conformation changes and phosphorylation of the Thr 172 residues of α-subunit by the liver kinase B1 (LKB1) (Towler and Hardie, 2007; Gruzman *et al.,* 2009). AMPK activation is regulated by antagonistic binding of ATP to the γ-subunit sites (Hardie, 2011). AMPK can also be activated independently of AMP and ADP by rising cytosolic Ca^{2+} levels via calmodulin-dependent protein kinase kinase (CaMKK) (Hawley *et al.,* 2010). As Ca^{2+} influx into the cytosol initiates various energy consuming processes, it is proposed that the activation of AMPK by this mechanism is in anticipation of increased energy expenditure (Hardie, 2011). In skeletal muscle activation of AMPK via CaMKK increases mitochondrial activity and increases GLUT4 synthesis via myocyte enhancer factor (MEF) mediated transcription. During exercise, AMPK increases glucose transport in skeletal muscle by enhancing GLUT4 expression and translocation (Ojuka *et al.,* 2012). This is also taught to be the mechanism whereby GLUT4 expression is increased during myocytic differentiation of C2C12 myoblasts (Richardson *et al.,* 1993) and during differentiation of 3T3-L1 adipocytes (Kaestner *et al.,* 1990). In muscle, as with other cell types, AMPK activation rapidly acts by promoting catabolic pathways yielding ATP such as glycolysis and lipid oxidation (Musi and Goodyear, 2006). It also appears that in skeletal muscle fatty acids such as palmitate could directly active AMPK by enhancing LKB1 activity. For palmitate, activation of AMPK appears to be concentration and time dependent (Watt *et al.,* 2006; Pimenta *et al.,* 2008). In muscle this mechanism makes sense as the downstream effects include inhibition of lipid synthesis and therefore limits the accumulation excessive amounts of intracellular lipids and of potentially harmful fatty acid intermediate metabolites such as ceramide and diacylglycerol (DAG). To facilitate long chain fatty acid oxidation, AMPK activation inhibits acetyl-CoA carboxylase (ACC) and stimulates malonyl-CoA decarboxylase, which together decreases malonyl-CoA concentrations. Concomitantly, fatty acid transport into the mitochondria is increased by releasing the rate limiting effects of malonyl-CoA on CPT1 and thereby enhancing fatty acid oxidation (Watt *et al.,* 2006).

In adipocytes and hepatocytes, AMPK activation suppresses glycerophosphate acyltransferase (GPAT) activity, which controls triglyceride and phospholipid synthesis (Daval *et al.,* 2005). In adipocytes, AMPK controls lipolysis by suppressing hormone-

sensitive lipase (HSL) and adipose triglyceride lipase (ATGL) (Daval *et al.,* 2005). In differentiated 3T3-L1 adipocytes (Salt *et al.,* 2000) and in primary isolated rat adipocytes (Wu *et al*., 2003), as with muscle, AMPK activation enhanced glucose uptake by increasing GLUT4 translocation. However, Gaidhu *et al*. (2006) using isolated rat adipocytes, found that activation of AMPK with 5-aminoimidazole-4-carboxamide-1-β-D-ribofuranoside (AICAR) inhibited both basal and insulin stimulated glucose uptake, lipid uptake, lipid synthesis, glucose and lipid oxidation. The authors proposed that in adipocytes, AMPK has contrasting effects to that of muscle and the liver (Gaidhu *et al.,* 2006). However in 2009, the same author demonstrated that chronic activation of AMPK with AICAR (15 h) supressed adipocytic lipogenesis, increased lipid oxidation and suppressed lipolysis through modulation of HSL and ATGL. This demonstrated that in adipocytes, AMPK-induced effects on lipid and glucose metabolism was time dependent, probably due to AMPK-induced genetic alterations in the expression of key adipogenic and lipolytic genes such as PPARγ and PPARα which occurs during prolonged activation of AMPK (Gaidhu *et al.,* 2009). Pharmacological targeting of AMPK by drugs such as biguanides and thiazolidinediones effectively reduces high blood glucose levels in T2D. Suppression of hepatic glucose release into the circulation is taught to be the major mechanism responsible for the hypoglycemic effects of these drugs. As with muscle and adipose tissue, activation of AMPK suppresses fatty acid, cholesterol and glycerolipid synthesis mainly via its inhibitory effects on ACC and 3-hydroxy-3-methylglutaryl-coenzyme (HMG-CoA) reductase and glycerolphosphate acyltransferase (GPAT), while increasing CPT1 activity enhances lipid oxidation (Viollet *et al.,* 2010). However the major effect of AMPK activation in the liver is related to its suppressive effects on transcription of genes that control endogenous hepatic glucose production. AMPK activation inhibits gluconeogenesis and glycogenolysis by suppressing phosphoenolpyruvate carboxykinase (PEPCK) and glucose-6-phophatase (G6Pase) activity. The inability of insulin to substantially inhibit hepatic glucose production by inactivating PEPCK and G6Pase contributes greatly to diabetic hyperglycemia. During periods of fast, and in T2D, PEPCK increases gluconeogenenic substrate by converting oxalacetic acid to phosphoenolpyruvate while G6Pase initiates the final step of gluconeogenesis and glycogenolysis by converting G6P back to glucose, which is transported back into the circulation via GLUT2. The gluconeogenic activity of

PEPCK and G6Pase is further regulated by Forkhead box protein O1 (FOXO1), which is phosphorylated by AKT, thereby linking insulin signalling with AMPK activation (Huang *et al.,* 2012).

2.8. Insulin resistance

Insulin resistance, which is more prevalent than T2D, is a major pathophysiological risk factor for developing T2D (D'Adamo and Caprio, 2011). Insulin resistance is defined as the impairment of insulin to achieve its physiological effects (Kraegen *et al*., 1991; Weigert *et al*., 2003; Bouzakri *et al*., 2006; Prashanth *et al*., 2009). This affects the action of insulin in major target tissues such as muscle, fat and liver, leading to an increase in circulating fatty acids and hyperglycemia (Storlien *et al.,* 1987). Insulin resistance, sometimes referred to as pre-diabetes, ultimately leads to T2D (Goalstone and Draznin, 1997; Prashanth *et al.*, 2009). To maintain euglycaemia and compensate for insulin resistance, the pancreatic β-cells produce more insulin, but this is at the expense of the negative physiological effects of chronic hyperinsulinemia. In the liver hyperinsulinemia is associated with hepatic steatosis (Reaven, 2005). The prolonged demand on β-cells to produce excessive amounts of insulin results in a progressive apoptotic loss of β-cells, and failure to compensate for the demand leads to the development of impaired glucose tolerance and eventually T2D (Kahn *et al*., 1993; Youngren, 2007; Corpeleijn *et al*., 2009). Therefore approaches to treat T2D must target insulin resistance as enhancement in insulin action allows endogenous insulin to be more effective, protects β-cells and reduces several associated metabolic risk factors.

2.8.1 Mitochondrial dysfunction and insulin resistance

Mitochondria are small oblong organelles found in most eukaryotic cells. Ultrastructurally they consist of an outer and inner membrane enclosing the inner compartment or matrix. Their main function is to produce energy in the form of ATP. The catalytic enzymes and their coenzymes responsible for electron transport and oxidative phosphorylation are bound to the inner mitochondrial membrane. The matrix contains the enzymes of the tricarboxylic acid cycle (TCA cycle) and fatty acid

oxidation as well as the mitochondrial DNA, RNA, and ribosomes for making mitochondrial proteins (Szewczyk and Wojtczak, 2002). In mitochondria energy in the form of ATP, the final product of glycolysis and β oxidation is produced by the respiratory chain where NADH and $FADH_2$ are oxidised leading to the phosphorylation of ADP to ATP (Lodish *et al.,* 2000; Schrauwen and Hesselink, 2002). Recent studies have reported that insulin resistance is associated with reduced mitochondrial ATP synthesis (Kim *et al.,* 2008; Abdul-Ghani and DeFronzo, 2010). A study conducted by Lim *et al.* (2006) showed that oligomycin reduced mitochondrial ATP synthase activity in myotubules, resulting in increased intracellular fat content and impaired insulin signalling, thereby linking mitochondrial dysfunction to insulin resistance and T2D (Befroy *et al.,* 2007; Sivitz and Yorek, 2010, Martins *et al.,* 2012).

2.8.2. Obesity and insulin resistance

Globally, the incidence of obesity is increasing rapidly with more than 1 billion adults overweight and at least 300 million of them clinically obese (Bhutani and Gohil, 2010). Obesity is closely linked to insulin resistance, however, the molecular mechanisms underlying the link between obesity and insulin resistance are not fully understood and thought to be multifactorial (Li *et al.,* 2013). Obesity represents a state of chronic inflammation, with increased levels of inflammatory cytokines, including IL-6 and TNF-α, which are produced by macrophages in the adipose tissue, resulting in pathological changes to insulin-sensitive tissues and β-cells (Qatanani and Lazar, 2007). In obese individuals the limited capacity of adipose tissue to properly store fat is over-run with resultant hyperlipidemia which leads to increased ectopic lipid storage in organs such as the liver and skeletal muscle (Heilbronn *et al.,* 2004; Snel *et al.,* 2012). Chronic hyperlipidemia eventually exceeds the ability of the liver to secrete fatty acids in the form of very-low-density lipoprotein (Fabbrini *et al.*, 2010), causing non-alcoholic fatty liver disease. This surplus lipid storage in the liver causes lipid-induced dysfunction (Fabbrini *et al.*, 2010) and lipid-induced programmed cell death (lipoapoptosis) (Shimabukuro *et al.,* 1998). In obese individuals intracellular levels of intermediate lipid metabolites such as DAG and ceramide inhibit insulin signalling in skeletal muscle and have cytotoxic effects on liver and β-cells thereby impairing function, survival and regeneration (Nguyen *et al*., 2010). Adipose tissue, apart from being a fatty storage

depot, functions as an endocrine organ to secrete a variety of hormones or adipokines such as adiponectin and leptin (Nguyen *et al*., 2010). Adiponectin, by activating AMPK and PPARα plays a major role in regulating ACC phosphorylation, fatty acid oxidation and reduces hepatic glucose production (Yoon *et al*., 2006). In obese individuals, the increasing insulin resistance is associated with decreasing adiponectin concentrations. In contrast to adiponectin, leptin secretion is proportional to fat mass and obesity is linked to hyperleptinemia. Leptin regulates appetite and satiety via its hypothalamic actions and controls adipogenesis and lipolysis by activation of PPARγ (Yadav *et al*., 2013). Leptin or leptin-receptor deficiency cause spontaneous obesity in animals. Paradoxically obese individuals normally present with hyperleptinemia resulting from leptin resistance. In muscle leptin resistance is mediated by overexpression of suppressor of cytokine signalling 3 (SOCS3), which causes ectopic accumulation of lipids and insulin resistance (Jorgensen *et al.,* 2013). Furthermore, hyperleptinemia perpetuates obesity-related inflammation by enhancing macrophage activation (Loffreda *et al.*, 1998).

2.9. Effect of lipids on insulin resistance

Lipid accumulation has been strongly associated with development of insulin resistance (Martins *et al.,* 2012). As mentioned previously, SFAs such as palmitate have been reported to cause insulin resistance in muscle fat and liver. In adipocytes inadequate lipid storage causes increased circulating FAs and this has been associated with insulin resistance (Karpe *et al,* 2011). Increased circulating FAs and chronic hyperglycemia, caused by insulin resistance, increases ectopic lipid accumulation in the liver and skeletal muscle which results in reduced glucose uptake, increased hepatic glucose release, fatty acid oxidation and lipotoxicity (Fig. 2.3).

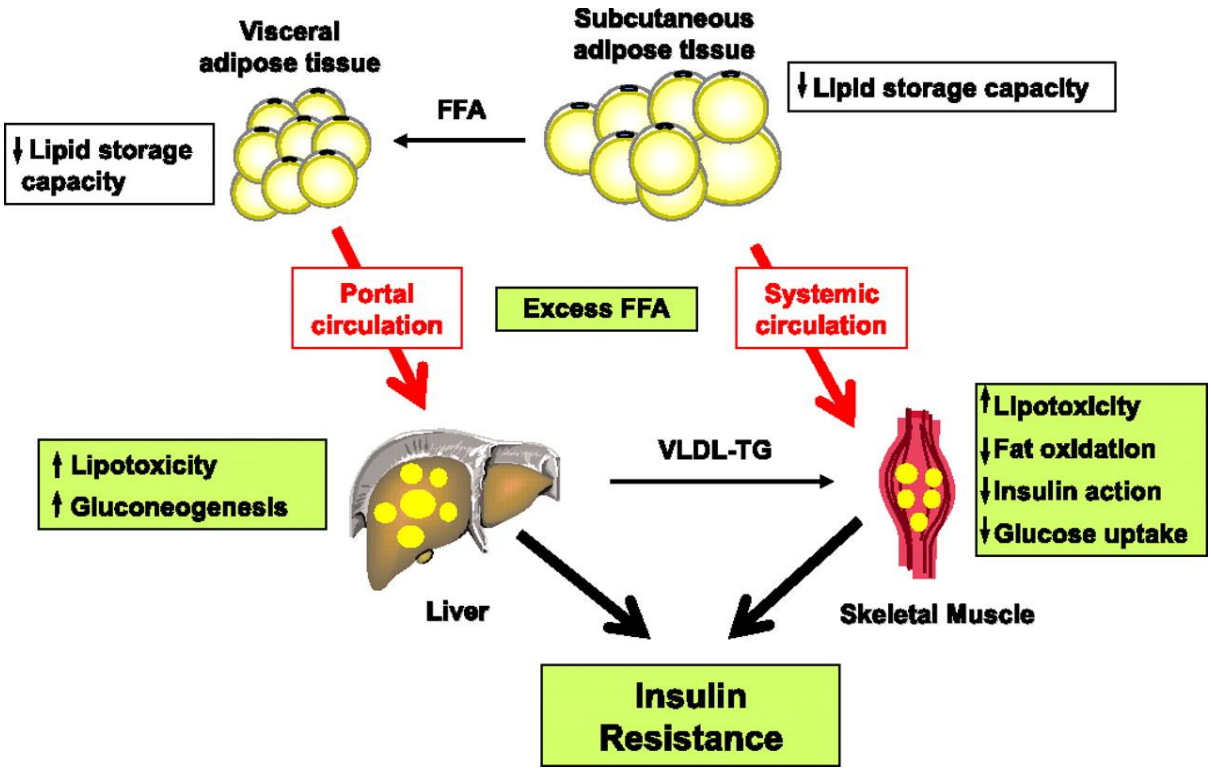

Figure 2.3. Illustration of lipid-induced insulin resistance in adipocytes, liver and muscle. Illustration obtained from Galgani *et al.,* 2008. Insulin resistance is related to the ineffective actions of insulin on its target organs. Under the control of insulin, circulating fatty acids (FA) are removed from the circulation and stored in adipose tissue. However, if insulin action is impaired, adipose tissues fail to remove FA effectively from the circulation and FA accumulates in other tissues such as the skeletal muscle and liver. In the muscle and liver the metabolites of saturated FA further exacerbates insulin resistance.

2.10. Signal transduction defects in insulin resistance in muscle fat and liver

The chronic exposure of cells to increased levels of FAs, particularly SFAs such as palmitate, results in the accumulation of intracellular intermediate lipid metabolites including ceramide and DAG (Boden *et al.,* 1994; Criddle *et al.,* 2006; Glatz *et al.,* 2010). These lipid metabolites lead to increased serine (307) phosphorylation of the IRS1 facilitated by protein kinase C theta (PKCθ) activation, while in the muscle these metabolites activate the inflammation pathway nuclear factor kappa-light-chain-enhancer of activated B (NF-κB). In the liver these metabolites activate protein kinase

C epsilon (PKCε). Taken together in muscle and fat, serine (307) phosphorylation of IRS1 attenuates downstream insulin transduction and ultimately glucose transporter type 4 (GLUT4) translocation to the cell membrane, resulting in deficient insulin-stimulated glucose uptake (Bhattacharya *et al.,* 2007; Yuzefovych *et al.,* 2010). In a recent review by Ragheb and Medhat (2011), it was suggested that muscle insulin resistance was associated with a defective lipid metabolism and high levels of circulating SFAs. The mechanism(s) whereby high levels of SFAs, particularly palmitate, contribute to insulin resistance are still contradictory. Accumulation of the intermediate lipid metabolites, DAG and ceramide, has been reported in palmitate-treated cells (Yuzefovych *et al.,* 2010). Furthermore, Jové *et al.* (2006) demonstrated that palmitate causes an increase in the gene expression of TNF-α in skeletal muscle, and this was strongly associated with activation of PKCθ. Dimopoulos *et al.* (2006) showed that palmitate impaired insulin sensitivity and glucose uptake by reducing activation of AKT in L6 muscle cells. In the adipocytes Wang *et al.* (2009) reported that palmitate induced insulin resistance through the activation of NF-kB and c-jun N-terminal kinase activation (JNK) pathway and this was reversed by curcumin.

2.11 Interaction between carbohydrate and lipid metabolism

In addition to substrate competition, as hypothesized by Randle *et al.* (1964), other processes and factors are known to regulate lipid metabolism. Recent evidence suggests that once inside the cell, fatty acids bind and activates peroxisome proliferators-activated receptors (PPARs), which are members of the steroid hormone receptor superfamily. Their natural activating ligands are fatty acids and lipid-derived substrates (Yoon, 2009).

There are three subtypes of peroxisome proliferators-activated receptors, PPARα, PPARγ and PPARδ. They play a key role in the regulation of energy homeostasis and inflammation (Berger *et al.,* 2005; Rakhshandehroo *et al.,* 2010). PPARα is expressed predominantly in tissues that have a high level of fatty acid catabolism and lipoprotein metabolism, such as liver, heart, and skeletal muscle (Ferré, 2004; Berger *et al.,* 2005). Fibrates, a class of PPARα ligand, have been used for the treatment of dyslipidemia due to their ability to lower plasma triglyceride levels and elevate HDL

cholesterol levels (Staels and Fruchart, 2005; Oyekan, 2009). Furthermore PPARα activators have been shown to regulate obesity in rodents by both increasing hepatic fatty acid oxidation and decreasing the levels of circulating triglycerides (Jeong and Yoon, 2009). PPARγ is a dominant isoform found in fat cells. Several *in vitro* studies have demonstrated that this receptor is important for adipocyte differentiation, and that it promotes lipid accumulation in adipocytes (Rosen *et al.,* 2000; Berger *et al.,* 2005; Sanderson *et al*., 2014). As mentioned previously PPARγ activation alters the expression of genes involved in lipid metabolism and enhance adipocyte insulin signalling, lipid uptake and attenuates lipolysis and FFA release (Fabris *et al.,* 2001).

2.12. Diabetes mellitus

Diabetes mellitus (DM) is a common metabolic disease, characterised by elevated blood glucose levels, either because in type 1 diabetes mellitus (T1D) insulin production is inadequate, or in type 2 diabetes mellitus cells do not respond properly to insulin. The onset of T1D normally occurs in adolescence and is due to the inability of the pancreas to secrete insulin (Skyler, 2007; Van Belle *et al.,* 2011). T2D has an adult-onset and is the most common type of diabetes accounting for approximately 90% of diabetes (Lieberman, 2003; Nolan *et al.,* 2006). T2D is characterised by high blood glucose levels and reduced insulin sensitivity (Prashanth *et al.,* 2009). Currently, T2D is a major cause of morbity and mortality worldwide. Approximately 347 million individuals worldwide are affected with T2D (Danaei *et al.,* 2011). Predictions are that this figure is expected to rise to 366 million individuals by 2030 (Wild *et al.,* 2004; Kumar and Singh, 2010). In addition to hyperglycemia, T2D is characterized by dyslipidemia due to defective or inaffective insulin signalling,a major risk factor for cardiovascular disease (CV) (Prashanth *et al.,* 2009; Fernandes *et al.,* 2010). Insulin resistance, obesity, hyperglycemia, hyperlipidemia and mitochondrial dysfunction are causal risk factors associated with T2D (Qatanani and Lazar 2007).

Chapter 3

Rooibos composition and bioactivity

3.1. Overview of *Aspalathus linearis* (rooibos) and its metabolic effects

3.1.1. *Aspalathus linearis*

Aspalathus linearis known as rooibos is a shrub-like bush that is endemic to South Africa and grows naturally in the Cederberg area, 250 km north of Cape Town where it is extensively cultivated for its commercial use as herbal tea (Fig. 3.1) (Joubert and De Beer, 2011).

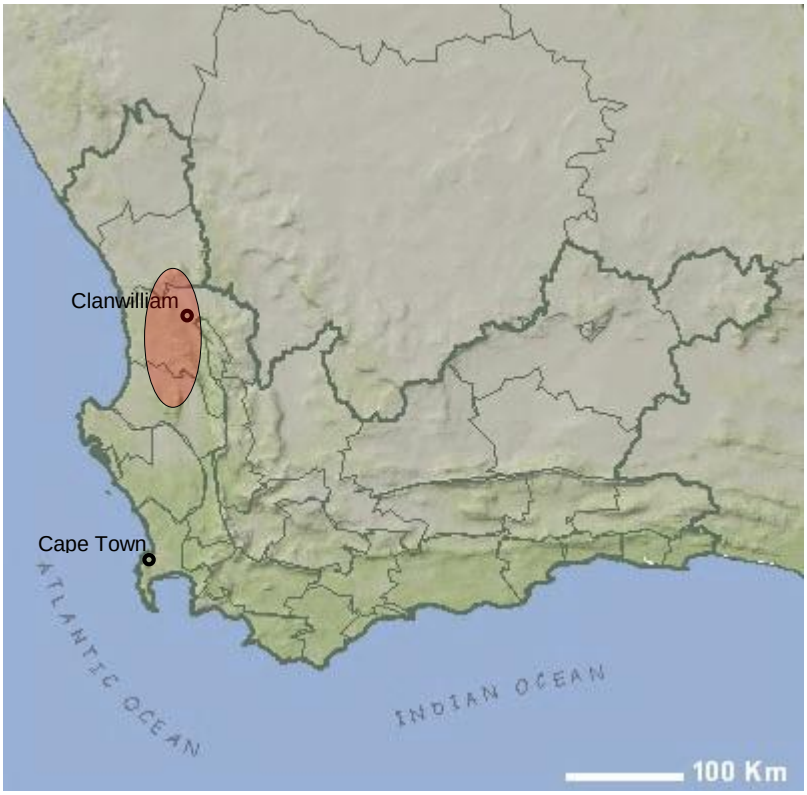

Figure 3.1. Distribution of rooibos. A geographical map illustrating the production and distribution areas of *Aspalathus linearis* in the Western Cape Province of South Africa.

Rooibos is an upright growing shrub, which can grow up to 2 m in nature. The branches are often reddish in colour, with green needle-like leaves. In spring and summer, the plant yields yellow flowers in dense groups at the tips of the branches (Fig. 3.2 A and B). After harvesting the leaves and stems are bruised and then left to “ferment” prior to drying (fermented) or dried immediately to avoid oxidation (unfermented). During the fermentation process the colour changes from green to red-brown due to oxidation (Fig. 3.2 C). The unfermented product remains green in colour and is referred to as green or unfermented rooibos (Fig. 3.2 D) (Joubert and De Beer, 2011).

Figure 3.2. Rooibos plants (A) and its flowers (B), fermented rooibos (C) and unfermented or green rooibos (D). Photographs were obtained from Prof. E Joubert (A), Dr. C Muller (B and C) and (D) downloaded from http://www.carmientea.co.za/tea-variants/rooibos/.

3.2. Chemical composition and bioactivity of rooibos

The consumption of rooibos is increasing worldwide (Joubert and De Beer, 2011). The reason for its popularity, apart from its taste and aroma, can be attributed to its perceived health benefits. Pure rooibos tea contains no additives, colourants or preservatives and is caffeine-free. Rooibos is low in tannins compared to green or black teas (Erickson, 2003). There is strong anecdotal evidence that rooibos alleviates many conditions such as colic, allergies, asthma, increases appetite and helps with dermatological problems such as eczema (Joubert and Schulz, 2006; Joubert *et al.,* 2008). Green rooibos is particularly rich in antioxidants. Many of the health benefits of rooibos have been attributed to the antioxidant activity of its polyphenolic constituents. However, recently, there is growing scientific evidence that rooibos could directly affect glucose and lipid metabolism. Its effects include modulation or stimulation of biological signal transduction pathways, particularly those affected by metabolic disease. Rooibos has been demonstrated to have anti-diabetic effects, cardiovascular protection and anti-obesity properties. Muller *et al.* (2012) showed that unfermented rooibos reduced blood glucose *in vivo*. A study conducted in humans by Marnewick *et al.* (2011) showed that six cups of rooibos per day reduced several relevant biomarkers associated with cardiovascular disease. Pantsi *et al.* (2011) showed that rooibos protected rat hearts from ischemia, whereas Dludla *et al.* (2013) demonstrated that a fermented rooibos extract (same extract used in this study referred to as FRE) protected isolated diabetic rat cardiomyocytes from exogenous oxidants and ischemic stress. In terms of anti-obesity properties, Beltrán-Debón *et al.* (2011) reported that rooibos reduced serum cholesterol, triglyceride and fatty acid levels in mice with diet-induced hyperlipidemia. Sanderson *et al.* (2014) demonstrated that a fermented rooibos infusion inhibited adipogenesis in 3T3-L1 adipocytes, suggesting its potential in inhibiting obesity. Rooibos has the ability to protect vulnerable tissues, such as the liver against exogenous toxin-induced injury. Rooibos was shown to protect rat livers against the effects of the known liver toxins, carbon tetrachloride and *tert*-butyl-hydroperoxide. The hepatoprotective effects were related to the *in vivo* antioxidant capacity of rooibos that prevented lipid peroxidation-induced cell damage (Uličná *et al.,* 2003, 2008; Ajuwon *et al.,* 2013). In STZ-induced diabetic rats, rooibos reduced

advanced glycation end-products and malondialdehyde levels, both associated with diabetic complications including β-cell dysfunction and apoptosis (Uličná *et al.,* 2006).

The phenolic content of rooibos tea differs greatly according to agro-processing methods (fermented and unfermented rooibos), as well as seasonal variation and time of harvest (Joubert and De Beer, 2011). This phenomenon is not unique to rooibos but is a complication common to all phytochemical research. In addition, complex mixtures such as extracts contain a whole plethora of chemical constituents with different physical and biochemical characteristics. Although when present in a mixture, effects such as synergism and antagonism may play a role, it is important to establish the bioactivity of the chemical constituents to gain understand the possible affect when present in these extracts. The most abundant flavonoid of rooibos, aspalathin a *C-C* linked dihydrochalcone glucoside (Fig. 3.3 A), is unique to this herbal tea (Joubert *et al.,* 2008). Many of the health benefits of rooibos has been attributed to aspalathin (Kreuz *et al.,* 2008; Kawano *et al.,* 2009; Fernandes *et al.,* 2010; Son *et al.,* 2013). Another dihydrochalcone, present in rooibos, is nothofagin, a 3-deoxy analog of aspalathin. Rooibos also contains several *C-C* linked β-D- glucopyranosyl flavones such as orientin, isoorientin (Fig. 3.3 B and C), vitexin and isovitexin (Rabe *et al.,* 1994). These are some of the major constituents of rooibos (Joubert *et al.,* 2012, 2013). Orientin has been shown to protect human lymphocytes against the effect of radiation. This radioprotection was associated with its antioxidant activity (Vrinda and Devi, 2001). In addition, orientin was shown to suppress adipogenesis and lipid accumulation in 3T3-L1 cells by inhibiting C/EBPα and PPARγ protein expression, suggesting that orientin could have anti-obesity properties (Kim *et al.,* 2010). In a study conducted by Alonso-Castro *et al.* (2012), isoorientin showed to exert anti-diabetic effects by ameliorating TNF-α induced insulin resistance and activating genes involved in the insulin signalling pathway in adipocytes. In another study isoorieintin protected HepG2 cells against oxidative stress injury by increasing endogenous antioxidant enzyme activity of NAD(P)H:quinone acceptor oxidoreductase 1 (NQO1). The protective effect was mediated by PI3K/AKT transduction and involved Nrf 2 transcription (Lim *et al.,* 2007). A study conducted by Sezik *et al.* (2005) showed that isoorientin had antihyperlipidemic and antihypoglycemic effects in STZ-induced diabetic rats. Isoorientin has also been shown to have significant PPARγ ligand activity

and therefore shows potential as a novel antidiabetic drug candidate (Fidan *et al.,* 2009). Also present in significant amounts are flavonols such as rutin (Fig. 3.3 D), quercetin-3-*O*-robinobioside, hyperoside and isoquercitrin (Joubert *et al.,* 2012). Rutin has been shown to be effective in attenuating the high-fat diet induced symptoms of metabolic syndrome by reducing oxidative stress and inflammation within the liver and heart of rats (Panchal *et al.,* 2011). Al-Rejaie *et al.* (2013) reported that rutin protected rats from hepatotoxicity induced by a high cholesterol diet, concluding that this hepatoprotective effect might be mediated by mechanisms that ameliorate oxidative stress genes. A recent study conducted by Renuka *et al.* (2013) showed that rutin improved glucose and fatty acid metabolism by reducing body weight, plasma triglycerides and total cholesterol in high fructose fed rats. For this study we assessed the bioactivity of rooibos and its major phenolic compound constituents (aspalathin, orientin, isoorientin and rutin). Specific emphasis was placed on the activity of aspalathin, as it is unique to rooibos, on glucose and lipid metabolism.

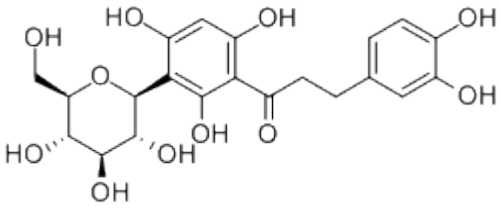

Aspalathin

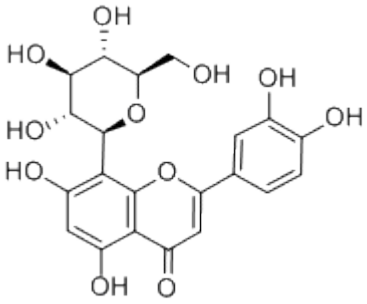

Orientin

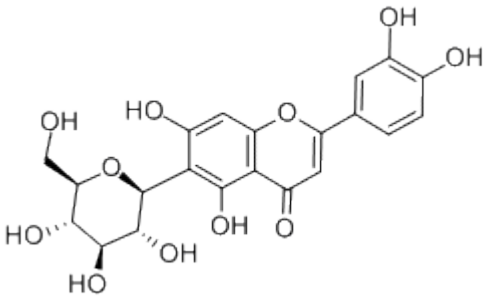

Isoorientin

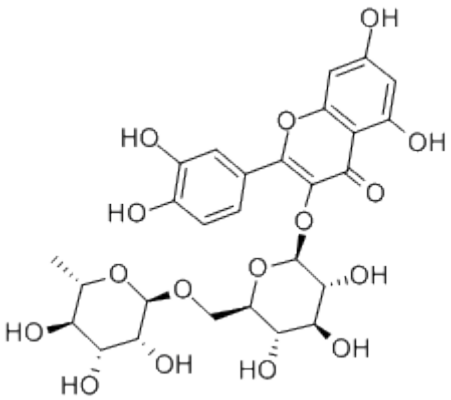

Rutin

Figure 3.3. Structure of aspalathin (A) orientin (B), isoorientin (C) and rutin (D).

Chapter 4

Experimental models of insulin resistance

4.1. *In vitro* models

In vitro models are widely used as an initial method for screening products such as extracts and plant-derived compounds for their effects on cell physiology and metabolism (Fidock *et al.,* 2004). The advantage of using *in vitro* models is that they offer a controlled environment such as temperature, pH and nutrient concentrations to test a specific cellular and molecular hypothesis. Using *in vitro* models to test for efficacy prior to *in vivo* studies is ethically more appropriate, saves time and allows for complex down-stream molecular testing. Furthermore *in vitro* models allow researchers to study chemical metabolism, evaluating mechanism of toxicity, measure enzyme kinetics and examine dose response studies (Soldatow *et al.,* 2013). In this study we used immortalized cell lines derived from skeletal muscle (C2C12), adipocytes transformed from fibroblasts (3T3-L1) and liver (C3A) cells. These cell lines were selected as they represent the major tissues involved in glucose hemostasis.

4.1.1 C2C12 muscle cells

C2C12 cells are murine myoblast cells derived from satellite cells, which have characteristics of skeletal muscle cells. In culture, C2C12 myoblasts differentiate into myocytes that spontaneously form myotubules (Burattin *et al.,* 2004). During muscle differentiation a group of transcriptional factors known as myogenic regulatory factors (MRFs) play a crucial role. MRFs, Myf5 and MyoD are essential for the development, proliferation and survival of skeletal muscle, while *myogenin* controls the differentiation process (Montesano *et al.,* 2013). Expression of MyoD is linked to the conversion of myocytes to myotubules, contractile function and expression of increased levels of muscle proteins including GLUT4, the insulin responsive glucose transporter (Andrés and Walsh, 1996). C2C12 muscle cells provide a good *in vitro* model and have been used to study cell proliferation and differentiation, glucose metabolism and insulin signalling (Li *et al.,* 2013). Several studies have been done on glucose metabolism

using C2C12 myotubes. Elkalaf *et al.* (2013) showed that low glucose concentrations enhances oxidative mitochondrial metabolism in C2C12 myoblasts and myotubes. Capell *et al.* (2010) reported that fatty acids increase glucose uptake and metabolism in C2C12 myoblasts stably transfected with human lipoprotein lipase.

4.1.2. 3T3-L1 pre-adipocytes

The 3T3-L1 pre-adipocyte was originally derived from murine Swiss 3T3 cells. They are embryonic fibroblasts that are chemically transformed in culture into lipid-accumulating adipocytes (Reed *et al.,* 1977; Zebisch *et al.,* 2012). The most commonly used agents for differentiation are insulin, dexamethasone and isobutylmethylxanthine (IBMX) that initiates transcriptional activation of genes involved in adipogenesis. Adipocyte differentiation is a highly regulated process that involves sequential activation of several transcription factors, such as CCAAT-enhancer-binding proteins beta and alpha (C/EBPβ and C/EBPα) and PPARγ. Once differentiated, 3T3-L1 adipocytes display similar characteristic to adipocytes *in vivo*, and are therefore a good model to study adipocytes metabolism (Sakoda *et al.,* 2000; Giri *et al.,* 2006; Ejaz *et al.,* 2009; Dudhia *et al.,* 2013; Ikeda *et al.,* 2013; Sanderson *et al.,* 2014).

4.1.3. C3A liver cells

C3A, also known as HepG2/C3A cells, are a clonal derivative of the human hepatoma cell line (HepG2) that is commonly used to resemble liver cells for *in vitro* screening (Zhou *et al.,* 2012). C3A cells display many liver specific characteristics, including gluconeogenesis, glycogen synthesis in response to insulin stimulation, synthesizes cholesterol as well as liver specific proteins, such as alpha-fetoprotein and express GLUT2. Zang *et al.* (2006) demonstrated that the plant stilbene, resveratrol, activated AMPK and lowered intracellular lipid content in HepG2 cells. Similarly Lian *et al.* (2011) reported that a novel AMPK activator, WS070117, ameliorated oleic acid-induced steatosis by activating AMPK in HepG2 cells, which suppressed HMG-CoA and ACC, key enzymes in liver cholesterol and lipid synthesis. Xie *et al.* (2003) showed that estrogen ameliorated insulin resistance in HepG2 cells and increased the activity of enzymes and genes involved in glucose metabolism. In a recent study, Do *et al.* (2013)

reported that phillyrin prohibited lipid accumulation by hindering the expression of sterol regulatory element-binding protein-1c (SREBP-1c) and fatty acid synthase (FAS) via the activation of LKB1/AMPK in HepG2 cells.

4.2. Induction of insulin resistance in C2C12 muscle, 3T3-L1 adipocytes and C3A liver cells

Insulin resistance is a physiological condition whereby tissues such as muscle, fat and liver fail to respond to insulin action (Morton and Schwartz, 2011; Ye, 2013). To help understand the mechanism of insulin resistance several studies have been conducted using *in vivo* and *in vitro* models in which insulin resistance is experimentally induced (Li and Messina, 2009). Zhang *et al.* (2010) showed that culturing C2C12 muscle cells with palmitate at a concentration of 0.25 mM had no effect, while exposure to concentrations of 0.5 and 0.75 mM for 16 h induced insulin resistance as defined by a reduction in insulin-stimulated glucose uptake and activation of NF-κB. In another study, Tsuchiya *et al.* (2010) reported that 1.0 mM palmitate down-regulated sortilin and impaired GLUT4 protein expression confirming insulin resistance in C2C12 muscle cells. Feng *et al.* (2012) reported that C2C12 muscle cells cultured with 0.5 mM palmitate for 16 h became insulin-resistant which was confirmed by a reduction in AKT phosphorylation. Yang *et al.* (2013) demonstrated that treating C2C12 muscle cells with lower concentrations of palmitate (0.2- 0.6 mM) for 24 h reduced glucose uptake, AKT phosphorylation and Glut4 gene expression. In 3T3-L1 adipocytes, McCall *et al.* (2010) reported that exposure to 0.75 mM palmitate for 16 h increased IRS1 (Ser307) phosphorylation which is associated with insulin resistance, however no effect was observed for AKT activation. In HepG2 liver cells, Lee *et al.* (2012) showed that incubation with 0.5 mM palmitate overnight induced insulin resistance defined by increased JNK and reduced AKT phosphorylation. Furthermore, Gao *et al.* (2010) showed that HepG2 hepatocytes cultured with 0.15 to 0.35 mM palmitate became insulin resistant with a concomitant reduction in intracellular glycogen synthesis. Based on the above and our own findings in C2C12 muscle, 3T3-L1 adipocytes and C3A liver cells for this study we decided to use 0.75 mM for 16 h to induce insulin resistance.

4.3. *In vivo* models

There are a number of *in vivo* models that are available for use in research specifically in T2D research such as monogenic obese models (*ob/ob* mice, *db/db* mice and Zucker diabetic rats) and polygenic models (KK mice, NZO mice and OLETF rat) (Wang *et al.,* 2013). Son *et al.* (2013) used the *ob/ob* mice model to assess the effect of aspalathin on hyperglycemia and glucose intolerance.

For this study a diet-induced obese insulin resistant rat model was used. Feeding Wistar rats a high fat diet (40% fat calorific content) for 12 weeks from weanling induced obesity and insulin resistance that was associated with impaired insulin-stimulated glycolysis and glycogen synthesis (Krygsman *et al.,* 2010). At 12 weeks the peripheral insulin-responsive tissues, such as muscle and adipose tissue, displayed an impaired response to insulin resulting in increased glucose and fatty acids in the circulating blood (Kim *et al.,* 2000). The ensuing insulin resistance results in a decrease in glycolysis which in turn initiates gluconeogenesis and glycolysis in the liver, both of which are controlled by insulin under normal conditions. Insulin resistance also differentially affects tissues involved with maintaining homeostatic glucose levels such as muscle, fat and kidney. To compensate for insulin resistance, the pancreatic β-cells produce more insulin, resulting in chronic hyperinsulinemia. Hyperinsulinemia leads to several negative physiological effects including hepatic steatosis and an attenuated insulin response in responsive tissues such as skeletal muscle and fat (Reaven, 2005).

Chapter 5

Materials and methods

5.1. Materials

Murine C2C12 myoblasts (ATTC Cat. No. CRL 1722), murine 3T3-L1 fibroblasts (ATTC Cat No. CL-173), and human C3A liver cells (ATTC Cat. No. CRL-10741) originating from the American Type Culture Collection, VA, USA were used in this study. The rooibos extracts FRE and GRE, and aspalathin used in this study, were supplied by Professor E Joubert, Post-Harvest and Wine Technology Division, Agricultural Research Council (ARC), Infruitec-Nietvoorbij, Stellenbosch, South Africa. Orientin and isoorientin were purchased from Extrasynthese (Genay Cedex, France), while rutin was purchased from Sigma-Aldrich (St Louis, MO, USA). All other materials, suppliers and product numbers are listed in Appendix 1.

5.2. Methods

5.2.1. Cell Culture

5.2.1.1. Thawing of cells

Cryopreserved cells, stored under liquid N2 in freezing media (Appendix 2) adapted specifically for C2C12 cells, 3T3-L1 adipocytes and C3A liver cells, respectively, were thawed by placing cells in a 37 °C water bath. Immediately, after thawing, cell suspensions were transferred from cryotubes to 15 mL tubes containing 10 mL of pre-warmed 37°C growth media (Table 5.1). Cells were pelleted by centrifugation at 800 g for 5 min. The supernatant was gently removed by aspiration and the cell pellet was lightly vortexed. Cells were resuspended in 5 mL growth media (Table 5.1) and gently mixed by pipetting. For consistency between experiments and to prevent depletion of specific cell phenotypes by excessive passaging, for all experiments, sub-culturing of cells were kept below 20 passages.

Table 5.1. Media used for for different cell type.

Cell type	Media	Supplement
C2C12 muscle cells	DMEM, with 4.5 g/L glucose, with L-glutamine	10% FCS
3T3-L1 adipocytes	DMEM, with 4.5 g/L glucose, with L-glutamine	10% NCS
C3A liver cells	EMEM with Earle's balanced salt solution, essential amino acids, and sodium pyruvate, without L-glutamine	10%FCS

5.2.1.2. Counting of cells

A sample of the cell suspension was stained with 0.4% (w/v) trypan blue in phosphate buffered saline (PBS) and counted using Countess® automated cell counter (Invitrogen, Paisley, Scotland,UK). Briefly, 10 µl trypan blue solution was added to 10 µl of the cell suspension and mixed. Thereafter, 10 µl of the trypan blue/cell suspension was pipetted into the cell counting chamber (Fig. 5.1). The cells were counted using a Countess® automated cell counter to determine cells/mL.

Figure 5.1 An illustration of Countess® automated cell counter. Cells suspension is mixed with trypan blue, pipetted into the counting chamber then counted with the countess automated cell counter.Picture dowloaded from: http://product.invitrogen.com/ivgn/product/C10227?ICD=search-product

5.2.1.3. Sub-culture of cells

After counting, cells were seeded in 75 cm^2 flasks at a density of 2.5 x 10^4 cells/mL for C2C12 muscle cells, 2.0 x 10^4 cells/mL for 3T3-L1adipocytes and 5.5 x 10^4 cells/mL for C3A liver cells. A total volume of 18 mL of pre-warmed growth media was added to the cells. Cells were then incubated at 37°C in 5% CO_2 and humidified air for three days until they were approximately 70% confluent. Media was refreshed every second day.

5.2.1.4. Seeding of cells into multi-well plates

When cells were approximately 70% confluent, media was removed by aspiration and cells were rinsed with 8 mL warm (37°C) Dulbecco`s phosphate buffered saline (DPBS). Cells were trypsinized by adding 2 mL trypsin/versene to the cell culture and incubated at 37°C in 5% CO_2 and humidified air for 7min to allow cells to dislodge from the flask. An inverted light microscope was used to confirm that cells have been dislodged. Trypsinization was stopped by adding 8 mL of growth media (Table 5.1). To ensure a single cell suspension and minimise clumping, the cell suspension was mixed by pipetting up and down against the growth surface of the flask. The cells were counted as previously described in section 5.2.1.2. Cells were seeded into multi-well plates at the densities listed in (Table 5.2). Cells were incubated at 37°C in 5% CO_2 and humidified air for three days until 80-90% confluence was reached, thereafter C2C12 cells and 3T3-L1 cells were differentiated according to the below protocol described in section 5.2.1.5 and 5.2.1.6 respectively. The C3A liver cells do not require differentiation therefore the relevant assays were perfomed in sub-confluent cultures.

Table 5.2.Cell densities used for seeding different cells and plate types.

Cell type	Plate type	Cell concentration	Volume (µl)	Cell density
C2C12	96 well	2.5 x 10^4 cells/mL	200 µl	5 x 10^3 cells/well
	24 well	2.5 x 10^4 cells/mL	1000 µl	2.5 x 10^4 cells/well
	6 well	2.5 x 10^4 cells/mL	3000 µl	7.5 x 10^4 cells/well
3T3	96 well	2.0 x 10^4 cells/mL	200 µl	4 x 10^3 cells/well
	24 well	2.0 x 10^4 cells/mL	1000 µl	2.0 x 10^4 cells/well
	6 well	2.0 x 10^4 cells/mL	3000 µl	6.0 x 10^4 cells/well
C3A	96 well	5.5 x 10^4 cells/mL	200 µl	11.0 x 10^3 cells/well
	24 well	5.5 x 10^4 cells/mL	1000 µl	5.5 x 10^4 cells/well
	6 well	5.5 x 10^4 cells/mL	3000 µl	1.65 x 10^5 cells/well

96 well plates were used for the colourometric glucose uptake, MTT and ATP assays, 24 well plates were used for the 2-deoxy-[3H]–D-glucose assays and 6 well plates were used for Western blot and RNA assays.

5.2.1.5. Myoblast differentiation (C2C12 muscle cells)

To induce differentiation of myoblasts into myocytes that form myotubes, the growth media (Table 5.1) was replaced when cells reached 80-90% confluency (after approximately three days) with Dulbecco's Modified Eagle's Medium (DMEM) containing 2% horse serum (HS) (growth factor poor media) and incubated at 37°C in 5% CO_2 and humidified air for a further two days. Myotubule formation was observed and confirmed using an inverted microscopy and phase contrast (Olympus ck x31). Thereafter the cells were treated with the rooibos extracts and compounds and various assays were perfomed.

5.2.1.6. Adipocyte differentiation (3T3-L1 pre-adipocytes)

3T3-L1 pre-adipocytes were cultured in DMEM growth medium (Table 5.1) at 37°C in humidified air with 5% CO_2 for three days until confluent. At confluence the growth media was replaced with differentiation media containing 10% FBS, dexamethasone (1 µM), 3-isobutyl-1-methylxanthine (0.5 mM) and insulin (1 µg/mL). After a further three days of culture, the differentiation media was substituted with adipocyte maintenance medium (DMEM, 10% FBS, 1 µg/mL insulin) and cells were cultured for a further two days. On day five, the 3T3-L1 cells were fully differentiated, the adipocyte medium was changed to DMEM containing 10% FBS and cells were cultured for a further two days, prior to performing the relevant treatments and assays.

5.3. Preparation of Extracts

The aspalathin-enriched green rooibos extract SB1, previously investigated by Muller *et al.* (2012) was used “as-is” and for the purpose of this study designated GRE (green rooibos extract). The manufacturing process of aspalathin-enriched green rooibos extract from unfermented rooibos was done according to a patented process (Grüner-Richter *et al.,* 2008). This entailed in short extraction of the plant material with an 80% ethanol-water mixture at room temperature, filtration and vacuum-drying, followed by extraction with ethyl acetate to reduce the chlorophyll content. The fermented rooibos extract (FRE), previously investigated by Dludla *et al.* (2013), was prepared on an industrial scale. In brief, the processing entailed hot water (> 90°C) extraction of a 1:10 solid: solvent mixture (m/m) for 30 min (ca 11% dry extract yield), followed by centrifugation, concentration, high-temperature short-time sterilization and vacuum-drying. The phenolic composition of GRE and FRE, previously characterised in terms of phenolic composition by HPLC-DAD was published by Muller *et al.* (2012); Dludla *et al.* (2013) and is summarised in Table 5.3.

Table 5.3. Phenolic content (g/100 g extract) of GRE and FRE

Compound	GRE	FRE
Aspalathin	18.440	0.364
Nothofagin	1.292	0.070
Orientin	1.050	0.721
Isoorientin	2.054	0.924
Luteolin-7-*O*-glucoside	nd	0.069
Vitexin	0.270	0.152
Isovitexin	0.389	0.140
Rutin	0.531	0.185
Quercetin-3-*O*-robinobioside	1.053	0.446
Hyperoside	0.266	0.087
Isoquercitrin	0.377	0.063
PPAG	0.491	0.713
Total	26.218	3.931

FRE and GRE composition as reported by Dludla et al. (2013) and Muller et al. (2012), respectively. PPAG, Z-2-(β-D-glucopyranosyloxy)-3-phenylpropenoic acid nd = not detected

5.4. Dose study

5.4.1. Preparation of extract and compounds for in vitro dose study

The effect of the extracts and compounds on glucose uptake by C2C12 muscle cells, 3T3-L1 adipocytes and C3A liver cells were used to determine the optimal effective concentration *in vitro*. The extracts FRE and GRE were freshly made up in cell culture tested sterile water at a stock concentration of 0.1 mg/µl, the stock solution was further diluted 1:10 in DMEM to give a working solution of 100 µg/µl and log dilutions were then prepared from the working solution. For the compounds (aspalathin, orieintin, isorieintin and rutin), Weighed amounts of ca. 10 mg were dissolved in 100 µL DMSO (100%), the molar amounts calculated e.g. 10 mg aspalathin (MW 452.41) in 100 µL = 221.03 mM. The compounds dissolved in DMSO were then aliquoted and stored at – 80 ºC for subsequent use. Stock solutions of 1 mM were prepared by diluting the appropriate amounts of concentrated compound into DMEM yielding a final DMSO content for the stock solution of < 0.001%. This was further diluted by at least 1:10 of

the working solutions (100, 10, 1, 0.1, 0.01, 0.001, 0.0001 µM). In comparison to the aqueous vehicle controls, DMSO at a concentration of 0.01% did not have any significant effect on glucose uptake, MTT and ATP concentrations (appendix 3).The controls (1 µM insulin), working solutions and dilutions thereof were prepared in DMEM without phenol red or pyruvate containing 8 mM glucose and pre-warmed to 37°C before use.

5.5. Glucose uptake (fluorometric method)

To quantify glucose uptake by the cells treated with the extracts and compounds at different concentrations, an indirect method that measures the amount of glucose remaining in the media after incubation was used. The two extracts GRE and FRE and four compounds, aspalathin, orientin, isoorientin and rutin were tested at various concentrations descibed in section 5.4.1.

After 1 h incubation with the extracts, compounds or insulin, the concentration of glucose remaining in the media was determined by transferring 10 µl of culture media into a new 96 well plate. The medium sample was diluted by adding 90 µl of deionised water, and further diluted to 1:10 with deionised water and the glucose concentration was determined using a commercial kit according to the manufacturer's instructions (Biovision Glucose Assay kit).

A standard curve was prepared by pipetting 0, 2, 4, 6, 8, and 10 µl of a 0.1 nmol/µl glucose standard in a 96 well plate and adjusted to 50 µl using glucose reaction buffer. Ten microlitres of diluted media samples and standards were added to the 384 well plate. Thereafter, 10 µl of glucose reaction mix consisting of substrate detecting dye, glucose oxidase and reaction buffer was added to the wells. The plate was incubated at 37°C for 30 minutes, thereafter the plate was read at Ex/Em of 535/590 in a BioTek® ELX 800 microplate plate reader using Gen 5® software. Glucose uptake was calculated using the formula:

$$\text{Concentration} = \frac{\text{Sample amount from standard curve (Sa) nmol X 100}}{\text{Sample volume added into the sample (Sv) µl}}$$

Results were expressed to % activity of control (8 mM glucose).

5.6. Insulin-resistant models

5.6.1. Free fatty acid preparation

Palmitate (16:0) containing culture media was prepared using a modified method described by Dimopoulos *et al. (*2006) with slight modifications. Briefly, 75 mM palmitate was dissolved in ethanol and heated to 95°C, filter sterilised, diluted 1:100 in DMEM containing 8 mM glucose supplemented with 2% bovine serum albumin (BSA) to yield a final working concentration of 0.75 mM palmitate. The palmitite/BSA solutions were kept at 37°C for 1 h to allow palmitate to conjugate with the BSA. The final concentration of ethanol was >1%. The presence of the palmitate did not affect the pH of the media which remained between 7.4 -7.5. The effect of 1% ethanol on C2C12 and 3T3-L1 cells were previously tested in our laboratory. No measurable differences on glucose uptake and cell viability in comparison to the aqueous vehicle controls were demonstrated (Mazibuko, 2011).

5.6.2. Preparation of extracts and compounds

The extracts FRE and GRE were freshly made up in cell culture tested sterile water prior to each assay at a stock concentration of 0.1 mg/µl. The stock solutions were diluted to a concentration of 10 µg/µl in DMEM containing 0.75 mM palmitate, 2% BSA and 8 mM glucose. For each of the flavonoids, aspalathin, orientin, isoorientin and rutin, stock solutions of 100 µM were prepared in DMSO, which was then diluted to a final working solution of 10 µM in DMEM containing 75 mM palmitate, 2% BSA and 8 mM glucose.

5.6.3. Experimental design

To induce insulin resistance in C2C12 muscle, 3T3-L1 adipocytes and C3A liver cells, the cells were pre-exposed to palmitate by culturing in DMEM containing 5 mM glucose supplemented with 0.75 mM palmitate for 16 h. Thereafter, cells were glucose and serum starved by incubating them with Dulbecco's phosphate buffered saline (DPBS) at 37°C in 5% CO_2 and humidified air for 30 min. After glucose starvation the

cells were exposed to DMEM containing 8 mM glucose with or without 0.75 mM palmitate, containing either GRE, FRE, aspalathin, orientin, isoorientin, rutin or metformin (1 µM) for 3 h at 37°C in 5% CO_2 and humidified air. Insulin (1 µM) and metformin were used as positive controls and a vehicle control (8mM glucose) served as an untreated control. Insulin was added during the last 15 min of the 3 h incubation period. Thereafter relevant assays were performed. The controls were treated exactly the same as the samples although they were not treated with the compounds or extracts.

5.7. 2-Deoxy-[^{3}H]-D-glucose uptake

The determination of 2-deoxy-[^{3}H]-D-glucose (^{3}H-2-DOG) uptake involves adding radioactively labelled ^{3}H-2-DOG to cells and then measuring the concentration of intracellular ^{3}H-2-DOG . 2-Deoxy-D-glucose is a fierce competitor with D-glucose for glucose transport across the cell membrane and can therefore be used to estimate the rate of D-glucose uptake. Once transported into the cell labeled 2-deoxy-D-glucose is phosphorylated by hexokinase to 2-deoxy-D-glucose-6-phosphate but unlike D-glucose, due to a missing hydroxyl group, it cannot be metabolised further and remains as an inert intracellular metabolite. Liquid scintillation counting was used to measure intracellular ^{3}H-2-DOG.

To quantify glucose uptake, cells were treated as described in section 5.6.3, media was removed and cells were washed twice with 1 mL of warm DPBS. Thereafter, 250 µL of DMEM containing 8 mM glucose, 2% BSA and 0.5 µCi/mL ^{3}H-2-DOG was added to each well. Cells were incubated at 37°C in 5% CO_2 and humidified air for 15 min. After incubation ^{3}H-2-DOG uptake was stopped by washing the cells with 1 mL of ice cold DPBS twice. Cells were lysed by adding 500 µL of 0.3 M sodium hydroxide (NaOH)/1% sodium dodecyl sulfate (SDS) and incubated for 45 minutes at 37^{o}C. Lysed cells were mixed into suspension by pipetting. Five microlitres of the cell lysate was used for protein determination using the Bradford method as described below (see sub-section 5.8 below).

For scintillation analyses, the cell lysate was thawed at room temperature and the entire suspension was added to a scintillation vial containing 1 mL distilled water. Thereafter, 2.5 mL of Ready Gel Ultima Gold scintillation fluid was added to the vials and the samples were mixed by vigorous shaking until a whitish gel formed. Vials were placed into a liquid scintillation analyser (2200 CA, Parkard Tricarb series) and left in the analyser overnight to allow samples to equilibrate to room temperature and darkness. The following day, the samples were read with a program for quantifying the ^{3}H-isotope. Results were calculated using the counts per minute (CPM) to determine ^{3}H-2-DOG uptake, and disintegrations per minute (DPM) to determine counter efficiency. The specific radioactivity of ^{3}H-2-DOG and the counter efficiency were used to determine CPM/fmol. The averaged CPM and protein values were used to determine the fmol/mg. Results were reported as ^{3}H-2-DOG fmol/mg protein using the GraphPad radioactivity calculator (GraphPad software): (http://graphpad.com/quickcalcs/radcalcform.cfm).

5.8. Protein determination (Bradford method)

Protein concentrations of cell lysates were determined using the Bradford protein method according to the manufacturer's instructions. A BSA protein standard curve was included in the 96 well plates by adding 5 µl of BSA standards (0.125, 0.25, 0.5, 0.75, 1, 1.5 and 2.0 mg/mL) into the first row. Thereafter, 5 µl of each sample as prepared in section 5.7.2 were added to the remaining wells of the 96 well plate in duplicate for each sample. Two hundred and fifty microlitres of Bradford reagent was then added to each well containing standards or samples and mixed by pipetting up and down twice. The plate was incubated at room temperature for 10 min and the absorbance was read at 570_{nm} in a BioTek® ELX800 plate reader (BioTek Instruments Inc., Winooski, VT, USA). The amount of protein in the sample was quantified by subtracting the absorbance of the blank from the standard and sample absorbance values. A standard curve was graphed by plotting absorbance values of the BSA standards against their concentrations. The protein concentrations of samples were determined from the BSA standard curve. Protein concentration expressed as mg/mL was used to normalise the ^{3}H-2-DOG uptake results.

5.9. [4, 5-Dimethylthiazol-2-yl]-2, 5 diphenyl tetrazolium bromide (MTT) assay

The method described by Mossman. (1983) was used to assess the effect of the rooibos extracts and compounds on cell viability. After the cells were treated as described in sub-section 5.6.3, MTT solution (2 mg/mL DPBS) was added to each well of the plate containing controls or treated cells and incubated for 1 h at 37˚C in humidified air and 5% CO_2. Absorbance was read at 570 nm, using a BioTek® ELX 800 plate reader and Gen 5® software for data acquisition.

5.10. ATP assay

Cells seeded in 96 well plates were treated as previously described in section 5.6.3. Thereafter, an ATP assay was performed using the ViaLight™ plus ATP kit according to the manufacturer's recommendations. Briefly, 50 µL of lysis buffer was added to each well of a 96 well plate and incubated at room temperature for 10 min, thereafter 100 µl ATP reaction mixture was added for further 2 min at room temperature before reading the luminescence in a BioTek® FLX 800 plate reader using Gen 5® software.

5.11. Enzyme-linked immunosorbent assay (ELISA) assay

For IRS1 (Ser 307) in C2C12 muscle cells, an enzyme-linked immunosorbant assay (ELISA) was conducted using a commercial kit, according to the manufacturer's instructions. Briefly C2C12 muscle cell lysates were added in a ratio of 1:1 with the sample diluent from the kit in a 96 well plate coated with primary antibody and incubated overnight at 4°C. The following day the content of the 96 well plates were discarded and the plates were washed three times with wash buffer. Thereafter 100 µL detection antibody was added for 1 h and incubated at 37°C, followed by thorough washing and addition of HRP-linked secondary antibody for 30 min. The TMB substrate was added to each well and further incubated for 30 min. The reaction was terminated by adding 100 µL of stop solution. The plate was shaken for ~10 sec and absorbance was read at 570 nm, using a BioTek® ELX 800 plate reader and Gen 5® software for data acquisition.

5.12. ^{14}C palmitate uptake

To determine palmitate uptake, cells were treated as described in section 5.6.3. Briefly upon induction of insulin resistance, cells were glucose and serum starved by incubating them with Dulbecco's phosphate buffered saline (DPBS) at 37°C in 5% CO_2 and humidified air for 30 min. After glucose starvation, the cells were cultured in DMEM containing 8 mM glucose with 1 µCi/mL ^{14}C palmitate containing either, GRE, FRE, aspalathin, orientin, isoorientin and rutin for 3 h at 37°C in 5% CO_2 and humidified air. Insulin (1 µM) was added during the last 15 min. After incubation ^{14}C palmitate was stopped by washing the cells with 1 mL of ice cold DPBS twice. Cells were lysed by adding 500 µL of 0.3 M sodium hydroxide (NaOH)/1% sodium dodecyl sulfate (SDS) and incubated for 45 minutes at 37^{o}C. Lysed cells were mixed into suspension by pipetting. Five microlitres of the cell lysate was used for protein determination using the Bradford method as described in section 5.8. Samples were analysed using the scintillation analyses as described before using the the isotope ^{14}C.

5.13. Western blots

5.13.1. Cell extraction

Western blot analyses was performed using a standardised protocol (Mahmood and Yang, 2012). Briefly, cells were seeded in 6 well plate and treated as described in section 5.6.3. After treatment, cells were lysed with 300 µL of lysis buffer (50 mM Tris pH 7.5, 1 mM DTT, 50 mM NaF, 100 µM Na_3VO_4, 1% NP40, 1% Triton X114, 25 µg/mL RNase, 1 mM PMSF, protease and phosphatase inhibitor tablets). Three replicates were pooled into a 2 mL Eppendorf tube and stored at -20°C until extraction .

5.13.2. Protein isolation

Cells frozen in 2 mL tubes were thawed on ice, a stainless bead ball was added and the tubes transferred into pre-cooled tissue lyser blocks. Samples were then homogenised in a tissue lyser at 25 Hz for 60 sec, and samples put back on ice after every 60 sec (this step was repeated 5 times). Tubes containing cell lysate were then

centrifuged for 15 min at 13 000 rpm at 4°C. The supernatant was carefully removed and added to a clean 1.5 mL tube.

5.13.3. Protein concentration determination

Protein concentrations were determined using the reducing agent and detergent compatible (RC DC) protein assay as per manufactures recommendations. A BSA protein standard curve was included in the 96 well plates by adding 5 µL of BSA standards (0, 0.2, 0.5, 1, 1.4 and 2.0 mg/mL) into the first two row. Thereafter 5 µL of the samples isolated as described in section 5.13.2 were added into a 96 well plate in duplicate. Twenty five microlitres of reagent A was added to all the wells including the standards. Two hundred microlitres of reagent B was added and the 96 well plate placed on a shaker and mixed for 10 sec. Thereafter the plate was incubated at room temperature for 10 min and the absorbance read at 695 nm in a BioTek® ELX 800 plate reader.

5.13.4. Gel profiling

To check if the isolated proteins were intact, gel profiling was performed for all the cell lines after protein determination. Briefly 20 µg of protein was diluted 1:1 with sample buffer and mixed well. Proteins were denatured by heating at 95°C for 5 min on the heating block, spun down and placed on ice.Thereafter 5 µl of page ruler was added in the first lane and 20 µg of sample was added to the remaining lanes of the 10% SDS-PAGE gel. The gel was run for 70 min at 150 V or until the dye reached the bottom of the gel. The gel was then stained with Coomassie brilliant blue stain overnight. The following day it was destainied with destaining solution until clear. After the gel was destained the gel profilling picture was captured using Biorad Chemidoc.

5.13.5. Running gels (Electrophoresis)

SDS-PAGE gels were prepared using a standard protocol (Mahmoon and Yang, 2012) as described above in sub-section 5.13.4, except that 40 µg of protein was loaded into each lane. To facilitate the transfer of proteins, Santa Cruz Marker™ molecular weight standards (HRP-labeled marker) were added to the last lane.

5.13.6. Transfer of gel to a PVDF membrane for Western blots

An illustration of the assemble and transfer sandwich is seen below (Fig. 5.2). Briefly**,** the sandwich was set in a following order: Fiber pad/sponge, Whatman paper, gel, Polyvinylidene fluoride (PVDF) membrane, Whatman paper and fiber pad/sponge was loaded into a transfer cassette. The casset was then placed in the tank with the cassette facing the corresponding colour coded electrode, black to black and red to red. Enough transfer buffer was added to cover the casset and the transfer performed at 4°C for 20 h at 30 V.

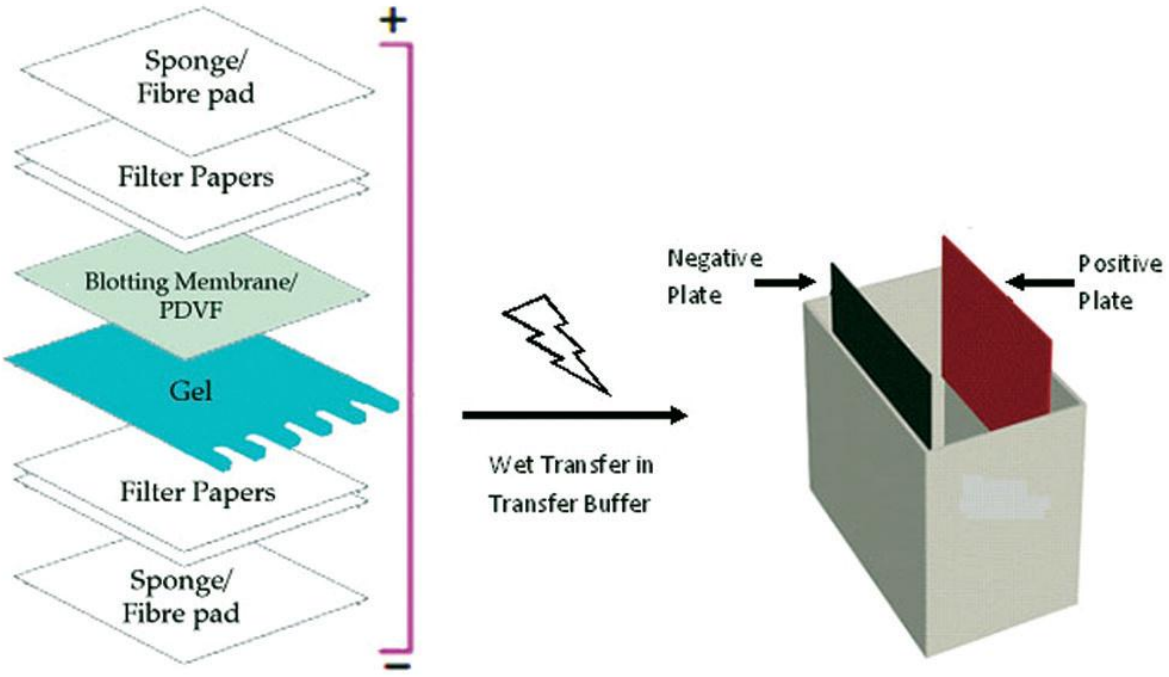

Figure 5.2 Schematic representation of the transfer Sandwich used to transfer proteins for Western blots. Illustration was obtained from Mahmood and Yang, 2012.

5.13.7. Ponceau S stain

Following the transfer the PVDF membrane was removed from the sandwich and placed in a container with Ponceau S stain and shaken gently on an orbital shaker for 5 min at room temperature. Thereafter membrane was rinsed with distilled water until the back ground was clear. To confirm that the proteins were successfully transferred an image of the membrane was taken using the Biorad Chemidoc system. To remove the stain the membrane was washed with 1X TBST buffer (Appendix 2).

5.13.8.Western blot analyses

After removal of the ponceau S stain, non-specific protein labelling was blocked by incubating the membrane in 5% (w/v) low-fat milk powder in TBST at room temperature for 2 h. Membranes were then labelled with the relevant primary antibody overnight (Table 5.4). The following day membranes were washed in 1X TBST 3 times for 10 min each, and incubated with horseradish peroxidase (HRP) conjugated secondary antibodies diluted in TBST with 2.5% (w/v) low-fat milk powder. Proteins were detected and quantified by chemiluminenscence using a Chemidoc-XRS imager and Quantity One 1-D software (Biorad), respectively. β-actin was used as the reference control. The proteins that were assesed in C2C12 muscle, 3T3-L1 adipocytes and C3A liver cells respectively, are listed in Table 5.4.

Table 5.4. List of antibodies, dilutions and gel concentrations used for Western blot analyses

C2C12 muscle cells	**Dilution**	**% gel**
Phosphoprotein kinase thetha (PKCθ)	1:1000	10
Insulin receptor (INSR)	1:1000	10
Threonine kinase B (AKT)	1:1000	10
5'adenosine monophosphate activated protein kinase (AMPK)	1:800	10
Glucose transporter 4 (GLUT4)	1:500	7.5
Phosphatidylinositol 3 kinase (PI3K)	1:800	7.5
3T3-L1 adipocytes cells	**Dilution**	**% gel**
Nuclear factor kappa beta (NFkB)	1:1000	10
Insulin receptor (INSR)	1:1000	10
Threonine kinase B (AKT)	1:1000	10
5'adenosine monophosphate activated protein kinase (AMPK)	1:800	10
Glucose transporter 4 (GLUT4)	1:500	7.5
Phosphatidylinositol 3 kinase (PI3K)	1:800	7.5
Malonly CoA	1:2500	7.5
Carnitine palmitoyltransferase I (CPT1)	1:1000	10
Peroxisome proliferator-activated receptor gamma (PPARγ)	1:1000	10
Peroxisome proliferator-activated receptor gamma (PPARα)	1:1000	10
C3A liver cells	**Dilution**	**% gel**
Phosphatidylinositol 3 kinase (PI3K)	1:800	7.5
Glucose transporter 2 (GLUT2)	1:500	7.5
5'adenosine monophosphate activated protein kinase (AMPK)	1:800	7.8
FOXO1	1:1000	10
Malonly CoA	1:2500	7.5
Carnitine palmitoyltransferase I (CPT1)	1:1000	10

5.14 In vivo OB/IR Wistar rat model

5.14.1. Diet-induced obese insulin-resistant Wistar rat model

Three weeks old weaning male Wistar rats were fed a high fat diet (40% fat as energy) and 30% sucrose and fructose (1:1) in the drinking water *ad libitum* for 12 weeks to induce obesity and insulin resistance (OB/IR).

5.14.2. Ethical approval

The Ethical approval for this study was granted by the ethics committee at the Medical Research Council of South Africa (ECRA 11/03/H). The study was performed in accordance with the principles and guidelines of the South African Medical Research Council as outlined in Guidelines on Ethics for Medical Research: Use of Animals in Research and Training, 2004 (http://www.mrc.ac.za/ethics/ethicsbook3.pdf).

5.14.3. Animal housing

Male Wistar rats (n = 64) bred at the Medical Research Council (MRC), Primate Unit were used in this study. All procedures were carried out at the Primate Unit and the rats were maintained and managed according to standard operating procedures (SOP) of the Primate Unit. The rats were maintained in a temperature controlled room of 24-26°C, humidity of 45-55% with 15-20 air changes per hour and on a 12 h light/dark cycle.

5.14.4. Diet and calorie composition

The high fat diet consisted of 40% fat, of which 18.3% was saturated fats and 44% carbohydrates (2.06 Kcal/g). In addition, 30% sucrose/fructose (1:1 w/w) were added to the drinking water contributing a further 6 Kcal/100 mL. After 12 weeks on the obesity diet, the rats were maintained on the diet for a further 12 weeks with daily administration of GRE at different doses.

5.14.5 Dosages for rooibos extract (GRE)

Rooibos dosages were extrapolated from human equivalent consumption of 1 (32 mg/kg), 3 (97 mg/kg) and 6 (195 mg/kg) cups of tea daily. The dose was calculated by dividing the soluble solid content of a cup of rooibos infusion (~230 mg/200 mL) by 70 (average human weight) and then multiplying the sum with an equivalent surface area dosage conversion factor of 10x for rats (Freireich *et al.,* 1966). Vildagliptin, the drug reference control, was administred at a dose of 10.0 mg/kg, previously shown to be effective (Muller *et al.,* 2012).

5.14.6. Experimental design of the study

After 12 weeks on the respective diets, rats were divided into 5 groups:

Group 1: control group of OB/IR rats (n = 14) received jelly with no extract for 12 weeks.

Group 2: treated group of OB/IR rats (n = 13) received jelly containing 10.0 mg/kg of Vildagliptin daily for 12 weeks.

Group 3: treated group of OB/IR rats (n = 12) received jelly containing 32 mg/kg of GRE daily for 12 weeks.

Group 4: treated group of OB/IR rats (n = 12) received jelly containing 97 mg/kg of GRE daily for 12 weeks.

Group 5: treated group of OB/IR rats (n = 12) received jelly containing 195 mg/kg of GRE daily for 12 weeks.

5.14.7. Administration of extracts and vildagliptin

Gelatine-jelly (80 g of gelatine-jelly was dissolved in 450 mL of water and 7 g additional gelatine added to increase the consistency of the jelly) was used as a vehicle to administer GRE and vildagliptin. Specific dosages were aliquoted into moulds equivalent to the body weight of a specific rat. The jelly was allowed to set in a 4°C before feeding to the rats.

5.14.8. Body weight and fasting plasma glucose

Rats were fasted for 4 h (food was removed and juice replaced with normal drinking water) prior to glucose measurements. A drop of blood was collected from the tip of the tail and the blood glucose concentration determined using a glucometer (OneTouch Select®, LifeScan Inc., Milipitas, CA). Body weights and blood glucose concentrations were determined every 4 weeks.

5.14.9. Oral glucose tolerance tests (OGTT)

After 12 weeks of treatment with GRE, oral glucose tolerance tests were performed. Rats were starved for 16 h (food was removed and juice replaced with normal drinking water). Fasting rats were gavaged with GRE treatments (t = -60 min) and 1 h later a glucose bolus (t = 0 min) was gavaged at 2 g/kg glucose (50% Dextrose-Fresenius 50%, Intramed, Port Elizabeth, S.A.). Plasma glucose concentrations were determined at -60 and at 0, 15, 30, 60, 120 and 240 min relative to the glucose bolus (t = 0).

5.14.10. Blood collection and organ harvesting

Rats were fasted for 16 h (food was removed and sucrose/fructose containing water was replaced with normal drinking water). After 16 h fast the rats received their final treatment dose of GRE in jelly, 2 h before being anaesthetised by inhalation of 98% oxygen and 2% fluothane. Paddle reflex was tested to establish response under anaesthesia and blood was collected in Vacutainer® SST™ gel tubes from the abdominal vena cava. After blood collection the rats were euthanised by exsanguination under anaesthesia, the muscle and liver tissues were removed, weighed and stored in the RNA later solution to preserve the mRNA integrity. The other tissues were frozen in liquid nitrogen and stored at -80°C for the Western blots analyses.

5.14.11. Serum insulin

After collection, the blood was centrifuged at 4000 rpm for 15 min at 4°C and serum was removed and stored at -20°C for the insulin determination. Serum insulin concentrations were determined by radioimmunoassay (RIA) using a Linco rat insulin kit. The procedure was done over two days. On the first day, standards and quality controls were prepared according to manufacturer's instructions and samples were prepared in duplicate. Two hundred microliters of assay buffer was added to borosilicate tubes followed by 100 µl of the rat serum samples. One hundred microliters of ^{125}I-Insulin were then added to samples. One hundred microliters of rat insulin antibody was added to all the samples. Samples were vortexed, covered and incubated overnight (20-24 h) at 4 °C. The following day, 1 mL precipitating reagent was added, the samples vortexed and incubated for 20 min at 4 °C. Samples were centrifuged at 4 °C for 30 min at 4000 x g. The supernatant was aspirated and the visible pellet remaining in tube was resuspended. Samples were analysed using a gamma counter (Perkin-Elmer Wizard 1470 automatic gamma counter, Monza, Italy). Results were expressed in ng/mL.

5.14.12. Calculation of homeostatic model assessment of insulin resistance (HOMA-IR)

HOMA-IR was used to estimate the degree of insulin resistance (Bonora *et al.,* 2002).HOMA-IR was calculated using the fasting plasma glucose concentrations (fPG) (mmol/L) multiplied by the fasting serum insulin concentrations (fINS) (ng/mL) divided by 22.5 ((fPG x fINS) / 22.5). A low HOMA-IR value indicates high insulin sensitivity and a high HOMA-IR indicates low insulin sensitivity (insulin resistance) (Bonora *et al.,* 2002).

5.15. mRNA analyses on muscle and liver tissue

5.15.1. RNA extraction

In brief: The muscle and liver tissues were removed from the RNA later solution weighed and ~30 mg placed into a new 2 mL tube containing 1 mL of Trizol and a stainless steel bead. Tissues were then homogenized using the Qiagen Tissue lyser at 25Hz for 2 min and this was repeated twice.
The lysate was centrifuged at 12 000 g for 10 min at 4°C and the supernatant was transferred to a new Eppendorf tube. Thereafter, 0.2 mL of chloroform was added to each tube, mixed intermittently for 3 min and then centrifuged at 12 000 g for 15 min at 4°C. The upper aqueous phase was transferred to a new 1.5 mL Eppendorf tube without disturbing the interphase or organic phase. For RNA precipitation, 0.5 mL of isopropanol was added and mixed thoroughly and samples incubated at -20°C overnight. The following day, the RNA was pelleted by centrifuging at 12 000 g for 20 minutes at 4°C. The supernatant was discarded, the RNA pellet was washed with 1 mL 75% ethanol and centrifuged at 12 000 g for 15 min at 4°C. This wash step was repeated. After the final wash, the fluid was drained from the Eppendorf tubes by blotting on paper towel and the pellet in the tube was allowed to air dry for 15 min. The RNA pellet was re-suspended by adding 100 µL RNase free water, mixed by pipetting up and down ten times and then incubated at 55°C for 10 min. Thereafter, RNA was cleaned up using the RNeasy Mini kit according to the instructions given by the manufacturer.

A volume of 350 µL of RLT lysis buffer was added to the RNA solution, followed by 250 µL of 96% ethanol and mixing by pipetting the samples up and down. The samples were transferred to an RNeasy spin column in a 2 mL collection tube and centrifuged at 12 000 g for 15 sec. The flow-through was discarded. Five hundred microliters RPE buffer was added to the RNeasy spin column, centrifuged at 12 000 g for 15 sec and the flow-through discarded. This step was repeated twice. Thereafter, the RNeasy spin column was placed in a new 2 mL collection tube and centrifuged at 12 000 g for 1 min to ensure that the membrane was completely dry. To elute the RNA following the washing steps described above, the RNeasy spin column was placed in a new 1.5 mL

collection tube and 40 µL of RNase free water was added directly to the spin column membrane. Samples were allowed to stand at room temperature for 1 min before RNA was eluted by centrifugation at 12 000 g for 1 min. The elution step was repeated to ensure that all RNA was retrieved from the spin column. Thereafter RNA elutants were pooled and placed on ice for RNA quantification.

5.15.2. RNA quantification and purity

Nucleic acids (RNA and DNA) absorb at 260 nm (A_{260}), while proteins and other contaminants absorb at 280 nm (A_{280}). Thus, the ratio of 260 nm to 280 nm was used to assess the purity of a sample. A ratio of two is generally accepted as sufficiently pure for RNA analyses. The ratio of A_{260} to A_{230} is used as a secondary measure of purity, and indicates DNA contaminants that absorb at or near 230 nm. RNA concentration and purity was determined by measuring the absorbance at A_{260}, A_{280} and A_{230} in a Nanodrop 1000 spectrophotometer. The spectrophotometer was initialised by pipetting 2 µL distilled water onto the pedestal of the spectrophotometer, and blanked with 2 µL RNase free water. Thereafter, 2 µL sample was pipetted onto the pedestal and the absorbance determined. Each sample was read in triplicate.

5.15.3. DNase treatment

RNA samples were DNase treated to remove contaminating genomic DNA from RNA preparations by using a Turbo DNase kit according to the manufacturer's recommendations. Briefly, 5 µL of 10x DNase buffer and 1.5 µL of DNase was added to 20 µg of RNA and RNase-free water in a total reaction volume of 50 µL. Samples were mixed and incubated at 37°C for 30 min, after which another 1.5 µL of DNase was added and incubated at 37°C for a further 30 min. The reaction was stopped by adding 10 µL DNase inactivation reagent and mixed by placing tubes on an orbital shaker for two min. Thereafter, the tubes were centrifuged at 10 000 g for 1.5 min and the supernatant transferred to a new tube. RNA concentrations were determined using a Nanodrop 1000 spectrophotometer.

5.15.4. Reverse transcription

Total RNA was reverse transcribed into cDNA using the High-Capacity cDNA kit according to the manufacturer's instructions. One microgram DNase treated RNA sample was added to 10 µL RNase-free water and placed on ice. A reaction mix consisting of reaction buffer, dNTPs, random primers, RNase-inhibitor (5000 units/mL), reverse transcriptase and nuclease-free water was prepared into two separate tubes labelled RT plus and RT minus. The RT minus reaction mix tube (negative control) contained the same reaction mix as the RT plus tube, but with the reverse transcription enzyme replaced by water (Table 5.5). After adding the RT plus and RT minus mix components, the prepared reaction mixes were mixed by pipetting and the tubes centrifuged briefly. Ten microlitres of plus or minus RT reaction mixes were added to 0.2 mL tubes containing RNA samples. The tube contents were mixed, briefly centrifuged and placed in a 2720 thermal cycler. Reactions were incubated at 25°C for 10 min, 37°C for 120 min, and 85°C for 5 sec to inactivate the reverse transcriptase enzyme. Samples were stored at -20°C until gene expression analyses by quantitative real-time PCR. The RT minus tube (negative control) was used to calculate the amount of genomic DNA contamination.

Table 5.5. Components used for the reverse transcription reaction

Component	**Volume (µL)**	
	Plus RT	**Minus RT**
1 µg DNase-treated RNA in RNase-free water	10	10
10 x RT buffer	2	2
25 x dNTP mix	0.8	0.8
10 x random primers	2	2
RNase inhibitor	1	1
Nuclease-free water	3.2	4.2
Reverse Transcriptase	1	0
Total volume	**20**	**20**

5.15.5. Quantitative Real-time PCR determination of genomic DNA contamination

To assess the extent of genomic DNA contamination in RNA samples, cDNA generated from plus and minus reverse transcription reactions were amplified with exon spanning primers that would amplify both mRNA and genomic DNA. A reaction mix consisting of 12.5 µL SYBR Green mix, 1 µL of 10 µM ActB Forward Primer (400 nM), 1 µL of 10 µM ActB Reverse Primer (400 nM) and H_2O to a final volume of 24 µL was prepared. The reaction mix was scaled up according to the number of test samples.

Twenty four microlitres of reaction mix was aliquoted into a PCR plate, followed by 1 µL (50 ng) of undiluted cDNA (plus or minus RT reactions). The plate was sealed with adhesive film, mixed on a plate shaker for 10 min and then briefly centrifuged at 3 000 g. The PCR reactions were conducted on the ABI 7500 Sequence Detection System Instrument (Applied Biosystems) using the Absolute Quantification (AQ) Software (SDS V1.4). Universal cycling conditions; 50ºC for 2 min and 95ºC for 10 min, followed by 40 cycles of 95°C for 15 sec and 60°C for 1 min were used. A dissociation curve was added for secondary product detection. Data was acquired during the extension step (60°C for 1 min). After the run, default settings for the threshold cycle (Ct) and baseline were used and Ct values were exported to Microsoft Excel for analyses.

5.15.6. Quantitative Real-time PCR for gene expression analyses

Quantitative real-time PCR (qRT-PCR) is one of the most sensitive and commonly used techniques to study gene expression. In this study Taqman® gene expression assays from Applied Biosystems were used. Taqman® gene expression assays consists of a Taqman® probe with a FAM™ or VIC® dye label and minor groove binder (MGB) moiety on the 5' end, and non-fluorescent quencher (NFQ) dye on the 3' end. For qRT-PCR, a reaction mixture consisting of 5 µL of Taqman® universal PCR master mix, 0.5 µL of pre-developed Taqman® gene expression assays and water to a final volume of 9 µL was prepared.

Standard curve was prepared from Total Rat Liver RNA (Ambion). The reaction mix was scaled up according to the number of samples to be analysed. Nine microlitres of the reaction mix was aliquoted into a well of the PCR plate, followed by 1 µL of a 10-fold dilution series of the standard curve or test samples cDNA. A No Template Control (NTC) negative control used to rule out cross contamination of reagents and surfaces was included by using water instead of cDNA. The NTC was used as a negative control in all PCR reactions. All samples were analysed in duplicate. PCR plates were covered with adhesive film, briefly centrifuged for 10 sec and placed in a shaker for 10 min and again briefly centrifuged at 3000 g. The PCR reactions were conducted on the ABI 7500 Sequence Detection System Instrument (Applied Biosystems) using universal cycling conditions as described before in sub-section 5.15.5. Data generated on the ABI 7500 Instrument was analysed with the ABI Standard Quantification (AQ) software (SDS V1.4) using a Ct of 0.1 and a baseline of between 3 and 15 cycles. Taqman® gene expression assays, Beta actin (ActB) and glyceraldehyde-3-phosphate dehydrogenase (Gapdh) (Table 5.6) were used as endogenous controls. Messenger RNA levels in test samples were normalised to the average of the two endogenous controls. The Taqman® gene expression assays that were used in this study are listed in (Table 5.6). The suffix _m represents an assay whose probe spans an exon-exon junction of the associated gene and therefore will not detect genomic DNA.

Table 5.6. Taqman® gene probes that were used in the study

Probes	**Assay ID**
Insulin receptor (Insr)	mM01211875_m1
Insulin receptor substrate 1(Irs1)	Mm01278327_m1
Insulin receptor substrate 2 (Irs2)	Mm03038435_m1
Phosphatidylinositol 3 Kinase (Pi3k)	Mm00803160_m1
5'adenosine monophosphate activated protein kinase (Ampk)	Mm01297600
Glucose transporter 4 (Glut4)	mM01245502
Glucose transporter 2 (Glut2)	Mm01245502_m1
Beta actin (ActB)	4352339E
Glyceraldehyde-3-phosphate dehydrogenase (Gapdh)	4352341E

5.16. Western blots on muscle and liver tissue

Western blot analyses were performed as previously described in section 5.13 with minor modifications to accommodate protein extraction from tissues. Briefly, 100 mg of tissue (muscle and liver) was weighed and placed in 2 mL tube and washed in cold DPBS. The DPBS was discarded, replaced with 500 µL lysis buffer and the tissue lysed in a Qiagen Tissue lyser at 25Hz for 1 min (this was repeated 5 times). Thereafter protein was extracted and Western blots performed.

5.17 Statistical analyses

In vitro results are expressed as the mean ± SEM of three independent experiments. Statistical significance were calculated using an one-way multivariate ANOVA statistical assessment with Turkey *post hoc* test if $p \leq 0.05$, which was deemed significantly different.

The *in vivo* results are expressed as mean ± SEM of n = 6 animals per group. An one-way ANOVA with a Dunnett's *post hoc* if $p \leq 0.05$, which was performed to demonstrate significant differences between groups (Graphpad Prism version 5.0) was used. Area under the curve values were calculated using the trapezoidal method with Graphpad Prism version 5.

CHAPTER 6

RESULTS

6.1. Dose finding

The use of *in vitro* studies to evaluate the glucose uptake in cell lines following stimulation with insulin and other active compounds including plant extracts, is a direct and sensitive method of determining the glucose lowering effect of these agents. It allows for rapid screening of extracts and compounds in terms of their efficacy and toxicity in an ethically acceptable manner. C2C12 muscle, 3T3-L1 adipocytes and C3A liver cells were selected for screening as they represent three tissues primarily involved in insulin-stimulated glucose uptake and are directly involved with glucose homeostasis. The first approach of this project was to perform an *in vitro* glucose uptake study to determine the most active concentration for FRE, GRE and the major phenolic compounds present in rooibos including the flavonoids aspalathin (ASP), orientin (ORE), isoorientin (ISO) and rutin (RUT).The cells screening dosage for GRE in C2C12 muscle cells was not performed as this was already established in our laboratory by Muller *et al.* (2012).

6.1.1. Phenolic composition of rooibos extracts

The total phenolic content of GRE and FRE (Table 5.3) was 26.2 and 3.9% respectively. The GRE extract contained substantially higher levels of all the phenolic compounds determined except for PPAG. Luteolin-7-*O*-glucoside was not detected in GRE, but was present in FRE. The largest difference in content of the individual compounds between GRE and FRE was for the dihydrochalcones, aspalathin and its 3-deoxy analogue, nothofagin (respectively 50.7 and 18.5 times higher in GRE). The other compounds were 1.5 to 6 times higher in GRE compared to FRE. The major compound in FRE was isoorientin (0.92%), one of the flavone analogues of aspalathin.

6.1.2. Dose-response effect of fermented rooibos extract (FRE) in C2C12 muscle, 3T3-L1 adipocytes and C3A liver cells

Glucose uptake was perfomed using a fluorometric method to determine the dose-response of FRE in C2C12 muscle, 3T3-L1 adipocytes and C3A liver cells. Insulin (1 µM) and metformin (1 µM) were used as positive controls. Results showed that both insulin and metformin increased glucose uptake from 100.0 ± 3.1% to 128.8 ± 5.1% ($p < 0.01$) and 130.5 ± 4.1% ($p < 0.001$). In the C2C12 muscle cells FRE significantly increased glucose uptake in the concentration range of 0.0001 to 10 µg/mL (Fig. 6.1 A). In 3T3-L1 adipocytes and C3A liver cells FRE increased glucose uptake in all the concentrations tested from 0.0001 to 100 µg/mL (Fig. 6.1 B and C).

A

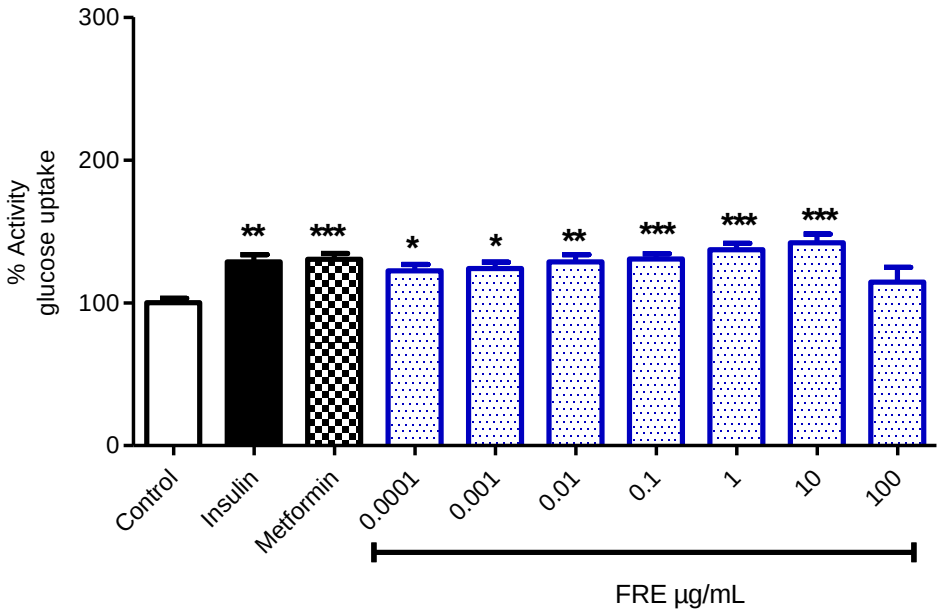

B

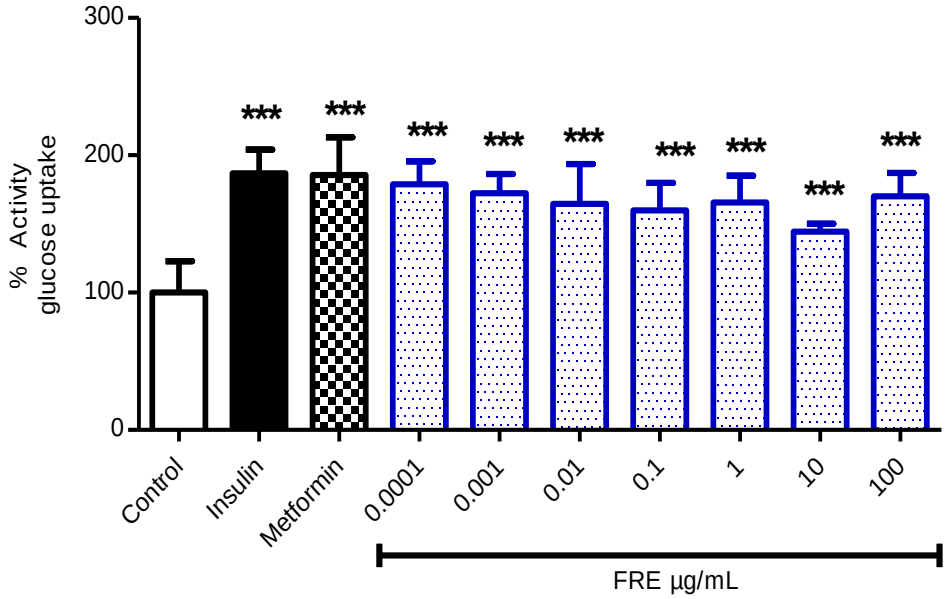

C

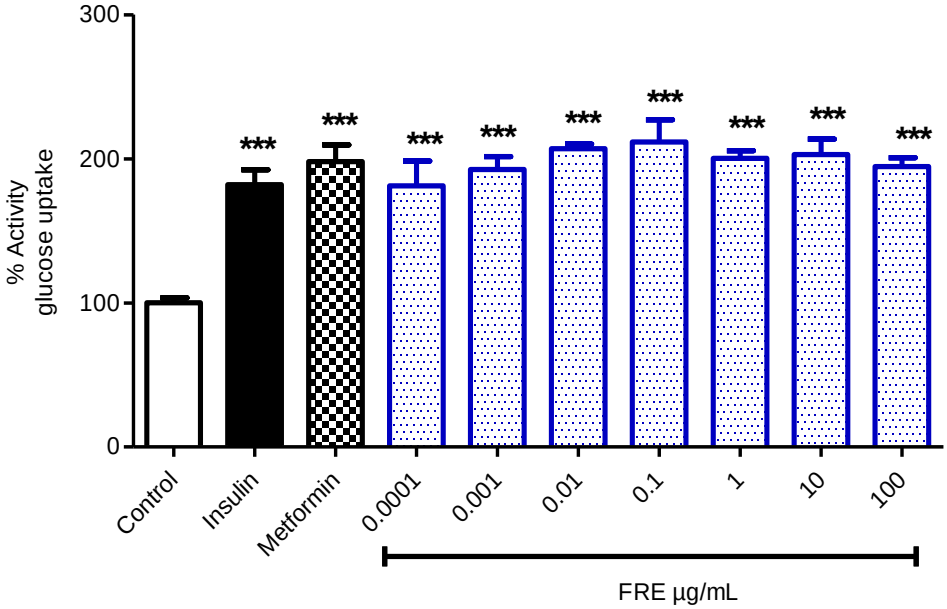

Figure 6.1. The effect of fermented rooibos extract (FRE) on glucose uptake in C2C12 muscle cells (A), 3T3-L1 adipocytes (B) and C3A liver cells (C). Cells were cultured in 8 mM glucose in DMEM without phenol red and pyruvate containing FRE at log concentrations for 1 h in C2C12 muscle and for 3 h in 3T3-L1 adipocytes and C3A liver cells, respectively. Glucose uptake was measured using a fluorometric assay. Results are expressed as the mean of three independent experiments expressed relative to control (8 mM glucose) at 100% ± SEM; *$p < 0.05$, **p <0.01 and ***$p < 0.001$.

6.1.3. Dose response for aspalathin-enriched unfermented green rooibos extract (GRE) in 3T3-L1 adipocytes and C3A liver cells

A dose response for GRE was only perfomed for 3T3-L1 adipocytes and C3A liver cells. An effective dose for C2C12 muscle cells has previously been established to be between 0.05 and 50 µg/mL (Muller *et al.,* 2012). In 3T3-L1 adipocyes and C3A liver cells glucose uptake was enhanced in a dose-dependent manner by GRE at all concentrations tested (Fig. 6.2 A and B).

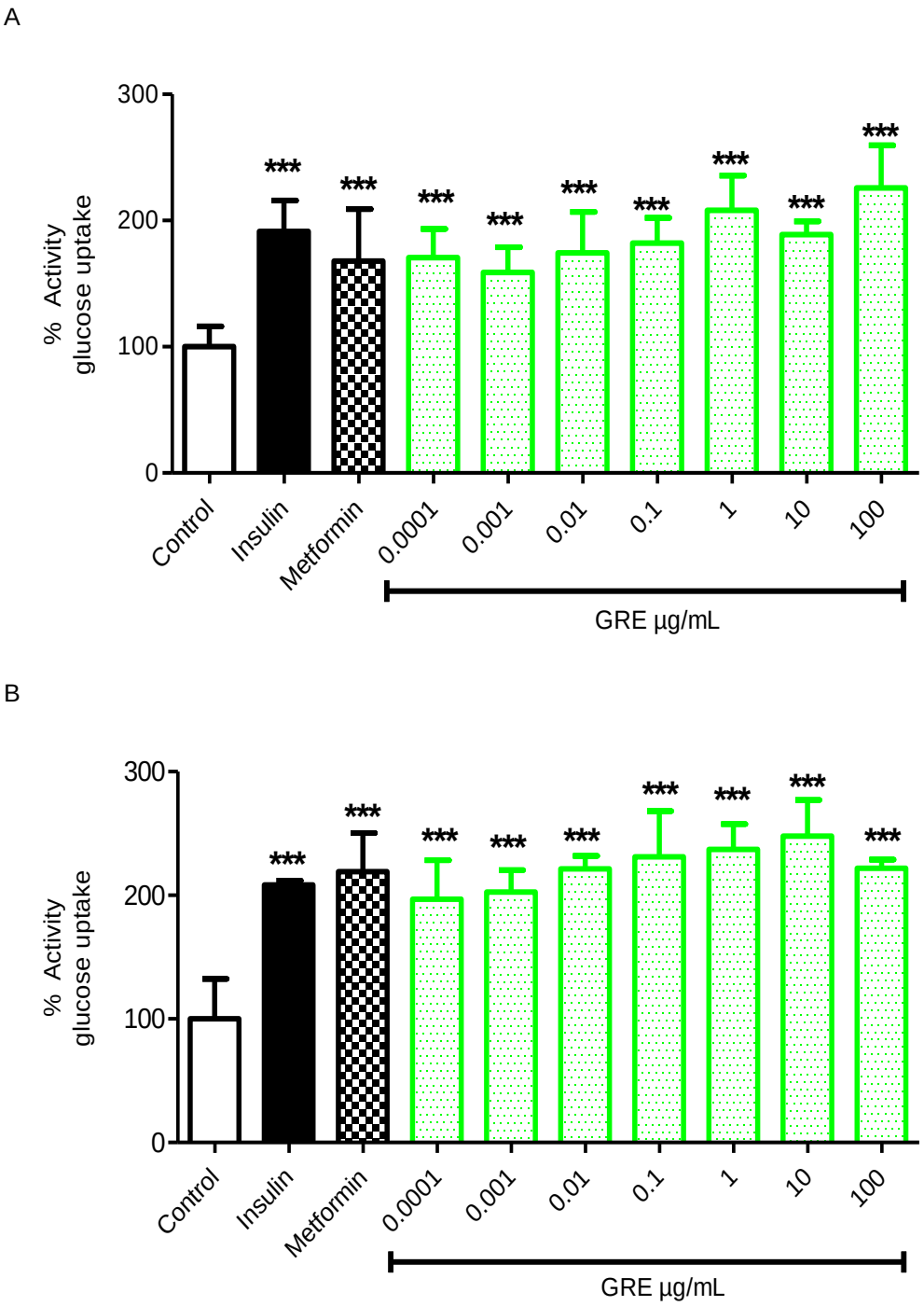

Figure 6.2. The effect green rooibos extract (GRE) on glucose uptake on 3T3-L1 adipocytes (A) and C3A liver cells (B). Cells were cultured in 8 mM glucose in DMEM without phenol red and pyruvate containing log dilutions of GRE for 1 h in C2C12 muscle and for 3 h in 3T3-L1 adipocytes and C3A liver cells, respectively. Glucose uptake was measured using a fluorometric assay. Results are expressed as the mean of three independent experiments expressed relative to control (8 mM glucose) at 100% ± SD; ***$p < 0.001$.

6.1.4. Dose response for aspalathin in C2C12 muscle, 3T3-L1 adipocytes and C3A liver cells

Glucose uptake was perfomed in C2C12 muscle, 3T3-L1 adipocytes and C3A liver cells, using the fluorometric method described previously. Results showed that treatment with aspalathin increased glucose uptake at all concentrations tested in C2C12 muscle cells (Fig. 6.3 A). In 3T3-L1 adipocytes glucose uptake was enhanced in a dose dependant manner (Fig. 6.3 B). Similar results were observed in C3A liver cells whereas treatment with aspalathin increased glucose uptake in a dose-dependent manner at all concentrations tested (Fig. 6.3 C).

A

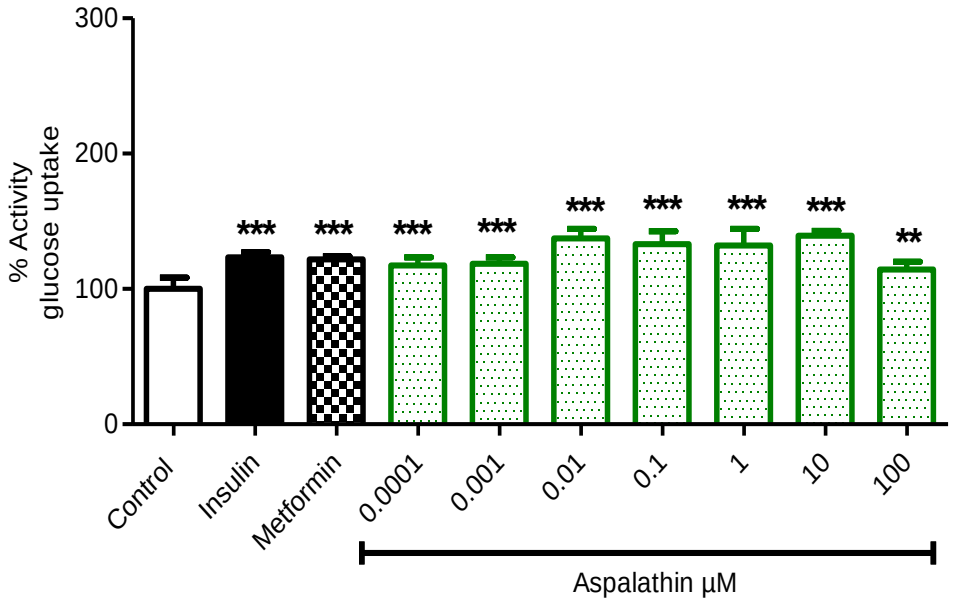

B

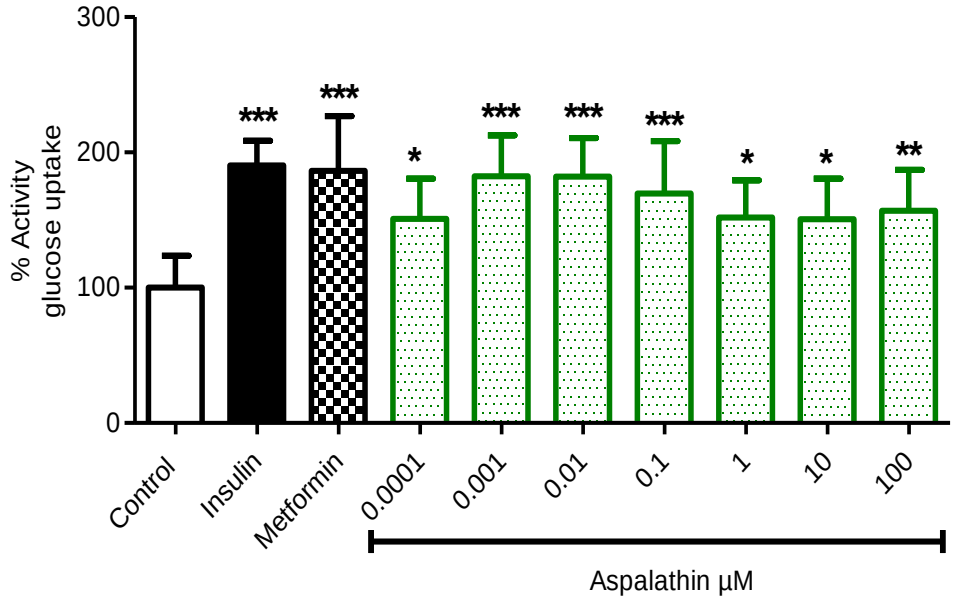

C

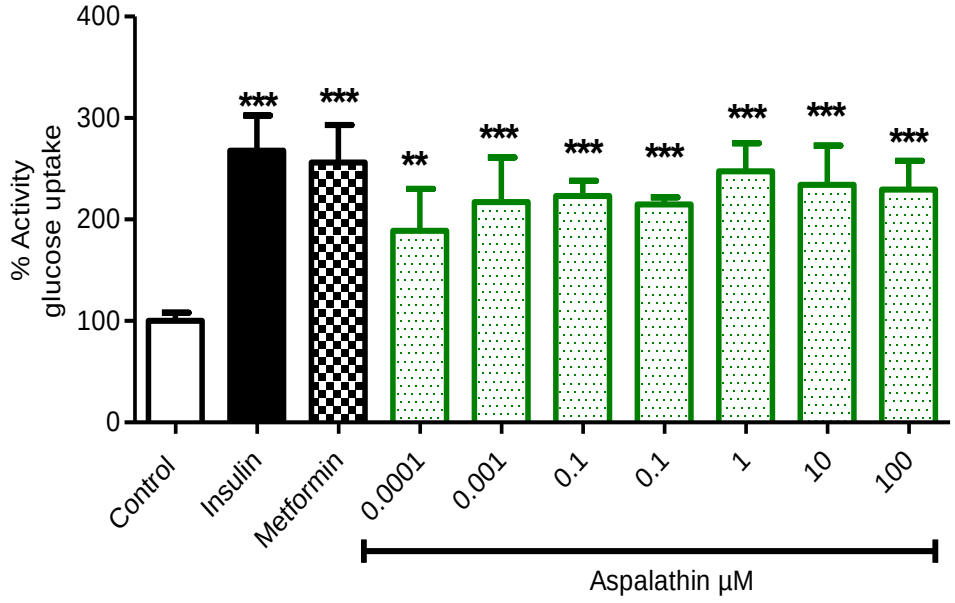

Figure 6.3. The effect of aspalathin on glucose uptake in C2C12 muscle cells (A), 3T3-L1 adipocytes (B) and C3A liver cells (C). Cells were cultured in 8 mM glucose in DMEM without phenol red and pyruvate containing log dilutions of aspalathin for 1 h in C2C12 muscle and for 3 h in 3T3-L1 adipocytes and C3A liver cells, respectively. Glucose uptake was measured using a fluorometric assay. Results are expressed as the mean of three independent experiments expressed relative to control (8 mM glucose) at 100% ± SEM; *$p < 0.05$, **$p < 0.01$ and ***$p < 0.001$.

6.1.5. Effect of orientin on glucose uptake in C2C12 muscle, 3T3-L1 adipocytes and C3A liver cells

Orientin significantly increased glucose uptake in C2C12 musle cells at concentrations of 10 and 100 µM, respectively (Fig. 6.4 A). In 3T3-L1 adipocytes and C3A liver cells orientin increased glucose uptake at all concentrations tested (Fig. 6.4 B and C).

A

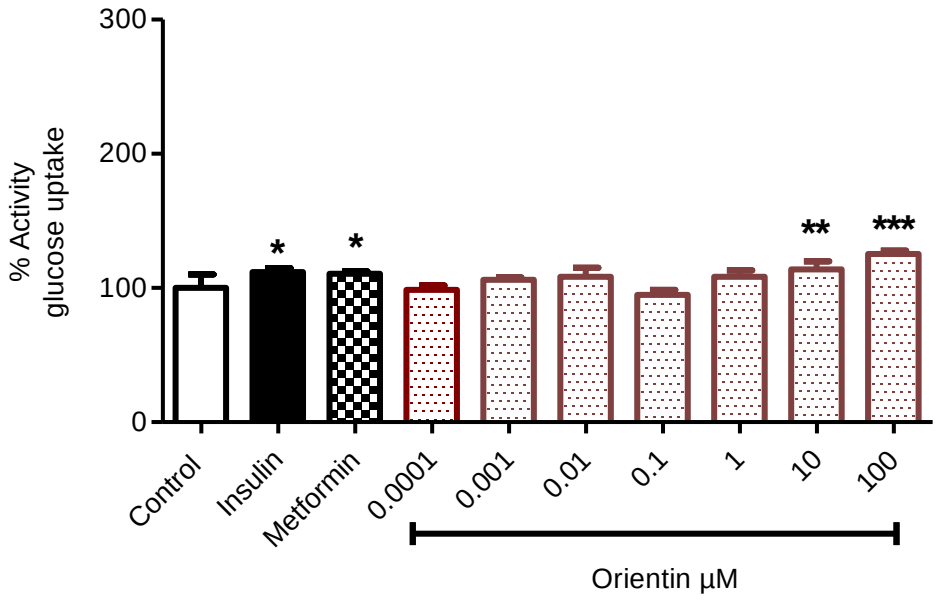

B

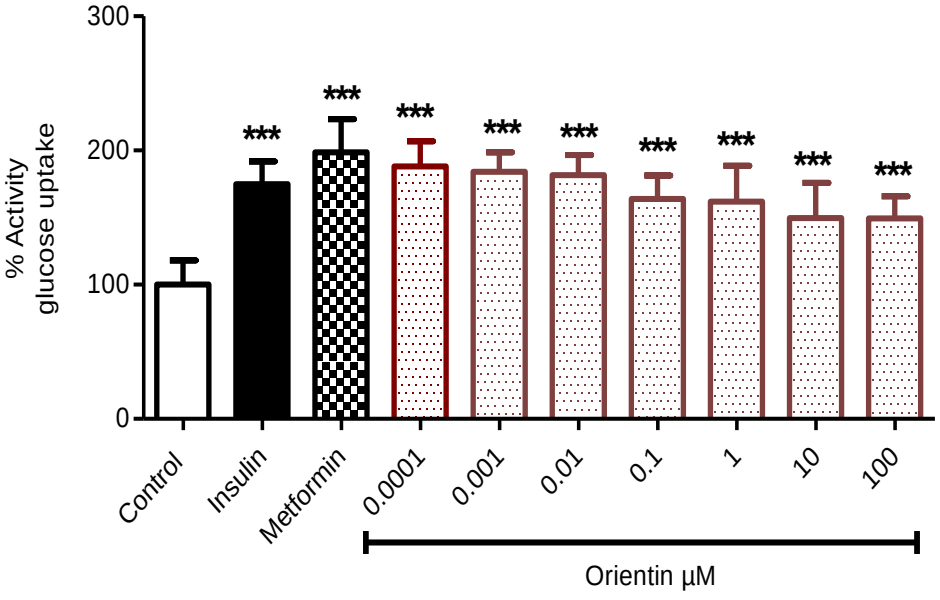

C

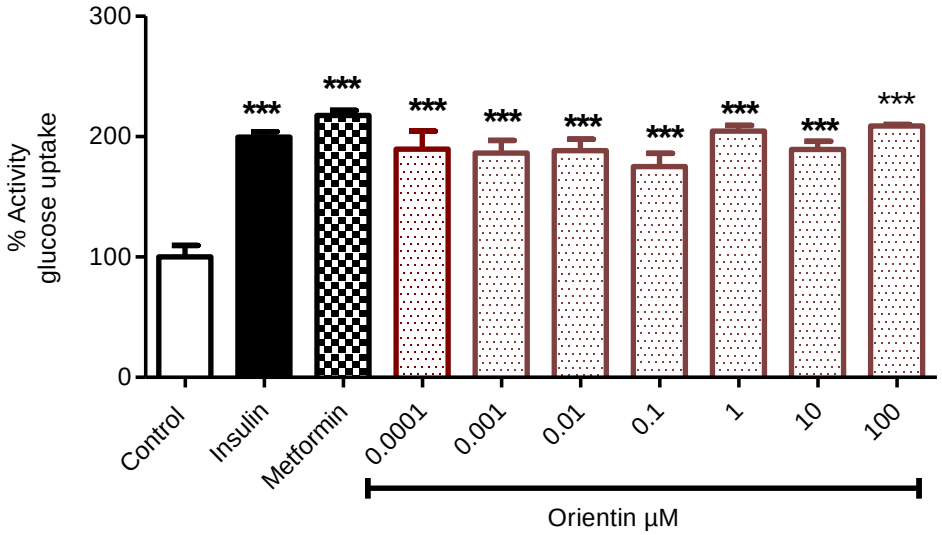

Figure 6.4. The effect of orientin on glucose uptake in C2C12 muscle cells (A), 3T3-L1 adipocytes (B) and C3A liver cells (C). Cells were cultured in 8 mM glucose in DMEM without phenol red and pyruvate containing log dilutions of orientin for 1 h in C2C12 muscle and for 3 h in 3T3-L1 adipocytes and C3A liver cells, respectively. Glucose uptake was measured using a fluorometric assay. Results are expressed as the mean of three independent experiments expressed relative to control (8 mM glucose) at 100% ± SEM; *$p < 0.05$, **$p < 0.01$ and ***$p < 0.001$.

6.1.6. Effect of isoorientin on glucose uptake in C2C12 muscle, 3T3-L1 and C3A liver cells

Isoorientin was most effective at increasing glucose uptake in C2C12 muscle cells at the concentrations of 0.001 to 10 µM (Fig. 6.5 A). In 3T3-L1 adipocytes and C3A liver cells at all the concentrations tested increased glucose uptake (Fig. 6.5 B and C).

A

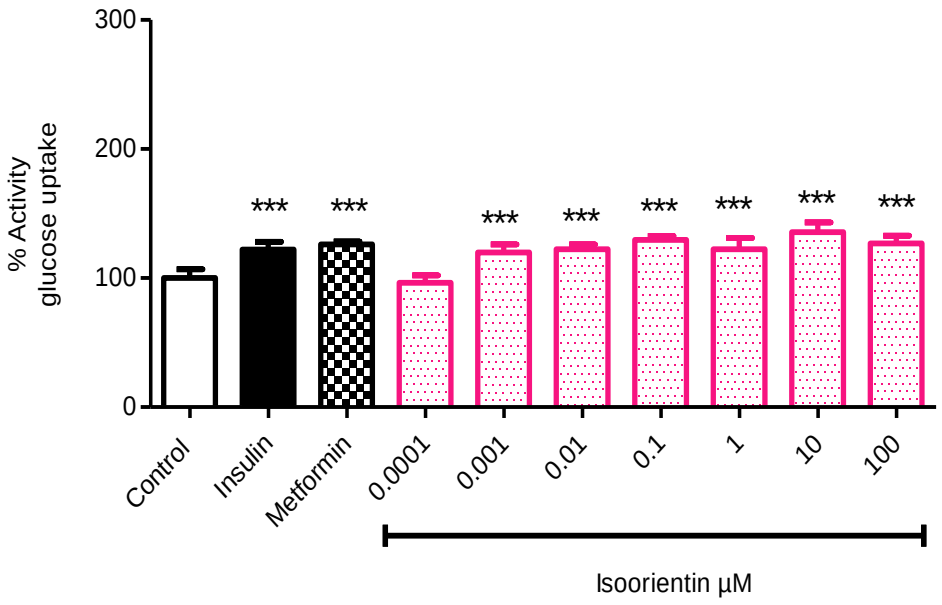

B

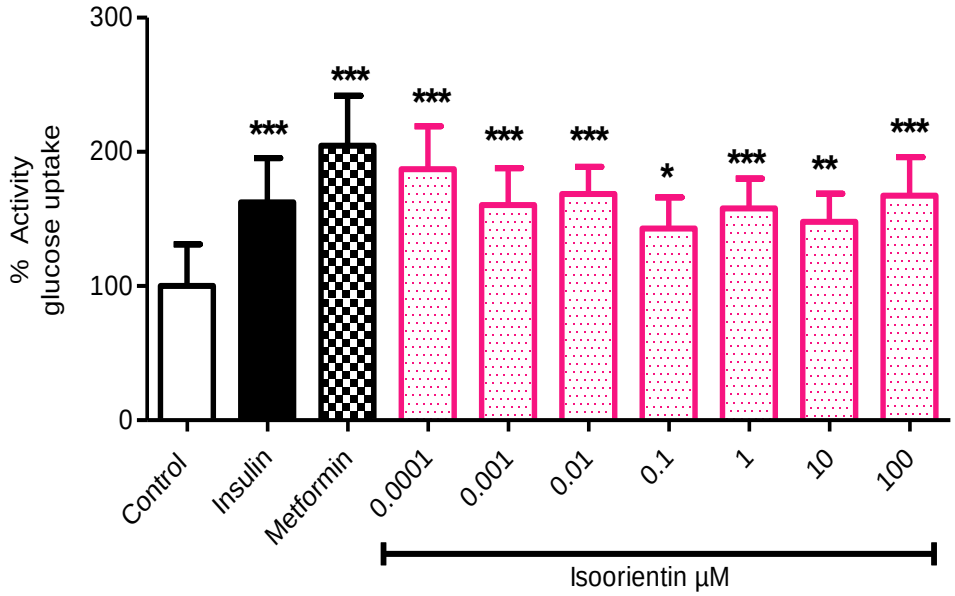

C

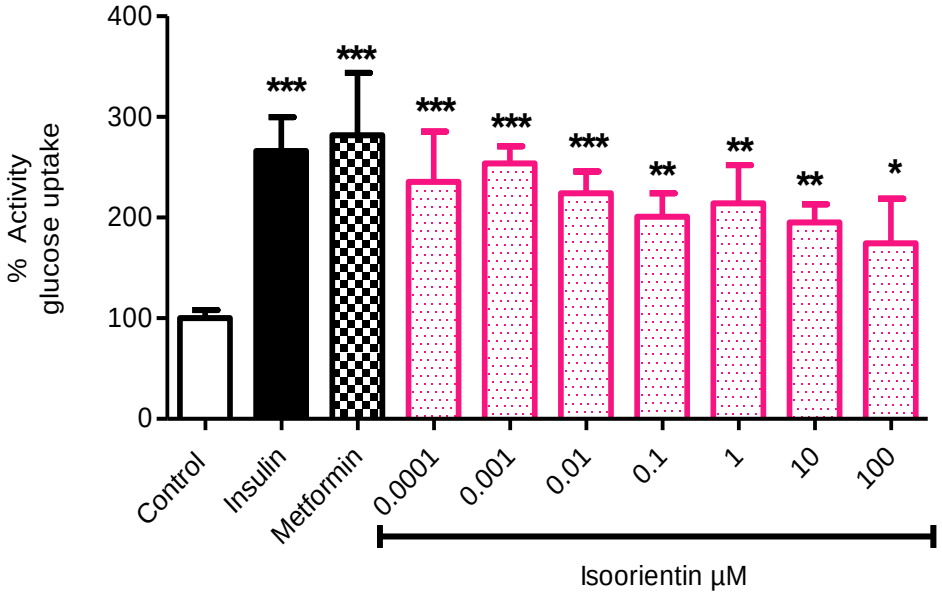

Figure 6.5 .The effect isoorientin on glucose uptake in C2C12 muscle cells (A), 3T3-L1 adipocytes (B) and C3A liver cells (C). Cells were cultured in 8 mM glucose in DMEM without phenol red and pyruvate containing log dilutions of isoorientin for 1 h in C2C12 muscle and for 3 h in 3T3-L1 adipocytes and C3A liver cells, respectively. Glucose uptake was measured using a fluorometric assay. Results are expressed as the mean of three independent experiments expressed relative to control (8 mM glucose) at 100% ± SEM; *$p < 0.05$, **$p < 0.01$ and ***$p < 0.001$.

6.1.7. Effect of rutin on glucose uptake in C2C12 muscle, 3T3-L1 adipocytes and C3A liver cells

In C2C12 muscle cells treated with rutin showed an increase in glucose uptake within a relatively narrow concentration range of 10 to 100 µM (Fig. 6.6 A). In 3T3-L1 adipocytes and C3A liver cells rutin significantly increased glucose uptake across all the concentrations tested (Fig. 6.6 B and C).

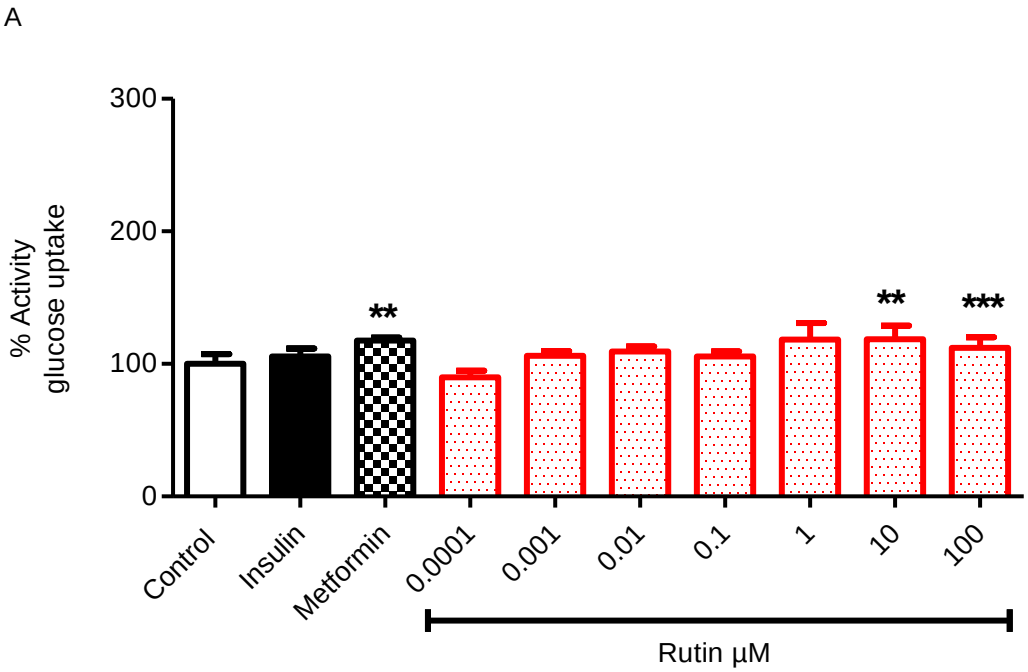

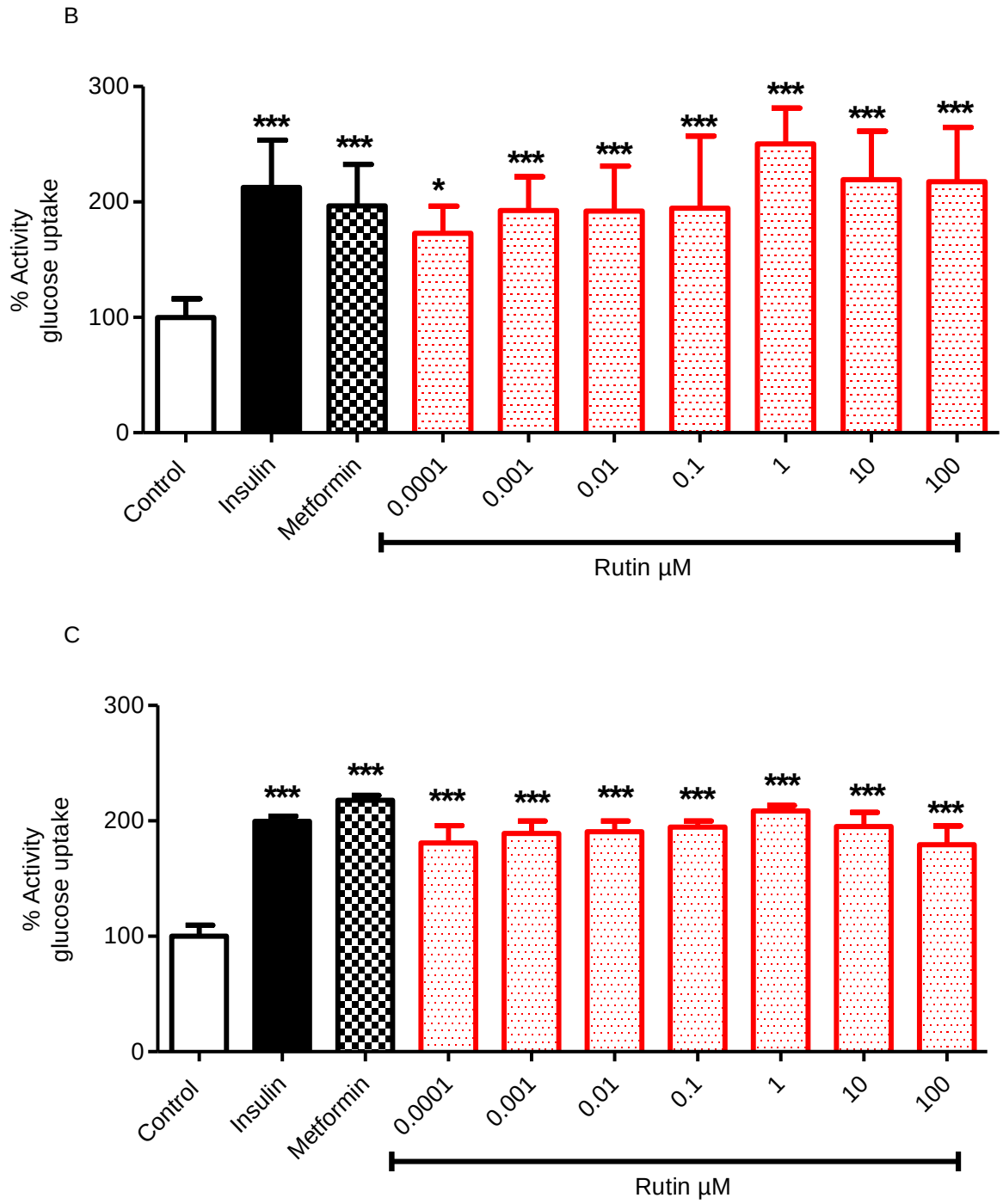

Figure 6.6. The effect of rutin on glucose uptake in C2C12 muscle cells (A), 3T3-L1 adipocytes (B) and C3A liver cells. Cells were cultured in 8 mM glucose in DMEM without phenol red and pyruvate containing log dilutions of rutin for 1 h in C2C12 muscle and for 3 h in 3T3-L1 adipocytes and C3A liver cells, respectively. Glucose uptake was measured using a fluorometric assay. Results are expressed as the mean of three independent experiments expressed relative to control (8 mM) at 100% ± SEM; *$p < 0.05$, **$p < 0.01$ and ***$p < 0.001$.

6.2 Glucose metabolism and insulin resistance in muscle cells

The results below describes the induction of insulin resistance in C2C12 muscle cells, by palmitate (16:0), a SFA. The results further cover the effects of the extracts and phenolic compounds using singular concentrations (10 µg/mL for FRE and GRE and 10 µM for aspalathin, orientin, isoorientin and rutin) on glucose metabolism. The aspalathin-enriched green rooibos extract (GRE) at 10 µg/mL and aspalathin at a concentration of 10 µM, were chosen to assess their effects on the glucose and lipid molecular mechanisms in insulin resistant cells.

6.2.1 Palmitate-induced insulin resistance in C2C12 muscle

Insulin resistance was confirmed by the lower insulin-stimulated glucose uptake (34.7 ± 2.8%; $p < 0.001$) in the palmitate-treated C2C12 muscle cells compared to the normal control C2C12 cells. In the normal control cells insulin (1 µM) and metformin (1 µM), used as controls, increased glucose uptake (129.6 ± 3.4%; $p < 0.001$ and 116.0 ± 2.4%; $p < 0.001$, respectively), however, insulin and metformin failed to increase glucose uptake by the palmitate-treated C2C12 muscle cells (Fig. 6.7).

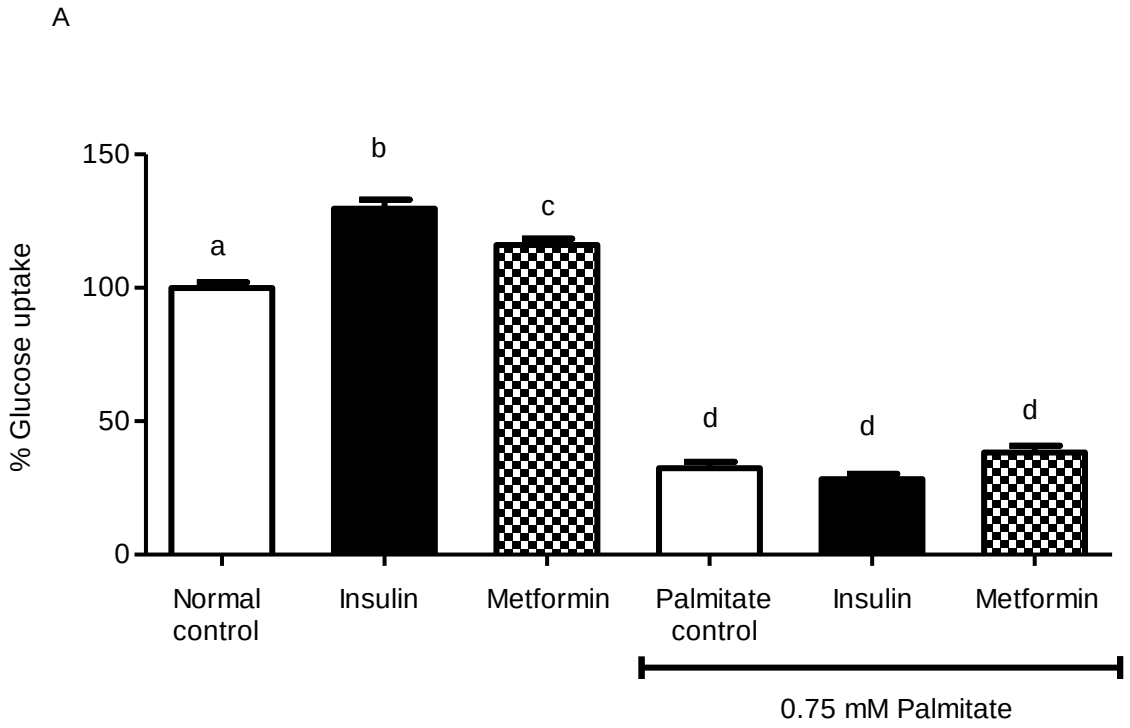

Figure 6.7. Effect of palmitate on glucose uptake. C2C12 muscle cells, cultured in 8 mM glucose with or without 0.75 mM palmitate for 16 h, were treated with 1 µM insulin (15 min) or 1 µM metformin (3 h). Glucose uptake was measured using [^{3}H]-2-deoxy-D-glucose. Results are expressed as the mean of three independent experiments relative to the control set at 100% ± SEM. Bars with different letters denote statistical differences at $p \leq 0.05$.

.

6.2.2 Effect of rooibos extracts (FRE and GRE) on glucose uptake, mitochondrial dehydrogenase activity (MTT) and intracellular ATP content in insulin-resistant C2C12 muscle cells

The ability of rooibos extracts to protect or reverse palmitate-induced insulin resistance was assessed by adding FRE or GRE for 3 h to the media of palmitate-treated C2C12 muscle cells. Results showed that basal glucose uptake was increased by rooibos treatment from 34.7 ± 2.8% to 70.2 ± 7.1% ($p < 0.001$) and 93.4 ± 6.2% ($p < 0.001$) for FRE and GRE, respectively. Insulin-stimulated glucose uptake increased from 30.3 ± 2.5% to 66.2 ± 5.2% ($p < 0.001$) and 103.7 ± 9.0% ($p < 0.001$) for FRE and GRE, respectively. Compared to FRE, GRE was more effective at increasing both basal and insulin-stimulated glucose uptake. In addition, GRE normalised basal glucose uptake by palmitate-treated cells compared to the normal controls not exposed to palmitate (Fig. 6.8 A). Mitochondrial dehydrogenase activity was determined using the MTT assay and intracellular ATP was determined with a luminescence kit. Results obtained from the MTT assay showed that FRE increased mitochondrial activity in both basal and insulin-stimulated palmitate-treated C2C12 cells from 37.4 ± 1.0% to 131.7 ± 11.7% ($p < 0.001$) and 38.5 ± 1.7 to 134.4 ± 8.1 % ($p < 0.001$), respectively. Similar results were obtained for GRE (37.4 ± 1.0% to 98.9 ± 5.1%; ($p < 0.001$) and 38.5 ± 1.7 to 114.1 ± 3.9%; ($p < 0.001$) (Fig. 6.8 B). In terms of ATP content FRE treatment increased basal and insulin-stimulated ATP concentrations from 40.7 ± 0.8 to 140.4 ± 11.4% ($p < 0.001$) and from 34.1 ± 0.7 to 149.4 ± 13.35 ($p < 0.001$), respectively. GRE increased the basal and insulin-stimulated ATP from 40.7 ± 0.8 to 135.2 ± 17.0% ($p < 0.001$) and 34.1 ± 0.7 to 165.0 ± 11.6% ($p < 0.001$), respectively (Fig. 6.8 C).

A

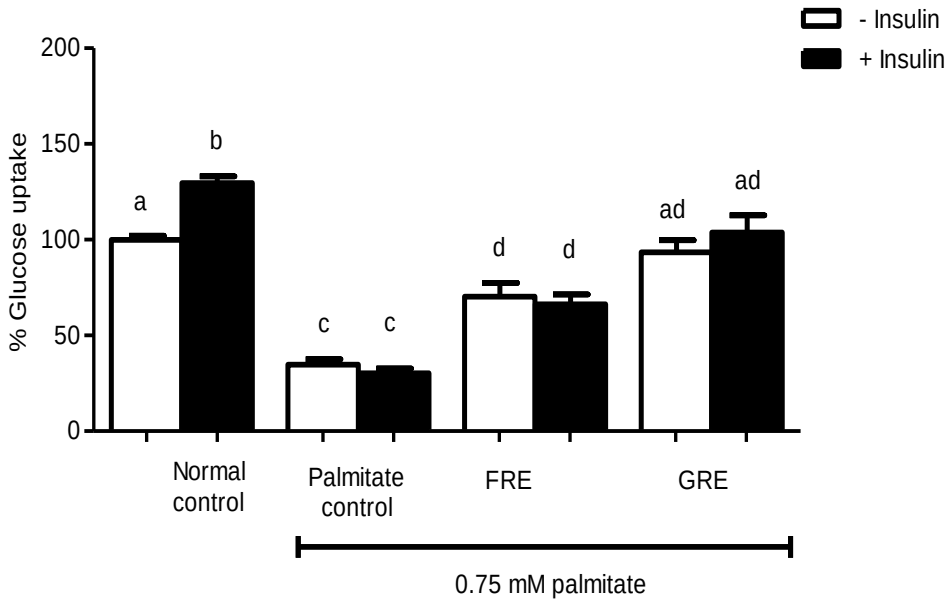
- Insulin
+ Insulin
% Glucose uptake
200
150
100
50
0
a
b
c
c
d
d
ad
ad
Normal control
Palmitate control
FRE
GRE
0.75 mM palmitate

B

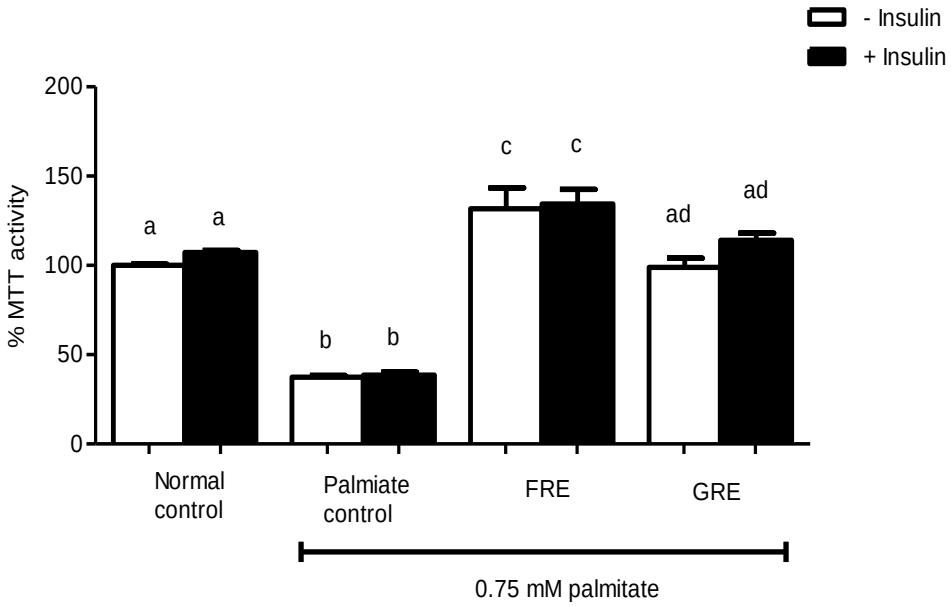
- Insulin
+ Insulin
% MTT activity
200
150
100
50
0
a
a
b
b
c
c
ad
ad
Normal control
Palmiate control
FRE
GRE
0.75 mM palmitate

C

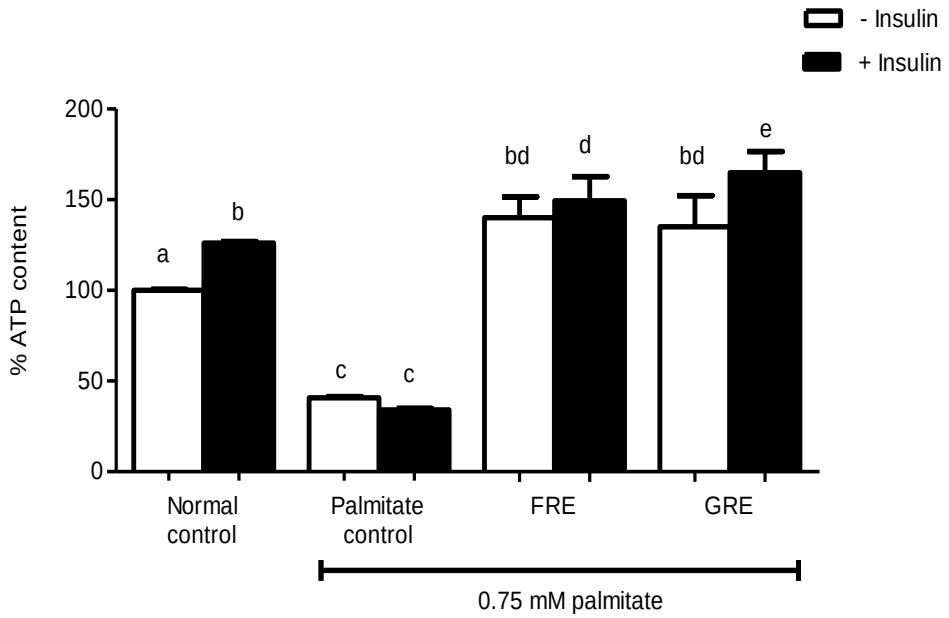

Figure 6.8. Effect of rooibos extracts (FRE and GRE) on glucose uptake (A), mitochondrial dehydrogenase activity (B) and intracellular ATP content (C). C2C12 muscle cells, cultured in 8 mM glucose with or without 0.75 mM palmitate for 16 h, were treated with FRE or GRE (10 µg/mL) for 3 h. Insulin (1 µM) was used for insulin-stimulated glucose uptake. Glucose uptake was measured using [^{3}H]-2-deoxy-D-glucose method, mitochondrial dehydrogenase activity was measured using the MTT assay and intracellular ATP was measured using the ATP luminescence kit. Results are expressed as the mean of three independent experiments relative to the respective normal control at 100% ± SEM. Bars with different letters denote statistical differences at $p \leq 0.05$.

6.2.3. Effect of phenolic compounds on glucose uptake mitochondrial dehydrogenase activity (MTT) intracellular ATP content in insulin-resistant C2C12 muscle cells

The effect of four major flavonoids present in rooibos (aspalathin (ASP), orientin (ORE), isoorientin (ISO) and rutin (RUT)) on palmitate-induced insulin resistance was assessed. Results demonstrated that aspalathin, orientin, isoorientin and rutin increased basal glucose uptake from 34.7 ± 2.8% for the palmitate-treated control to 96.5 ± 19.2%, 95.3 ± 10.4% and 106.9 ± 17.3% and 82.9 ± 6.3% ($p < 0.001$), respectively. Insulin-stimulated glucose uptake was increased by orientin, isoorientin and rutin from 30.3 ± 2.5% for the palmitate-treated control to 95.9 ±10.4% ,102.7 ± 15.2% and 77.5 ± 5.1%, ($p < 0.001$) respectively. Although there were no significant differences between the individual compounds, orientin and isoorientin appeared to have the greatest effect on insulin-stimulated glucose uptake (Fig .6.9 A).

The effect of aspalathin, orientin, isoorientin and rutin on mitochondrial activity and cellular ATP was assessed in insulin-resistant C2C12 muscle cells. Results showed that aspalathin, orientin, isoorientin and rutin increased basal mitochondrial activity from 37.4 ± 1.0% to 118.1 ± 4.1%, 145.8 ± 14.9%,144 ± 7.9% and 115.9 ± 9.2% ($p < 0.001$) and by insulin-stimulation from 38.5 ± 1.7% to 113.7 ± 3.7%, 156.9 ± 12.3, 153.2 ± 12.9% and 97.99 ± 9.2%, ($p < 0.001$) respectively (Fig. 6.9 B). Of these phenolic compounds, orientin and isoorientin appeared to be most effective at increasing the MTT activity. In terms of ATP content results showed that aspalathin, orientin, isoorientin and rutin increased basal energy production in C2C12 muscle cells from 40.7 ± 0.7% to 100.5 ± 7.3%, 100.6 ± 12.9%, 85.3 ± 1.6% and 159.3 ± 7.8% ($p < 0.001$) and insulin-stimulated ATP content from 34.1 ± 0.7% to 106.5 ± 11.2%, 93.9 ± 7.7%, 89.9 ± 4.9% and 115.9 ± 7.8% ($p < 0.001$), respectively (Fig. 6.9 C). Interestingly it appeared that rutin had the greatest effect on ATP content.

A

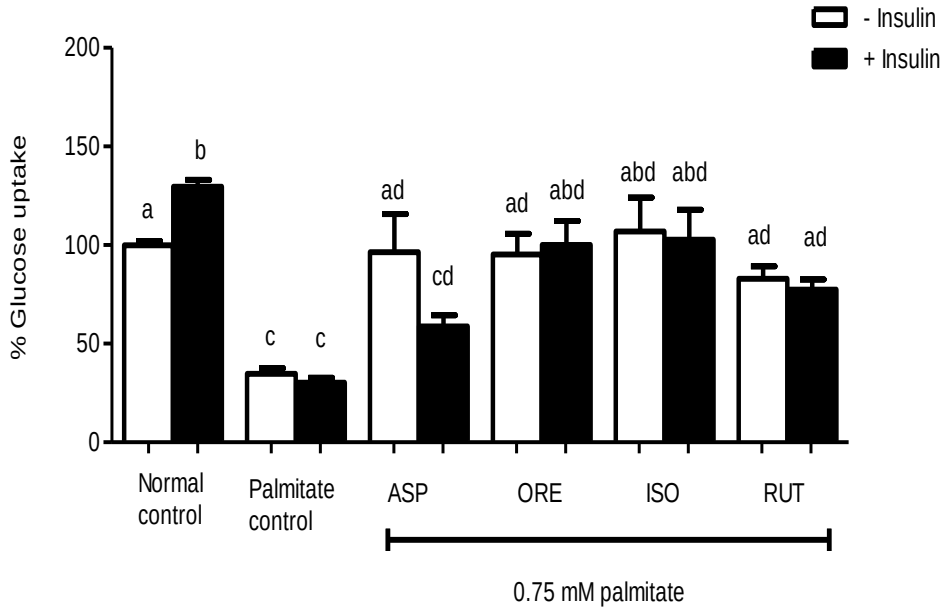
- Insulin
+ Insulin
% Glucose uptake
200
150
100
50
0
a
b
c
c
ad
cd
ad
abd
abd
abd
ad
ad
Normal control
Palmitate control
ASP
ORE
ISO
RUT
0.75 mM palmitate

B

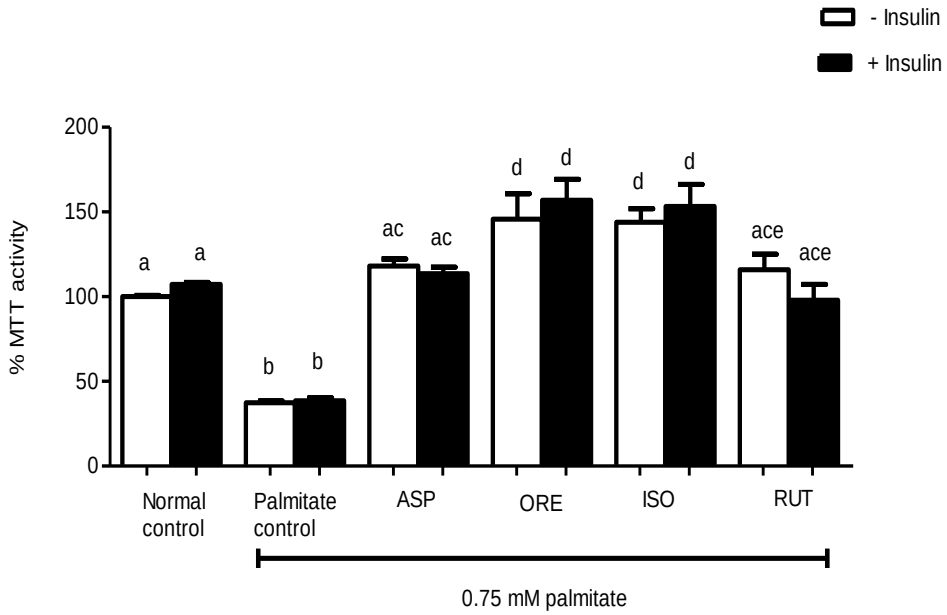
- Insulin
+ Insulin
% MTT activity
200
150
100
50
0
a
a
b
b
ac
ac
d
d
d
d
ace
ace
Normal control
Palmitate control
ASP
ORE
ISO
RUT
0.75 mM palmitate

C

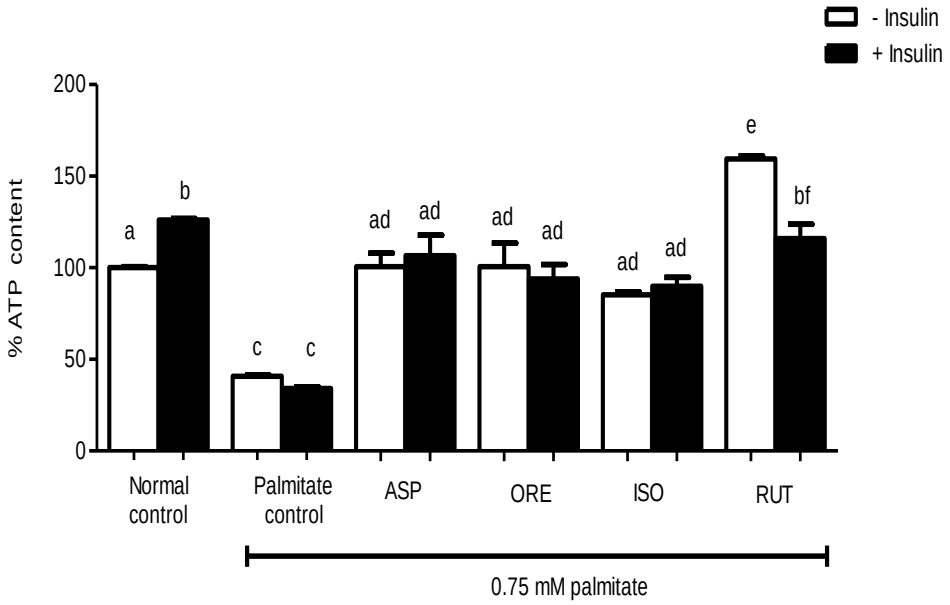

Figure 6.9. Effect of aspalathin (ASP), orientin (ORE), isoorientin (ISO) and rutin (RUT) on glucose uptake (A) mitochondrial dehydrogenase activity (B) and ATP content (C). C2C12 muscle cells, cultured in DMEM with 8 mM glucose with or without 0.75 mM palmitate for 16 h, were treated with aspalathin, orientin, isoorientin or rutin (10 µM) for 3 h. Glucose uptake was measured using [^{3}H]-2-deoxy-D-glucose method. Mitochondrial dehydrogenase activity was measured using the MTT assay and ATP content determined using a luminescence kit. Results are expressed as the mean of three independent experiments relative to control cells (100%) ± SEM. Bars with different letters denote statistical differences at $p \leq 0.05$.

6.2.4. Aspalathin-enriched green rooibos extract (GRE) and aspalathin down-regulated PKCθ activation in palmitate-treated C2C12 muscle cells

Western blot analyses showed that palmitate increased basal PKCθ activation from 100.0 ± 9.2% to 265.9 ± 25.7% ($p < 0.001$) and from 43.2 ± 4.7% to 321.2 ± 15.2% ($p < 0.001$) following insulin stimulation, respectively. GRE and aspalathin reduced the pPKC θ / tPKCθ ratio in basal and insulin-stimulated palmitate-treated C2C12 muscle cells. Basal pPKCθ ratio levels were reduced from 265.9 ± 25.7% to 153.7 ± 31.3% ($p < 0.01$) and 103.9 ± 11.0% ($p < 0.001$); and insulin-stimulated levels were reduced from 321.2 ± 15.1% to 93.3 ± 23.2% ($p < 0.001$) and 135.8 ± 9.1% ($p < 0.001$) for GRE and aspalathin treatments, respectively (Fig. 6.10).

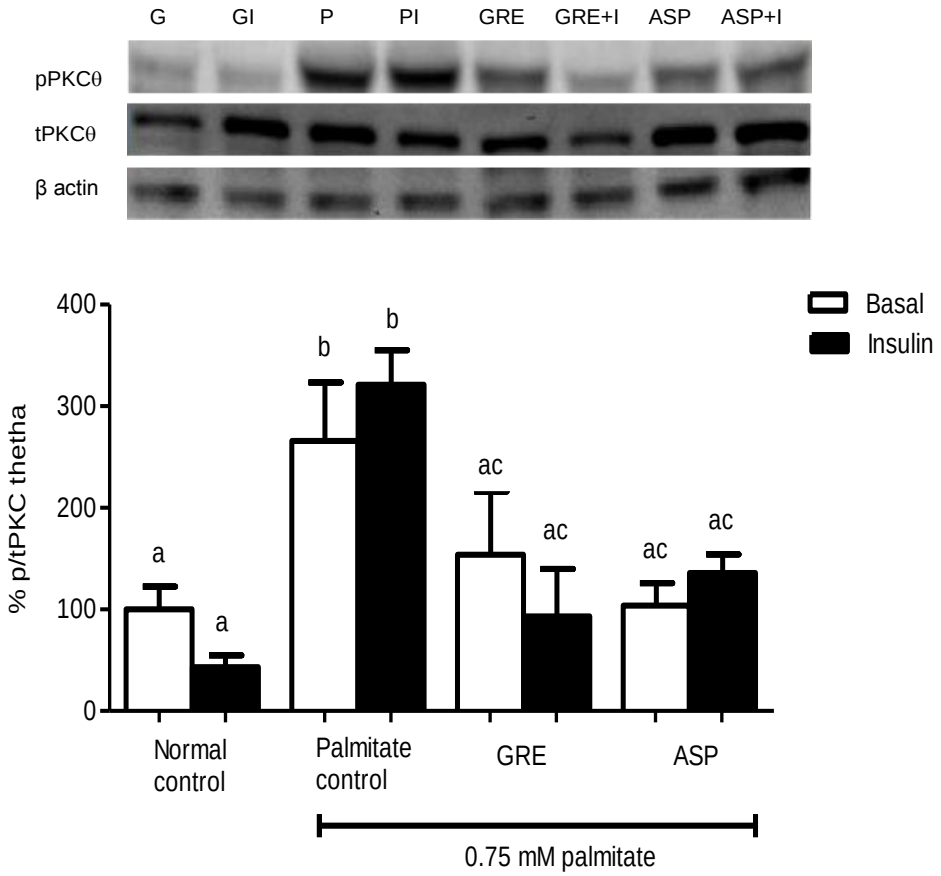

Figure 6.10. Effect of green rooibos extract (GRE) and aspalathin (ASP) on PKCθ activation. C2C12 muscle cells, cultured in DMEM with 8 mM glucose with or without 0.75 mM palmitate for 16 h, were treated with GRE (10 µg/mL) or aspalathin (10 µM) for 3 h. Insulin (1 µM) was used for insulin stimulation. Cells were lysed and subjected to Western blot analyses. The % of pPKCθ/tPKCθ was used to estimate the level of PKCθ activation. Results are expressed as the mean of three independent experiments relative to control at 100% ± SEM. Bars with different letters denote statistical differences at $p \leq 0.05$.

6.2.5 Effect of aspalathin-enriched green rooibos extract (GRE) and aspalathin on insulin receptor (INSR) protein expression

GRE and aspalathin increased basal INSR protein expression from 70.2 ± 3.0% to 159.0 ± 6.3% and 123.1 ± 6.2% ($p < 0.001$) and the insulin-stimulated INSR expression from 70.2 ± 3.0% to 165.4 ± 5.5% ($p < 0.001$) and 132.1 ± 1.5% ($p < 0.01$), compared to palmitate-treated controls, respectively (Fig. 6.11).

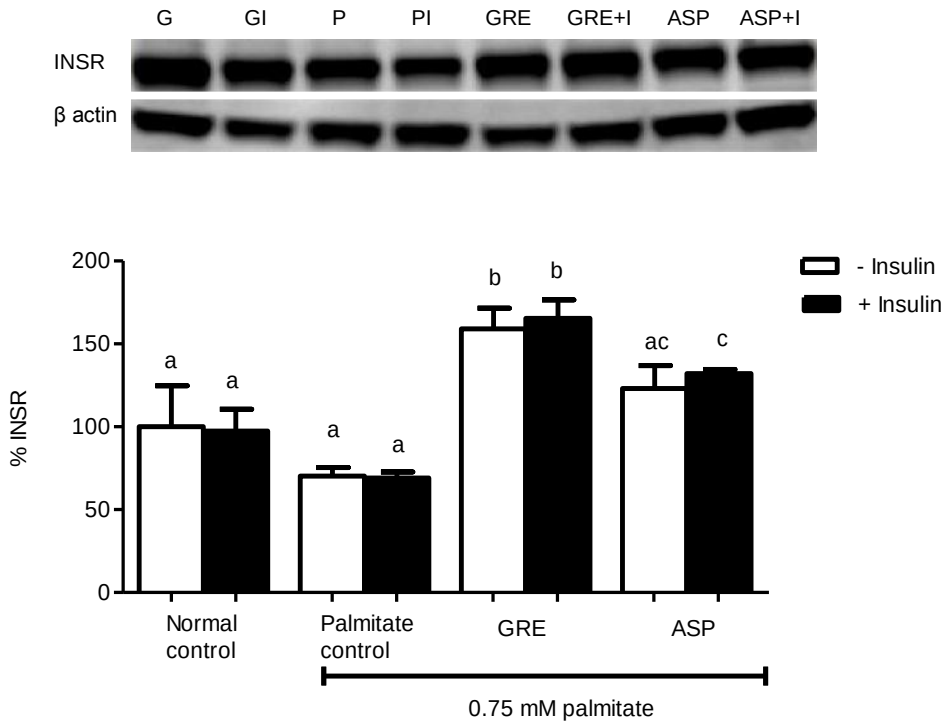

Figure 6.11. Effect of green rooibos extract (GRE) and aspalathin (ASP) on INSR protein expression. C2C12 muscle cells, cultured in DMEM with 8 mM glucose with or without 0.75 mM palmitate for 16 h, were treated with GRE (10 µg/mL) or aspalathin (10 µM) for 3 h. Insulin (1 µM) was used for insulin stimulation. Cells were lysed and subjected to Western blot analyses. Results are expressed as the mean of three independent experiments relative to control at 100% ± SEM. Bars with different letters denote statistical differences at $p \leq 0.05$.

6.2.6 Effect of aspalathin-enriched green rooibos (GRE) and aspalathin on IRS1 (Ser 307)

Enzyme-linked immunosorbent assay (ELISA) was used to determine the protein expression of IRS1 (Ser 307). The results showed that palmitate treatment of C2C12 muscle cells increased the protein expression of IRS1 (Ser 307) (76.2 ± 5.5% to 223.8 ± 40.1% ($p < 0.05$)). This occurs both with and without insulin stimulation and the effects can be attenuated by addition of aspalathin or neutralised by GRE (223.8 ± 40.1% to 111.1 ± 22.9% ($p < 0.01$)) (Fig. 6.12).

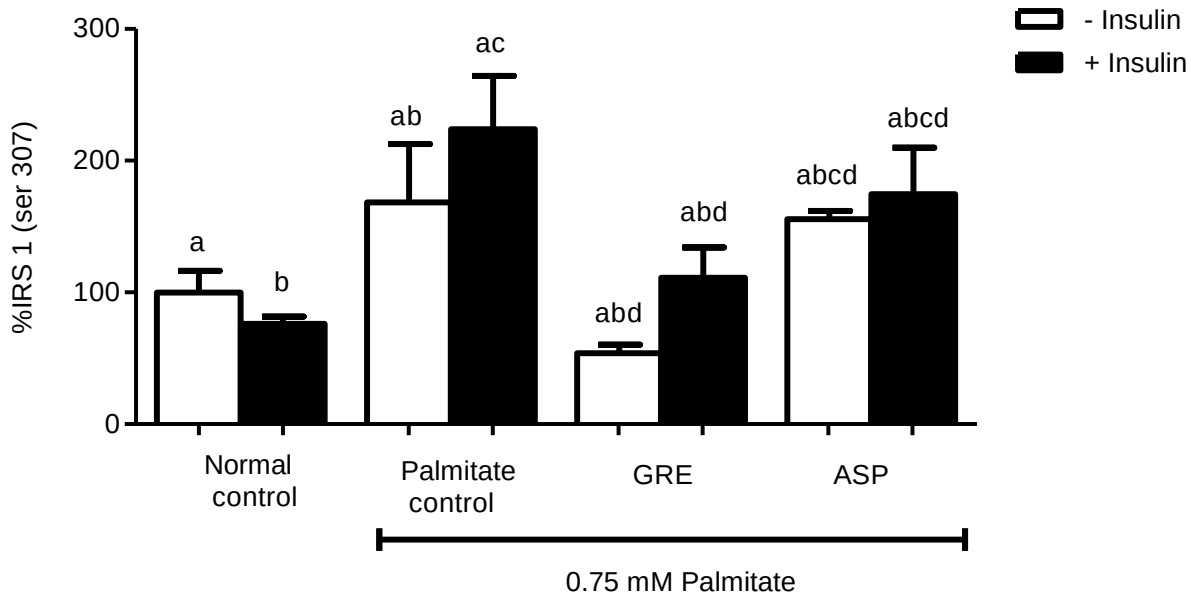

Figure 6.12. Effect of green rooibos extract (GRE) and aspalathin (ASP) on IRS1 (Ser 307) protein expression. C2C12 muscle cells, cultured in DMEM with 8 mM glucose with or without 0.75 mM palmitate for 16 h, were treated with GRE (10 µg/mL) or aspalathin (10 µM) for 3 h. Insulin (1 µM) was used for insulin stimulation. Cells were lysed and subjected to ELISA. Results are expressed as the mean of three independent experiments relative to control at 100% ± SEM. Bars with different letters denote statistical differences at $p \leq 0.05$.

6.2.7. Aspalathin-enriched green rooibos extract (GRE) and aspalathin increased protein expression of pPI3K (p85) in palmitate-induced insulin-resistant C2C12 muscle cells

Treatment with GRE and aspalathin significantly increased phosphorylation of insulin-stimulated PI3K (p85) in palmitate-treated C2C12 muscle cells from 88.8 ± 4.8% to 144.2 ± 5.7% ($p < 0.001$) and 158.5 ± 10.9% ($p < 0.001$), respectively. The basal pPI3K (p85) levels were also increased by GRE and aspalathin to above that of the normal controls, however, the increase was not significant for GRE (Fig. 6.13).

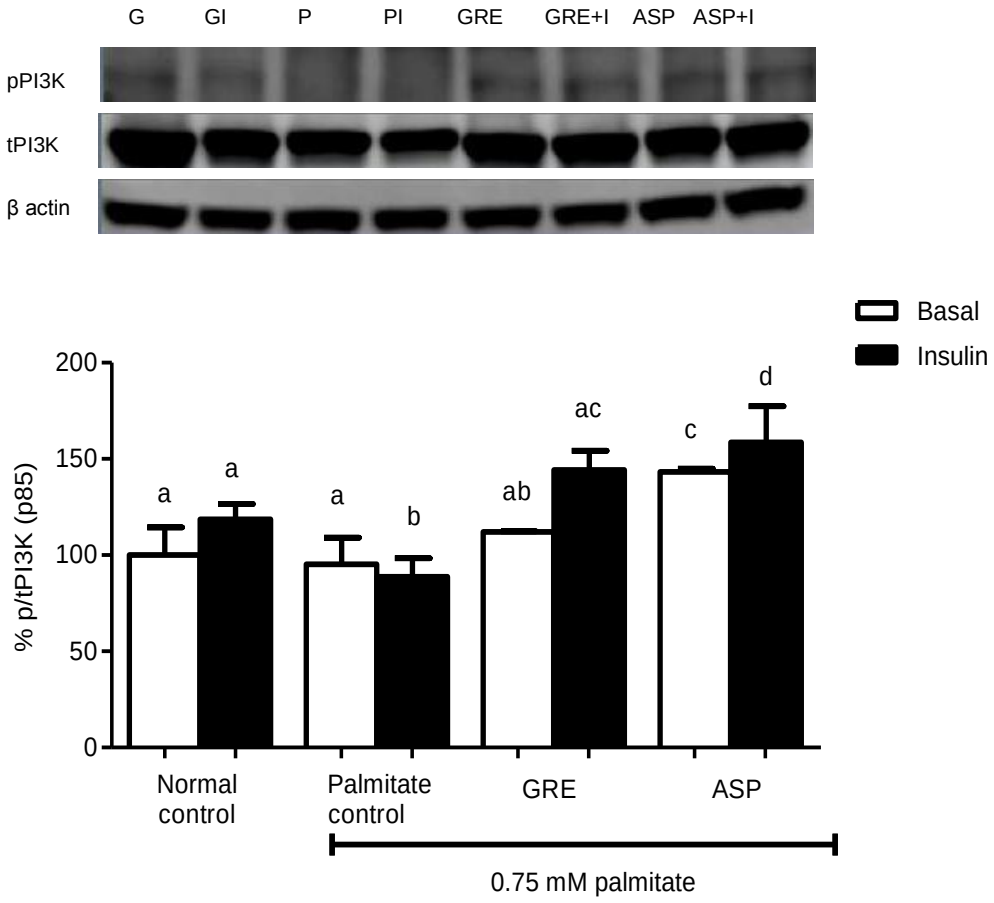

Figure 6.13. Effect of green rooibos extract (GRE) and aspalathin (ASP) on PI3K(p85) activation. C2C12 muscle cells, cultured in DMEM with 8 mM glucose with or without 0.75 mM palmitate for 16 h, were treated with GRE (10 µg/mL) or aspalathin (10 µM) for 3 h. Insulin (1 µM) was used for insulin stimulation. Cells were lysed and subjected to Western blot analyses. The % of pPI3K /tPI3K was used to estimate the levels of PI3K p85) activation. Results are expressed as the mean of three independent experiments relative to control at 100% ± SEM. Bars with different letters denote statistical differences at $p \leq 0.05$.

6.2.8. Effect of aspalathin-enriched green rooibos extract (GRE) and aspalathin on pAKT (Ser 473) protein expression in insulin-resistant C2C12 muscle cells

Insulin stimulation increased AKT (Ser 473) activation from 100.0 ± 27.7% to 4215.0 ± 213.2% ($p < 0.001$). Culturing with palmitate significantly reduced this increased from 4215 ± 213.2% to 1438.0 ± 342.7% ($p < 0.001$). In palmitate-treated C2C12 muscle cells, GRE and aspalathin increased AKT (Ser 473) phosphorylation in the presence of insulin from 1438.0 ± 342.7% to 3722.0 ± 468.5%; ($p < 0.001$) and 2911.0 ± 224.9%; ($p < 0.001$), respectively. GRE and aspalathin had no effect on basal (non-insulin-stimulated) AKT (Ser 473) phosphorylation (Fig. 6.14).

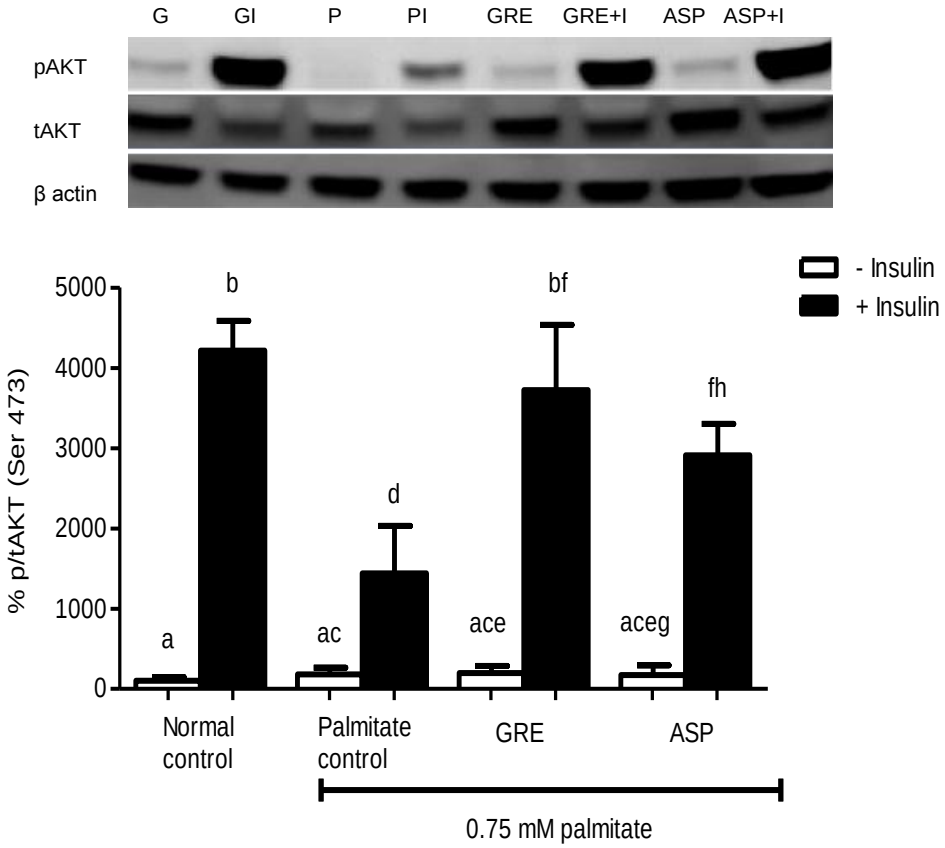

Figure 6.14 Effect of green rooibos extract (GRE) and aspalathin (ASP) on AKT (Ser 473) activation. C2C12 muscle cells, cultured in DMEM with 8 mM glucose with or without 0.75 mM palmitate for 16 h, were treated with GRE (10 µg/mL) or ASP (10 µM) for 3 h. Insulin (1 µM) was used for insulin stimulation. Cells were lysed and subjected to Western blot analyses. The % of pAKT/tAKT was used to estimate the level of AKT (Ser 473) activation. Results are expressed as the mean of three independent experiments relative to control at 100% ± SEM. Bars with different letters denote statistical differences at $p \leq 0.05$.

6.2.9. Effect of aspalathin-enriched green rooibos extract (GRE) and aspalathin on pAMPK in palmitate-induced insulin-resistant C2C12 muscle cells

Treatment with GRE had no effect on AMPK activation. Aspalathin increased the percentage of phosphorylated basal AMPK in palmitate-treated C2C12 muscle cells from 145.6 ± 52.2% to 368.0 ± 49.1% ($p < 0.05$) (Fig. 6.15).

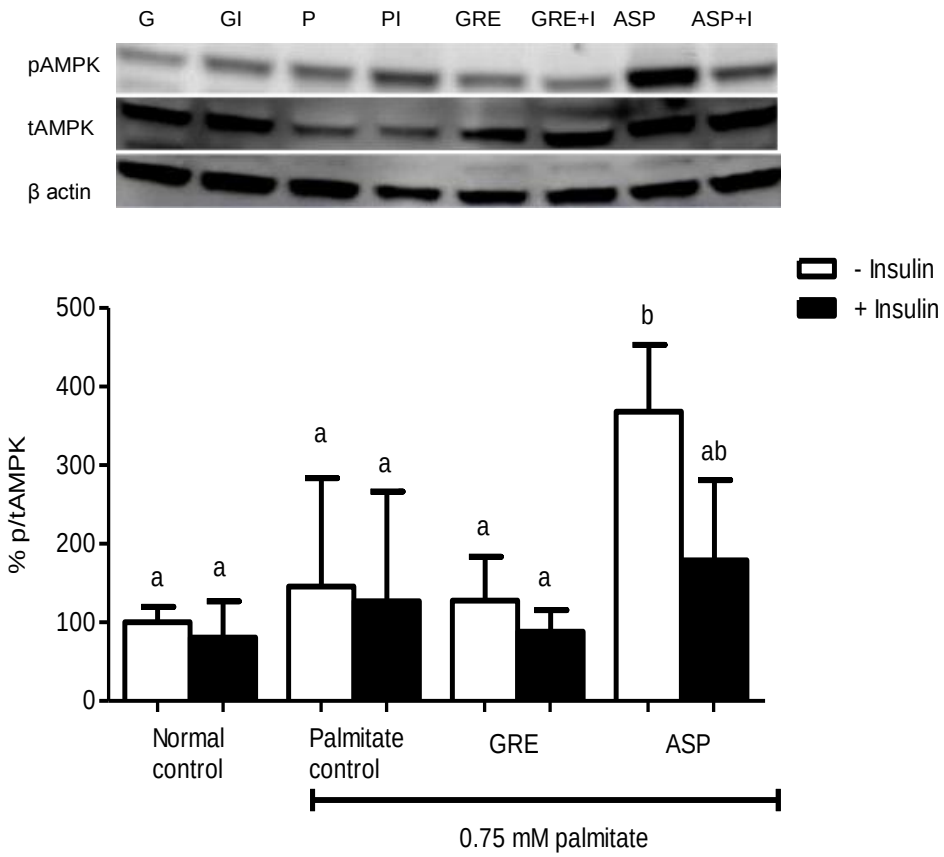

Figure 6.15. Effect of green rooibos extract (GRE) and aspalathin (ASP) on AMPK activation. C2C12 muscle cells, cultured in DMEM with 8 mM glucose with or without 0.75 mM palmitate for 16 h, were treated with GRE (10 µg/mL) or aspalathin (10 µM) for 3 h. Insulin (1 µM) was used for insulin stimulation. Cells were lysed and subjected to Western blot analyses. The % of pAMPK/tAMPK was used to estimate the level of AMPK activation Results are expressed as the mean of three independent experiments relative to control at 100% ± SEM. Bars with different letters denote statistical differences at $p \leq 0.05$.

6.2.10. Effect of aspalathin-enriched green rooibos extract (GRE) and aspalathin on GLUT4 protein expression

GRE and aspalathin increased insulin-stimulated GLUT4 protein expression compared to palmitate-treated controls from 66.9 ± 18.4% to 196.1 ± 14.9% ($p < 0.001$) and 183.1 ± 22.5% ($p < 0.01$), respectively. The GRE extract increased basal GLUT4 expression from 100.0 ± 8.9% to 227.2 ± 11.4% ($p < 0.001$) (Fig. 6.16).

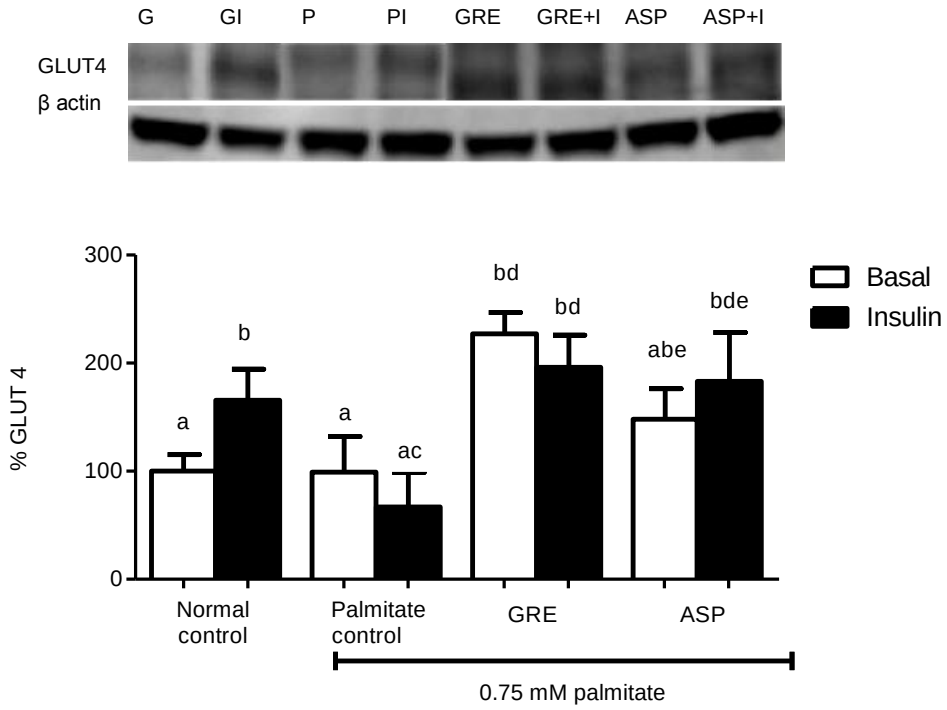

Figure 6.16. Effect of green rooibos extract (GRE) and aspalathin (ASP) on GLUT4 protein expression. C2C12 muscle cells, cultured in DMEM with 8 mM glucose with or without 0.75 mM palmitate for 16 h, were treated with GRE (10 µg/mL) or aspalathin (10 µM) for 3 h. Insulin (1 µM) was used for insulin stimulation. Cells were lysed and subjected to Western blot analyses. Results are expressed as the mean of three independent experiments relative to control AT 100% ± SEM. Bars with different letters denote statistical differences at $p \leq 0.05$.

6.3. Glucose metabolism and insulin resistance in 3T3-L1 adipocytes

The following results describe the induction of insulin resistance in differentiated adipocytes using palmitate. The effects of fermented rooibos (FRE) and aspalathin-enriched green rooibos (GRE) at a concentration of 10 µg/mL and aspalathin, orientin, isoorientin and rutin at a concentration of 10 µM in insulin-resistant 3T3-L1 adipocytes will be further demonstrated. Insulin (1 µM) was used for insulin stimulation. GRE (10 µg/mL) and aspalathin at a concentration of 10 µM, were chosen to assess their effects on the glucose and lipid molecular mechanisms in insulin-resistant 3T3-L1 adipocyte.

6.3.1. Palmitate reduces insulin sensitivity in 3T3-L1 adipocytes

The effect of palmitate on 3T3-L1 adipocyte insulin sensitivity was assessed using a glucose uptake assay. In the normal control cells insulin (1 µM) and metformin (1 µM) were used as controls. Both insulin and metformin increased glucose uptake from 100.0 ± 3.1% to 189.4 ± 10.9% ($p < 0.001$) and 130.6 ± 14.9% ($p < 0.001$), respectively compared to the normal control. Results showed that palmitate reduced insulin activity in 3T3-L1 adipocytes from 100.0 ± 3.1% to 69.9 ± 1.8% ($p < 0.05$). In palmitate-treated cells insulin increased glucose uptake compared to the palmitate control. Metformin, however had no effect on glucose uptake in palmitate-treated 3T3-L1 adipocytes (Fig. 6.17).

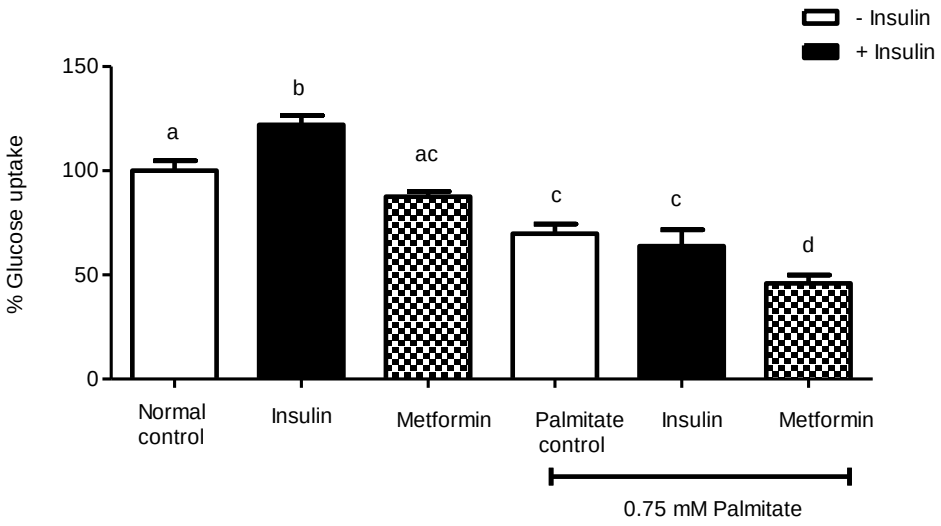

Figure 6.17. Effect of palmitate on glucose uptake in 3T3-L1 adipocytes. 3T3-L1 adipocytes were cultured in DMEM with 8 mM glucose with or without 0.75 mM palmitate for 16 h, then treated with 1 µM insulin (15 min) or 1 µM metformin (3 h). Glucose uptake was measured using [^{3}H]-2-deoxy-D-glucose. Results are expressed as the mean of three independent experiments relative to the control set at 100% ± SEM. Bars with different letters denote statistical differences at $p \leq 0.05$.

6.3.2. Fermented rooibos extract (FRE) and aspalathin-enriched green rooibos extract (GRE) increased glucose uptake, MTT activity and ATP content in insulin-resistant 3T3-L1 adipocytes

Rooibos extracts (FRE and GRE) ameliorated palmitate-induced insulin resistance in 3T3-L1 adipocytes. This was evaluated by culturing insulin-resistant 3T3-L1 adipocytes with FRE or GRE in the media that contained 0.75 mM palmitate for 3 h. Results showed that basal glucose uptake was significantly increased by GRE from 69.9 ± 1.8% to 128.5 ± 3.6% ($p < 0.001$). Insulin-stimulated glucose uptake increased from 126.3 ± 6.8% to 175.0 ± 6.1% ($p < 0.001$) and 177.3 ± 5.7% ($p < 0.001$) for FRE and GRE, compared to palmitate control (Fig. 6.18 A). Palmitate treatment of 3T3-L1 adipocytes reduced basal 100.0 ± 2.2% to 67.2 ± 2.8% ($p < 0.001$) and insulin-stimulated mitochondrial dehydrogenase activity from 102.2 ± 2.6% to 72.8 ± 3.7% ($p < 0.001$) respectively. Culturing 3T3-L1 adipocytes with FRE and GRE increased basal mitochondrial dehydrogenase activity that was suppressed palmitate from 67.2 ± 2.8% to 106.7 ± 2.9% and 106.9 ± 2.5% ($p< 0.001$), and for insulin-stimulated activity from 72.8 ± 3.7% to 103.9 ± 3.9% and 108.3 ± 2.8% ($p < 0.001$), respectively (Fig. 6.18 B). Intracellular ATP content was reduced by palmitate from 100.0 ± 2.7% to 77.1 ± 3.5% ($p < 0.001$) in basal and from 109.2 ± 3.3% to 80.9 ± 3.9% ($p < 0.05$) in insulin-stimulated 3T3-L1 adipocytes, respectively. Addition of FRE to palmitate-treated cells increased basal and insulin-stimulated ATP content from 77.1 ± 3.5 to 104.6 ± 4.6% ($p < 0.001$) and from 80.9 ± 3.9% to 114.8 ± 4.5%, ($p < 0.001$),respectively. Similarly GRE increased the basal and insulin-stimulated ATP content from 77.1 ± 3.5 to 112.1 ± 5.8% ($p < 0.001$) and 80.9 ± 3.9 to 126.4 ± 5.8% ($p < 0.001$), respectively (Fig. 6.18 C).

A

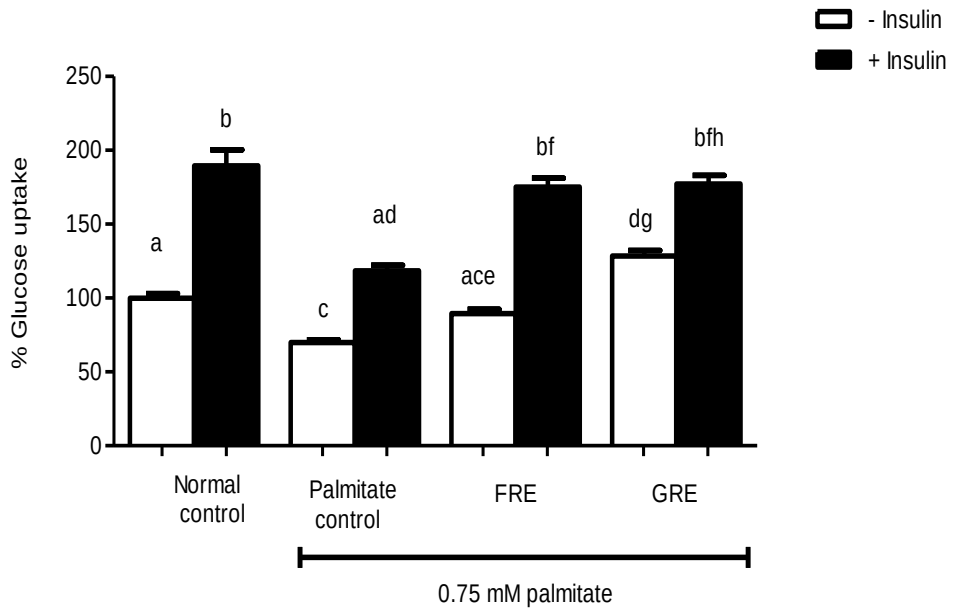
- Insulin
+ Insulin
% Glucose uptake
250
200
150
100
50
0
a
b
c
ad
ace
bf
dg
bfh
Normal control
Palmitate control
FRE
GRE
0.75 mM palmitate

B

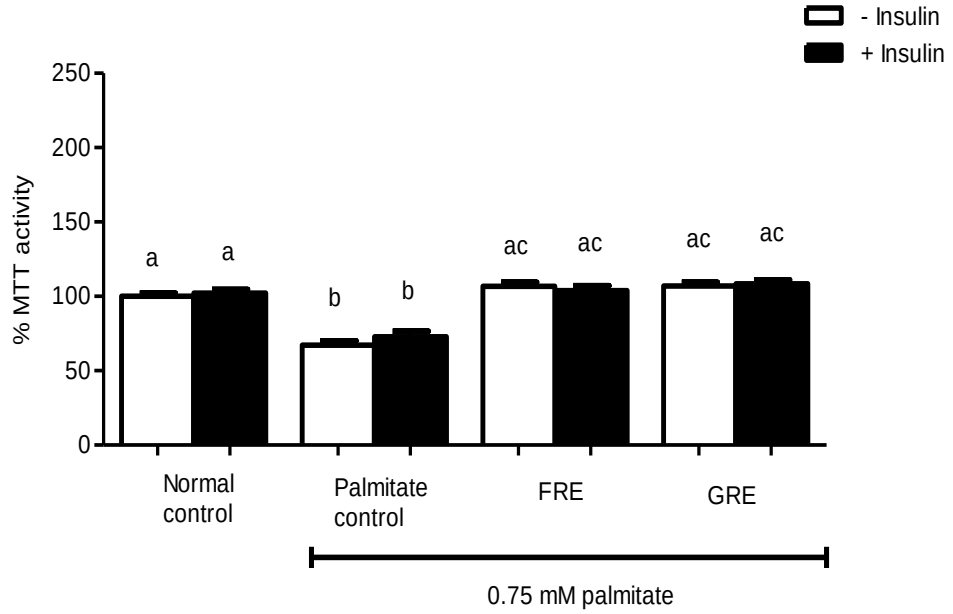
- Insulin
+ Insulin
% MTT activity
250
200
150
100
50
0
a
a
b
b
ac
ac
ac
ac
Normal control
Palmitate control
FRE
GRE
0.75 mM palmitate

C

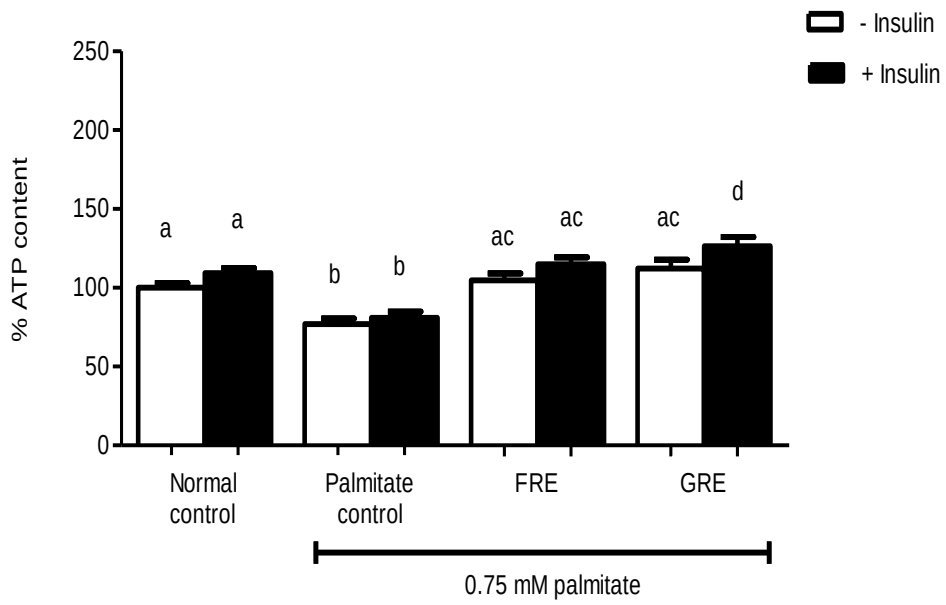

Figure 6.18. Effect of rooibos extracts (GRE and FRE) on glucose uptake (A), mitochondrial dehydrogenase activity (B) and intracellular ATP content (C). 3T3-L1 adipocytes, cultured in DMEM with 8 mM glucose with or without 0.75 mM palmitate for 16 h, were treated with FRE or GRE (10 µg/mL) for 3 h. Insulin (1 µM) was used to assess insulin-stimulated glucose uptake. Glucose uptake was measured using [^{3}H]-2-deoxy-D-glucose method, mitochondrial dehydrogenase activity was measured using the MTT assay and intracellular ATP content was measured using the ATP luminescence kit. Results are expressed as the mean of three independent experiments relative to the control at 100% ± SEM. Bars with different letters denote statistical differences at $p \leq 0.05$.

6.3.3 Effect of aspalathin, orientin, isoorientin and rutin on glucose metabolism in palmitate-induced insulin-resistant 3T3-L1 adipocytes

To evaluate the effect of rooibos flavonoids on palmitate-induced insulin resistance, aspalathin, orientin, isoorientin and rutin were added to the media of palmitate-treated 3T3-L1 adipocytes for 3 h. Results showed that rutin increased basal glucose uptake from 69.9 ± 1.8% to 176.8 ± 9.3% ($p < 0.001$) compared to the palmitate control. Insulin-stimulated glucose uptake was increased by all the compounds tested from 125.3 ± 7.7% to 163.1 ± 6.1% ($p < 0.01$), 164.8 ± 3.6% ($p < 0.001$), 158.6 ± 7.4% ($p < 0.05$) and 171.9 ± 7.5% ($p < 0.001$) for aspalathin, orientin, isoorientin and rutin, respectively (Fig. 6.19 A).

Addition of palmitate in 3T3-L1 adipocytes reduced basal mitochondrial dehydrogenase activity from 100.0 ± 2.2% to 67.2 ± 2.8% ($p < 0.001$) and from 102.2 ± 2.6% to 72.8 ± 3.7% ($p < 0.001$) for the insulin-stimulated cells. Futhermore, results showed that 3T3-L1 adipocytes treated with aspalathin, orientin, isoorientin or rutin increased basal mitochondrial activity from 67.2 ± 2.8% to 115.5 ± 5.1%, 102.8 ± 3.6%, 108.2 ± 3.5% and 101.8 ± 3.3% ($p < 0.001$), respectively. In the insulin-stimulated cells MTT activity was increased from 72.8 ± 3.7% to 104.6 ± 4.2%, 103.5 ± 2.2, 108.0 ± 5.6% and 102.0 ± 3.03% ($p < 0.001$) for the respective compounds compared to the palmitate-treated control (Fig. 6.19 B). In terms of intracellular ATP content, results showed that palmitate reduced basal ATP content from 100.0 ± 2.7% to 77.1 ± 3.5% ($p < 0.001$) and from 109.2 ± 3.3% to 80.9 ± 3.9% ($p < 0.05$) for basal and insulin-stimulated cells compared to the normal control. Aspalathin, orientin, isoorientin and rutin increased the basal cellular ATP content from 77.1 ± 3.5% to 108.9 ± 4.7%, 110.5 ± 5.6%, 112.7 ± 7.2% and 115.0 ± 6.7% ($p < 0.001$) and insulin-stimulated ATP from 80.9 ± 3.9% to 121.6 ± 4.2% ($p < 0.01$), 123.8 ± 4.4%, 134.4 ± 4.4% and 129.5 ± 5.1% ($p < 0.001$), respectively (Fig. 6.19 C).

A

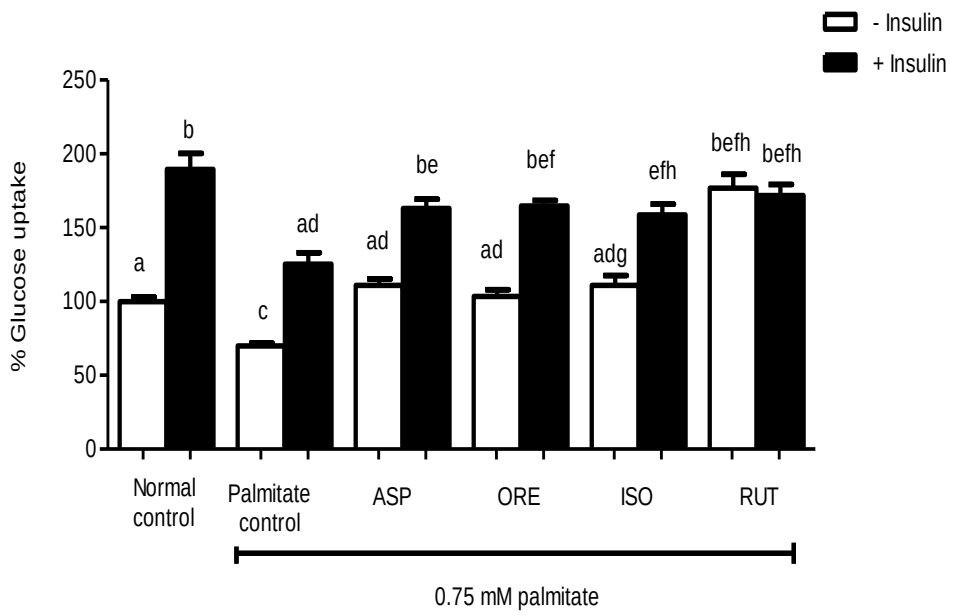
- Insulin
+ Insulin
% Glucose uptake
250
200
150
100
50
0
a
b
c
ad
ad
be
ad
bef
adg
efh
befh
befh
Normal control
Palmitate control
ASP
ORE
ISO
RUT
0.75 mM palmitate

B

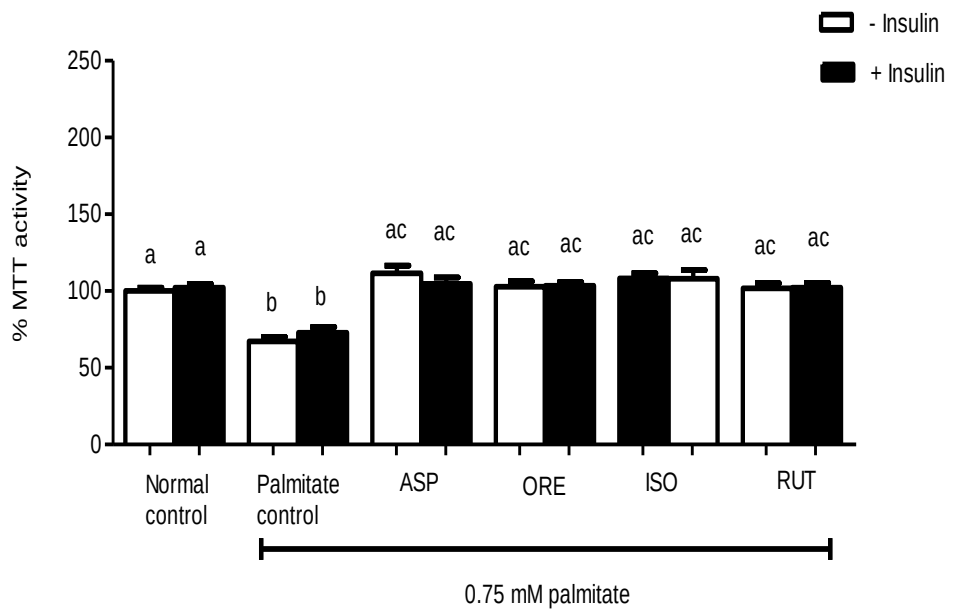
- Insulin
+ Insulin
% MTT activity
250
200
150
100
50
0
a
a
b
b
ac
ac
ac
ac
ac
ac
ac
ac
Normal control
Palmitate control
ASP
ORE
ISO
RUT
0.75 mM palmitate

C

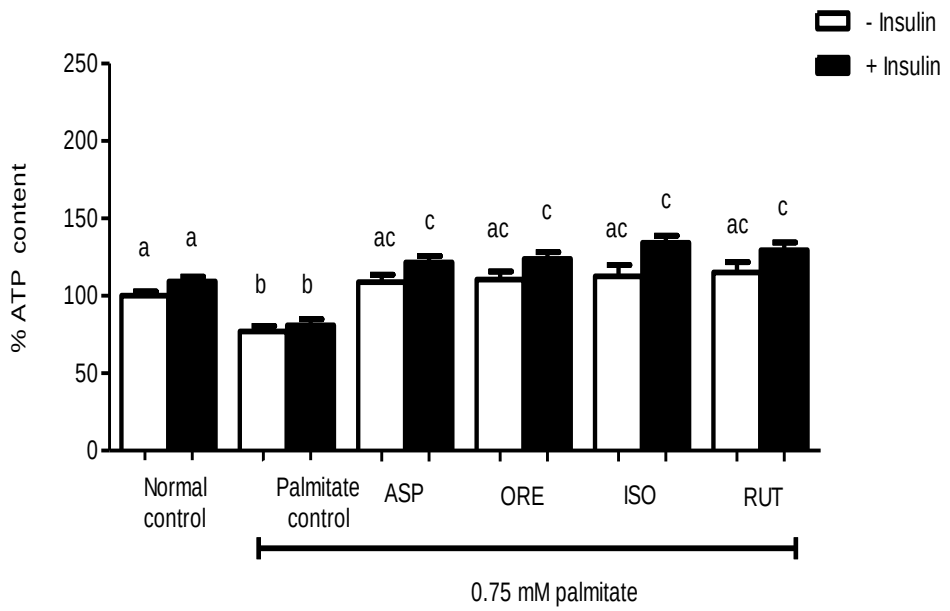

Figure. 6.19. Effect of aspalathin (ASP), orientin (ORE), isoorientin (ISO) and rutin (RUT), on glucose uptake (A) mitochondrial dehydrogenase activity (B) and ATP content (C) in 3T3-L1 adipocytes. 3T3-L1 adipocytes, cultured in DMEM with 8 mM glucose with or without 0.75 mM palmitate for 16 h, were treated with aspalathin, orientin, isoorientin and rutin (10 µM) for 3 h. Insulin (1 µM) was used for insulin stimulation. Glucose uptake was measured using [^{3}H]-2-deoxy-D-glucose method, mitochondrial dehydrogenase activity was measured using the MTT assay and intracellular ATP content was measured using the ATP luminescence kit. Results are expressed as the mean of three independent experiments relative to the control at 100% ± SEM. Bars with different letters denote statistical differences at $p \leq 0.05$.

6.3.4 Effect of an aspalathin-enriched green rooibos extract (GRE) and aspalathin on NF-κB activation in 3T3-L1 adipocytes

We investigated the effect of GRE and aspalathin on the NF-κB activation. Western blot analyses showed that palmitate activated NF-κB expression three-fold from 100.0 ± 16.8% to 304.8 ± 65.8% ($p < 0.001$). GRE and aspalathin reduced palmitate-induced basal NF-κB activation from 304.8 ± 65.8% to 18.2 ± 3.7% ($p < 0.001$) and 53.6 ± 8.9% ($p < 0.001$), respectively. Insulin-stimulated NF-κB activity was reduced from 90.6 ± 4.4% to 31.1 ± 10.5% ($p < 0.001$) and 66.9 ± 6.4% ($p < 0.001$), respectively (Fig. 6.20).

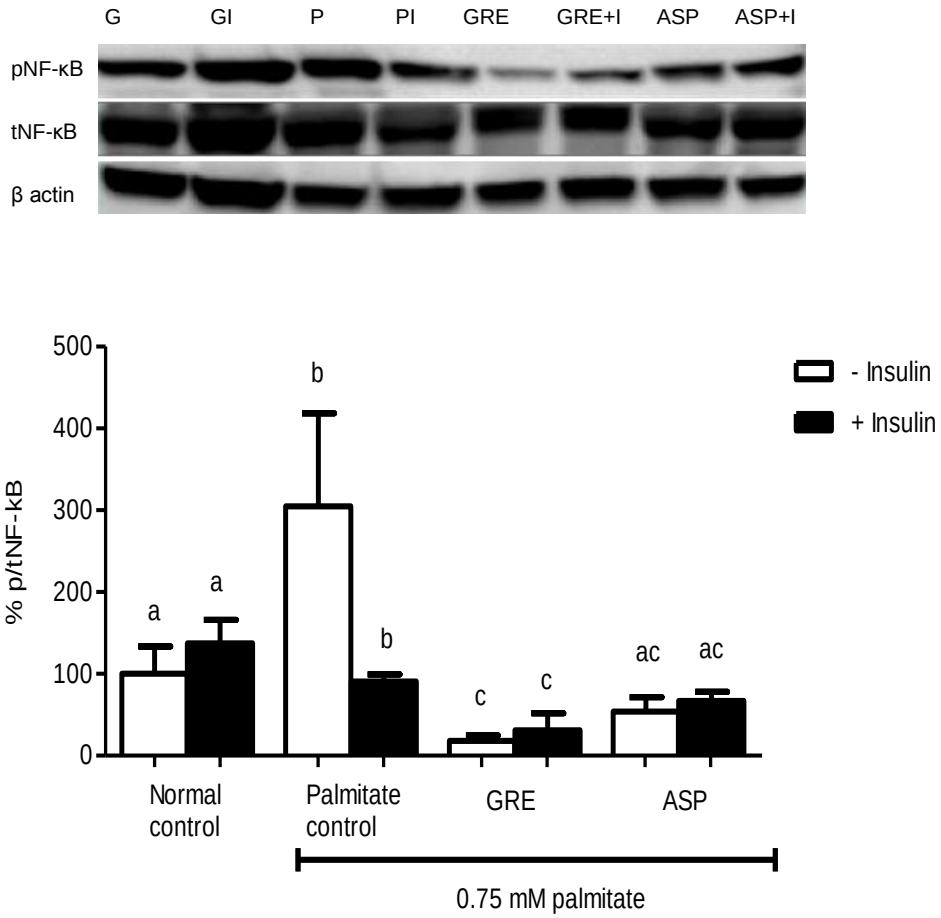

Figure 6.20. Effect of green rooibos extract (GRE) and aspalathin (ASP) on NF-κB activation. 3T3-L1 adipocytes, cultured in DMEM with 8 mM glucose with or without 0.75 mM palmitate for 16 h, were treated with GRE (10 µg/mL) or aspalathin (10 µM) for 3 h. Insulin (1 µM) was used for insulin stimulation. Cells were lysed and subjected to Western blot analyses. The % of pNF-κB/tNF-κB was used to estimate the level of NF-κB activation. Results are expressed as the mean of three independent experiments relative to control cells at 100% ± SEM. Bars with different letters denote statistical differences at $p \leq 0.05$.

6.3.5 Effect of aspalathin-enriched green rooibos extract (GRE) and aspalathin on insulin receptor (INSR) protein expression in 3T3-L1 adipocytes

We evaluated the effect of GRE and aspalathin on INSR protein expression in 3T3-L1 adipocytes. Treating 3T3-L1 adipocytes with palmitate reduced INSR protein expression from 100.0 ± 14.7% to 79.3 ± 5.5% ($p < 0.05$). Aspalathin increased basal and insulin-stimulated INSR protein expression compared to palmitate-treated controls from 79.3 ± 5.5% to 157.3 ± 9.7% ($p < 0.01$) and from 91.6 ± 8.4% to 181.6 ± 5.2% ($p < 0.001$), respectively. The GRE had no effect on the INSR protein expression (Fig. 6.21).

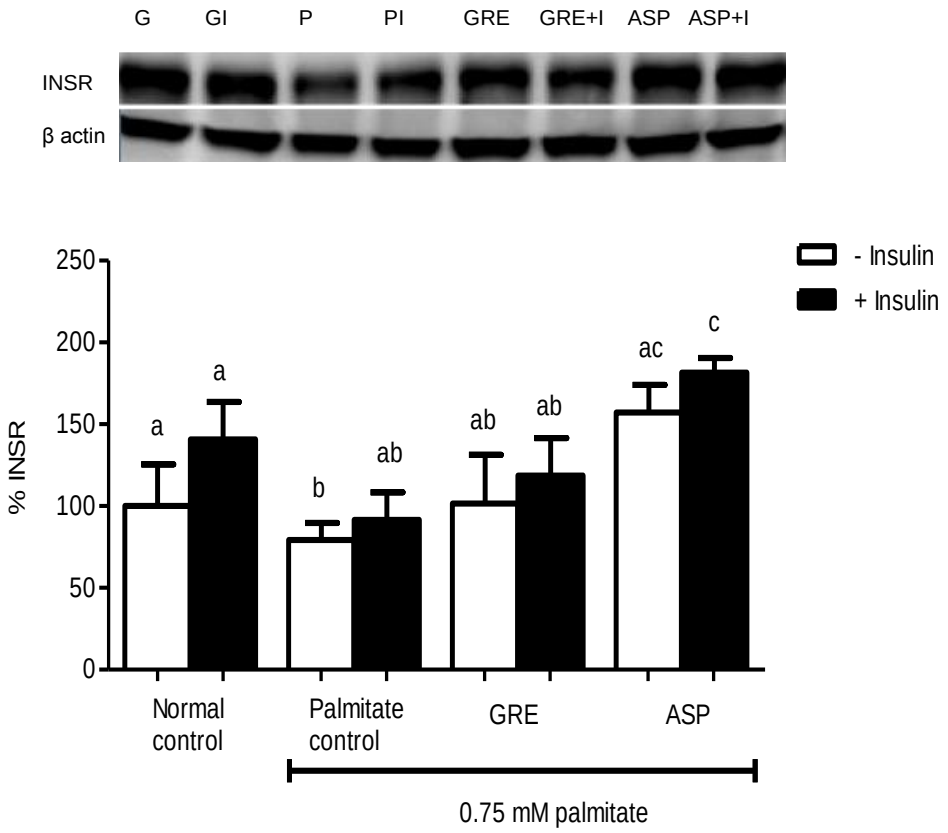

Figure 6.21. Effect of green rooibos extract (GRE) and aspalathin (ASP) on INSR protein expression. 3T3-L1 adipocytes, cultured in DMEM with 8 mM glucose with or without 0.75 mM palmitate for 16 h, were treated with GRE (10 µg/mL) or aspalathin (10 µM) for 3 h. Insulin (1 µM) was used for insulin stimulation. Cells were lysed and subjected to Western blot analyses. Results are expressed as the mean of three independent experiments relative to control set at 100% ± SEM. Bars with different letters denote statistical differences at $p \leq 0.05$.

6.3.6. Effect of aspalathin-enriched green rooibos extract (GRE) and aspalathin on PI3K (p85) protein activation on 3T3-L1 adipocytes

Albeit not significant, insulin stimulation increased PI3K (p85) activation in normal cells. Culturing cells with palmitate had no effect on 3T3-L1 adipocytes, similarly GRE and aspalathin had no effect on PI3K (p85) activation (Fig. 6.22).

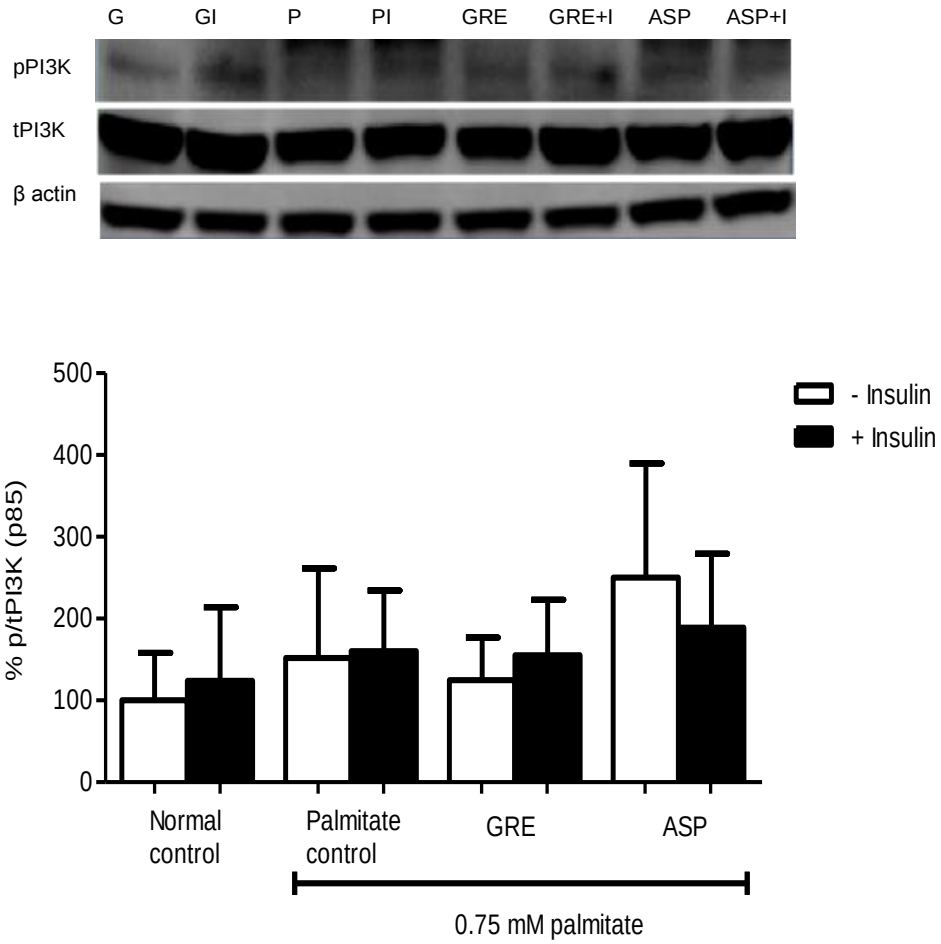

Figure 6.22. Effect of green rooibos extract (GRE) and aspalathin (ASP) on PI3K (p85) protein expression. 3T3-L1 adipocytes, cultured in DMEM with 8 mM glucose with or without 0.75 mM palmitate for 16 h, were treated with GRE (10 µg/mL) or aspalathin (10 µM) for 3 h. Insulin (1 µM) was used for insulin stimulation. Cells were lysed and subjected to Western blot analyses. The % of pPI3K/tPI3K was used to estimate the level of PI3K (p85) activation. Results are expressed as the mean of three independent experiments relative to control at 100% ± SEM.

6.3.7. Effect of aspalathin-enriched green rooibos extract (GRE) and aspalathin on AKT (Ser 473) protein expression in 3T3-L1 adipocytes

The protein expression results showed that insulin increased AKT (Ser 473) phosphorylation in 3T3-L1 adipocytes from 100.0 ± 3.7% to 399.4 ± 23.9% ($p < 0.001$). Addition of palmitate to the culture media of 3T3-L1 adipocytes reduced insulin-stimulated AKT (Ser 473) protein expression from 399.4 ± 3.7% to 90.7 ± 10.5% ($p < 0.001$) of the normal control. Both the GRE and aspalathin increased AKT (Ser 473) phosphorylation in the presence of insulin from 90.7 ± 10.5% to 257.7 ± 24.5 % ($p < 0.001$) and 174.0 ± 26.3% ($p < 0.001$), respectively. GRE and aspalathin had no effect on basal (non-insulin-stimulated) AKT (Ser 473) phosphorylation (Fig. 6.23).

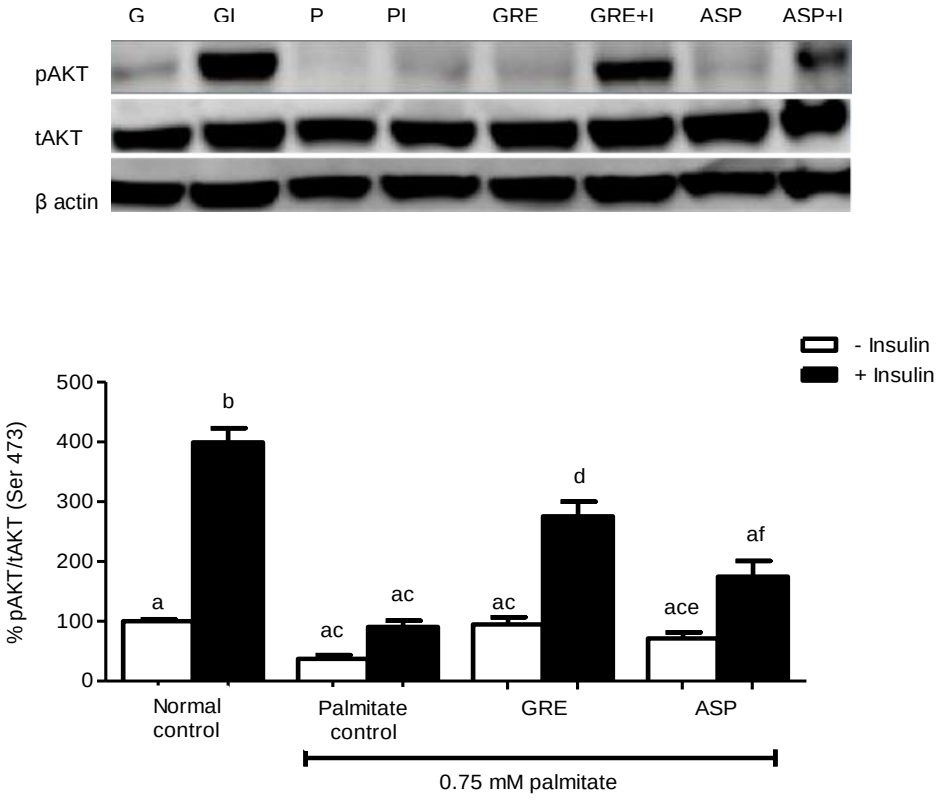

Figure 6.23. Effect of green rooibos extract (GRE) and aspalathin (ASP) on AKT (Ser 473) protein expression. 3T3-L1 adipocytes, cultured in DMEM with 8 mM glucose with or without 0.75 mM palmitate for 16 h, were treated with GRE (10 µg/mL) or aspalathin (10 µM) for 3 h. Insulin (1 µM) was used for insulin stimulation. Cells were lysed and subjected to Western blot analyses. The % of pAKT/tAKT was used to estimate the level of AKT (473) activation. Results are expressed as the mean of three independent experiments relative to control at 100% ± SEM. Bars with different letters denote statistical differences at $p \leq 0.05$.

6.3.8. Effect of aspalathin-enriched green rooibos extract (GRE) and aspalathin on AMPK activation in 3T3-L1 adipocytes

At a protein level, addition of palmitate to culture media of 3T3-L1 adipocytes increased the activation of AMPK in both basal and insulin-stimulated adipocytes from 100.0 ± 5.9% to 1383.0 ± 124.8% and from 102.4 ± 7.1% to 1501.0 ± 169.1% ($p < 0.001$), respectively. GRE had no effect on basal and insulin-stimulated AMPK activation compared to the normal control, however, if compared to the palmitate control, AMPK activation was reduced from 1383.0 ± 124.8% to 125.7 ± 23.1% ($p < 0.001$) for basal and from 1501.0 ± 169.1% to 163.1 ± 26.2% ($p < 0.001$) for the insulin-stimulated adipocytes, respectively. Although not significant, aspalathin increased the basal AMPK phosphorylation compared to the normal control (Fig. 6.24).

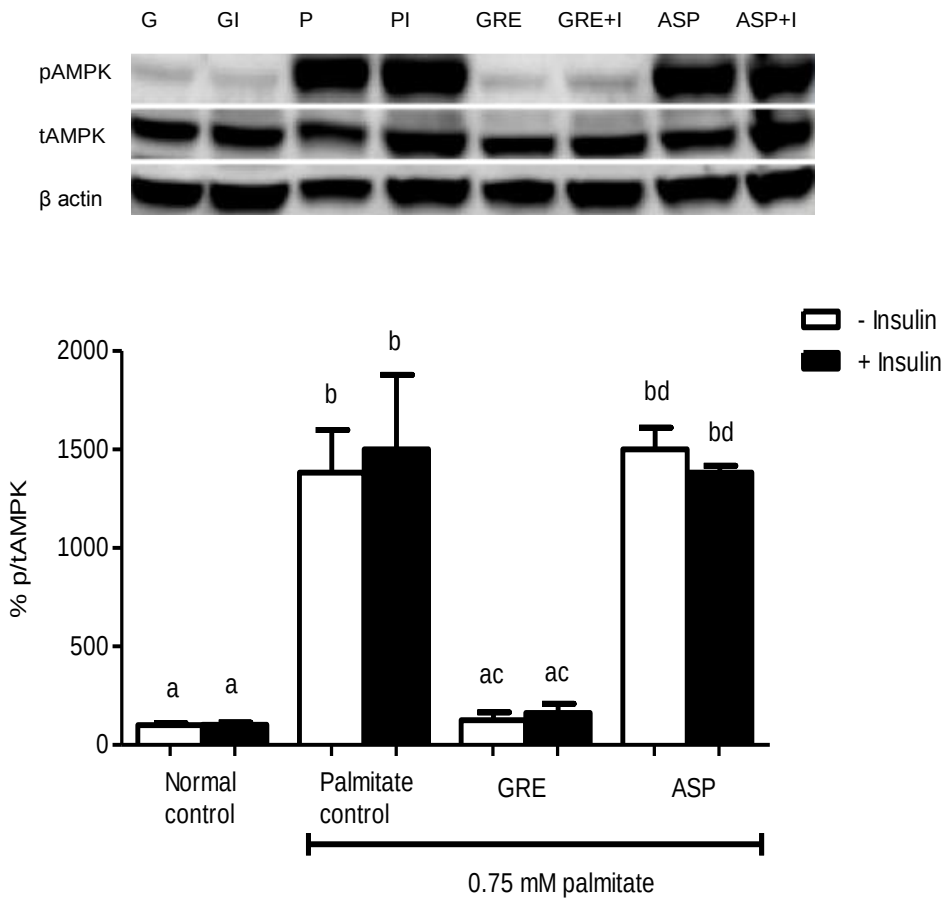

Figure 6.24. Effect of green rooibos extract (GRE) and aspalathin (ASP) on AMPK protein expression. 3T3-L1 adipocytes, cultured in DMEM with 8 mM glucose with or without 0.75 mM palmitate for 16 h, were treated with GRE (10 µg/mL) or aspalathin (10 µM) for 3 h. Insulin (1 µM) was used for insulin stimulation. Cells were lysed and subjected to Western blot analyses. The % of pAMPK/tAMPK was used to estimate the level of AMPK activation. Results are expressed as the mean of three independent experiments relative to control set at 100% ± SEM. Bars with different letters denote statistical differences at $p \leq 0.05$.

6.3.9. Effect of aspalathin-enriched green rooibos extract (GRE) and aspalathin on GLUT4 protein expression in 3T3-L1 adipocytes

GRE increased basal GLUT4 protein expression compared to palmitate-treated controls from 116.5 ± 17.1% to 199.0 ± 10.9% ($p < 0.001$ and from 143.1 ± 18.0% to 188.0 ± 11.9% ($p < 0.01$) for insulin-stimulated GLUT4 protein expression. Aspalathin slightly increased both basal and insulin-stimulated GLUT4 protein expression although this was not significant (Fig. 6.25).

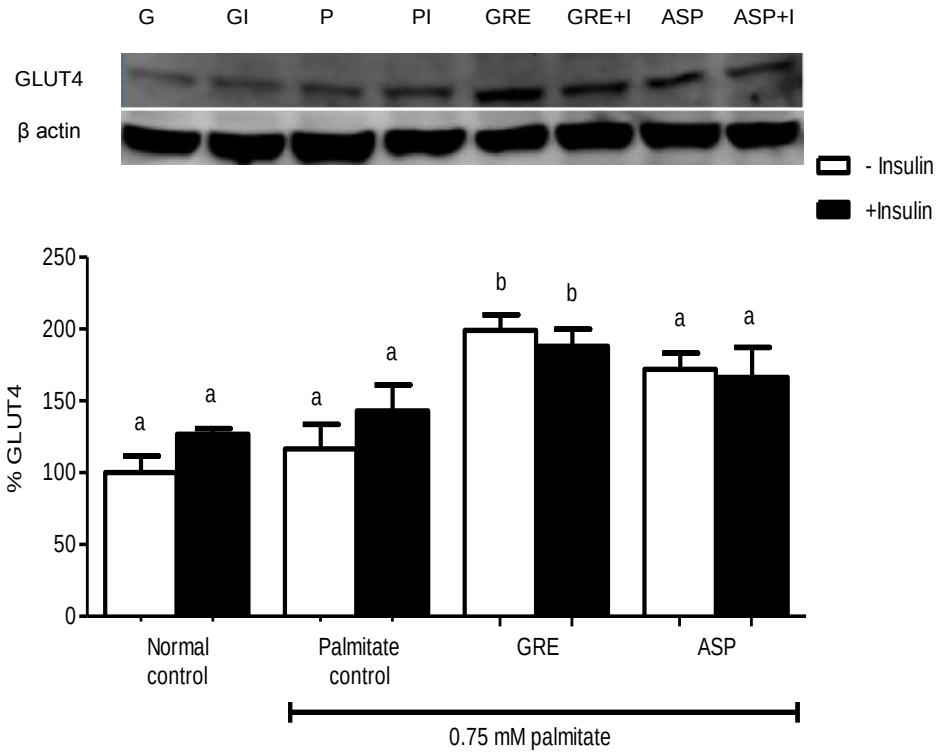

Figure 6.25. Effect of green rooibos extract (GRE) and aspalathin (ASP) on GLUT4 protein expression. 3T3-L1 adipocytes, cultured in DMEM with 8 mM glucose with or without 0.75 mM palmitate for 16 h, were treated with GRE (10 µg/mL) or aspalathin (10 µM) for 3 h. Insulin (1 µM) was used for insulin stimulation. Cells were lysed and subjected to Western blot analyses. Results are expressed as the mean of three independent experiments relative to control at 100% ± SEM. Bars with different letters denote statistical differences at $p \leq 0.05$.

6.3.10. Lipid metabolism studies in 3T3-L1 adipocytes

6.3.10.1. Effect of rooibos extracts on palmitate uptake in 3T3-L1 adipocytes

Fatty acid uptake was measured using radiolabelled ^{14}C palmitate. Addition of palmitate reduced the fatty acid uptake both in basal and insulin-stimulated cells from 100.0 ± 4.4% to 43.0 ± 7.7% ($p < 0.01$) and from 101.7 ± 13.8% to 42.1 ± 8.6% ($p < 0.01$), respectively. Treating the palmitate-induced insulin-resistant 3T3-L1 adipocytes with FRE and GRE, increased palmitate uptake from 43.0 ± 7.7% to 122.7 ± 9.3% ($p < 0.001$) and 110.2 ± 3.9% ($p < 0.001$) for basal cells and from 42.1 ± 8.6% to 98.1 ± 8.8% ($p < 0.001$) and 89.5 ± 10.9 ($p < 0.05$) for insulin-stimulated cells, respectively (Fig. 6.26).

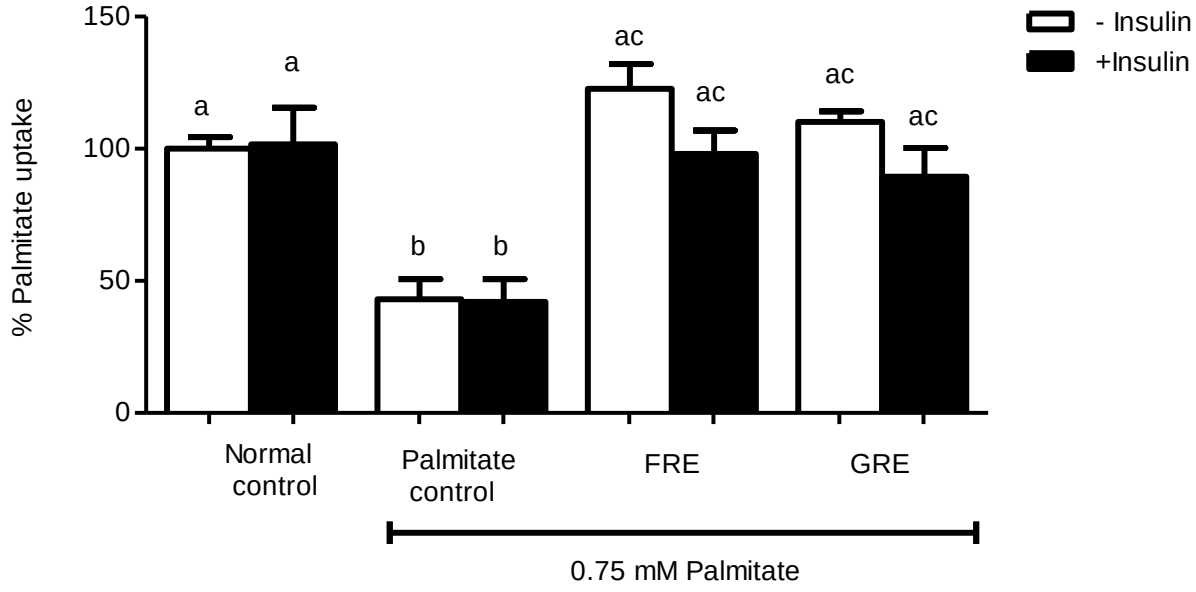

Figure 6.26. Effect of rooibos extract (GRE and FRE) on palmitate uptake. 3T3-L1 adipocytes, were cultured in DMEM supplemented with 8 mM glucose with or without 0.75 mM palmitate for 16 h, and treated with FRE or GRE (10 µg/mL) for 3 h. Palmitate uptake was measured using ^{14}C palmitate. Results are expressed as the mean of three independent experiments relative to the control at 100% ± SEM. Bars with different letters denote statistical differences at $p \leq 0.05$.

6.3.10.2. Effect of aspalathin, orientin, isoorientin and rutin on palmitate uptake in 3T3-L1 adipocytes

Aspalathin, orientin, and rutin increased basal palmitate uptake in palmitate treated cells from 43.0 ± 7.7% to 90.2 ± 10.1% ($p < 0.05$), 110.7 ± 6.5% ($p < 0.001$) and 102.1 ± 8.5% ($p < 0.001$), respectively. Isoorientin did not significantly affect basal palmitate uptake in palmitate treated cells. Orientin, isoorientin and rutin enhanced insulin-stimulated palmitate uptake from 42.1 ± 8.6% to 107.3 ± 5.9% ($p < 0.001$), 93.7 ± 3.7% ($p < 0.001$) and 107.8 ± 8.5 ($p < 0.001$), respectively. Aspalathin did not significantly affect insulin-stimulated palmitate uptake compared to the palmitate treated controls. It should be noted however that, aspalathin, orientin, isoorientin and rutin were equally effective at normalising palmitate uptake relative to the normal controls not exposed to palmitate (Fig. 6.27).

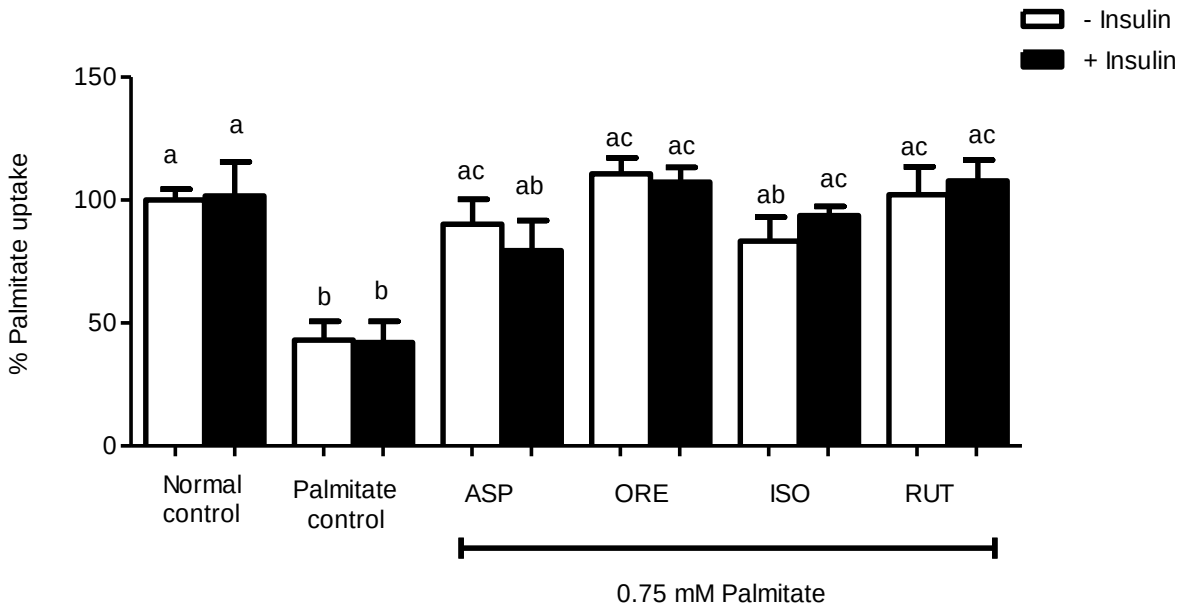

Figure 6.27. Effect of aspalathin (ASP), orientin (ORE), isoorientin (ISO) and rutin (RUT) on palmitate uptake. 3T3-L1 adipocytes, were cultured in DMEM containing 8 mM glucose with or without 0.75 mM palmitate for 16 h, and treated with ASP, ORE, ISO and RUT (10 µM) for 3 h. Palmitate uptake was measured using ^{14}C palmitate. Results are expressed as the mean of three independent experiments relative to the control at 100% ± SEM. Bars with different letters denote statistical differences at $p \leq 0.05$.

6.3.10.3. Effect of aspalathin-enriched green rooibos extract (GRE) and aspalathin on PPARγ protein expression

Treatment with palmitate induced a slight, non-significant reduction in the PPARγ protein expression in 3T3-L1 cells. GRE had no effect on PPARγ expression in 3T3-L1 adipocytes, while the aspalathin increased both basal and insulin-stimulated PPARγ protein expression from 62.7 ± 8.4% to 234.8 ± 31.4% ($p < 0.001$) and from 77.8 ± 2.8% to 172.4 ± 23.5% ($p < 0.01$), respectively compared to the palmitate-treated control (Fig. 6.28).

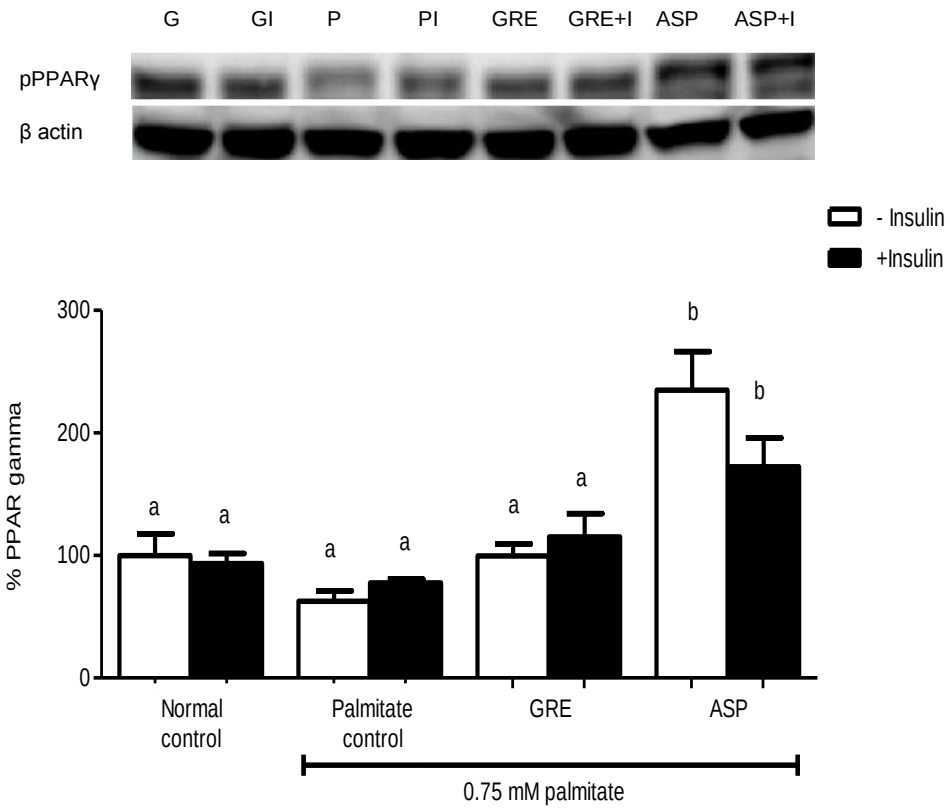

Figure 6.28. Effect of green rooibos extract (GRE) and aspalathin (ASP) on PPARγ protein expression. 3T3-L1 adipocytes, cultured in DMEM with 8 mM glucose with or without 0.75 mM palmitate for 16 h, were treated with GRE (10 µg/mL) or aspalathin (10 µM) for 3 h. Insulin (1 µM) was used for insulin stimulation. Cells were lysed and subjected to Western blot analyses. Results are expressed as the mean of three independent experiments relative to control set at 100% ± SEM. Bars with different letters denote statistical differences at $p \leq 0.05$.

6.3.10.4. Effect of aspalathin-enriched green rooibos extract (GRE) and aspalathin on PPARα protein expression

Insulin stimulation of palmitate treated cells increased PPARα protein expression from 100.0 ± 14.4% to 175.4 ± 10.1% ($p < 0.05$). GRE had no effect of PPARα expression in 3T3-L1 adipocytes while the aspalathin increased insulin-stimulated protein expression from 117.3 ± 9.8% to 181.6 ± 5.2% ($p < 0.05$), compared to the palmitate-treated control (Fig. 6.29).

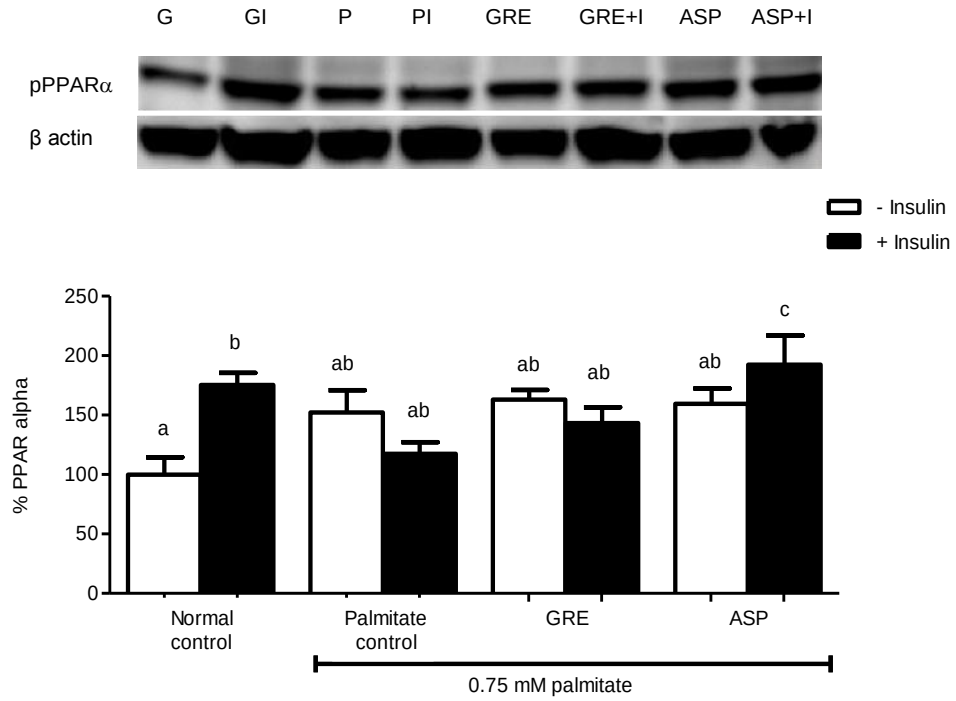

Figure 6.29. Effect of green rooibos extract (GRE) and aspalathin (ASP) on PPARα protein expression. 3T3-L1 adipocytes, cultured in DMEM with 8 mM glucose with or without 0.75 mM palmitate for 16 h, were treated with GRE (10 µg/mL) or aspalathin (10 µM) for 3 h. Insulin (1 µM) was used as insulin stimulation. Cells were lysed and subjected to Western blot analyses. Results are expressed as the mean of three independent experiments relative to control at 100% ± SEM. Bars with different letters denote statistical differences at $p \leq 0.05$.

6.3.10.5. Effect of aspalathin-enriched green rooibos extract (GRE) and aspalathin on malonyl-CoA protein expression

Albeit not significant, culturing with palmitate increased malonyl-CoA protein expression compared to the normal control, while aspalathin reduced this increase (Fig. 6.30).

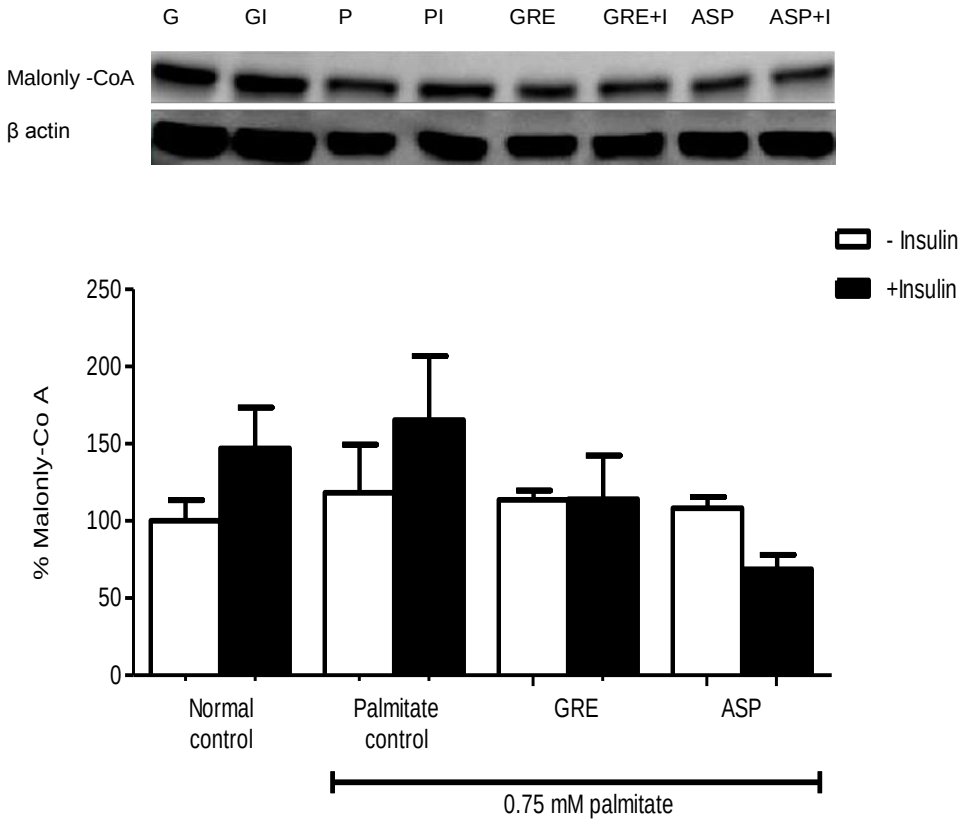

Figure 6.30. Effect of green rooibos extract (GRE) and aspalathin (ASP) on malonyl-CoA protein expression. 3T3-L1 adipocytes, cultured in DMEM with 8 mM glucose with or without 0.75 mM palmitate for 16 h, were treated with GRE (10 µg/mL) or aspalathin (10 µM) for 3 h. Insulin (1 µM) was used as insulin stimulation. Cells were the lysed and subjected to Western blot analyses. Results are expressed as the mean of three independent experiments relative to control at 100% ± SEM. Bars with different letters denote statistical differences at $p \leq 0.05$.

6.3.10.6. Effect of aspalathin-enriched green rooibos extract (GRE) and aspalathin on carnitine palmitoyltransferase I (CPT1) protein expression

Palmitate reduced CPT1 protein expression from 100.0 ± 3.4% to 44.3 ± 3.3% (p < 0001) in 3T3-L1 adipocytes. Addition of GRE and aspalathin increased the basal CPT1 protein expression from 44.3 ± 3.3% to 111.1 ± 5.7% and 93.9 ± 6.3 (p < 0.001), respectively. In the insulin-stimulated palmitate-treated 3T3-L1 cells aspalathin increased CPT1 protein expression from 54.1 ± 5.6% to 87.6 ± 8.6% (p < 0.05) (Fig. 6.31).

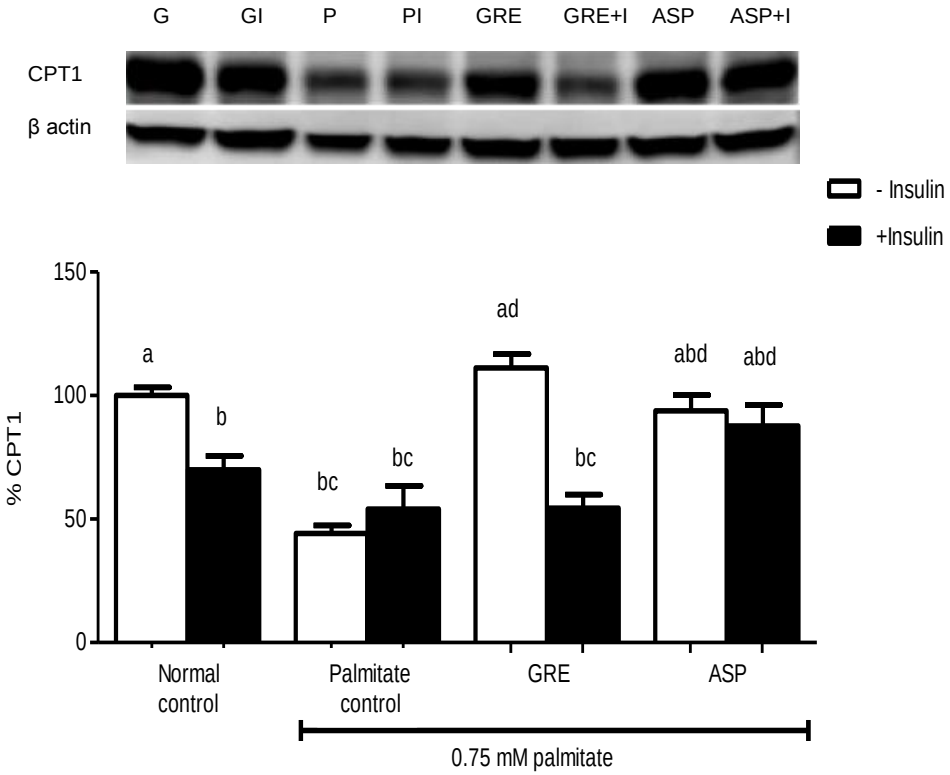

Figure 6.31. Effect of green rooibos extract (GRE) and aspalathin (ASP) on CPT1 protein expression. 3T3-L1 adipocytes, cultured in DMEM with 8 mM glucose with or without 0.75 mM palmitate for 16 h, were treated with GRE (10 µg/mL) or aspalathin (10 µM) for 3 h. Insulin (1 µM) was used for insulin stimulation. Cells were lysed and subjected to Western blot analyses. Results are expressed as the mean of three independent experiments relative to control set at 100% ± SEM. Bars with different letters denote statistical differences at $p \leq 0.05$.

6.4. Insulin resistance in C3A liver cells

Following results describe the induction of insulin resistance in C3A liver cells by palmitate. The effects of fermented rooibos extract (FRE) and aspalathin-enriched green rooibos extract (GRE) at a concentration of 10 µg/mL and aspalathin (ASP), orientin (ORE), isoorientin (ISO) and rutin (RUT) at a concentration of 10 µM in insulin-resistant C3A liver cells will be further demonstrated. Insulin (1 µM) was used for insulin stimulation. GRE (10 µg/mL) and aspalathin at a concentration of 10 µM, were chosen to assess their effects on the glucose and lipid molecular mechanisms in insulin resistant C3A liver cells.

6.4.1. Effect of palmitate on glucose uptake in C3A liver cells

Addition of palmitate to C3A liver cells reduced basal glucose uptake and induced insulin resistance. This was confirmed by a reduction of basal and insulin-stimulated glucose uptake from 100.0 ± 4.8% to 69.8 ± 4.6% and from 122.0 ± 4.6% to 63.8 ± 7.9% ($p < 0.01$) compared to the control cells not exposed to palmitate (Fig. 6.32).

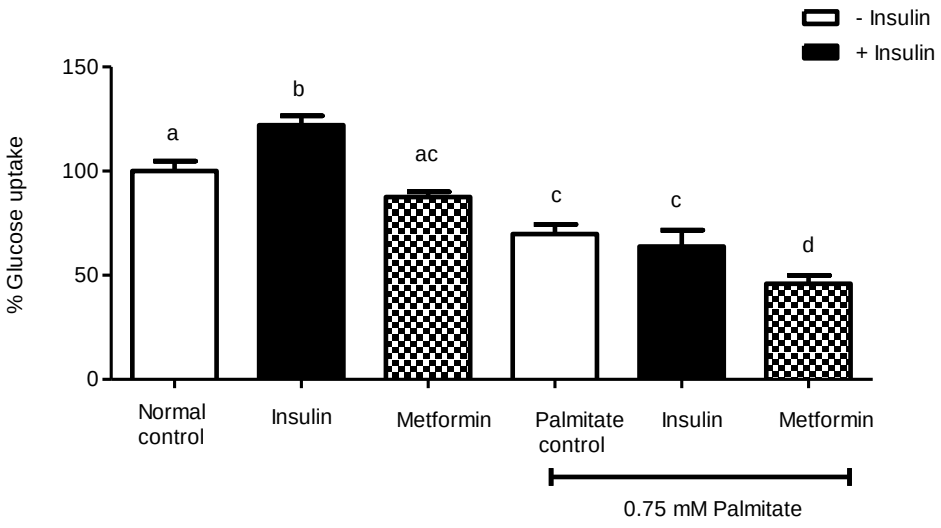

Figure 6.32. Effect of palmitate on glucose uptake in C3A liver cells. C3A liver cells were cultured in DMEM with 8 mM glucose with or without 0.75 mM palmitate for 16 h, and treated with insulin (15 min) or metformin (3 h), respectively. Glucose uptake was estimated using [^{3}H]-2-deoxy-D-glucose. Results are expressed as the mean of three independent experiments relative to the control set at 100% ± SEM. Bars with different letters denote statistical difference at $p \leq 0.05$.

6.4.2. Effect of fermented rooibos extracts (FRE) and aspalathin-enriched green rooibos extract (GRE) on glucose uptake, mitochondrial dehydrogenase activity and intracellular ATP content in palmitate-treated C3A liver cells

Addition of FRE for 3 h to the media of palmitate-treated C3A liver cells enhanced insulin-stimulated glucose uptake from 63.8 ± 7.9% to 97.4 ± 6.2% ($p < 0.01$), GRE also increased insulin-stimulated glucose uptake, however, the increase was not significant compared to the palmitate control (Fig. 6.33 A).Treating C3A liver cells with palmitate for 16 h had no effect on MTT activity however in the palmitate treated cells GRE increased MTT activity from 90.6 ± 3.0% to 129.8 ± 13.3% compared to palmitate control respectively (Fig. 6.33 B). Palmitate treatment reduced ATP content. FRE and GRE increased the ATP content under basal conditions from 76.2 ± 6.2% to 130.4 ± 6.7 ($p < 0.0001$) and 139.8 ± 11.9% ($p < 0.01$), respectively. FRE and GRE increased insulin-stimulated ATP content in palmitate-treated cells from 90.1 ± 6.8% to 119.9 ± 7.3% ($p < 0.01$) and 138.6 ± 7.3% ($p < 0.001$), respectively compared to the palmitate control (Fig. 6.33 C).

A

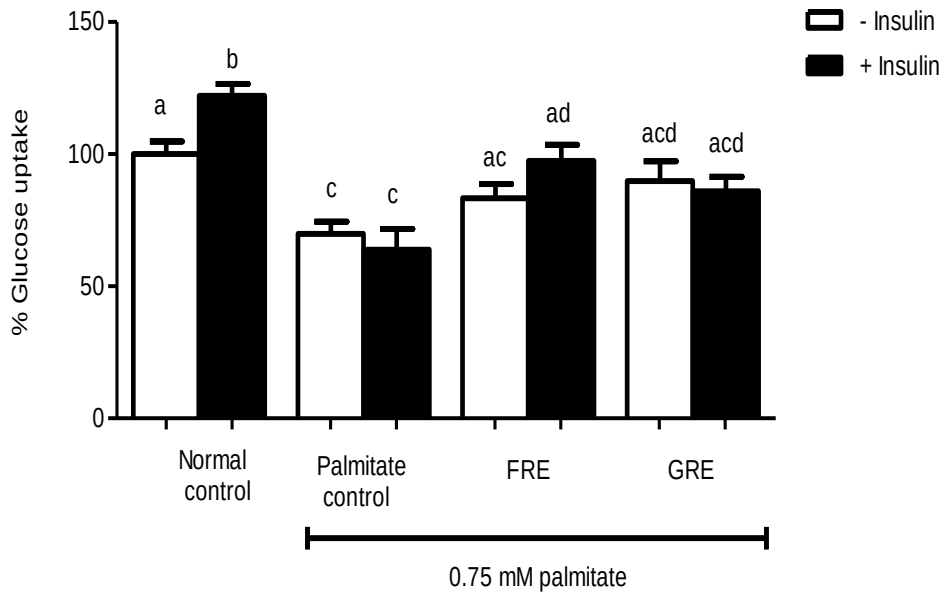
- Insulin
+ Insulin
% Glucose uptake
150
100
50
0
a
b
c
c
ac
ad
acd
acd
Normal control
Palmitate control
FRE
GRE
0.75 mM palmitate

B

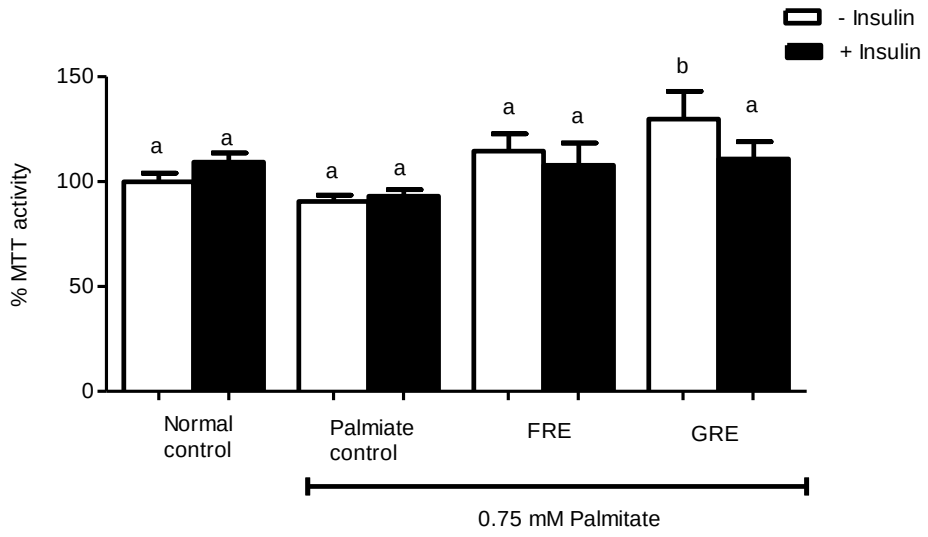
- Insulin
+ Insulin
% MTT activity
150
100
50
0
a
a
a
a
a
a
b
a
Normal control
Palmiate control
FRE
GRE
0.75 mM Palmitate

C

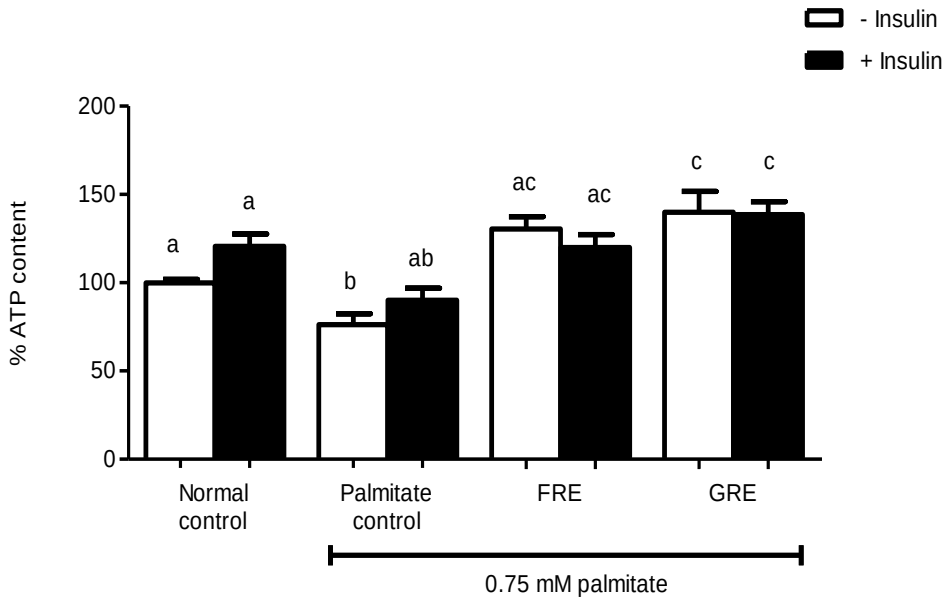

Figure 6.33. Effect green rooibos extracts (FRE and GRE) on glucose uptake (A), mitochondrial activity (B) and intracellular ATP content (C). C3A liver cells were cultured in DMEM with 8 mM glucose with or without 0.75 mM palmitate for 16 h, and then treated with insulin (15 min). Glucose uptake was measured using [^{3}H]-2-deoxy-D-glucose, mitochondrial dehydrogenase activity was measured using the MTT assay and ATP content was measured using a luminescent assay. Results are expressed as the mean of three independent experiments relative to the control, which was set at 100% ± SEM. Bars with different letters denote statistical differences at $p \leq 0.05$.

6.4.3. Effect of aspalathin, orientin, isoorientin and rutin on glucose uptake, mitochondrial dehydrogenase activity and intracellular ATP content in palmitate-treated C3A liver cells

Of the compounds tested, only rutin had a significant effect on the palmitate-induced reduction of basal glucose uptake from 69.8 ± 4.7% to 91.9 ± 2.8% (p <0.05). In terms of insulin-stimulated glucose uptake, aspalathin, orientin and isoorientin had no effect. (Fig. 6.34A). Treating C3A liver cells with palmitate for 16 h had no effect on MTT activity. Aspalathin and rutin increased basal MTT activity from 90.6 ±3.0% to 138 ± 143% and 137.9 ± 14.5% compared to palmitate control (Fig. 6.34 B). Aspalathin, orientin, isoorientin and rutin increased basal ATP content from 76.2 ± 6.2% to 145.1 ± 7.6%, 141.1 ± 10.2%, 137.3 ± 7.5% and 146.0 ± 10.1% (p < 0.001), respectively, and insulin-stimulated ATP content from 90.1 ± 6.8% to 137.3 ± 7.3%, 144.7 ± 8.9%, 137.1 ± 6.8% and 135.5 ± 12.3% (p < 0.001), respectively with respect to basal and insulin-stimulated palmitate controls. As demonstrated for GRE and FRE, treatment with the compounds induced similar increases between the basal and insulin-stimulated ATP content (Fig. 6.34 C).

A

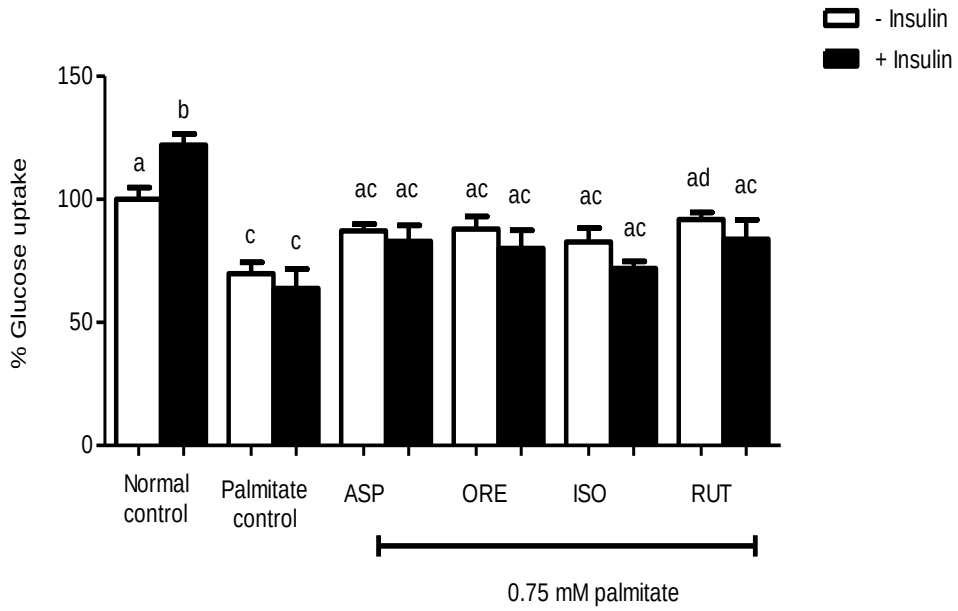
- Insulin
+ Insulin
% Glucose uptake
150
100
50
0
a
b
c
c
ac
ac
ac
ac
ac
ac
ad
ac
Normal control
Palmitate control
ASP
ORE
ISO
RUT
0.75 mM palmitate

B

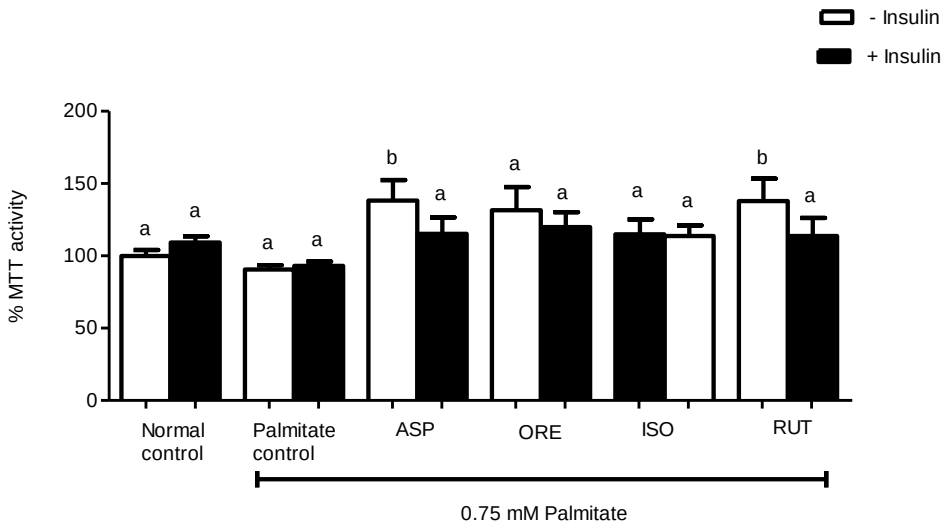
- Insulin
+ Insulin
% MTT activity
200
150
100
50
0
a
a
a
a
b
a
a
a
a
a
b
a
Normal control
Palmitate control
ASP
ORE
ISO
RUT
0.75 mM Palmitate

C

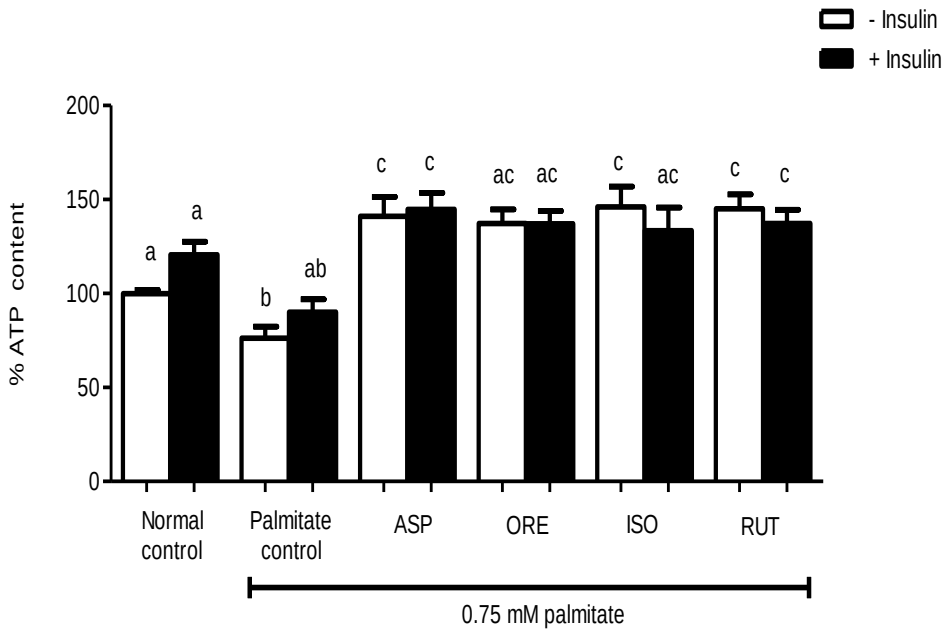

Figure 6.34. Effect of aspalathin (ASP), orientin (ORE), isoorientin (ISO) and rutin (RUT), on glucose uptake (A), mitochondrial activity (B) and intracellular ATP content (C). C3A liver cells were cultured in DMEM with 8 mM glucose with or without 0.75 mM palmitate for 16 h, and then treated with insulin (15 min). Glucose uptake was measured using [^{3}H]-2-deoxy-D-glucose, mitochondrial dehydrogenase activity was measured using the MTT assay and ATP content was measured using a luminescent assay. Results are expressed as the mean of three independent experiments relative to the control which was set at 100% ± SEM. Bars with different letters denote statistical differences at $p \leq 0.05$.

6.4.4. Effect of aspalathin-enriched green rooibos extract (GRE) and aspalathin on PI3K (p85) activation in C3A liver cells

Palmitate reduced the basal levels of activated PI3K (p85) but had no effect on the insulin-stimulated activation of PI3K (p85). GRE and aspalathin increased basal PI3K (p85) activation relative to the normal control (not exposed to palmitate) and the palmitate-treated controls, respectively. Under basal conditions levels of activated PI3K were increased from 86.6 ± 11.1% to 171.0 ± 3.5% ($p < 0.001$) and 195.6 ± 22.2% ($p < 0.001$) for GRE and aspalathin relative to the palmitate-treated control. (Fig. 6.35).

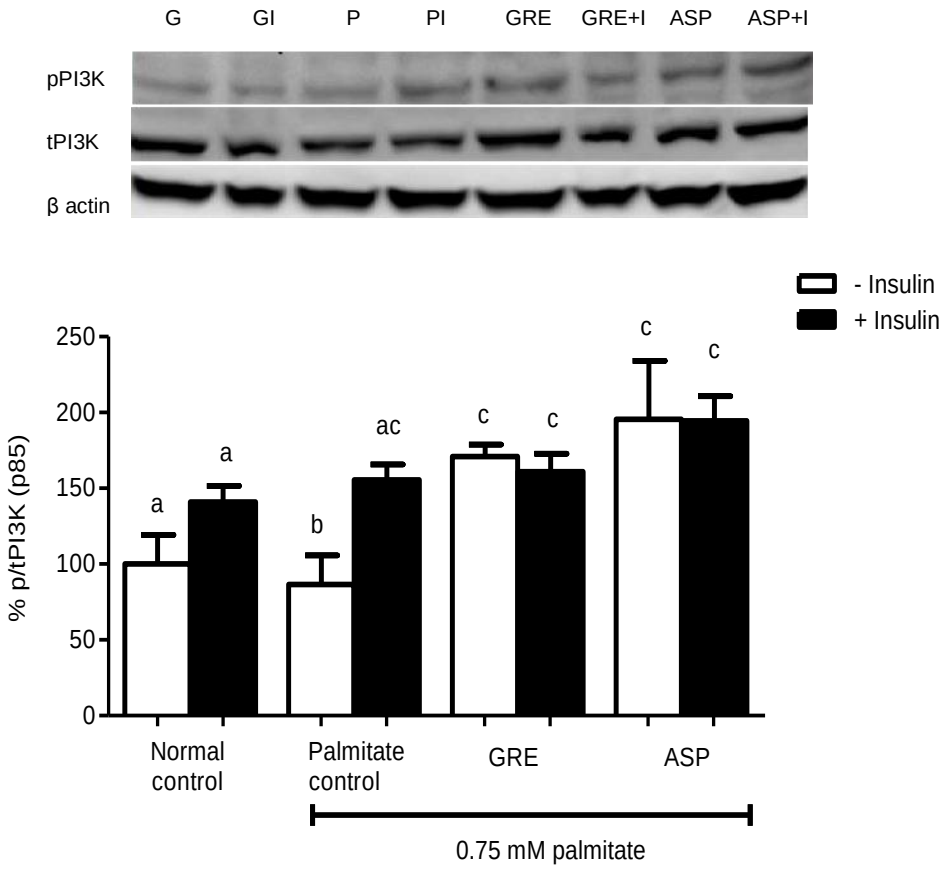

Figure 6.35 Effect of green rooibos extract (GRE) and aspalathin (ASP) on PI3K activation.
C3A liver cells were cultured in DMEM supplemented with 8 mM glucose with or without 0.75 mM palmitate for 16 h and then treated with GRE (10 µg/mL) or aspalathin (10 µM) for 3 h. Cells were lysed and subjected to Western blot analyses. The % of pPI3K/tPI3K was used to estimate the level of PI3K activation. Results are expressed as the mean of three independent experiments relative to the control at 100% ± SEM. Bars with different letters denote statistical differences at $p \leq 0.05$.

6.4.5. Effect of aspalathin-enriched green rooibos extract (GRE) and aspalathin on AKT (Ser 473) activation in C3A liver cells

In normal C3A liver cells insulin stimulation increased AKT (Ser 473) activation by ~ 400 % ($p < 0.001$). Palmitate reduced insulin-stimulated AKT (Ser 473) activation from 418.1 ± 15.6% to 151.9 ± 25.3% ($p < 0.001$) compared to the normal control. GRE increased AKT (Ser 473) phosphorylation in the presence of insulin from 151.9 ± 25.3% to 300.0 ± 39.5 % ($p < 0.001$). Aspalathin had no effect on basal and insulin-stimulated AKT (Ser 473) phosphorylation (Fig. 6.36).

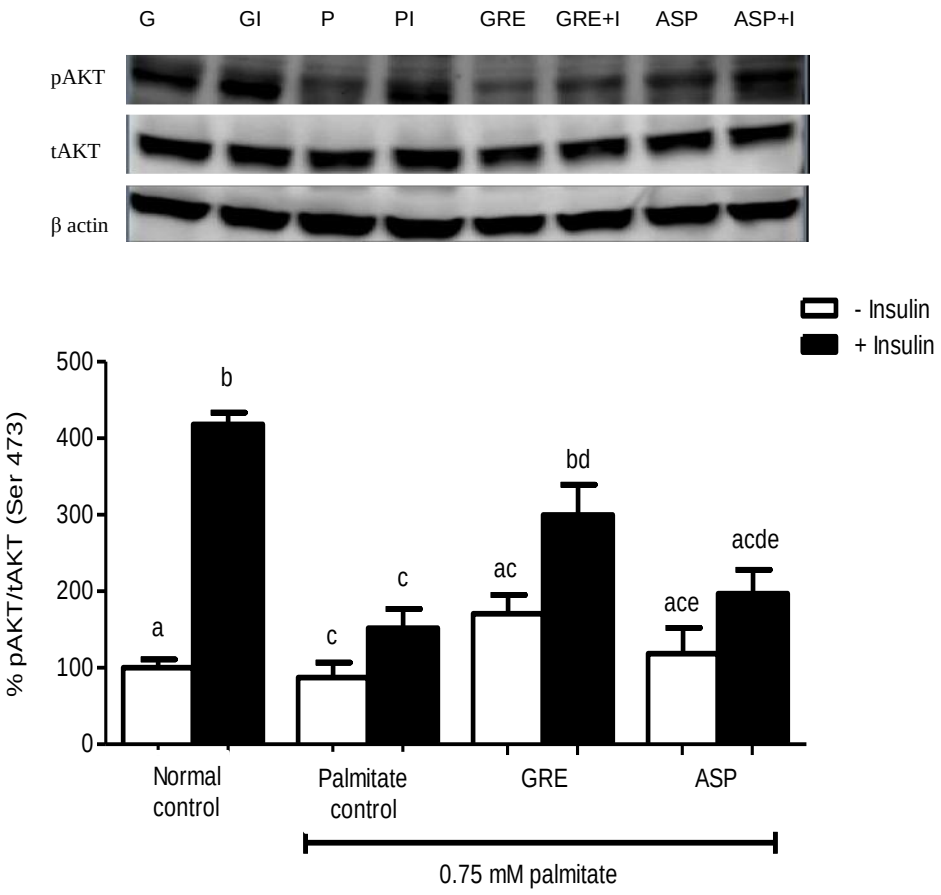

Figure 6.36. Effect of green rooibos extract (GRE) and aspalathin (ASP) on AKT (Ser 473) activation. C3A liver cells were cultured in DMEM supplemented with 8 mM glucose with or without 0.75 mM palmitate for 16 h and then treated with GRE (10 µg/mL) or aspalathin (10 µM) for 3 h. Cells were lysed and subjected to Western blot analyses. The % of pAKT/tAKT was used to estimate the level of AKT (Ser 473) activation. Results are expressed as the mean of three independent experiments relative to controls set at 100% ± SEM. Bars with different letters denote statistical differences at $p \leq 0.05$.

6.4.6. Effect of aspalathin-enriched green rooibos extract (GRE) and aspalathin on AMPK activation in C3A liver cells

GRE and aspalathin increased AMPK activation from 228.8 ± 14.7% to 332.7 ± 4.4% and 580.1 ± 20.4% ($p < 0.001$) in basal and from 279.2 ± 16.4% to 533.0 ± 14.2% and 485.0 ± 11.8% ($p < 0.001$) in the insulin-stimulated cells respectively (Fig. 6.37).

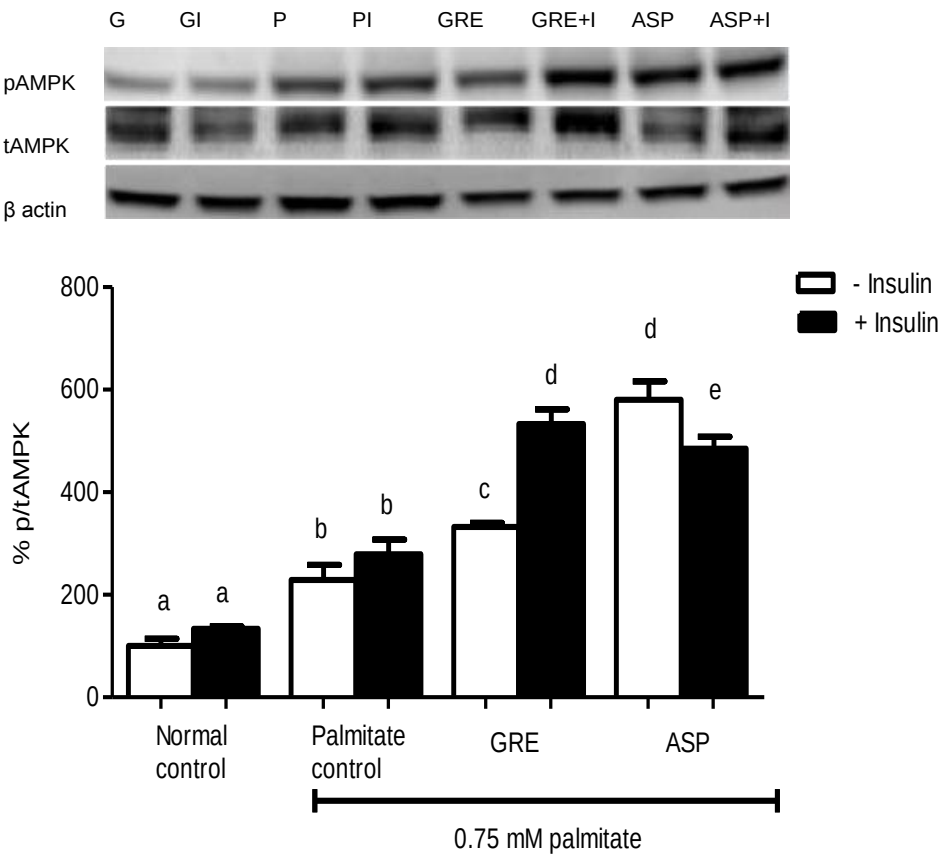

Figure 6.37. Effect of green rooibos extract (GRE) and aspalathin (ASP) on AMPK activation. C3A liver cells were cultured in DMEM containing 8 mM glucose with or without 0.75 mM palmitate for 16 h and then treated with GRE (10 µg/mL) or ASP (10 µM) for 3 h. Cells were lysed and subjected to Western blot analyses. The % of pAMPK/tAMPK was used to estimate the level of AMPK activation. Results are expressed as the mean of three independent experiments relative to the control set at 100% ± SEM. Bars with different letters denote statistical differences at $p \leq 0.05$.

6.4.7. Effect of aspalathin-enriched green rooibos extract (GRE) and aspalathin on GLUT2 protein expression in C3A liver cells

Treating C3A liver cells with palmitate reduced insulin-stimulated GLUT2 protein expression from 106.1 ± 11.9% to 43.7 ± 4.2% ($p < 0.05$). Addition of GRE and aspalathin to the palmitate-treated C3A liver cells increased basal GLUT2 protein expression from 59.4 ± 3.4% to 114.4 ± 18.7% ($p < 0.05$) and 137.5 ± 11.2% ($p < 0.01$),respectively. Insulin-stimulated GLUT2 protein expression was also increased from 43.7 ± 4.2% to 105.2 ± 10.2% ($p < 0.01$) and 175.8 ± 12.7%, respectively. Aspalathin significantly increased insulin-stimulated GLUT2 protein expression relative to the normal control, palmitate control and GRE treated C3A cells (Fig. 6.38).

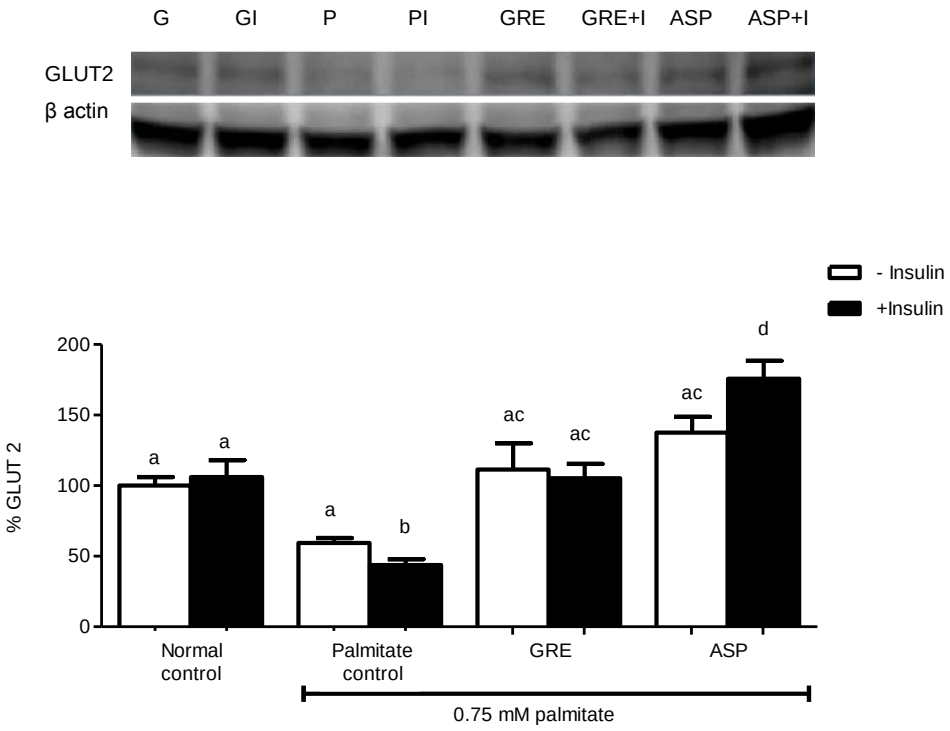

Figure 6.38. Effect of green rooibos extract (GRE) and aspalathin (ASP) on GLUT2 protein expression. C3A liver cells were cultured in DMEM containing 8 mM glucose with or without 0.75 mM palmitate for 16 h and then treated with GRE (10 µg/mL) or aspalathin (10 µM) for 3 h. Cells were lysed and subjected to Western blot analyses. Results are expressed as the mean of three independent experiments relative to the control at 100% ± SEM. Bars with different letters denote statistical differences at $p \leq 0.05$.

6.4.8. Lipid metabolism in insulin-resistant C3A liver cells

6.4.8.1. Effect of rooibos extracts on palmitate uptake in C3A liver cells

Palmitate uptake was measured using radiolabelled ^{14}C palmitate. In the normal controls, insulin increased palmitate uptake but not significantly. Addition of palmitate reduced palmitate uptake, both under basal and insulin-stimulated conditions from 100.0 ± 4.1% to 65.0 ± 3.6% ($p < 0.01$) and from 149.6 ± 24.9% to 61.2 ± 2.3% ($p < 0.01$), respectively. Treating the palmitate-induced insulin-resistant C3A liver cells with FRE and GRE increased palmitate uptake from 65.0 ± 3.6% to 150.7 ± 12.2% ($p < 0.01$) and 137.7 ± 6.9% ($p < 0.5$), respectively under basal conditions. Insulin-stimulation increased palmitate uptake of GRE and FRE treated cells from 61.2 ± 2.3% to 111.0 ± 19.1% ($p < 0.05$) and 132.8 ± 7.7 ($p < 0.05$), respectively (Fig. 6.39).

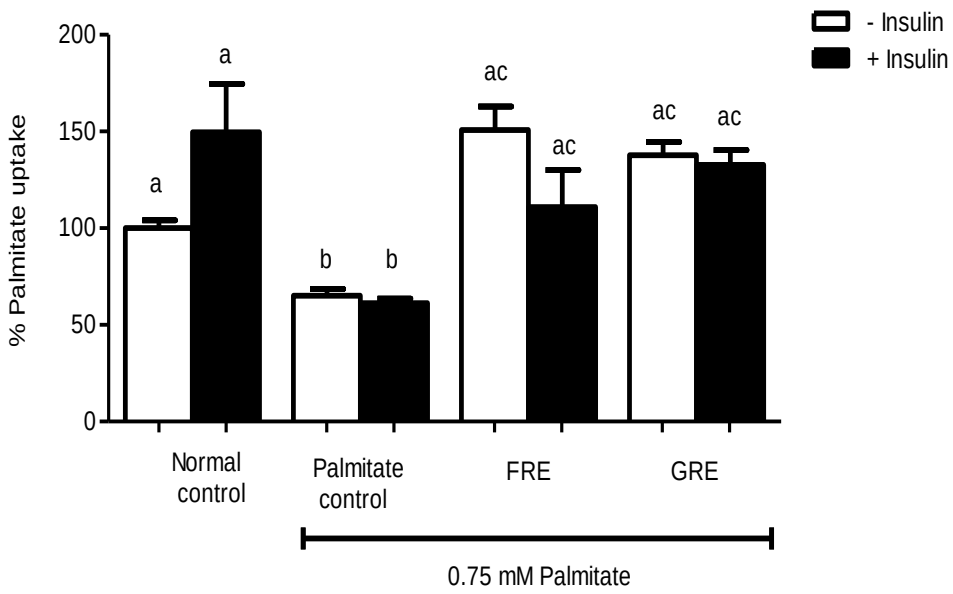

Figure 6.39. Effect of rooibos extracts (GRE and FRE) on palmitate uptake. C3A liver cells were cultured in DMEM supplemented with 8 mM glucose with or without 0.75 mM palmitate for 16 h and treated with GRE (10 µg/mL) or aspalathin (10 µM) for 3 h. Palmitate uptake was measured using ^{14}C palmitate. Results are expressed as the mean of three independent experiments relative to the control set at 100% ± SEM. Bars with different letters denote statistical differences at $p \leq 0.05$.

6.4.8.2. Effect of aspalathin, orientin, isoorientin and rutin on palmitate uptake

Aspalathin, orientin , isoorientin and rutin reversed the palmitate-induced reduction of basal palmitate uptake from 65.0 ± 3.6% to 152.8 ± 5.9% ($p < 0.001$), 139.9 ± 6.0% ($p < 0.001$), 122.6 ± 11.8% ($p < 0.05$) and 150.9 ± 5.5% ($p < 0.05$),respectively. Although the compounds tested increased insulin-stimulated palmitate uptake, only orientin and isoorientin showed significant increases from 61.2 ± 2.3% to 118.1 ± 12.5% ($p < 0.05$) and 121.8 ± 10.1% ($p < 0.05$), respectively (Fig 6.40).

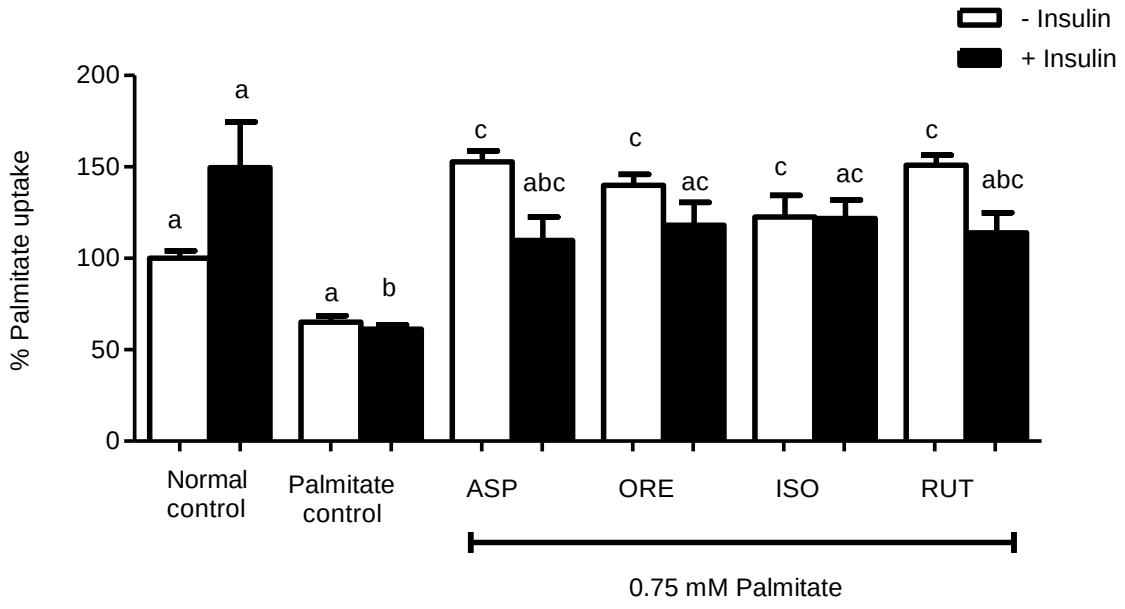

Figure 6.40. Effect of aspalathin (ASP), orientin (ORE), isoorientin (ISO) and rutin (RUT) on palmitate uptake. C3A liver cells were cultured in DMEM containing 8 mM glucose with or without 0.75 mM palmitate for 16 h and treated with ASP, ORE, ISO and RUT (10 µM) for 3 h. Palmitate uptake was measured using ^{14}C palmitate. Results are expressed as the mean of three independent experiments relative to the control set at 100% ± SEM. Bars with different letters denote statistical differences at $p \leq 0.05$.

6.4.10. Aspalathin-enriched green rooibos extract (GRE) and aspalathin reduced malonyl-CoA protein expression

Palmitate increased malonyl-CoA protein expression, in both basal and insulin-stimulated C3A liver cells by ~ 23.0% and 54.0% ($p < 0.01$), respectively. Treating the C3A liver cells with GRE or aspalathin reduced the palmitate-induced increase of malonyl-CoA from 123.7 ± 3.9% to 77.2 ± 6.2% ($p < 0.001$) and 84.7 ± 10.9% ($p < 0.01$) for basal cells and from 123.0 ± 5.5% to 85.3 ± 9.9% ($p < 0.001$) and 76.6 ± 3.7% ($p < 0.001$), respectively for insulin-stimulated cells (Fig. 6.41).

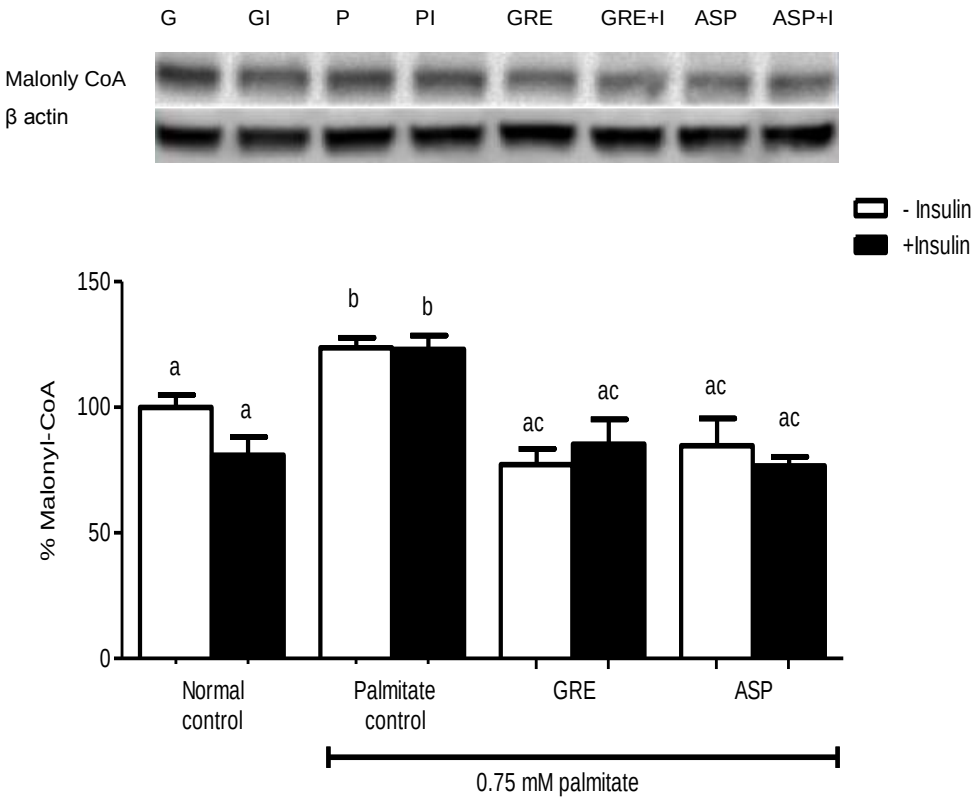

Figure 6.41. Effect of green rooibos extract (GRE) and aspalathin (ASP) on malonyl-CoA protein expression. C3A liver cells, cultured in 8 mM glucose with or without 0.75 mM palmitate for 16 h, were treated with GRE (10 µg/mL) or aspalathin (10 µM) for 3 h. Cells were lysed and subjected to Western blot analyses. Results are expressed as the mean of three independent experiments relative to the control set at 100% ± SEM. Bars with different letters denote statistical differences at $p \leq 0.05$.

6.4.11 Effect of aspalathin-enriched green rooibos extract (GRE) and aspalathin on CPT1 protein expression

Palmitate reduced basal CPT1 protein expression in C3A liver cells by ~59% ($p < 0.05$). GRE and aspalathin increased the protein expression of CPT1 in palmitate-treated C3A liver cells from 41.4 ± 2.4% to 120.0 ± 8.1% ($p < 0.001$) and 209.2 ± 4.2% ($p < 0.001$) for basal and from 73.5 ± 7.7% to 168.9 ± 11.5% ($p < 0.001$) and 318.9 ± 37.3% ($p < 0.001$) for insulin-stimulated CPT1 protein expression, respectively (Fig. 6.42).

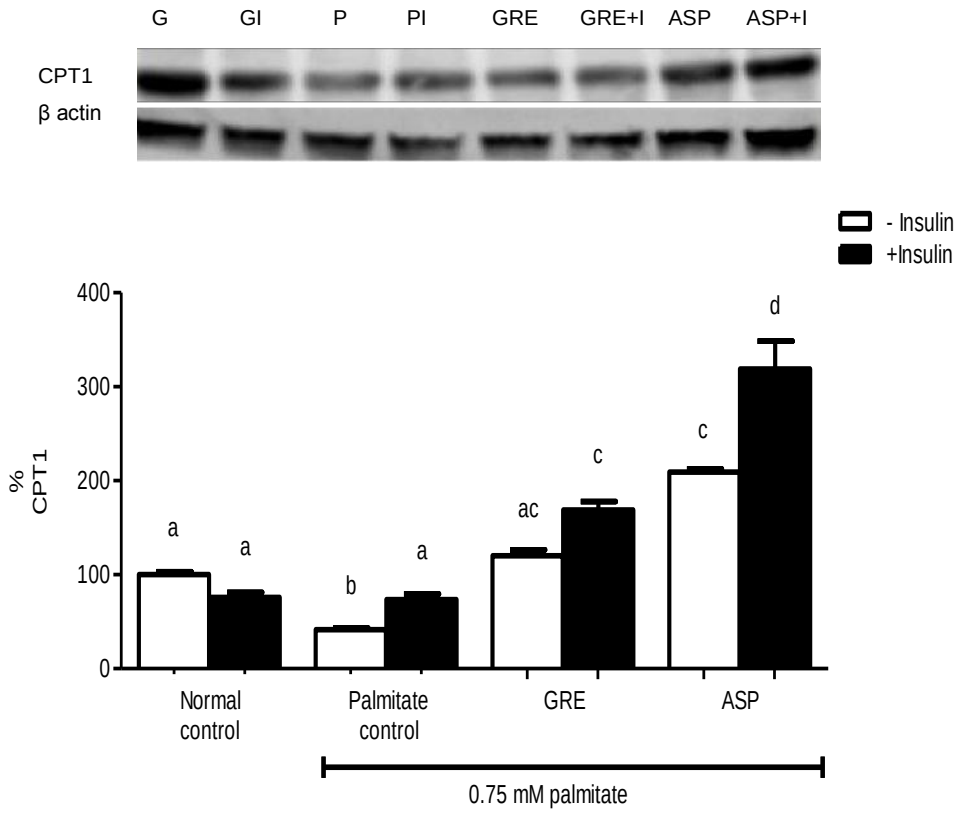

Figure 6.42. Effect of green rooibos extract (GRE) and aspalathin (ASP) on CPT1 protein expression. C3A liver cells were cultured in DMEM supplemented with 8 mM glucose with or without 0.75 mM palmitate for 16 h, and treated with GRE (10 µg/mL) or aspalathin (10 µM) for 3 h. Cells were lysed and subjected to Western blot analyses. Results are expressed as the mean of three independent experiments relative to the set at 100% ± SEM. Bars with different letters denote statistical differences at $p \leq 0.05$.

6.4.12. Effect of aspalathin-enriched green rooibos extract (GRE) and aspalathin on FOXO1 activation in C3A liver cells

Insulin increased FOXO1 activation by ~ 51% compared to the normal control. Palmitate treatment inhibited insulin-stimulated activation of FOXO1 from 151.7 ± 13.4% to 87.7 ± 10.6% ($p < 0.01$). GRE and aspalathin reversed the palmitate-induced inhibition of insulin-stimulated FOXO1 activation from 87.7 ± 10.6% to 203.3 ± 12.4% ($p < 0.001$) and 196.5 ± 12.8% ($p < 0.001$),respectively. In addition, aspalathin significantly increased basal activation by ~ 200% ($p < 0.001$) (Fig. 6.43).

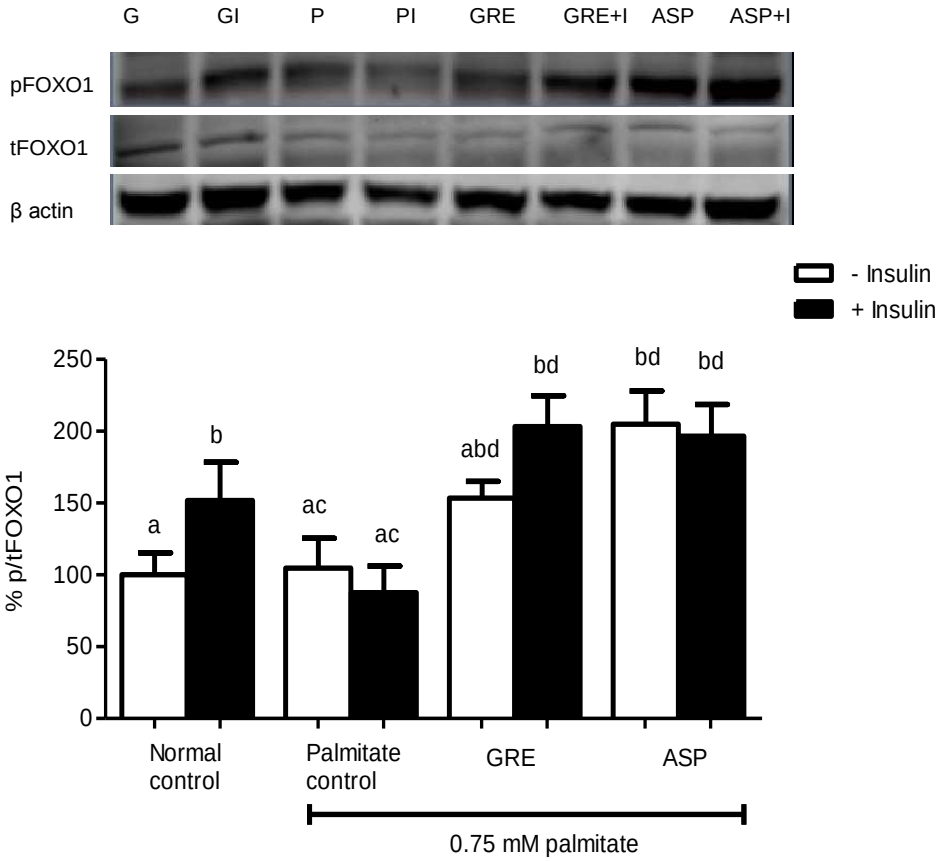

Figure 6.43. Effect of green rooibos extract (GRE) and aspalathin (ASP) on FOXO1 activation.
C3A liver cells were cultured in DMEM supplemented with 8 mM glucose with or without 0.75 mM palmitate for 16 h and treated with GRE (10 µg/mL) or aspalathin (10 µM) for 3 h. Cells were lysed and subjected to Western blot analyses. The % of pFOXO1/tFOXO1 was used to estimate FOXO1 activation. Results are expressed as the mean of three independent experiments relative to the control cells set at 100% ± SEM. Bars with different letters denote statistical differences at $p \leq 0.05$.

6.5. Effect of an aspalathin-enriched green rooibos extract (GRE) on obese insulin-resistant Wistar rats

In this study, male Wistar rats were fed an obesity-inducing diet ad *libitum* from weaning for twelve weeks to induce obesity and insulin resistance. OB/IR rats were treated daily with GRE at various doses (32, 97 and 195 mg/kg BW) for 12 weeks. Vildagliptin, a dipeptidyl peptidase-4 (DPP-4) inhibitor and a new generation hypoglycemic drug, was selected as a positive drug reference control. Vildagliptin improves dyslipidemia and reduces hyperglycemia in T2D. (Ahrén *et al.,* 2005). The purpose of the study was to investigate the effect of GRE on insulin resistance in diet-induced obese insulin-resistant Wistar rats.

6.5.1. Effects of aspalathin-enriched green rooibos extract (GRE) on body weight and fasting blood glucose concentrations in OB/IR Wistar rats

Body weights were measured before treatment (baseline), during and after treatment (4 weeks, 8 weeks and 12 weeks). There were no significant differences in body weight in any of the treatment groups for the duration of the study (Fig. 6.44 A and B). The GRE extract at doses of 97 and 195 mg/kg/day reduced glucose concentrations at 4 and 8 weeks compared to their baseline values. However, after 12 weeks of treatment GRE had no effect on blood glucose concentrations.

A

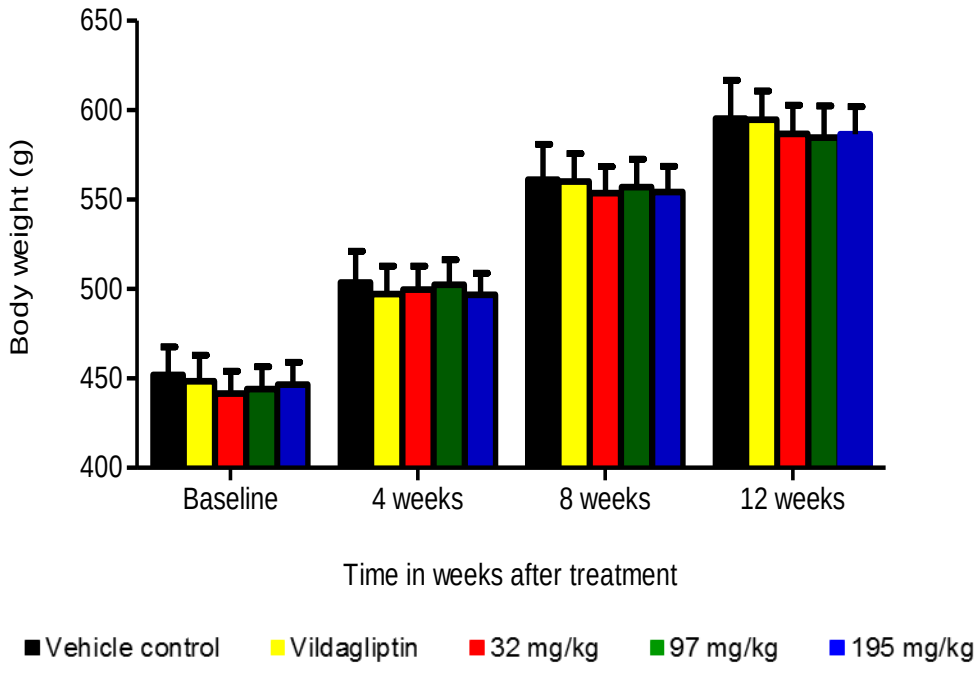

B

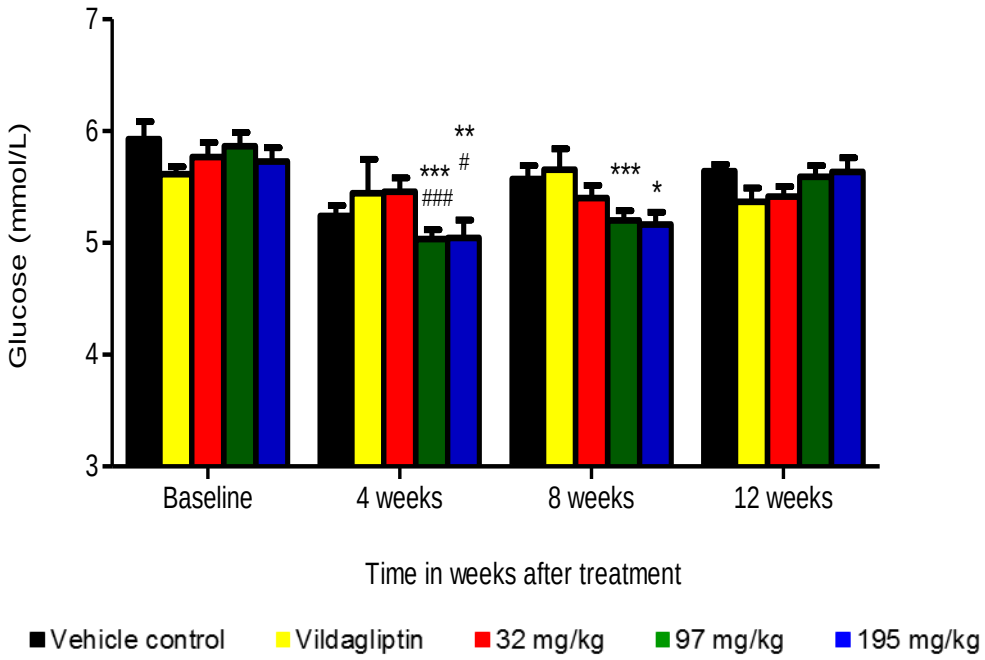

Figure 6.44. Body weights (A) and blood glucose (B) of OB/IR Wistar rats treated with GRE.
The body weights and blood glucose concentrations of OB/IR rats treated daily with GRE were measured at baseline, 4 weeks, 8 weeks and 12 weeks. The results are presented as mean ± SEM. * $p \leq 0.05$, ** $p < 0.01$, *** $p < 0.001$, vs. respective baseline values; # $p \leq 0.05$, ### $p < 0.001$ vs. untreated .control at 4 weeks after treatment.

6.5.2. Aspalathin-enriched green rooibos extract (GRE) reduces insulin concentrations after 12 weeks of treatment in OB/IR Wistar rats

The results showed that after 12 weeks of treatment, GRE at a dose of 195 mg/kg/day significantly reduced insulin concentrations compared to the control after a 16 h fast (Fig. 6.45 A) and reduced HOMA-IR values compared to control (Fig. 6.45 B).

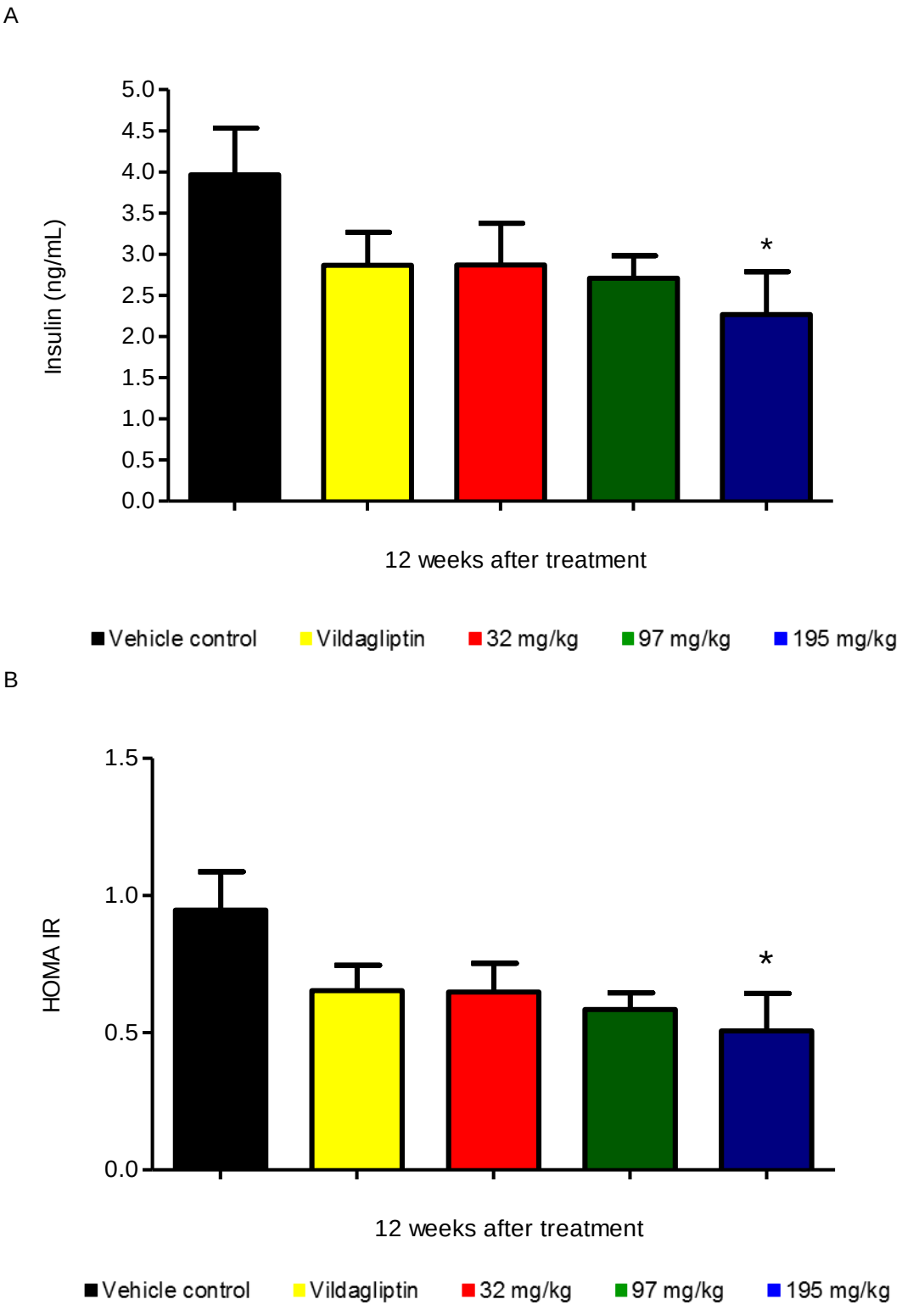

Figure 6.45. Insulin concentrations (A) and HOMA-IR values (B) of OB/IR Wistar rats after 12 weeks of treatment. HOMA-IR as calculated from fasting glucose and insulin concentrations after 12 weeks of treatment. The results are presented as mean ± SEM. * $P \leq 0.05$.

6.5.3. Effect of aspalathin-enriched green rooibos extract (GRE) on insulin receptor (Insr) mRNA and protein expression in muscle of OB/IR Wistar rats

GRE (195 mg/kg) increased Insr mRNA expression from 100.0 ± 25.9 to 1223.0 ± 404.7% (p < 0.001) (Fig. 6.46 A.). In contrast to mRNA expression, GRE and vildagliptin reduced INSR protein expression albeit not significantly (Fig. 6.46 B).

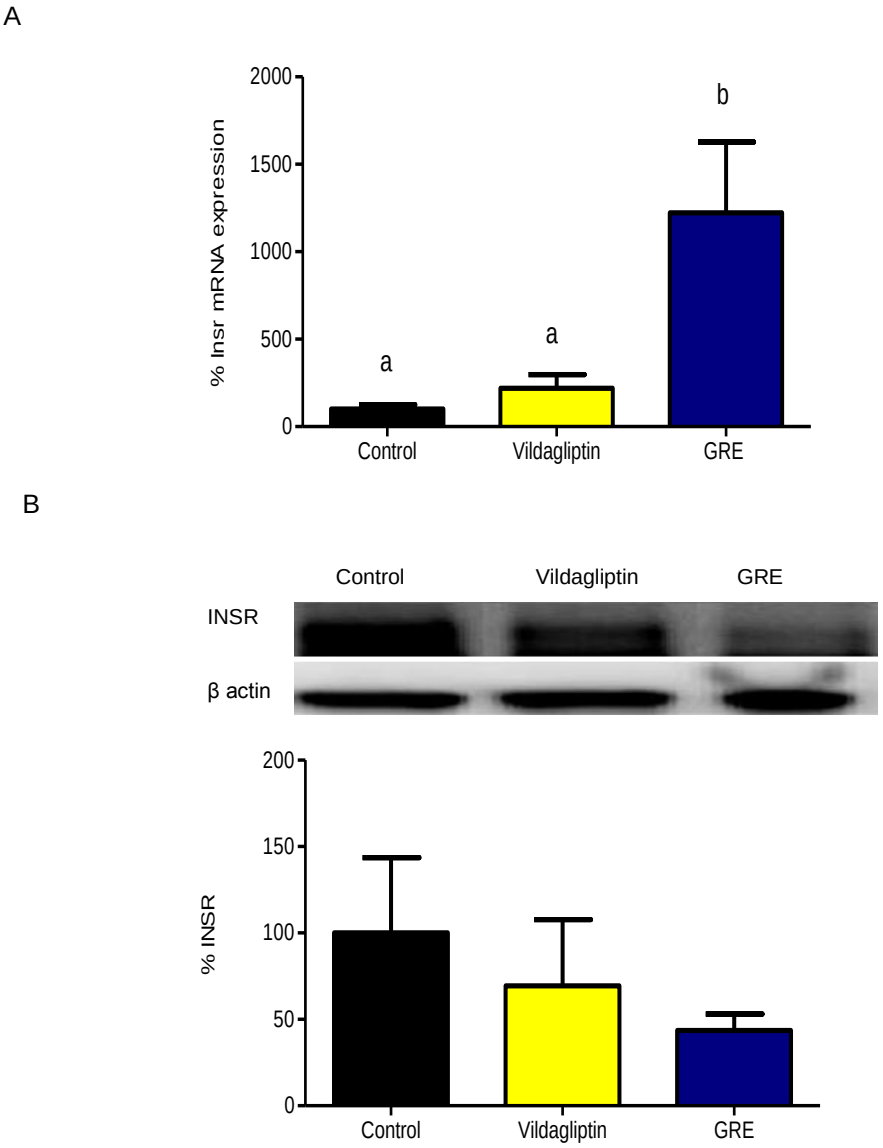

Figure 6.46. Effect of green rooibos extract (GRE) on Insr mRNA (A) and INSR protein expression (B) in the muscle of OB/IR Wistar rats. OB/IR rats were treated with Vildagliptin (10 mg/kg) or GRE (195 mg/kg) for 12 weeks. Messenger RNA was extracted from skeletal muscle tissue and quantified by RT-PCR. Protein expression was analysed by Western blot. Data are reported as mean ± SEM of OB/IR rats (n = 6). Bars with different letters denote statistical differences between results at $p \leq 0.05$.

6.5.4. Effect of aspalathin-enriched green rooibos extract (GRE) on Irs1 and Irs2 mRNA expression in the muscle of OB/IR Wistar rats

The effect of GRE on Irs1 and Irs2 mRNA expression was measured. The Irs1 mRNA expression was slightly increased compared to the non-treated control, however, this increase was not significant (Fig. 6.47 A). Similar results were observed with Irs2 expression in muscle (Fig. 6.47 B).

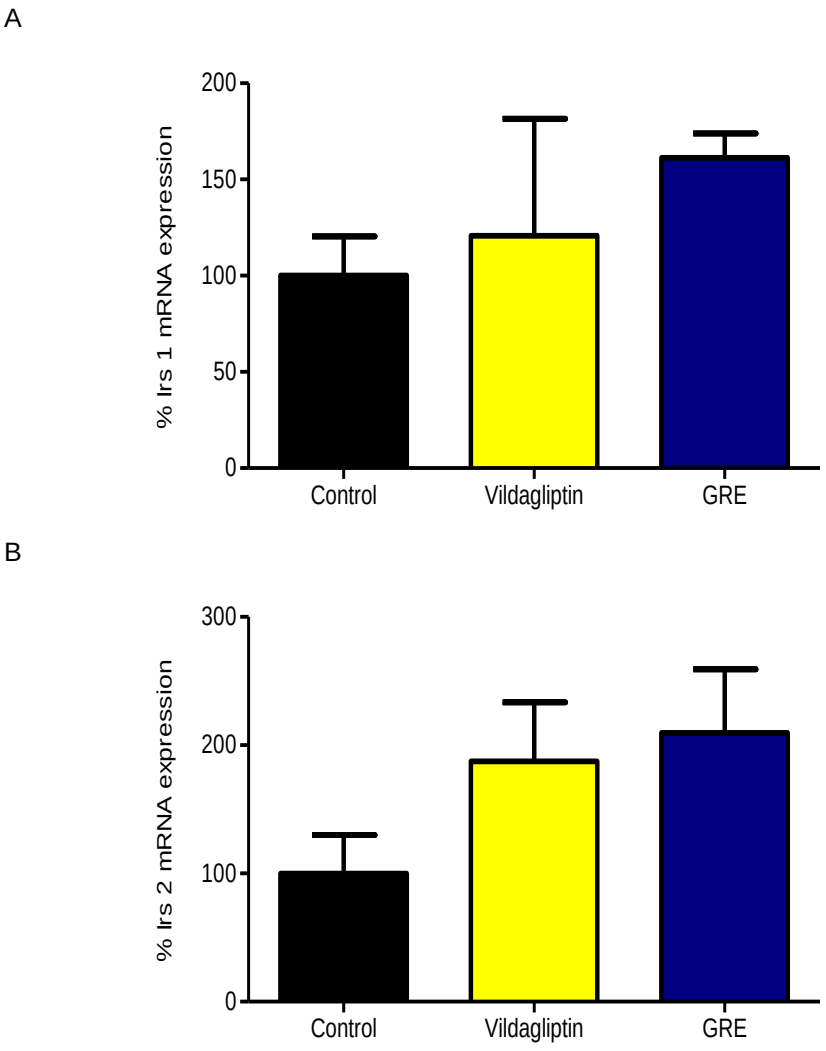

Figure 6.47. Effect of green rooibos extract (GRE) on Irs1 (A) and Irs2 (B) mRNA expression in the muscle of OB/IR Wistar rats. OB/IR rats were treated with Vildagliptin (10 mg/kg) or GRE (195 mg/kg) for 12 weeks. Messenger RNA was extracted from skeletal muscle tissue and quantified by RT-PCR. Data are reported as mean ± SEM of OB/IR rats (n = 6).

6.5.5. Effect of aspalathin-enriched green rooibos extract (GRE) on Pi3k, mRNA and protein expression in the muscle of OB/IR male Wistar rats

OB/IR rats treated with GRE for 12 weeks showed an increase in Pi3k mRNA expression from 100 ± 19.9% to 249 ± 69.5% ($p < 0.05$) (Fig. 6.48 A). GRE had no detectable effect on PI3K protein expression (Fig.6.48 B).

A

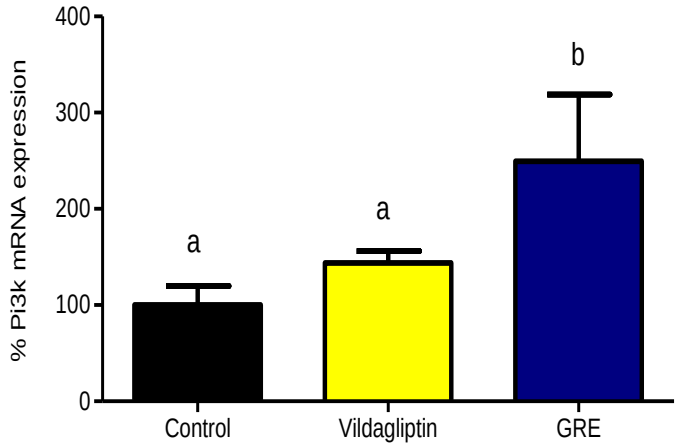

B

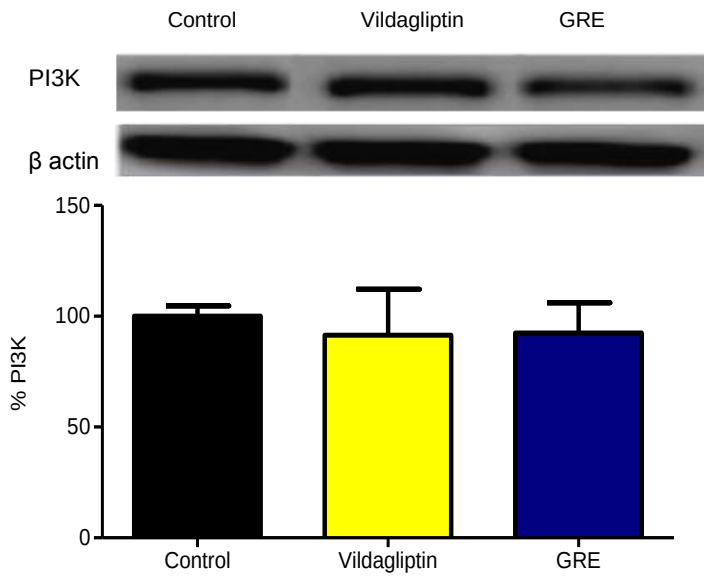

Figure 6.48. Effect of green rooibos extract (GRE) on Pi3k mRNA (A) and PI3K protein (B) expression in the muscle of OB/IR Wistar rats. OB/IR rats were treated with Vildagliptin (10 mg/kg) or GRE (195 mg/kg) for 12 weeks. Messenger RNA was extracted from skeletal muscle tissue and quantified by RT-PCR. Protein expression was analysed by Western blot. Data are reported as mean ± SEM of OB/IR rats (n = 6). Bars with different letters denote statistical differences between results at $p \leq 0.05$.

6.5.6. Effect of aspalathin-enriched green rooibos extract (GRE) on Ampk mRNA and protein expression in the muscle of OB/IR rats

GRE significantly increased Ampk mRNA expression from 100.0 ± 18.4% to 358.0 ± 61.4% ($p < 0.001$) (Fig. 6.49 A). At a protein level, GRE resulted in a slight non-significant increase in AMPK activation (Fig. 6.49 B).

A

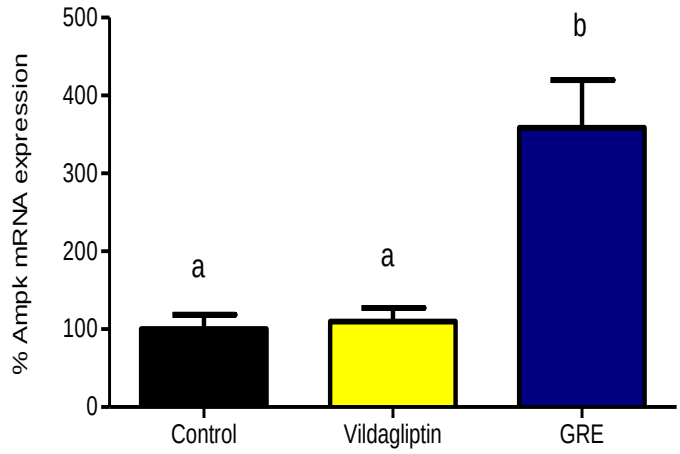

B

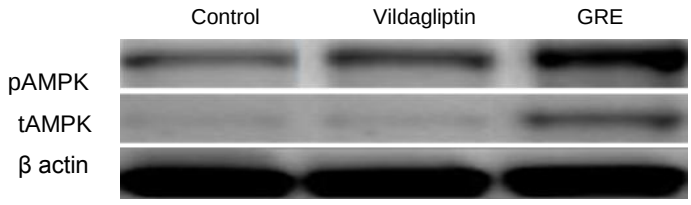

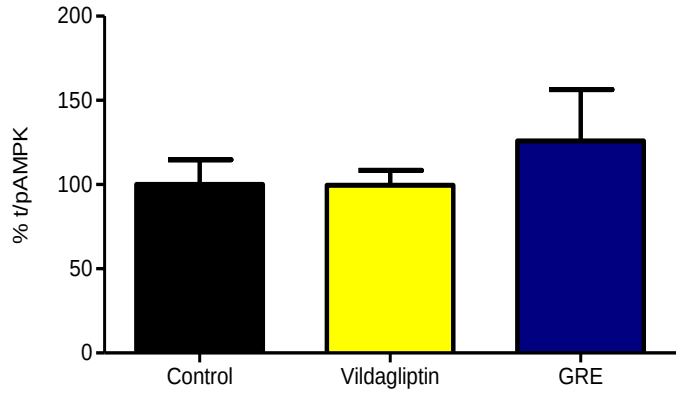

Figure 6.49. Effect of green rooibos extract (GRE) on Ampk mRNA expression (A) and AMPK protein expression (B) in the skeletal muscle of OB/IR Wistar rats. OB/IR rats were treated with Vildagliptin (10 mg/kg) or GRE (195 mg/kg) for 12 weeks, Messenger RNA was extracted from skeletal muscle tissue and quantified by RT-PCR. Proteins were analysed by Western blot. Data are reported as mean ± SEM of OB/IR rats (n = 6). Results are reported as mean ± SEM of n = 6 rats. Bars with different letters denote statistical differences between results at $p \leq 0.05$.

6.5.7. Effect of aspalathin-enriched green rooibos extract (GRE) on Glut4 mRNA expression in the muscle of OB/IR Wistar rats

GRE increased Glut4 mRNA expression in the skeletal muscle of OB/IR rat from 100 ± 10.3% to 223 ± 29.2% ($p < 0.01$) compared to untreated control (Fig. 6.50).

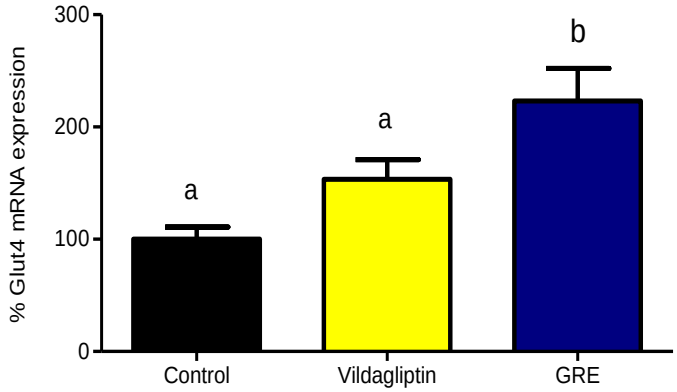

Figure 6.50 Effect of green rooibos extract (GRE) on Glut4 mRNA expression in the skeletal muscle of OB/IR Wistar rats. OB/IR rats were treated with Vildagliptin (10 mg/kg) or GRE (195 mg/kg) for 12 weeks. Messenger RNA was extracted from skeletal muscle tissue and quantified by RT-PCR. Data are reported as mean ± SEM of OB/IR rats (n = 6). Bars with different letters denote statistical differences between results at $p \leq 0.05$.

6.5.8. Effect of aspalathin-enriched green rooibos extract (GRE) on insulin receptor (Insr) mRNA and protein expression in the liver of OB/IR Wistar rats

GRE significantly increased Insr mRNA expression from 100 ± 9.8% to 170.4 ± 7.8% ($p < 0.01$) (Fig. 6.51A). GRE had no detectable effect on INSR protein expression (Fig. 6.51 B).

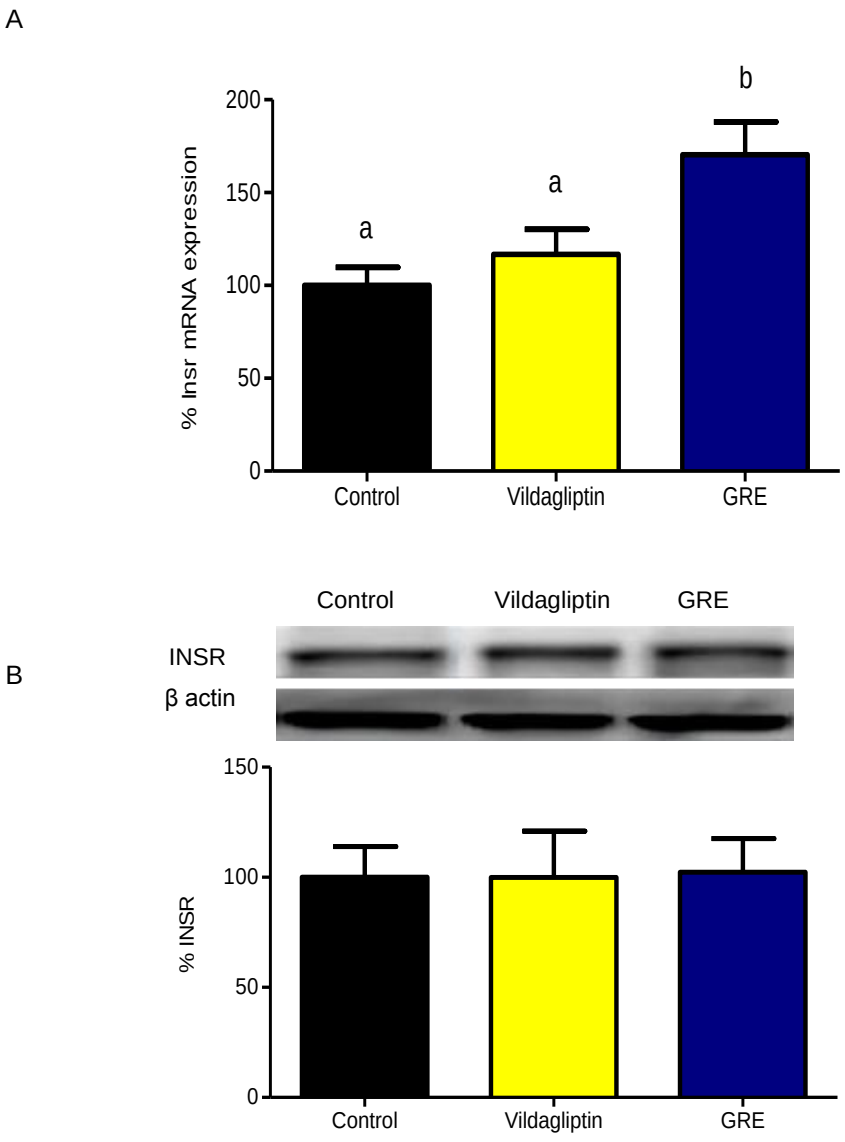

Figure 6.51. Effect of green rooibos extract (GRE) on Insr mRNA (A) and INSR protein (B) expression in the liver of OB/IR Wistar rats. OB/IR rats were treated with Vildagliptin (10 mg/kg) or GRE (195 mg/kg) for 12 weeks. Messenger RNA was extracted from liver tissue and quantified by RT-PCR. Protein expression was analysed by Western blot. Data are reported as mean ± SEM of OB/IR rats (n = 6). Bars with different letters denote statistical differences between results at $p \leq 0.05$.

5.5.9. Effect of aspalathin-enriched green rooibos extract (GRE) on Irs1 and Irs2 mRNA expression in the liver of OB/IR rats

GRE increased Irs1 mRNA expression in the liver from 100.0 ± 18.3% to 400.7 ± 68.9% ($p < 0.05$) (Fig. 6.52 A). Similarly, GRE enhanced the Irs2 mRNA expression from 100.0 ± 6.9% to 190.4 ± 36.9% ($p < 0.05$) (Fig. 6.52. B).

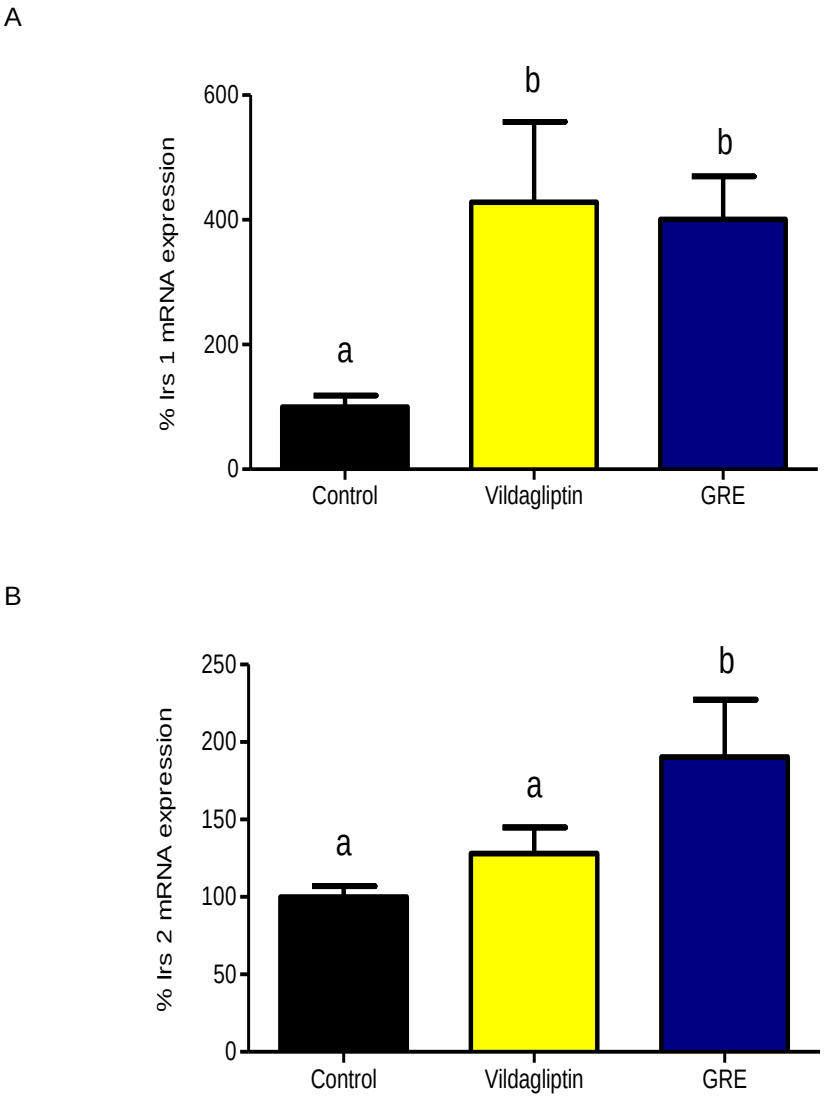

Figure 6.52. Effect of green rooibos extract (GRE) on Irs1 (A) and Irs2 (B) mRNA expression in the liver of OB/IR Wistar rats. OB/IR rats were treated with Vildagliptin (10 mg/kg) or GRE (195 mg/kg) for 12 weeks. Messenger RNA was extracted from liver tissue and quantified by RT-PCR. Data are reported as mean ± SEM of OB/IR rats (n = 6). Bars with different letters denote statistical differences between results at $p \leq 0.05$.

6.5.10. Effect of aspalathin-enriched green rooibos extract (GRE) on Pi3k gene and protein expression in the liver of OB/IR Wistar rats

GRE increased Pi3k mRNA expression from 100.0 ± 54.2% to 220.7 ± 28.6% ($p < 0.01$) (Fig. 6.53 A). GRE had no detectable effect on PI3K protein expression (Fig. 6.53 B).

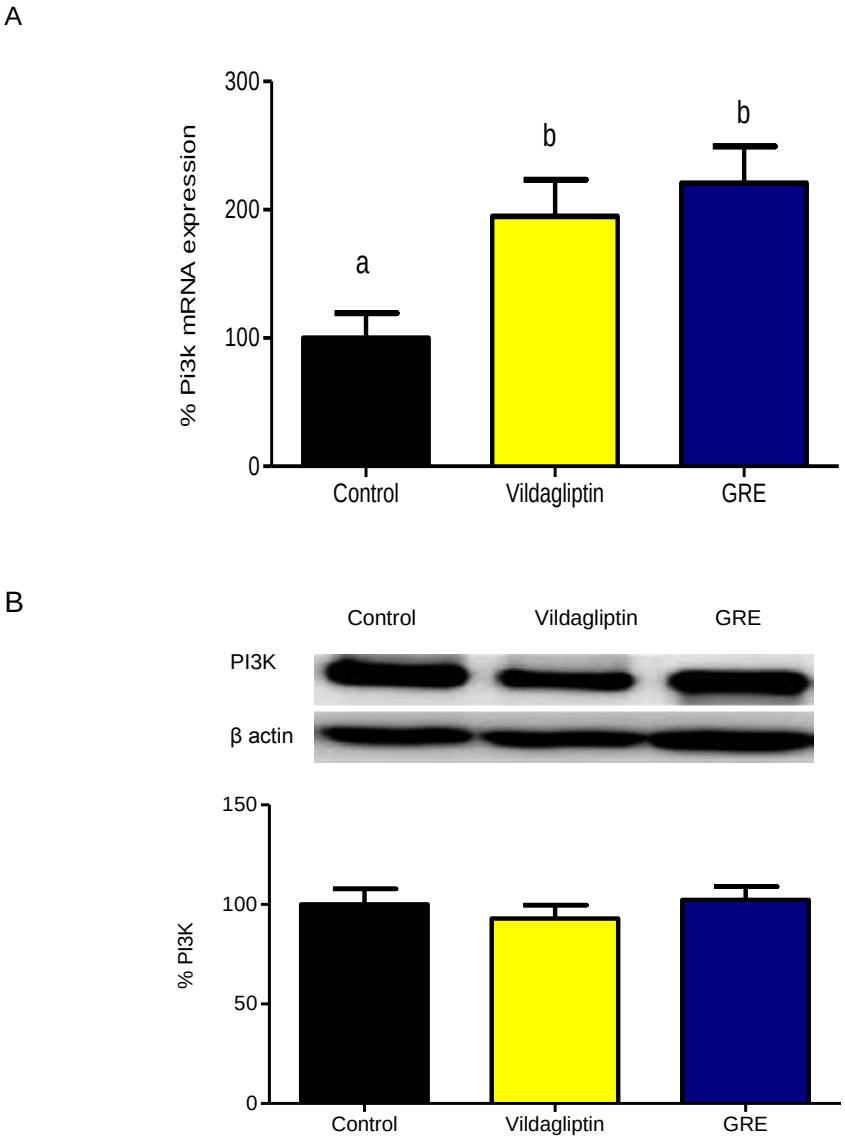

Figure 6.53. Effect of green rooibos extract (GRE) on the Pi3k mRNA (A) and PI3K protein (B) expression in the liver of OB/IR Wistar rats. OB/IR were treated with Vildagliptin (10 mg/kg) or GRE (195 mg/kg) for 12 weeks. Messenger RNA was extracted from liver tissue and quantified by RT-PCR. Protein expression was analysed by Western blot. Data are reported as mean ± SEM of OB/IR rats (n = 6). Bars with different letters denote statistical differences between results at $p \leq 0.05$.

6.5.11. Effect of aspalathin-enriched green rooibos extract (GRE) on AMPK mRNA and protein expression

GRE significantly increased Ampk mRNA expression from 100.0 ± 14.6 to 320.4 ± 54.9% ($p < 0.001$) (Fig. 6.54 A). GRE had no detectable effect on AMPK protein expression (Fig 6.54 B).

A

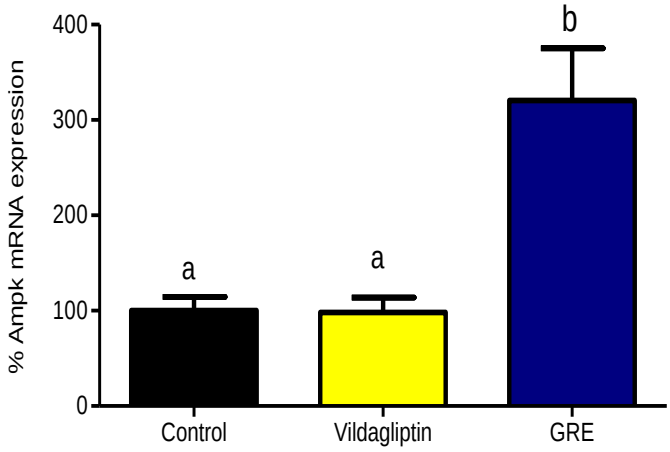

B

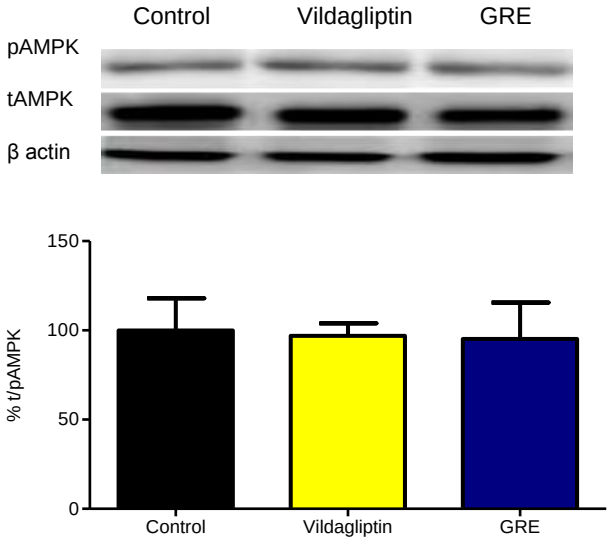

Figure 6.54. Effect of green rooibos extract (GRE) on Ampk mRNA (A) and AMPK protein (B) expression in the liver of OB/IR Wistar rats. OB/IR rats were treated with Vildagliptin (10 mg/kg) or GRE (195 mg/kg) for 12 weeks. Messenger RNA was extracted from liver tissue and quantified by RT-PCR. Proteins were analysed by Western blot. Data are reported as mean ± SEM of OB/IR rats (n = 6). Bars with different letters denote statistical differences between results at $p \leq 0.05$.

6.5.12. Effect of aspalathin-enriched green rooibos extract (GRE) on Glut2 mRNA expression in the liver of OB/IR Wistar rats

OB/IR Wistar rats treated with GRE had no effect on the Glut2 mRNA gene expression in the liver (Fig. 6.55).

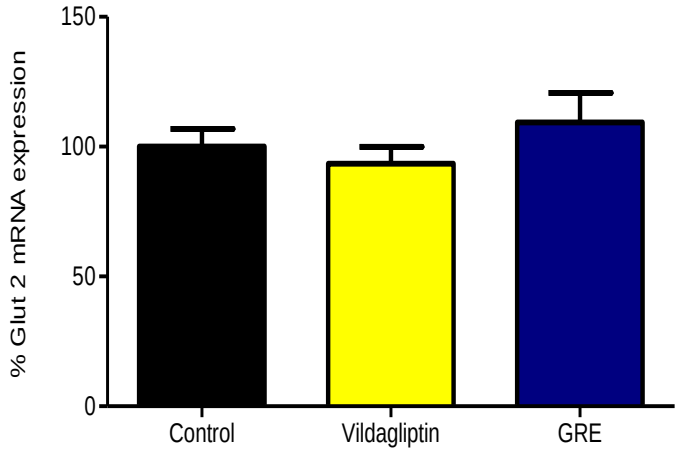

Figure 6.55. Effect of rooibos extract (GRE) on Glut2 mRNA gene expression of in the liver of OB/IR Wistar rats. OB/IR rats were treated with Vildagliptin (10 mg/kg) or GRE (195 mg/kg) for 12 weeks. Messenger RNA was extracted from liver tissue and quantified by RT-PCR. Data are reported as mean ± SEM of OB/IR rats (n = 6). The figure shows representative data presented as the mean ± SEM of n = 6 rats.

6.6. Summary of results

Table 6.1. Summary of the *in vitro* metabolic effects of FRE, GRE, aspalathin, orientin, isoorientin and rutin in C2C12 muscle cells, 3T3-L1 adipocytes and C3A liver cells.

		C2C12		3T3-L1		C3A	
Parameter	**Treatment**	**Basal**	**Insulin-stimulation**	**Basal**	**Insulin-stimulation**	**Basal**	**Insulin-stimulation**
Glucose uptake	FRE	↑	↑	NE	↑	NE	↑
	GRE	↑	↑	↑	↑	NE	NE
	ASP	↑	NE	↑	↑	NE	NE
	ORE	↑	↑	↑	↑	NE	NE
	ISO	↑	↑	↑	↑	NE	NE
	RUT	↑↑	↑↑	↑	↑	NE	NE
Palmitate uptake	FRE	ND	ND	↑	↑	↑	↑
	GRE	ND	ND	↑	↑	↑	↑
	ASP	ND	ND	↑	↑	↑	↑
	ORE	ND	ND	↑	↑	↑	↑
	ISO	ND	ND	↑	↑	↑	↑
	RUT	ND	ND	↑	↑	↑	↑
MTT	FRE	↑↑	↑↑	↑	↑	NE	NE
	GRE	↑	↑	↑	↑	NE	NE
	ASP	↑	↑	↑	↑	NE	NE
	ORE	↑↑	↑↑	↑	↑	NE	NE
	ISO	↑↑	↑↑	↑	↑	NE	NE
	RUT	↑	↑	↑	↑	NE	NE
ATP	FRE	↑	↑	↑	↑	↑	↑
	GRE	↑	↑↑	↑	↑↑	↑	↑
	ASP	↑	↑	↑	↑	↑	↑
	ORE	↑	↑	↑	↑	↑	↑
	ISO	↑	↑	↑	↑	↑	↑
	RUT	↑↑	↑↑	↑	↑	↑	↑

Activity relevant to the palmitate treated controls are indicated as follows:

NE no significant effect detected, ↑ increased from relevant palmitate control, ↑↑ increased relative to palmitate and normal controls and ND not done.

Table 6.2. Summary of signalling protein expression in palmitate-treated C2C12 muscle cells, 3T3-L1 adipocytes and C3A liver cells treated with GRE and aspalathin.

		C2C12		3T3-L1		C3A	
Proteins	**Treatment**	**Basal**	**Insulin-stimulation**	**Basal**	**Insulin-stimulation**	**Basal**	**Insulin-stimulation**
*PKCθ	GRE	↓	↓	ND	ND	ND	ND
	ASP	↓	↓	ND	ND	ND	ND
*N-FkB	GRE	ND	ND	↓	↑	ND	ND
	ASP	ND	ND	↓	↓	ND	ND
IR	GRE	↑	↑	↑	NE	ND	ND
	ASP	↑	↑	↑	↑	ND	ND
IRS1 Ser 307	GRE	NE	NE	ND	ND	ND	ND
	ASP	NE	NE	ND	ND	ND	ND
†PI3K(p85)	GRE	NE	NE	NE	NE	↑	NE
	ASP	↑	↑↑	NE	NE	↑	NE
†AKT(Ser 473	GRE	NE	↑	NE	↑↑	NE	↑
	ASP	NE	↑	NE	↑	NE	NE
†AMPK	GRE	NE	NE	↓	↓	↑↑	↑↑
	ASP	↑	NE	NE	NE	↑↑	↑↑
GLUT4	GRE	↑	↑	↑	↑	ND	ND
	ASP	NE	↑	NE	NE	ND	ND
GLUT2	GRE	ND	ND	ND	ND	↑	↑
	ASP	ND	ND	ND	ND	↑	↑↑
PPARg	GRE	ND	ND	NE	NE	ND	ND
	ASP	ND	ND	↑	↑	ND	ND
PPARα	GRE	ND	ND	NE	NE	ND	ND
	ASP	ND	ND	NE	↑	ND	ND
Malonyl CoA	GRE	ND	ND	NE	NE	↑	↑
	ASP	ND	ND	NE	NE	↑	↑
CPT1	GRE	ND	ND	↑↑	NE	↑	↑
	ASP	ND	ND	↑	↑	↑	↑↑
†FOXO1	GRE	ND	ND	ND	ND	↑	↑
	ASP	ND	ND	ND	ND	↑	↑

Protein expression expressed relative to β actin. Palmitate treated controls are indicated as follows:

†Indicates the activated protein as determined by total protein/phosphorylated protein % ratio.

NE no significant effect detected, ↑ increased from relevant palmitate control, ↑↑ increased relative to palmitate and normal controls and ND not done.

Table 6.3. Summary of muscle and liver gene and protein expression results following treatment of OB/IR Wistar rats with GRE for 12 weeks.

Proteins	Muscle	Liver	Genes	Muscle	Liver
IR	NE	NE	Ir	↑	↑
IRS1	ND	↑	Irs1	↑	↑
IRS2	ND	↑	Irs2	↑	↑
PI3K	NE	NE	Pi3k	↑	↑
†AMPK	↑	↑	Ampk	↑	↑
GLUT4	ND	ND	Glut4	↑	ND
GLUT2	ND	ND	Glut2	ND	NE

Protein expression expressed relative to β actin are indicated as follows:

†Indicates the activated protein as determined by total protein/phosphorylated protein % ratio.

NE no significant effect detected, ↑ increased from relevant palmitate control, ↑↑ increased relative to palmitate and normal controls and ND not done

Chapter 7

Discussion

7.1. Preparation and phenolic composition of rooibos extracts

Most commonly rooibos is consumed as an infusion of fermented rooibos. For this study two extracts, a hot water extract produced from fermented rooibos (FRE) and a solvent-based aspalathin-enriched extract from unfermented or green rooibos (GRE) were used. The phenolic composition of the hot water extract of fermented rooibos is similar to that of a hot water infusion of rooibos ("cup of tea") (Joubert *et al.,* 2012). The solvent-based extract of green rooibos provided not only increased levels of aspalathin, but also that of other flavonoids. To eliminate batch-to-batch variation, which presents a major problem for plant-based research, the extracts used in this study were from the same batches as previously used by Dludla *et al.* (2013) and Muller *et al.* (2012) for FRE and GRE, respectively. Extracts were stored under vacuum desiccation at room temperature. Based on HPLC-DAD analysis of the extracts the total content of the quantified phenolic compounds was approximately 670% higher in GRE compare to FRE, with aspalathin comprising ~70%. The other phenolic compounds shown to be present in increased amounts in GRE included orientin, isoorientin and rutin. Enolic phenylpyruvic acid-2-*O*-glucoside (PPAG) was the only phenolic compound present at a higher concentration in FRE.

7.2. Motivation for selecting rooibos extracts (GRE and FRE)

Many of the beneficial metabolic effects of rooibos have been attributed to the presence of the flavonoid, aspalathin. Kawano *et al.* (2009) reported that aspalathin increases glucose uptake in muscle cells and insulin secretion from pancreatic β-cells. In our laboratory, we confirmed the hypoglycemic activity of GRE both *in vitro* and *in vivo* (Muller *et al.,* 2012). Beltrán-Debón *et al.* (2011) demonstrated a hypolipidemic effect of an aqueous extract of rooibos in LDLr-/- mice fed a high fat diet, but this effect was stringently dependent on diet type. Although not explicitly stated, the total phenolic content of the extract as determined by the Folin-Ciocalteu method (25 g/100 g),

compared to previous chemical composition analyses of fermented and green rooibos extracts by Joubert *et al.* (2008), suggests the extract was prepared from fermented rooibos. Currently limited information is available on the effect of rooibos in insulin resistance, and no comparative studies that relate to the phenolic composition and efficacy of rooibos extracts are available. Previously Muller *et al.* (2012) demonstrated an effective concentration response for GRE on *in vitro* glucose uptake in C2C12 muscle and Chang cells. Furthermore, they also demonstrated that GRE was more effective than the single compounds, aspalathin and rutin. However, aspalathin and rutin in a 1:1 (m/m) combination further enhanced glucose uptake providing evidence of possible synergistic or addictive effects between the different polyphenolic compounds.

7.3. *In vitro* concentration response study

Optimal concentration-response studies for FRE and GRE, as well as the phenolic compounds aspalathin, orientin, isoorientin and rutin, were established by measuring glucose uptake in normal insulin responsive C2C12 muscle, 3T3-L1 adipocytes and C3A liver cells. Muller *et al.* (2012) showed that GRE increased glucose uptake in a concentration dependent manner within a concentration range of 0.00005 to 50 µg/mL in C2C12 muscle cells. Subsequently, FRE was shown to have a similar efficacy within a range of 0.0001-10 µg/mL. Maximal activity was shown to be in a range of 5 to 10 µg/mL (Fig. 6.1 A). For 3T3-L1 adipocytes and C3A liver cells both FRE and GRE enhanced glucose uptake across the concentration range tested (0.0001-100 µg/mL) (Fig. 6.1 B, C and 6.2 B, C). Although, we anticipated that, based on the higher flavonoid content of GRE, it would be more effective than FRE, the concentration-response studies showed that in terms of glucose uptake, MTT activity and intracellular ATP content, the extracts had similar activity. In FRE, however, the increased amount of Z-2-(β-D-glucopyranosyloxy)-3-phenylpropenoic acid (PPAG), previously shown to enhance glucose uptake (Muller *et al.,* 2013), could have enhanced its efficacy. The higher level of PPAG in FRE, however, can not fully explain the similar activity of FRE and GRE. Other factors such as synergistic effect, rather than the concentrations of the active compounds present in GRE and FRE, and compounds not considered could have contributed to the efficacy of the extracts.

Based on these findings 10 µg/mL for FRE and GRE was selected for all subsequent experiments.

For the phenolic compounds, based on the efficacy of orientin and rutin, shown to have the lowest activity and only effective in the 10-100 µM range in C2C12 muscle cells (Fig. 6.4 A and Fig. 6.6 A), a concentration of 10 µM was selected for further *in vitro* testing for all compounds. This is in agreement with Muller *et al.* (2012) who showed that aspalathin was effective in C2C12 muscle cells within a dose range of 0.05-50 µM. Furthermore, Son *et al.* (2013) showed increased glucose uptake by aspalathin in L6 muscle cells in a dose dependent manner from a concentration of 25-100 µM. No cytotoxicity was observed for the selected concentration ranges (results not shown).

7.4. Induction of insulin resistance by palmitate in muscle cells

Several other studies have reported on the effect of palmitate on glucose uptake (Usui *et al.,* 1999; Gaster *et al.,* 2005; Sawada *et al.,* 2012). Yang *et al.* (2013) showed a reduction in glucose uptake by palmitate at a concentration range of 0.1 to 0.6 mM, while Tsuchiya *et al.* (2010) reported a reduction in glucose uptake at a concentration of 0.5 mM. For this study, the addition of 0.75 mM palmitate significantly reduced glucose uptake in C2C12 muscle cells, 3T3-L1 adipocytes and C3A liver cells over a 16 h period (Fig. 6.7; 6.17 and 6.32) Insulin resistance was confirmed by the blunted effect of insulin on glucose uptake following palmitate exposure. In palmitate-treated C2C12 muscle and C3A liver cells insulin had no effect on glucose uptake, while in 3T3-L1 adipocytes some insulin response was still present, albeit significantly attenuated compared to the cells not exposed to palmitate. Metformin, a commonly used oral hypoglycemic drug to which an insulin sensitizing effect is attributed, failed to restore or to ameliorate insulin resistance.

7.5. Effect of rooibos extracts (FRE and GRE) and compounds on palmitate-induced insulin resistance

7.5.1. Glucose uptake and metabolism

Exposure of C2C12 muscle cells to FRE significantly increased basal glucose uptake from the reduced levels of the palmitate controls. However, glucose uptake was still significantly lower than that of the normal untreated control cells. FRE had no effect on insulin sensitivity as glucose uptake was not enhanced compared to basal glucose uptake. Treating palmitate-induced insulin resistant C2C12 muscle cells with GRE normalised basal glucose uptake, but failed to normalise insulin-stimulated glucose uptake compared to the insulin response of normal control cells (Fig. 6.8 A). In contrast to the insulin-resistant C2C12 muscle cells, FRE was able to normalise basal glucose uptake and to restore insulin sensitivity in 3T3-L1 adipocytes. GRE significantly increased basal glucose uptake, and restored insulin sensitivity relative to normal controls not exposed to palmitate (Fig. 6.18 A). In C3A liver cells, both FRE and GRE normalised basal glucose uptake but failed to restore insulin sensitivity (Fig. 6.33 A).

To further estimate the effect of the extracts on glucose metabolism, mitochondrial dehydrogenase activity and cellular ATP content were evaluated in palmitate-induced insulin-resistant cells. In palmitate-treated C2C12 muscle cells both FRE and GRE reversed the palmitate-induced reduction in mitochondrial dehydrogenase activity (Fig. 6.8 B). In terms of cellular ATP content, both FRE and GRE increased the ATP content to above that of the insulin-stimulated normal control (Fig. 6.8 C). In 3T3-L1 adipocytes, mitochondrial dehydrogenase activity was normalised by both FRE and GRE (Fig. 6.18 B). The palmitate-induced decrease in ATP content was reversed by both FRE and GRE and, in the case of GRE, insulin-stimulated ATP content was increased to above the normal control (Fig. 6.18 C). Similarly, significant increases in cellular ATP content were demonstrated for FRE and GRE in C3A liver cells, while the extracts had no effect on mitochondrial activity (Fig. 6.33 B).

In C2C12 muscle cells, the phenolic compounds tested (aspalathin, orientin, isoorientin and rutin) normalised basal glucose uptake from the palmitate-induced

decreased levels, however no significant increase in glucose uptake was detected following insulin stimulation (Fig. 6.9 A). In 3T3-L1 adipocytes basal glucose uptake was normalised by aspalathin, orientin and isoorientin. Rutin was most effective by increasing basal glucose uptake to the same level achieved by insulin in the normal control cells. Aspalathin, orientin, isoorientin and rutin significantly increased and restored insulin sensitivity (Fig. 6.19 A). However, with rutin insulin stimulation did not further increase the insulin-stimulated glucose uptake from the already increased basal glucose uptake level. This probably indicates that rutin maximally stimulates basal glucose uptake in 3T3-L1 adipocytes and therefore has reached saturation levels for adipocytes. In the C3A liver cells, aspalathin, orientin, isoorientin and rutin normalised basal glucose uptake, but did not improve the insulin-stimulated glucose response (Fig. 6.34 A).

In C2C12 muscle cells, mitochondrial activity was either restored (aspalathin and rutin) from the decreased palmitate-induced levels or increased in the case of orientin and isoorientin, however the compounds had no effect on insulin stimulation (Fig. 6.9 B). Similar results were evident for ATP where ATP content were normalised to basal levels and insulin stimulation had no additional effect (Fig. 6.9 C). Similar effects were observed in 3T3-L1 adipocytes for basal mitochondrial activity (Fig. 6.19 B). In 3T3-L1 adipocytes, aspalathin, orientin, isoorientin and rutin normalised basal ATP content, while insulin stimulation significantly increased ATP content to above the levels in the normal controls (Fig. 6.19 C). In C3A liver cells, aspalathin, orientin, isoorientin and rutin restored and increased basal ATP concentrations to above that of the normal control. However, the increases in basal ATP were not further stimulated by insulin (Fig. 6.34 B).

These results demonstrate clearly that both FRE and GRE enhanced glucose uptake, and that the four phenolic compounds tested (aspalathin, orientin, isoorientin and rutin) had similar effects on palmitate-induced insulin resistant muscle, fat and liver cells. It further appears that both FRE and GRE and the phenolic compounds stimulate glycolysis in these cells as demonstrated by increased mitochondrial activity with a resultant increase in cellular ATP. In the insulin-resistant state, glucose uptake in muscle is repressed by the accumulation of glucose-6-phosphate (G6P), which is a rate-limiting step in glucose uptake. The accumulation of G6P is the result of a

diminished activity of glycolytic flux substrate towards oxidative phosphorylation (Simoneau and Kelley, 1997). In adipocytes, glycolysis is mainly used to produce glycerol-3-phosphate and generate pyruvate that is further metabolised in the mitochondria to form acetyl CoA, a substrate for fatty acid synthesis. In the liver increased glycolysis results in either glycogen synthesis, glucose oxidation and ATP content or fatty acid synthesis via pyruvate and acetyl CoA (Guo *et al.,* 2012). It is interesting that the 3T3-L1 adipocytes appeared to be less insulin-resistant. Furthermore, although palmitate treatment reduced glucose uptake, some insulin sensitivity was retained. This insulin sensitivity was further enhanced by the extracts and compounds. In the C3A liver cells, basal glucose levels were restored by the extracts and compounds. However, because C3A liver cells do not express GLUT4, the insulin responsive glucose transporter, insulin did not further enhance glucose uptake. The increase in ATP following palmitate treatment further suggests that the increase in glucose uptake induced by FRE, GRE and the compounds was mainly as a result of increased glucose oxidation by the mitochondria. Although we present strong evidence for increased ATP production through mitochondrial respiration as supported by increased MTT levels, it is also true that the MTT assay could be affected by phenolic compounds (Han *et al.,* 2010). For this study, method controls to estimate the interaction between the MTT reagent and the extracts and compounds, at the respective concentrations used, did not have any direct measurable effect. Furthermore, the integrity of the MTT results are supported by the high degree of similarity to the ATP results.

Recently Beauvieux *et al.* (2013) using nuclear magnetic resonance (NMR), demonstrated that the stilbene resveratrol, increased ATP cellular concentrations in perfused and isolated liver cells via cytosolic glycolysis and not via oxidative phosphorylation. The authors further proposed that resveratrol might directly act on the glyceraldehyde-3-phosphate dehydrogenase/3-phosphoglycerate kinase (G3PDH/PGK) complex or alternatively via stimulation of AMPK, which stimulated phosphofructokinase activity (PFK) thereby increasing glycolytic flux. For this study, glycolytic substrates were not measured and therefore it is not possible to speculate whether the increased ATP content induced by the extracts and compounds, resulted from mitochondrial oxidation or cytosolic ATP synthesis. From our evidence, we

hypothesise, at least in part, that the increased ATP content were due to increased glucose oxidation.

7.6. Effect of rooibos extracts (FRE and GRE) and compounds on palmitate uptake by 3T3-L1 adipocytes and C3A liver cells

As both adipocytes and liver cells are involved in fatty acid synthesis, it was of interest to determine whether palmitate uptake would be affected by the extracts and phenolic compounds. Chronic palmitate exposure of 3T3-L1 adipocytes and C3A liver cells significantly reduced C^{14} palmitate uptake from the media. Both FRE and GRE and the compounds (aspalathin, orientin, isoorientin and rutin) were able to reverse the reduced palmitate uptake induced by chronic palmitate exposure (Fig 6.26, 6.27 and 6.39 and 6.40). Adipose tissue and the liver are the primary sites for fatty acid uptake from the circulation. The enhancement of lipid uptake by the extracts and compounds in 3T3-L1 adipocytes and C3A liver cells supports several *in vivo* findings demonstrating the anti-dyslipidemic effect of rooibos and aspalathin, previously demonstrated in *db/db* mice and humans at risk for developing CVD (Kawano e*t al.*, 2009; Marnewick *et al.,* 2011).

7.7. Effect of rooibos extracts (FRE and GRE) on signalling in C2C12 muscle cells

To gain insight into the possible mechanism(s) of action whereby the extracts elicit their bioactivity, biochemical signalling pathways involved with glucose metabolism and insulin palmitate-induced insulin resistance were assessed in C2C12 cells. These finding were published recently (Mazibuko *et al.,* 2013). We demonstrated that both extracts down-regulated PKCθ activation which is associated with palmitate-induced insulin resistance and inflammation. Furthermore, the extracts increased activation of the key regulatory proteins, AKT and AMPK, involved in insulin-dependent and non-insulin regulated signalling pathways. Protein expression of GLUT4, the glucose transporter involved in glucose transport via these two pathways, were also increased. The inhibition of PKCθ activation and increased activation of AMPK and AKT offer a plausible mechanistic explanation for this ameliorative effect that the extracts had on

palmitate-induced insulin resistance. Due to the similar mechanism of action demonstrated in these insulin-resistant C2C12 cells, and the fact that GRE was more effective, together with high costs involved in molecular analyses, it was decided to only perform further molecular mechanistic studies using GRE. Furthermore, because of the uniqueness of aspalathin to rooibos, and in terms of bioactivity (glucose uptake, MTT and ATP) in which no significant differences were observed between the efficacy of the compounds at an equimolar concentration (10 µM), it was decided to select aspalathin as a compound for further molecular studies.

7.8. Effect of aspalathin-enriched green rooibos extract (GRE) and aspalathin on insulin signalling

In a recent review by Ragheb and Medhat. (2011), muscle insulin resistance was associated with a defective lipid metabolism and high levels of circulating saturated FFAs. The mechanism(s) whereby high levels of SFA, particularly palmitate contribute to insulin resistance are still contradictory. Accumulation of the intermediate lipid metabolites, DAG and ceramide, in palmitate-treated cells could at least in part affect insulin signalling (Yuzefovych *et al.,* 2010). In muscle, increased levels of DAG and ceramide activate the serine kinase PKCθ, which phosphorylates IRS1 at the Ser 307 site and inhibits tyrosine phosphorylation resulting in attenuated downstream insulin signalling via IRS1 and PI3K. This reduces glucose uptake into the cell by GLUT4 (Yuzefovych *et al.,* 2010). Furthermore, Jové *et al.* (2006) demonstrated that palmitate causes an increase in the gene expression of the pro-inflammatory cytokine TNF-α in skeletal muscle, and this was strongly associated with activation of PKCθ. As expected, our results confirmed that palmitate increased PKCθ activation by ~300% in C2C12 muscle cells and that GRE and aspalathin reversed the palmitate-induced activation of PKCθ (Fig. 6.10). This study confirmed that palmitate significantly increased IRS1 phosphorylation at the serine 307 residue in C2C12 muscle cells and that both GRE and aspalathin attenuated the activation of IRS1 (Ser 307) (Fig. 6.11).

In 3T3-L1 adipocytes palmitate activated NF-κB, which is strongly associated with inflammation in adipocytes (Kennedy *et al.,* 2009; Han *et al.,* 2010; McCall *et al.,* 2010). Our results showed that GRE and aspalathin reversed the palmitate-induced

activation of NF-κB (Fig. 6.20). As both PKCθ and NF-κB supress insulin signalling via phosphorylation of IRS1 (Ser 307), it is plausible that at a mechanistic level, inhibition of these pathways could enhance insulin signalling.

In C2C12 muscle cells and 3T3-L1 adipocytes palmitate only had a marginal effect on insulin receptor protein expression (Fig. 6.12 and 6.21). However, both GRE and aspalathin enhanced insulin receptor expression compared to the palmitate-treated cells. In C2C12 muscle cells GRE increased INSR protein expression to above that of the normal controls. In 3T3-L1 adipocytes aspalathin was more effective than GRE at increasing INSR protein expression. In terms of PI3K, palmitate reduced the activation of PI3K in C2C12 muscle cells. Deng et al. (2012) reported similar results. GRE and aspalathin increased PI3K activation in C2C12 muscle with aspalathin showing the greater increase in PI3K activity (Fig. 6.13). In 3T3-L1 adipocytes and C3A liver cells, palmitate appeared to have no effect on the activation of PI3K (Fig. 6.22 and 6.35). In terms of AKT, the downstream target of PI3K, palmitate significantly decreased activation of AKT by insulin in all three cell lines (Fig. 6.14, 6.23 and 6.36). These findings are in agreement with previous findings in L6 muscle cells showing that palmitate impaired insulin sensitivity and glucose uptake by reducing activation of AKT (Dimopoulos *et al.,* 2006). GRE and aspalathin increased insulin-stimulated AKT activation from the reduced levels induced by palmitate, however, in the case of GRE, it normalised the activation of AKT by insulin. Aspalathin significantly improved AKT activation, but it was less effective than GRE. Similar results were reported by Deng *et al.,* (2012), showing that polyphenols such as the green tea flavanol, epigallocatechin gallate (EGCG) and the tumuric curcuminoid, curcumin, inhibited palmitate-induced PKC activation and suppressed phosphorylation of IRS1 (Ser 307), thereby enhancing PI3K/AKT signalling, suggesting ameliorative affectivity against palmitate-induced insulin resistance in C2C12 muscle cells. Alonso-Castro *et al.* (2012) showed that isoorientin, which is also present in GRE in high quantities; increased phosphorylation of AKT in TNF-α induced insulin-resistant adipocytes. Lim *et al.* (2007) reported that isoorientin protected HepG2 liver cells against oxidative damage by activating the Nrf2 pathway, which increased the expression of the endogenous antioxidant NQO1. The mechanism whereby isoorientin elicited the protective effect was PI3K/AKT dependent. Our study demonstrated that both GRE

and aspalathin activated the PI3K/AKT pathway in C3A liver cells and therefore, although we did not study the Nrf2 pathway, we can speculate that both GRE and aspalathin could have similar protective effects in the liver. It is interesting; however, that isoorientin at a high concentration (80 µM) inhibits AKT phosphorylation and induces apoptosis in HepG2 liver cells (Yuan *et al.,* 2012). In another study conducted by Lee *et al.* (2012), rutin and the combination of rutin and quercetin, a minor rooibos flavonoid (Joubert *et al.,* 2012) improved glucose uptake and activated AKT in hepatocytes.

In terms of GLUT4 protein expression in C2C12 muscle cells, palmitate significantly decreased insulin stimulated GLUT4 protein expression. GRE and aspalathin reversed the palmitate-induced decrease (Fig. 6.16). In 3T3-L1 adipocytes palmitate had no effect on GLUT4 protein expression, however GRE appeared to increase GLUT4 protein expression (Fig. 6.25). Further, we showed that FRE and GRE increased pAKT (Ser 473) and GLUT4 protein expression. AKT is a pivotal insulin-signalling protein responsible for GLUT4 expression and translocation to the cell membrane thereby increasing glucose uptake in response to insulin-signalling. It should be kept in mind that in this study, the total GLUT4 protein expression does not necessarily relate to the insulin-stimulated translocation of GLUT4, which was not determined.

In the C3A liver cells, GLUT2 is the major glucose transporter (Fisette *et al.,* 2013). GLUT2 protein expression was significantly decreased following palmitate treatment, while GRE and aspalathin normalised, and in a case of aspalathin even increased insulin-stimulated GLUT2 protein expression (Fig. 6.38).

7.9. Effect of aspalathin-enriched green rooibos extract (GRE) and aspalathin on AMPK

Activation of AMPK increases glucose uptake and ATP synthesis independently of insulin and is regarded as a major drug target in the treatment of T2D (Sajan *et al.,* 2010). During periods of starvation and deprivation of cellular energy, ATP content decrease with concomitant increases in AMP and ADP. AMPK, an energy-sensing

enzyme, responds to these shifts in the energy balance (AMP/ADP: ATP ratios) and acts by activating energy replenishing catabolic pathways that increase ATP, such as glycolysis and lipid oxidation at the expense of energy-consuming synthesising pathways (Musi and Goodyear, 2006).

In 3T3-L1 adipocytes and C3A liver cells, palmitate significantly activated AMPK, but it had little or no effect on the C2C12 cells (Fig. 6.24, 6.37 and 6.15). Previous studies have confirmed that AMPK is activated independently of AMP/ADP by increasing levels of cellular fatty acids including palmitate. AMPK was only activated by palmitate in L6 muscle at high concentrations (250 µM) and not at lower concentrations (75 µM) (Watt *et al.,* 2006), such as was used in this study. Of particular interest was that AMPK activation in both C2C12 muscle and 3T3-L1 adipocytes by aspalathin was more effective at increasing basal and insulin-stimulated AMPK activation. These findings are in keeping with those of Son *et al.* (2013) who demonstrated that aspalathin promoted AMPK phosphorylation in L6 cells. Activation of AMPK with metformin increased glucose uptake in human primary myocytes (Sarabia *et al.,* 1992) and in L6 myotubules (Ouyang *et al.,* 2011). The increase was shown to be related to increased translocation of GLUT1 and GLUT4 to the plasma membrane (Hundal *et al.,* 1992). In adipocytes AMPK plays a central role by inhibiting fatty acid synthesis and lipolysis (Daval *et al.,* 2005). Activation of AMPK suppresses acetyl-CoA carboxylase (ACC) activity thereby decreasing malonyl-CoA levels (inhibit synthetises and enhances breakdown by malonyl-CoA decarboxylase). By decreasing malonyl-CoA levels the inhibition of carnitine palmitoyl-transferase I (CPT1) is eased by increasing the entry of long-chain fatty acyl-CoA into mitochondria and fatty acid oxidation (Hardie, 2011). In 3T3-L1 adipocytes, AMPK activation enhances basal glucose uptake by a mechanism independent of insulin-signalling but involving translocation of GLUT4 (Salt *et al.,* 2000; Sakoda *et al.,* 2000). In C3A liver cells both GRE and aspalathin effectively increased AMPK activation. In the liver AMPK activation increases glucose uptake by enhancing energy producing catabolic processes such as glycolysis and fatty acid oxidation in favour of energy consuming synthesis pathways including those involved with glycogen, lipid and protein synthesis (Viollet *et al.,* 2010).

7.10. Effect of aspalathin-enriched green rooibos extract (GRE) and aspalathin on lipid metabolism in 3T3-L1 adipocytes and C3A liver cells

In 3T3-L1 cells palmitate treatment did not significantly affect the protein expression of peroxisome proliferator-activated receptor gamma (PPARγ) and alpha (PPARα), two key genes involved in adipogenesis, lipolysis and regulation of lipid oxidation. In both cases, aspalathin, but not GRE, significantly increased the protein expression of both these PPAR isoforms (Fig. 6.28 and 6.29). The PPARγ agonists, thiazolidinediones, used in the treatment of T2D, are known to reduce insulin resistance by restoring sensitivity to insulin in muscle and adipose tissue and by inhibiting hepatic gluconeogenesis (Kovacs and Stumvoll, 2005). The increased glucose uptake in 3T3-L1 adipocytes by kaempferol and quercetin has been attributed to the ability of these flavonoids to act as ligands to PPARγ (Fang *et al.,* 2008). Phenolic acids such as gallic acid have also been previously demonstrated to activate PPARγ expression (Sugii *et al.,* 2009; Huang *et al.,* 2005). Furthermore, Sheng *et al.* (2008) reported that cinnamon improved insulin sensitivity in *db/db* mice by increasing PPARγ and PPARα expression. Other downstream effects of GRE and aspalathin on 3T3-L1 adipocytes lipid metabolism included a slight, but not significant decrease in insulin-stimulated malonyl-CoA levels of the palmitate-treated cells and a concomitant increase of basal CPT1 levels (Fig. 6.30 and 6.31). In the C3A liver cells palmitate significantly increased both basal and insulin-stimulated malonyl-CoA levels which were reversed by both GRE and aspalathin (Fig. 6.41). GRE and aspalathin also significantly increased both basal and insulin-stimulated CPT1 protein expression (Fig. 6.42). In the liver, lipid oxidation is regulated both at the transcriptional level involving PPARα and by allosteric regulation of CPT1 by malonyl CoA (Muoio and Newgard, 2008). As discussed previously, by decreasing malonyl-CoA and increasing CPT1 protein expression, the capacity to transport long chain Acyl CoA into the mitochondria increases and therefore fatty acid oxidation is enhanced (Rasmussen *et al.,* 2002; Zammit, 2008; Hardie, 2011).

7.11. Effect of aspalathin-enriched green rooibos extract (GRE) and aspalathin on FOXO1

In the C3A liver cells, palmitate decreased insulin-stimulated FOXO1 activation. Treating the cells with GRE and aspalathin increased both basal and insulin-stimulated FOXO1 activation (Fig. 6.43). FOXO1 is known to play a central role in the regulation of glucose metabolism in the liver in particular, its role in promoting glyconeogenesis and lipid mobilisation, while supressing glycolysis and lipid synthesis during times of fast is important for maintaining normoglycemia. FOXO1 also enhances insulin signalling by promoting AKT phosphorylation and glycogen synthase kinase-3 activity when glucose levels are increased (Matsumoto *et al.,* 2006; Gross *et al.,* 2008).

7.12. Effect of aspalathin-enriched green rooibos extract (GRE) in the OB/IR rat

As the bioavailability of rooibos flavonoids, including aspalathin, is generally considered to be low and found to be almost undetectable in pig and human plasma (Kreuz *et al.,* 2008; Stalmach *et al.,* 2009), and in order to assess if we could corroborate the *in vitro* findings, GRE was administered daily to adult diet-induced OB/IR Wistar rats. Previously, Muller *et al.* (2012) demonstrated that GRE reduced glucose concentrations in STZ diabetic rats and OB/IR rats. GRE had no effect on body weight (Fig. 6.44 A). Importantly, however, GRE reduced fasting insulin concentrations by ~44%, thereby ameliorating diet induced insulin resistance, as calculated by HOMAR-IR (Fig. 6.45 A and B). To gain some insight into mechanism(s) of action at a gene level, the effect of GRE on key genes involved with insulin signalling and AMPK was assessed. In muscle and liver mRNA expression demonstrated increases in insulin receptor (Insr) (Fig. 6.46 A and 6.51 A), phosphatidylinositol 3-kinase (Pi3k) (Fig. 6.48 A and 6.53 A) and AMP-activated protein kinase (Ampk) (Fig 6.49 A and 6.54 A), while insulin receptor substrate 1 and 2 (Irs1 and 2) expression was increased in the liver but not in the muscle (Fig 6.52 A, B and 6.47 A, B). Messenger RNA expression of Glut4, the insulin sensitive glucose transporter, was increased in muscle (Fig. 6.50). With the exception of AMPK expression in muscle (Fig 6.49 A and B), the lack of correlation between mRNA expression and Western blot

protein expression in the liver and muscle tissue is an unfortunate aspect of the *in vivo* study. In terms of mRNA expression, the results are relevant to the effects observed following treatment. The discrepancy could be due to a technical issue in that our Western blot methods were not sensitive enough to detect the differences in tissue. This is particularly disappointing as proteins are the final effectors of biological processes. At a physiological level it is also possible that the the differences could be due to posttranslational effects such as protein synthesis regulation by mRNA degradation whereby a transcript for a particular protein is made, but the translation is never made or is restricted. Increased mRNA expression of key regulators in insulin transduction is of particular importance as the liver and skeletal muscle are the major tissues responsible for glucose disposal from the portal and peripheral circulation, respectively. Furthermore, the increased gene expression of the insulin signalling proteins Irs1/2 in the liver and of PI3K, demonstrated for both the muscle and liver along with GLUT4 in muscle, provides further evidence that GRE enhanced insulin-signalling. A number of studies have provided evidence suggesting that insulin resistance, the main cause of T2D, can potentially be treated by targeting PI3K itself or its modulators such as IRS (Jiang and Zhang, 2002; Karnieli and Armoni, 2008).

7.13. Mechanism of action whereby aspalathin-enriched green rooibos extract (GRE) and aspalathin ameliorate insulin resistance.

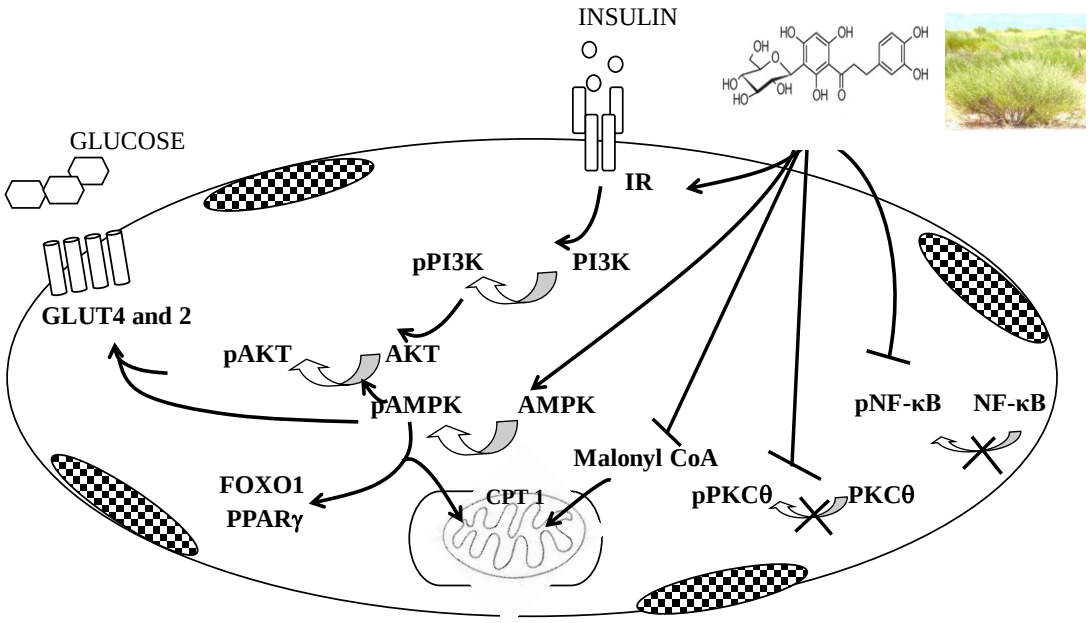

Figure 7.1. Schematic representation reflecting the mechanism of action whereby GRE and aspalathin ameliorate insulin resistance. GRE and aspalathin inhibit palmitate-induced activation of PKCθ and NF-κB, thereby suppressing the inflammatory pathway and restoring insulin sensitivity. Insulin transduction is enhanced by (i) increased INSR expression, (ii) activation of the PI3K/AKT and (iii) AMPK culminating in enhanced glucose transport and metabolism. Glucose transport capacity is improved by increasing GLUT4 (muscle and adipocytes) and GLUT2 (liver) expression. Reduced malonyl CoA and increased CPT1 protein expression favour fatty acid transport in to the mitochondria for oxidation. By increasing lipid oxidation, the accumulation of intracellular lipid metabolites such as DAG and ceramides, known to be responsible for insulin resistance, is reduced. The expression of PPARγ and FOXO1 further enhances insulin sensitivity by enhancing the activation of AMPK and by protecting tissues such as muscle and liver against lipid overload.

7.14. Conclusions

Rooibos and the major phenolic compounds present therein were shown to ameliorate experimentally-induced insulin resistance *in vitro* and *in vivo*. In terms of glucose metabolism suppressed by palmitate, FRE and GRE proved to be equally effective at restoring glucose uptake, mitochondrial dehydrogenase activity and intracellular ATP content in muscle, adipocytes and liver cells. The phenolic compounds (aspalathin, orientin, isoorientin and rutin) demonstrated similar ameliorative effects. In terms of mechanism of action GRE and aspalathin enhanced insulin-signalling by reducing palmitate-induced activation of PKCθ and NF-kB, thereby reducing IRS1 (Ser 307) phosphorylation known to attenuate insulin-signalling. Concomitantly, insulin-signalling effectors such as PI3K and AKT, as well as AMPK, were activated. Activation of these proteins are associated with enhanced glucose and lipid uptake. Increased protein expression of GLUT4 and GLUT2 provides further evidence for increased glucose uptake capacity in muscle, fat and liver cells, respectively. GRE and aspalathin increased palmitate uptake in 3T3-L1 adipocytes and C3A liver cells. In terms of lipid metabolism, GRE and aspalathin decreased malonyl-CoA and increased CPT1 protein expression, thereby increasing fatty acid oxidation. Increased levels of PPARγ and FOXO1 protein expression support the insulin sensitising effect of GRE and aspalathin in fat and liver, respectively. In an OB/IR rat model, GRE improved insulin resistance by reducing hyperinsulinemia. Gene and protein studies on the muscle and liver tissue collaborated the mechanism(s) of action demonstrated in the C2C12 muscle and C3A liver cells. Strong evidence is presented that amelioration of insulin resistance in an OB/IR rat involved enhanced insulin signalling, AMPK activation and increased Glut4 expression.

This study provides compelling evidence in support of the potential health benefits of rooibos and its phenolic compounds in the prevention of insulin resistance.

7.15. Shortcomings of the study

Due to budget restrictions and lack of laboratory resources, the following analyses were not performed:

Accumulation of intracellular SFA metabolites, such as DAG, and ceramide, were not determined. The presence of these intermediate lipid metabolites have been identified as an important additional parameter to estimate the level of insulin resistance in muscle, fat and liver cells.

Lipid metabolism studies, particularly palmitate uptake, were only done in 3T3-L1 adipocytes and C3A liver cells, which are the cell types primarily involved in lipid metabolism.

For Western blot analyses we had to prioritise and limit protein expression studies to the key proteins involved in transduction.

Western blot analysis was limited to cells treated with GRE and aspalathin.

In terms of glucose transport, it would have been valuable to look at GLUT4 translocation, in addition to protein expression.

Performing Western blot analyses on proteins with higher molecular weights such as IRS1, IRS2 and ACC were not successful due to technical reasons (proteins were not successfully transferred). As an alternative IRS1 (Ser 307) protein expression was assessed using ELISA. Due to the increased cost of the ELISA kit, the study was limited to C2C12 muscle cells.

In the OB/IR rat study, mRNA determination was limited to muscle and liver tissue. Attempts to extract mRNA from adipose tissue was unsuccessful due to its high fat content.

7.16. Future Studies

Providing sufficient funding is obtained, the following future studies are proposed:

Expand the study to include the effects of the other phenolic compounds present in GRE (orientin, isoorientin and rutin) on insulin resistance. This will give us a better understanding of how different phenolic compounds could differentially affect the metabolism thereby giving insight into structure-function relationships of these compounds.

Clarity the effect of rooibos and its compounds on cellular metabolism by analyses of metabolic substrates and enzymes to provide additional information regarding metabolic processes such as glycolysis, gluconeogenesis, glycogenolysis, oxidation, glycogen and lipid synthesis.

Gain a better understanding of the molecular mechanism(s) involved, by using specific inhibitors, genes silencing, and specific gene knock out animal models to provide definitive proof of concept.

In addition to mRNA and protein expression, GLUT4 translocation in response to insulin stimulation will provide functional proof that insulin signalling and AMPK activation is effective.

Perform pharmacokinetic studies to determine *in vivo* bioavailability and stability of the phenolic compounds. This will allow us to determine an optimal effective dosage for further *in vivo* experiments.

Chapter 8

References

Abdul-Ghani, M.A. & DeFronzo, R.A. 2010. Pathogenesis of insulin resistance in skeletal muscle. *J Biomed Biotechnol*., 2010, 476279.

Ahrén, B., Pacina, G., Foley, J.E., & Schweizer, A. 2005. Improved meal-related β-cell function and insulin sensitivity by the dipeptidyl peptidase-IV inhibitor vildagliptin in metformin-treated patients with type 2 diabetes over 1 year. *Diabetes Care*, 28,(8) 1936-1940.

Ajuwon, O.R., Katengua-Thamahane, E., Van Rooyen, J., Oguntibeju, O.O., & Marnewick, J.L. 2013. Protective effects of rooibos (*Aspalathus linearis*) and/or red palm oil (*Elaeis guineensis*) supplementation on *tert*-Butyl hydroperoxide-induced oxidative hepatotoxicity in Wistar rats. *Evid Based Complement Alternat Med*., 2013, 984273.

Alonso-Castro, A.J., Zapata-Bustos, R., Gómez-Espinoza, G., & Salazar-Olivo, L.A. 2012. Isoorientin reverts TNF- α- induced insulin resistance in adipocytes activating the insulin signalling pathway. *Endocrinol*., 153, (11) 5222-5230.

Al-Rejaie, S.S., Aleisa, A.M., Sayed-Ahmed, M.M., Al-Shabanah, O.A., Abuohashish, H.M., Ahmed, M.M., Al-Hosaini, K.A., & Hafez, M.M. 2013. Protective effect of rutin on the antioxidant genes expression in hypercholestrolemic male Wistar rat. *BMC Complement Altern Med*., 13, 136.

Anderson, J.W., Baird, P., Davis, R.H., Ferreri, S., Knudtson, M., Koraym, A., Waters, V., & Williams, C.L. 2009. Health benefits of dietary fiber. *Nutr Rev.*, 67, (4) 188-205.

Andrés, V. & Walsh, K. 1996. Myogenin expression, cell cycle withdrawal, and phenotypic differentiation are temporally separable events that precede cell fusion upon myogenesis. *J Cell Biol.*, 132, (4) 657-666.

Anhê, G.F., Okamoto, M.M., Kinote, A., Sollon, C., Lellis-Santos, C., Anhê, F.F., Lima,

G.A., Hirabara, S.M., Velloso, L.A., Bordin, S., & Machado, U.F. 2012. Quercetin decreases inflammatory response and increases insulin action in skeletal muscle of *ob/ob* mice and in L6 myotubes. *Eur.J Pharmacol.*, 689, (1-3) 285-293.

Ayah, R., Joshi, M.D., Wanjiru, R., Njau, E.K., Otieno, C.F., Njeru, E.K., & Mutai, K.K. 2013. A population-based survey of prevalence of diabetes and correlates in an urban slum community in Nairobi, Kenya. *BMC Public Health*., 13, 371.

Bahadoran, Z., Mirmiran, P., & Azizi, F. 2013. Dietary polyphenols as potential nutraceuticals in management of diabetes: a review. *J Diabetes Metab Disord*., 12, (1) 43.

Beauvieux, M.C., Stephant, A., Gin, H., Serhan, N., Couzigou, P., & Gallis, J.L. 2013. Resveratrol mainly stimulates the glycolytic ATP synthesis flux and not the mitochondrial one: a saturation transfer NMR study in perfused and isolated rat liver. *Pharmacol Res*., 78, 11-17.

Befroy, D.E., Petersen, K.F., Dufour, S., Mason, G.F., De Graaf, R.A., Rothman, D.L., & Shulman, G.I. 2007. Impaired mitochondrial substrate oxidation in muscle of insulin-resistant offspring of type 2 diabetic patients. *Diabetes*, 56, (5) 1376-1381.

Belfort, R., Mandarino, L., Kashyap, S., Wirfel, K., Pratipanawatr, T., Berria, R., DeFronzo, R.A., & Cusi, K. 2005. Dose-response effect of elevated plasma free fatty acid on insulin signalling. *Diabetes*, 54, (6) 1640-1648.

Beltrán-Debón, R., Rull, A., Rodriguez-Sanabria, F., Iswaldi, I., Herranz-López, M., Aragonès, G., Camps, J., Alonso-Villaverde, C., Menéndez, J.A., Micol, V., Segura-Carretero, A., & Joven, J. 2011. Continuous administration of polyphenols from aqueous rooibos (*Aspalathus linearis*) extract ameliorates dietary-induced metabolic disturbances in hyperlipidemic mice. *Phytomedicine*, 18, (5) 414-424.

Berg J.M., Tymoczko J.L., & Stryer L. 2002. Fatty acid metabolism 5th edition .New york, *W H Freeman*.

Berger, J.P., Akiyama, T.E., & Meinke, P.T. 2005. PPARs: therapeutic targets for metabolic disease. *Trends Pharmacol Sci*., 26, (5) 244-251.

Bhattacharya, S., Dey, D., & Roy, S.S. 2007. Molecular mechanism of insulin resistance. *J Biosci*., 32, (2) 405-413.

Bhutani, K.K. & Gohil, V.M. 2010. Natural products drug discovery research in India: status and appraisal. *Indian J Exp.Biol*., 48, (3) 199-207.

Blin, C., Panserat, S., Médale, F., Gomes, E., Brèque, J., Kaushik, S., & Krishnamoorthy, R. 1999. Teleost liver hexokinase- and glucokinase-like enzymes: partial cDNA cloning and phylogenetic studies in rainbow trout (*Oncorhynchus mykiss*), common carp (*Cyprinus carpio*) and gilthead seabream (*Sparus aurata*). *Fish Physiol Biochem.*, 21, (2) 93-102.

Boden, G., Chen, X., Ruiz, J., White, J.V., & Rossetti, L. 1994. Mechanisms of fatty acid-induced inhibition of glucose uptake. *J Clin Invest*., 93, (6) 2438-2446.

Bonora, E., Formentini, G., Calcaterra, F., Lombardi, S., Marini, F., Zenari, L., Saggiani, F., Poli, M., Perbellini, S., Raffaelli, A., Cacciatori, V., Santi, L., Targher, G., Bonadonna, R., & Muggeo, M. 2002. HOMA-estimated insulin resistance is an independent predictor of cardiovascular disease in type 2 diabetic subjects: prospective data from the Verona diabetes complications study. *Diabetes Care*, 25, (7) 1135-1141.

Bouzakri, K., Zachrisson, A., Al-Khalili, L., Zhang, B.B., Koistinen, H.A., Krook, A., & Zierath, J.R. 2006. siRNA-based gene silencing reveals specialized roles of IRS-1/Akt2 and IRS-2/Akt1 in glucose and lipid metabolism in human skeletal muscle. *Cell Metab*., 4, (1) 89-96.

Buchakjian, M.R. & Kornbluth, S. 2010. The engine driving the ship: metabolic steering of cell proliferation and death. *Nat Rev Mol Cell Biol*., 11, (10) 715-727.

Burattini, S., Ferri, P., Battistelli, M., Curci, R., Luchetti, F., & Falcieri, E. 2004. C2C12 murine myoblasts as a model of skeletal muscle development: morpho-functional characterization. *Eur J Histochem*., 48, (3) 223-233.

Capell, W.H., Schlaepfer, I.R., Wolfe, P., Watson, P.A., Bessesen, D.H., Pagliassotti, M.J., & Eckel, R.H. 2010. Fatty acids increase glucose uptake and metabolism in C2C12

myoblasts stably transfected with human lipoprotein lipase. *Am J Physiol Endocrinol Metab*., 299, (4) E576-E583.

Chang, L., Chiang, S.H., & Saltiel, A.R. 2004. Insulin signalling and the regulation of glucose transport. Mol Med., 10, (7-12) 65-71.

Colberg, S.R., Albright, A.L., Blissmer, B.J., Braun, B., Chasan-Taber, L., Fernhall, B., Regensteiner, J.G., Rubin, R.R., & Sigal, R.J. 2010. Exercise and type 2 diabetes. *Diabetes Care*, 33, (12) e147-e167.

Corcoran, M.P., Lamon-Fava, S., & Fielding, R.A. 2007. Skeletal muscle lipid deposition and insulin resistance: effect of dietary fatty acids and exercise. *Am J Clin Nutr*., 85, (3) 662-677.

Corpeleijn, E., Saris, W.H., & Blaak, E.E. 2009. Metabolic flexibility in the development of insulin resistance and type 2 diabetes: effects of lifestyle. *Obes.Rev*., 10, (2) 178-193.

Criddle, D.N., Sutton, R., & Petersen, O.H. 2006. Role of Ca2+ in pancreatic cell death induced by alcohol metabolites. *J Gastroenterol Hepatol*., 21, (3) s14-s17.

Da Poian A.T, El-Bacha T., & Luz M.R.M.P. 2010. Nutrient utilization in humans: metabolism pathways. *Nature Education*, 3 (9) 11.

D'Adamo, E. & Caprio, S. 2011. Type 2 diabetes in youth: epidemiology and pathophysiology. *Diabetes Care*, 34, (2) s161-s165.

Danaei, G., Finucane, M.M., Lu, Y., Singh, G.M., Cowan, M.J., Paciorek, C.J., Lin, J.K., Farzadfar, F., Khang, Y.H., Stevens, G.A., Rao, M., Ali, M.K., Riley, L.M., Robinson, C.A., & Ezzati, M. 2011. National, regional, and global trends in fasting plasma glucose and diabetes prevalence since 1980: systematic analysis of health examination surveys and epidemiological studies with 370 country-years and 2.7 million participants. *Lancet*, 378, (9785) 31-40.

Daudon, M., Traxer, O., Conort, P., Lacour, B., & Jungers, P. 2006. Type 2 diabetes increases the risk for uric acid stones. *J Am Soc Nephrol*., 17, (7) 2026-2033.

Daval, M., Diot-Dupuy, F., Bazin, R., Hainault, I., Viollet, B., Vaulont, S., Hajduch, E., Ferré,

P., & Foufelle, F. 2005. Anti-lipolytic action of AMP-activated protein kinase in rodent adipocytes. *J Biol Chem*., 280, (26) 25250-25257.

De Santa Olalla, L.M, Sánchez Muniz, F.J., & Vaquero, M.P. 2009. N-3 fatty acids in glucose metabolism and insulin sensitivity. *Nutr Hosp*., 24, 113-127

DeFronzo, R.A., & Tripathy, D. 2009. Skeletal muscle insulin resistance is the primary defect in type 2 diabetes. *Diabetes Care*, 32, (2) s157-s163.

DeFronzo, R.A., Davidson, J.A., & Del, P.S. 2012. The role of the kidneys in glucose homeostasis: a new path towards normalizing glycaemia. *Diabetes Obes Metab*., 14, (1) 5-14.

Deng, Y.T., Chang, T.W., Lee, M.S., & Lin, J.K. 2012. Suppression of free fatty acid-induced insulin resistance by phytopolyphenols in C2C12 mouse skeletal muscle cells. *J Agric Food Chem*., 60, (4) 1059-1066.

Dimitriadis, G., Mitrou, P., Lambadiari, V., Maratou, E., & Raptis, S.A. 2011. Insulin effects in muscle and adipose tissue. *Diabetes Res.Clin Pract*., 93, (1) s52-s59.

Dimopoulos, N., Watson, M., Sakamoto, K., & Hundal, H.S. 2006. Differential effects of palmitate and palmitoleate on insulin action and glucose utilization in rat L6 skeletal muscle cells. *Biochem J*., 399, (3) 473-481.

Dludla, P.V., Muller, C.J., Louw, J., Joubert, E., Salie, R., Opoku, A.R., & Johnson, R. 2013. The cardioprotective effect of an aqueous extract of fermented rooibos (Aspalathus linearis) on cultured cardiomyocytes derived from diabetic rats. Phytomedicine. doi: 10.1016/j.phymed.2013.10.029

Do, M.T., Kim, H.G., Choi, J.H., Khanal, T., Park, B.H., Tran, T.P., Hwang, Y.P., Na, M., & Jeong, H.G. 2013. Phillyrin attenuates high glucose-induced lipid accumulation in human HepG2 hepatocytes through the activation of LKB1/AMP-activated protein kinase-dependent signalling. *Food Chem*., 136, (2) 415-425.

Dokken, B. 2012. The kidney as a treatment target for type 2 diabetes. *Diabetes Spectrum*, 25, (1) 29-36.

Draznin, B. 2006. Molecular mechanisms of insulin resistance: serine phosphorylation of insulin receptor substrate-1 and increased expression of p85 α the two sides of a coin. *Diabetes*, 55, (8) 2392-2397.

Dudhia, Z., Louw, J., Muller, C., Joubert, E., De Beer, D., Kinnear, C., & Pheiffer, C. 2013. *Cyclopia maculata* and *Cyclopia subternata* (honeybush tea) inhibits adipogenesis in 3T3-L1 pre-adipocytes. *Phytomedicine*, 20, (5) 401-408.

Dutta-Roy, A.K. 2000. Cellular uptake of long-chain fatty acids: role of membrane-associated fatty-acid-binding/transport proteins. *Cell Mol Life Sci*., 57, (10) 1360-1372.

Ejaz, A., Wu, D., Kwan, P., & Meydani, M. 2009. Curcumin inhibits adipogenesis in 3T3-L1 adipocytes and angiogenesis and obesity in C57/BL mice. *J Nutr*., 139, (5) 919-925.

Elkalaf, M., Anděl, M., & Trnka, J. 2013. Low glucose but not galactose enhances oxidative mitochondrial metabolism in C2C12 myoblasts and myotubes. *PLoS One*, 8, (8) e70772.

Erickson L. 2003. Rooibos tea: research into antioxidant and antimutagenic properties. *HerbalGram*, 59, 34-45.

Fabbrini, E., Sullivan, S., & Klein, S. 2010. Obesity and nonalcoholic fatty liver disease: biochemical, metabolic, and clinical implications. *Hepatology*., 51, (2) 679-689.

Fabris, R., Nisoli, E., Lombardi, A.M., Tonello, C., Serra, R., Granzotto, M., Cusin, I., Rohner-Jeanrenaud, F., Federspil, G., Carruba, M.O., & Vettor, R. 2001. Preferential channeling of energy fuels toward fat rather than muscle during high free fatty acid availability in rats. *Diabetes*, 50, (3) 601-608.

Fang, X.K., Gao, J., & Zhu, D.N. 2008. Kaempferol and quercetin isolated from *Euonymus alatus* improve glucose uptake of 3T3-L1 cells without adipogenesis activity. *Life Sci*., 82, (11-12) 615-622.

Feng, X.T., Wang, T.Z., Leng, J., Chen, Y., Liu, J.B., Liu, Y., & Wang, W.J. 2012. Palmitate contributes to insulin resistance through downregulation of the Src-mediated

phosphorylation of Akt in C2C12 myotubes. *Biosci Biotechnol Biochem*., 76, (7) 1356-1361.

Fernandes, A.A., Novelli, E.L., Okoshi, K., Okoshi, M.P., Di Muzio, B.P., Guimarães, J.F., & Fernandes, J.A. 2010. Influence of rutin treatment on biochemical alterations in experimental diabetes. *Biomed Pharmacother*., 64, (3) 214-219.

Ferré, P. 2004. The biology of peroxisome proliferator-activated receptors: relationship with lipid metabolism and insulin sensitivity. Diabetes, 53, (1) S43-S50.

Fidan, O., Aslan, M., & Mor, M. 2009. Computational evaluation of isoorientin (*C-glycosyl* flavone) on PPAR gamma receptors and HMG- CoA reductase using MOE 2008.10. *Planta Medica*., 75, PH 27.

Fidock, D.A., Rosenthal, P.J., Croft, S.L., Brun, R., & Nwaka, S. 2004. Antimalarial drug discovery: efficacy models for compound screening. *Nat Rev Drug Discov*., 3, (6) 509-520.

Fillmore N, Alrob O.A and Lopaschuk G.D. 2011. Fatty acid β-oxidation. The American Oil Chemists' Society Lipid Library; *http://lipidlibrary.aocs.org/animbio/fa-oxid/index.htm*.

Fisette, A., Poursharifi, P., Oikonomopoulou, K., Munkonda, M.N., Lapointe, M., & Cianflone, K. 2013. Paradoxical glucose-sensitizing yet proinflammatory effects of acute ASP administration in mice. *Mediators Inflamm*., 2013, 713284.

Frayn, K.N., Arner, P., & Yki-Järvinen, H. 2006. Fatty acid metabolism in adipose tissue, muscle and liver in health and disease. *Essays Biochem*., 42, 89-103.

Freireich, E.J., Gehan, E.A., Rall, D.P., Schmidt, L.H., & Skipper, H.E. 1966. Quantitative comparison of toxicity of anticancer agents in mouse, rat, hamster, dog, monkey, and man. *Cancer Chemother Rep*., 50, (4) 219-244.

Funaki, M., Randhawa, P., & Janmey, P.A. 2004. Separation of insulin signalling into distinct GLUT4 translocation and activation steps. *Mol Cell Biol*., 24, (17) 7567-7577.

Gaidhu, M.P., Fediuc, S., & Ceddia, R.B. 2006. 5-Aminoimidazole-4-carboxamide-1-beta-D-ribofuranoside-induced AMP-activated protein kinase phosphorylation inhibits basal

and insulin-stimulated glucose uptake, lipid synthesis, and fatty acid oxidation in isolated rat adipocytes. *J Biol Chem*., 281, (36) 25956-25964.

Gaidhu, M.P., Fediuc, S., Anthony, N.M., So, M., Mirpourian, M., Perry, R.L., & Ceddia, R.B. 2009. Prolonged AICAR-induced AMP-kinase activation promotes energy dissipation in white adipocytes: novel mechanisms integrating HSL and ATGL. *J Lipid Res*., 50, (4) 704-715.

Galgani, J.E., Moro, C., & Ravussin, E. 2008. Metabolic flexibility and insulin resistance. *Am J Physiol Endocrinol Metab*., 295, (5) E1009-E1017.

Gao, D., Bailey, C.J., & Griffiths, H.R. 2009. Metabolic memory effect of the saturated fatty acid, palmitate, in monocytes. *Biochem Biophys Res Commun*., 388, (2) 278-282.

Gao, D., Nong, S., Huang, X., Lu, Y., Zhao, H., Lin, Y., Man, Y., Wang, S., Yang, J., & Li, J. 2010. The effects of palmitate on hepatic insulin resistance are mediated by NADPH oxidase 3-derived reactive oxygen species through JNK and p38MAPK pathways. *J Biol Chem*., 285, (39) 29965-29973.

García-Martínez, C., Marotta, M., Moore-Carrasco, R., Guitart, M., Camps, M., Busquets, S., Montell, E., & Gómez-Foix, A.M. 2005. Impact on fatty acid metabolism and differential localization of FATP1 and FAT/CD36 proteins delivered in cultured human muscle cells. *Am J Physiol Cell Physiol*., 288, (6) C1264-C1272.

Gaster, M., Rustan, A.C., & Beck-Nielsen, H. 2005. Differential utilization of saturated palmitate and unsaturated oleate: evidence from cultured myotubes. *Diabetes*, 54, (3) 648-656.

Ghafoorunissa, Ibrahim, A., Rajkumar, L., & Acharya, V. 2005. Dietary (n-3) long chain polyunsaturated fatty acids prevent sucrose-induced insulin resistance in rats. *J Nutr*., 135, (11) 2634-2638.

Giri, L., Mutalik, V.K., & Venkatesh, K.V. 2004. A steady state analysis indicates that negative feedback regulation of PTP1B by Akt elicits bistability in insulin-stimulated GLUT4 translocation. *Theor Biol Med Model*., 1, 2.

Giri, S., Rattan, R., Haq, E., Khan, M., Yasmin, R., Won, J.S., Key, L., Singh, A.K., & Singh, I. 2006. AICAR inhibits adipocyte differentiation in 3T3L1 and restores metabolic alterations in diet-induced obesity mice model. *Nutr Metab*., 3, 31.

Glatz, J.F., Luiken, J.J., & Bonen, A. 2010. Membrane fatty acid transporters as regulators of lipid metabolism: implications for metabolic disease. *Physiol Rev*., 90, (1) 367-417.

Goalstone, M.L. & Draznin, B. 1997. Insulin signalling. *West J Med*., 167, (3) 166-173.

Gross, D.N., Van Den Heuvel, A.P., & Birnbaum, M.J. 2008. The role of FOXO in the regulation of metabolism. *Oncogene*, 27, (16) 2320-2336.

Grüner-Richter S, Otto F and Weinreich B. 2008. Rooibos extract with increased aspalathin content, process for the preparation of such a rooibos extract, and cosmetic agent containing such a rooibos extract. U.S., Patent; Application No. US2008/0247974 A1.

Gruzman, A., Babai, G., & Sasson, S. 2009. Adenosine monophosphate-activated protein kinase (AMPK) as a new target for antidiabetic drugs: a review on metabolic, pharmacological and chemical considerations. *Rev Diabet Stud*., 6, (1) 13-36.

Guo, X., Li, H., Xu, H., Woo, S., Dong, H., Lu, F., Lange, A.J., & Wu, C. 2012. Glycolysis in the control of blood glucose homeostasis. *Acta Pharmaceutica Sinica B*., 2, (4) 358-367.

Haag, M., & Dippenaar, N.G., 2005. Dietary fats, fatty acids and insulin resistance: short review of a multifaceted connection. *Med Sci Monit*., 11, (12) RA359-RA367.

Han, M., Li J.F., Tan, Q., Sun, Y.Y., & Wang, Y.Y. 2010. Limitations of the use of MTT assay for screening in drug discovery. *J Chin Pharm Sci*., 1003-1057.

Hanhineva, K., Törrönen, R., Bondia-Pons, I., Pekkinen, J., Kolehmainen, M., Mykkänen, H., & Poutanen, K. 2010. Impact of dietary polyphenols on carbohydrate metabolism. *Int.J Mol Sci*., 11, (4) 1365-1402.

Hardie, D.G. 2011. AMP-activated protein kinase: an energy sensor that regulates all aspects of cell function. *Genes Dev*., 25, (18) 1895-1908.

Hawley, S.A., Ross, F.A., Chevtzoff, C., Green, K.A., Evans, A., Fogarty, S., Towler, M.C., Brown, L.J., Ogunbayo, O.A., Evans, A.M., & Hardie, D.G. 2010. Use of cells expressing gamma subunit variants to identify diverse mechanisms of AMPK activation. *Cell Metab*., 11, (6) 554-565.

Heilbronn, L., Smith, S.R., & Ravussin, E. 2004. Failure of fat cell proliferation, mitochondrial function and fat oxidation results in ectopic fat storage, insulin resistance and type II diabetes mellitus. *Int.J Obes Relat Metab Disord*., 28, (4) S12-S21.

Holloway, G.P., Thrush, A.B., Heigenhauser, G.J., Tandon, N.N., Dyck, D.J., Bonen, A., & Spriet, L.L. 2007. Skeletal muscle mitochondrial FAT/CD36 content and palmitate oxidation are not decreased in obese women. *Am J Physiol Endocrinol Metab*., 292, (6) E1782-E1789.

Huang, T.H., Peng, G., Kota, B.P., Li, G.Q., Yamahara, J., Roufogalis, B.D., & Li, Y. 2005. Anti-diabetic action of *Punica granatum* flower extract: activation of PPAR-gamma and identification of an active component. *Toxicol Appl Pharmacol.*, 207, (2) 160-169.

Huang, W., Yu, J., Jia, X., Xiong, L., Li, N., & Wen, X. 2012. Zhenqing recipe improves glucose metabolism and insulin sensitivity by repressing hepatic FOXO1 in type 2 diabetic rats. *Am J Chin Med*., 40, (4) 721-733.

Hundal, H.S., Ramlal, T., Reyes, R., Leiter, L.A., & Klip, A. 1992. Cellular mechanism of metformin action involves glucose transporter translocation from an intracellular pool to the plasma membrane in L6 muscle cells. *J Endocrinol*., 131, (3) 1165-1173.

Ikeda, Y., Tsuchiya, H., Hama, S., Kajimoto, K., & Kogure, K. 2013. Resistin affects lipid metabolism during adipocyte maturation of 3T3-L1 cells. *FEBS J*., 280, (22) 5884-5895.

Jenkins, D.J., Kendall, C.W., Marchie, A., Jenkins, A.L., Augustin, L.S., Ludwig, D.S., Barnard, N.D., & Anderson, J.W. 2003. Type 2 diabetes and the vegetarian diet. *Am J Clin Nutr*., 78, (3) s610-s616.

Jeong, S. & Yoon, M. 2009. Fenofibrate inhibits adipocyte hypertrophy and insulin resistance by activating adipose PPAR alpha in high fat diet-induced obese mice.

Exp.Mol Med., 41, (6) 397-405.

Jiang, G. & Zhang, B.B. 2002. Pi3-kinase and its up- and down-stream modulators as potential targets for the treatment of type II diabetes. *Front Biosci*., 7, d903-d907.

Jorgensen, S.B., O'Neill, H.M., Sylow, L., Honeyman, J., Hewitt, K.A., Palanivel, R., Fullerton, M.D., Öberg, L., Balendran, A., Galic, S., van der Poel, C., Trounce, I.A., Lynch, G.S., Schertzer, J.D., & Steinberg, G.R. 2013. Deletion of skeletal muscle SOCS3 prevents insulin resistance in obesity. *Diabetes*, 62, (1) 56-64.

Joubert E, Gelderblom, W.C.A, Louw, J., & De Beer, D. 2008. South African herbal teas: *aspalathus linearis*, *cyclopia spp*. and a*thrixia phylicoides* – a review. *J Ethnopharmaco*l., 119:376-412.

Joubert, E., & De Beer, D. 2011. Rooibos (*Aspalathus linearis*) beyond the farm gate: From herbal tea to potential phytopharmaceutical. *South African Journal of Botany*, 77, (4) 869-886.

Joubert, E., & Schulz, H. 2006. Production and quality aspects of rooibos tea and related products. *J Appl Bot Food Qual*., 80:138-144.

Joubert, E., Beelders, T., De Beer, D., Malherbe, C.J., De Villiers, A.J., & Sigge, G.O. 2012. Variation in phenolic content and antioxidant activity of fermented rooibos herbal tea infusions: role of production season and quality grade. *J Agric Food Chem*., 60, (36) 9171-9179.

Joubert, E., De Beer. D., Malherbe, C.J., Muller, N., Bonnet, S.L., Van Der Westhuizen, J.H., & Ferreira, D. 2013. Occurrence and sensory perception of *Z-2-(beta-d-glucopyranosyloxy)-3-phenylpropenoic acid* in rooibos (*Aspalathus linearis*). *Food Chem*., 136, (2) 1078-1085.

Jové, M., Planavila, A., Sánchez, R.M., Merlos, M., Laguna, J.C., & Vázquez-Carrera, M. 2006. Palmitate induces tumor necrosis factor-alpha expression in C2C12 skeletal muscle cells by a mechanism involving protein kinase C and nuclear factor-kappaB activation. *Endocrinol*., 147, (1) 552-561.

Kaestner, K.H., Christy, R.J., & Lane, M.D. 1990. Mouse insulin-responsive glucose transporter gene: characterization of the gene and trans-activation by the CCAAT/enhancer binding protein. *Proc Natl Acad Sci*., 87, (1) 251-255.

Kahn, C.R. & Saad, M.J. 1992. Alterations in insulin receptor and substrate phosphorylation in hypertensive rats. *J Am Soc Nephrol*., 3, (4) s69-s77.

Kahn, C.R. & White, M.F. 1988. The insulin receptor and the molecular mechanism of insulin action. *J Clin Invest*., 82, (4) 1151-1156.

Kahn, S.E., Prigeon, R.L., McCulloch, D.K., Boyko, E.J., Bergman, R.N., Schwartz, M.W., Neifing, J.L., Ward, W.K., Beard, J.C., Palmer, J.P., & . 1993. Quantification of the relationship between insulin sensitivity and beta-cell function in human subjects. Evidence for a hyperbolic function. *Diabetes*, 42, (11) 1663-1672.

Kalish B.T, Fallon E.M & Puder M. 2012. A tutorial on fatty acid biology. *J Parenter Enteral Nutr*., 36(4):380-388.

Karnieli, E. & Armoni, M. 2008. Transcriptional regulation of the insulin-responsive glucose transporter GLUT4 gene: from physiology to pathology. *Am J Physiol Endocrinol Metab*., 295, (1) E38-E45.

Karpe, F., Dickmann, J.R., & Frayn, K.N. 2011. Fatty acids, obesity, and insulin resistance: time for a reevaluation. *Diabetes*, 60, (10) 2441-2449.

Kasuga, M., Izumi, T., Tobe, K., Shiba, T., Momomura, K., Tashiro-Hashimoto, Y., & Kadowaki, T. 1990. Substrates for insulin-receptor kinase. *Diabetes Care*, 13, (3) 317-326.

Kawano, A., Nakamura, H., Hata, S., Minakawa, M., Miura, Y., & Yagasaki, K. 2009. Hypoglycemic effect of aspalathin, a rooibos tea component from *Aspalathus linearis*, in type 2 diabetic model *db/db* mice. *Phytomedicine*, 16, (5) 437-443.

Keizer, H.A., Schaart, G., Tandon, N.N., Glatz, J.F., & Luiken, J.J. 2004. Subcellular immunolocalisation of fatty acid translocase (FAT)/CD36 in human type-1 and type-2 skeletal muscle fibres. *Histochem Cell Biol*., 121, (2) 101-107.

Kennedy, A., Martinez, K., Chuang, C.C., LaPoint, K., & McIntosh, M. 2009. Saturated fatty acid-mediated inflammation and insulin resistance in adipose tissue: mechanisms of action and implications. *J Nutr*, 139, (1) 1-4.

Kerner, J. & Hoppel, C. 2000. Fatty acid import into mitochondria. *Biochim Biophys Acta*, 1486, (1) 1-17.

Kim, C.H., Youn, J.H., Park, J.Y., Hong, S.K., Park, K.S., Park, S.W., Suh, K.I., & Lee, K.U. 2000. Effects of high-fat diet and exercise training on intracellular glucose metabolism in rats. *Am J Physiol Endocrinol Metab*., 278, (6) E977-E984.

Kim, J., Lee, I., Seo, J., Jung, M., Kim, Y., Yim, N., & Bae, K. 2010. Vitexin, orientin and other flavonoids from *Spirodela polyrhiza* inhibit adipogenesis in 3T3-L1 cells. *Phytother Res*., 24, (10) 1543-1548.

Kim, J.A., Wei, Y., & Sowers, J.R. 2008. Role of mitochondrial dysfunction in insulin resistance. *Circ Res*., 102, (4) 401-414.

Koonen, D.P., Glatz, J.F., Bonen, A., & Luiken, J.J. 2005. Long-chain fatty acid uptake and FAT/CD36 translocation in heart and skeletal muscle. *Biochim Biophys Acta, 1736*, (3) 163-180.

Kottra, G. & Daniel, H. 2007. Flavonoid glycosides are not transported by the human Na+/glucose transporter when expressed in *Xenopus laevis* oocytes, but effectively inhibit electrogenic glucose uptake. *J Pharmacol Exp Ther*., 322, (2) 829-835.

Kovacs, P. & Stumvoll, M. 2005. Fatty acids and insulin resistance in muscle and liver. *Best Pract Res Clin Endocrinol Metab*., 19, (4) 625-635.

Kraegen, E.W., Clark, P.W., Jenkins, A.B., Daley, E.A., Chisholm, D.J., & Storlien, L.H. 1991. Development of muscle insulin resistance after liver insulin resistance in high-fat-fed rats. *Diabetes*, 40, (11) 1397-1403.

Kreuz, S., Joubert, E., Waldmann, K.H., & Ternes, W. 2008. Aspalathin, a flavonoid in *Aspalathus linearis* (rooibos), is absorbed by pig intestine as a *C-glycoside*. *Nutr Res*., 28, (10) 690-701.

Krygsman, A., Roux, C.R., Muller, C., & Louw, J. 2010. Development of glucose intolerance in Wistar rats fed low and moderate fat diets differing in fatty acid profile. *Exp Clin Endocrinol Diabetes.*, 118, (7) 434-441.

Kumar, A. & Singh, V. 2010. Atherogenic dyslipidemia and diabetes mellitus: what's new in the management arena? *Vasc.Health Risk Manag*., 6, 665-669.

Kurotani, K., Kochi, T., Nanri, A., Tsuruoka, H., Kuwahara, K., Pham, N.M., Kabe, I., & Mizoue, T. 2013. Plant oils were associated with low prevalence of impaired glucose metabolism in Japanese workers. *PLoS One*, 8, (5) e64758.

Laukkanen, O., Lindström, J., Eriksson, J., Valle, T.T., Hämäläinen, H., Ilanne-Parikka, P., Keinanen-Kiukaanniemi, S., Tuomilehto, J., Uusitupa, M., & Laakso, M. 2005. Polymorphisms in the SLC2A2 (GLUT2) gene are associated with the conversion from impaired glucose tolerance to type 2 diabetes: the Finnish Diabetes Prevention Study. *Diabetes*, 54, (7) 2256-2260.

Lebovitz, H.E. 1999. Type 2 diabetes: an overview. *Clin Chem*., 45, (Pt 2) 1339-1345.

Lee, C.C., Hsu, W.H., Shen, S.R., Cheng, Y.H., & Wu, S.C. 2012. *Fagopyrum tataricum* (buckwheat) improved high-glucose-induced insulin resistance in mouse hepatocytes and diabetes in fructose-rich diet-induced mice. *Exp Diabetes Res*., 2012, 375673.

Li, C., Hsieh, M.C., & Chang, S.J. 2013. Metabolic syndrome, diabetes, and hyperuricemia. *Curr Opin Rheumatol*., 25, (2) 210-216.

Li, L. & Messina, J.L. 2009. Acute insulin resistance following injury. *Trends Endocrinol Metab*., 20, (9) 429-435.

Li, M., Youngren, J.F., Manchem, V.P., Kozlowski, M., Zhang, B.B., Maddux, B.A., & Goldfine, I.D. 2001. Small molecule insulin receptor activators potentiate insulin action in insulin-resistant cells. *Diabetes*, 50, (10) 2323-2328.

Lian, Z., Li, Y., Gao, J., Qu, K., Li, J., Hao, L., Wu, S., & Zhu, H. 2011. A novel AMPK activator, WS070117, improves lipid metabolism discords in hamsters and HepG2 cells. *Lipids Health Dis*., 10, 67.

Lieberman, L.S. 2003. Dietary, evolutionary, and modernizing influences on the prevalence of type 2 diabetes. *Annu.Rev Nutr*., 23, 345-377.

Lim, J.H., Lee, J.I., Suh, Y.H., Kim, W., Song, J.H., & Jung, M.H. 2006. Mitochondrial dysfunction induces aberrant insulin signalling and glucose utilisation in murine C2C12 myotube cells. *Diabetologia*, 49, (8) 1924-1936.

Lim, J.H., Park, H.S., Choi, J.K., Lee, I.S., & Choi, H.J. 2007. Isoorientin induces Nrf2 pathway-driven antioxidant response through phosphatidylinositol 3-kinase signalling. *Arch Pharm Res*., 30, (12) 1590-1598.

Lobo, V., Patil, A., Phatak, A., & Chandra, N. 2010. Free radicals, antioxidants and functional foods: Impact on human health. *Pharmacogn Rev*, 4, (8) 118-126.

Lodish, H., Berk, A., Zipursky, L., Matsudaira, P., Baltimore, D., & Darnell, J. 2000., electron transport and oxidative phosphorylation, Molecular cell biology, 4th edition New York: *W. H. Freeman*.

Loffreda, S., Yang, S.Q., Lin, H.Z., Karp, C.L., Brengman, M.L., Wang, D.J., Klein, A.S., Bulkley, G.B., Bao, C., Noble, P.W., Lane, M.D., & Diehl, A.M. 1998. Leptin regulates proinflammatory immune responses. *FASEB J*., 12, (1) 57-65.

Ludewig, U. & Frommer, W.B. 2002. Genes and proteins for solute transport and sensing. *Arabidopsis.Book*., 1, e0092.

Mahmood, T. & Yang, P.C. 2012. Western blot: technique, theory, and trouble shooting. *N.Am J Med.Sci*., 4, (9) 429-434.

Makni, K., Mnif, F., Boudawara, M., Hamza, N., Rekik, N., Abid, M., Rebaï, A., Jarraya, F., Granier, C., & Ayadi, H. 2008. Association of glucose transporter 1 polymorphisms with type 2 diabetes in the Tunisian population. *Diabetes Metab Res Rev*., 24, (7) 544-548.

Marcel, Y.L. & Suzue, G. 1972. Kinetic studies on the specificity of long chain acyl coenzyme A synthetase from rat liver microsomes. *J Biol Chem*., 247, (14) 4433-4436.

Marnewick, J.L., Rautenbach, F., Venter, I., Neethling, H., Blackhurst, D.M., Wolmarans,

P., & Macharia, M. 2011. Effects of rooibos (*Aspalathus linearis*) on oxidative stress and biochemical parameters in adults at risk for cardiovascular disease. *J Ethnopharmacol*., 133, (1) 46-52.

Martins, A.R., Nachbar, R.T., Gorjao, R., Vinolo, M.A., Festuccia, W.T., Lambertucci, R.H., Cury-Boaventura, M.F., Silveira, L.R., Curi, R., & Hirabara, S.M. 2012. Mechanisms underlying skeletal muscle insulin resistance induced by fatty acids: importance of the mitochondrial function. *Lipids Health Dis*., 11, 30.

Matsumoto, M., Han, S., Kitamura, T., & Accili, D. 2006. Dual role of transcription factor FOXO1 in controlling hepatic insulin sensitivity and lipid metabolism. *J Clin Invest*., 116, (9) 2464-2472.

Mazibuko, S.E., Muller, C.J.F., Joubert, E., De Beer, D., Johnson, R., Opoku, A.R., & Louw, J. 2013. Amelioration of palmitate-induced insulin resistance in C2C12 muscle cells by rooibos (Aspalathus linearis). *Phytomedicine*, 20, (10) 813-819.

Mazibuko, SE. 2011. An in vitro study of the effects of free fatty acids on insulin mediated glucose uptake and metabolism by myocytes and fibroblast derived adipocytes. MSc Thesis, *University of Zululand.*

McAuley, K.A., Williams, S.M., Mann, J.I., Goulding, A., Chisholm, A., Wilson, N., Story, G., McLay, R.T., Harper, M.J., & Jones, I.E. 2002. Intensive lifestyle changes are necessary to improve insulin sensitivity: a randomized controlled trial. *Diabetes Care*, 25, (3) 445-452.

McCall, K.D., Holliday, D., Dickerson, E., Wallace, B., Schwartz, A.L., Schwartz, C., Lewis, C.J., Kohn, L.D., & Schwartz, F.L. 2010. Phenylmethimazole blocks palmitate-mediated induction of inflammatory cytokine pathways in 3T3-L1 adipocytes and RAW 264.7 macrophages. *J Endocrinol*., 207, (3) 343-353.

Montel-Hagen, A., Sitbon, M., & Taylor, N. 2009. Erythroid glucose transporters. *Curr Opin Hematol*., 16, (3) 165-172.

Montesano, A., Luzi, L., Senesi, P., & Terruzzi, I. 2013. Modulation of cell cycle progression by 5-azacytidine is associated with early myogenesis induction in murine myoblasts. *Int.J Biol Sci*., 9, (4) 391-402.

Morton, G.J. & Schwartz, M.W. 2011. Leptin and the central nervous system control of glucose metabolism. *Physiol Rev.*, 91, (2) 389-411.

Mossman, H.M.T. 1983. Rapid colorimetric assay for cellular growth and survival: application to proliferation and cytotoxic assays. *J Immunol Methods*., 65:55-63.

Mozaffarian, D., Pischon, T., Hankinson, S.E., Rifai, N., Joshipura, K., Willett, W.C., & Rimm, E.B. 2004. Dietary intake of trans fatty acids and systemic inflammation in women. *Am J Clin Nutr*, 79, (4) 606-612.

Muller, C.J., Joubert, E., De Beer, D., Sanderson, M., Malherbe, C.J., Fey, S.J., & Louw, J. 2012. Acute assessment of an aspalathin-enriched green rooibos (*Aspalathus linearis*) extract with hypoglycemic potential. *Phytomedicine*, 20, (1) 32-39.

Muller,C.J.F., Joubert, E., Pheiffer, C., Ghoor, S., Sanderson, M., Chellan, N., Fey, S.J., & Louw, J. 2013. Z-2-(*β*-d-glucopyranosyloxy)-3-phenylpropenoic acid, an α-hydroxy acid from rooibos (*Aspalathus linearis*) with hypoglycemic activity. *Mol Nutr Food Res*., 57(12) 2216-2222.

Muoio, D.M. & Newgard, C.B. 2008. Fatty acid oxidation and insulin action: when less is more. *Diabetes*, 57, (6) 1455-1456.

Musi, N. & Goodyear, L.J. 2006. Insulin resistance and improvements in signal transduction. *Endocrine*., 29, (1) 73-80.

Nguyen, D.M. & El-Serag, H.B. 2010. The epidemiology of obesity. *Gastroenterol Clin North Am*., 39, (1) 1-7.

Nkabinde, L. 2004. The establishment of a rat model of dietary induced obesity and insulin resistance. MSc Thesis, *University of Zululand.*

Nolan, J.J., O'Halloran, D., McKenna, T.J., Firth, R., & Redmond, S. 2006. The cost of treating type 2 diabetes (CODEIRE). *Ir Med J*., 99, (10) 307-310.

O'Boyle, R.N., & Beamish, F.W.H. 1977. Growth and intermediary metabolism of larval and metamorphosing stages of the landlocked sea lamprey, *Petromyzon marinus* L. *Env. Biol. Fish*., 2(2) 103-120.

Ojuka, E.O., Goyaram, V., & Smith, J.A. 2012. The role of CaMKII in regulating GLUT4 expression in skeletal muscle. *Am J Physiol Endocrinol Metab*., 303, (3) E322-E331.

Olson A.L. 2012.Regulation of GLUT4 and insulin-dependent glucose flux. *ISRN*., 856987.

Ouyang, J., Parakhia R.A., & Ochs R.S. 2011. Metformin activates AMP kinase through inhibition of AMP deaminase. *J. Biol. Chem*., 286:1-11

Oyekan, A. 2009. Peroxisome profilerator-activated receptors (PPARs)- The new frontiers in the treatment of cardiovascular diseases. *Trop J Pharm Res*., 8(2)101-103.

Panchal, S.K., Poudyal, H., Arumugam, T.V., & Brown, L. 2011. Rutin attenuates metabolic changes, nonalcoholic steatohepatitis, and cardiovascular remodeling in high-carbohydrate, high-fat diet-fed rats. *J Nutr*., 141, (6) 1062-1069.

Pantsi, W.G., Marnewick, J.L., Esterhuyse, A.J., Rautenbach, F., & Van Rooyen, J. 2011. Rooibos (*Aspalathus linearis*) offers cardiac protection against ischaemia/reperfusion in the isolated perfused rat heart. *Phytomedicine*, 18, (14) 1220-1228.

Pelsers, M.M., Stellingwerff, T., & Van Loon, L.J. 2008. The role of membrane fatty-acid transporters in regulating skeletal muscle substrate use during exercise. *Sports Med*., 38, (5) 387-399.

Pessin, J.E. & Saltiel, A.R. 2000. Signalling pathways in insulin action: molecular targets of insulin resistance. *J Clin Invest*, 106, (2) 165-169.

Pimenta, A.S., Gaidhu, M.P., Habib, S., So, M., Fediuc, S., Mirpourian, M., Musheev, M., Curi, R., & Ceddia, R.B. 2008. Prolonged exposure to palmitate impairs fatty acid oxidation despite activation of AMP-activated protein kinase in skeletal muscle cells. *J Cell Physiol*., 217, (2) 478-485.

Pohl, J., Ring, A., & Stremmel, W. 2002. Uptake of long-chain fatty acids in HepG2 cells involves caveolae: analysis of a novel pathway. *J Lipid Res*., 43, (9) 1390-1399.

Pohl, J., Ring, A., Ehehalt, R., Schulze-Bergkamen, H., Schad, A., Verkade, P., & Stremmel, W. 2004. Long-chain fatty acid uptake into adipocytes depends on lipid raft function. *Biochemistr*y, 43, (14) 4179-4187.

Prashanth, M., Ganesh, H.K., Vima, M.V., John, M., Bandgar, T., Joshi, S.R., Shah, S.R., Rathi, P.M., Joshi, A.S., Thakkar, H., Menon, P.S., & Shah, N.S. 2009. Prevalence of nonalcoholic fatty liver disease in patients with type 2 diabetes mellitus. *J Assoc Physicians India*, 57, 205-210.

Qatanani, M. & Lazar, M.A. 2007. Mechanisms of obesity-associated insulin resistance: many choices on the menu. *Genes Dev*., 21, (12) 1443-1455.

Rabe, C., Steenkamp, J.A., Joubert, E., Burger, J.f.W., & Ferreira, D. 1994. Phenolic metabolites from rooibos tea (*Aspalathus linearis*). *Phytochemistry*, 35, (6) 1559-1565.

Ragheb, R., & Medhat, A.M. 2011. Mechanisms of fatty acid-induced insulin resistance in muscle and liver. *Diabetes Metab J.,* 2 (4) 127.

Rakhshandehroo, M., Knoch, B., Müller, M., & Kersten, S. 2010. Peroxisome proliferator-activated receptor alpha target genes. *PPAR Res*., 2010, Article ID 612089.

Randle, P.J., Newsholme, E.A., & Garland, P.B. 1964. Regulation of glucose uptake by muscle. 8. Effects of fatty acids, ketone bodies and pyruvate, and of alloxan-diabetes and starvation, on the uptake and metabolic fate of glucose in rat heart and diaphragm muscles. *Biochem J*., 93, (3) 652-665.

Rasmussen, B.B., Holmbäck, U.C., Volpi, E., Morio-Liondore, B., Paddon-Jones, D., & Wolfe, R.R. 2002. Malonyl coenzyme A and the regulation of functional carnitine palmitoyltransferase-1 activity and fat oxidation in human skeletal muscle. J *Clin Invest*., 110, (11) 1687-1693.

Rasmussen, B.M., Vessby, B., Uusitupa, M., Berglund, L., Pedersen, E., Riccardi, G., Rivellese, A.A., Tapsell, L., & Hermansen, K. 2006. Effects of dietary saturated, monounsaturated, and n-3 fatty acids on blood pressure in healthy subjects. *Am J Clin Nutr.,* 83, (2) 221-226.

Reaven, G.M. 2005. Compensatory hyperinsulinemia and the development of an atherogenic lipoprotein profile: the price paid to maintain glucose homeostasis in insulin-resistant individuals. *Endocrinol Metab Clin North Am*., 34, (1) 49-62.

Reed, B.C., Kaufmann, S.H., Mackall, J.C., Student, A.K., & Lane, M.D. 1977. Alterations in insulin binding accompanying differentiation of 3T3-L1 pre-adipocytes. *Proc Natl Acad Sci*., 74, (11) 4876-4880.

Renuka, M., Rajani, G., Haritha, K., Swathi, M., & Raju, A.B. 2013. Effect of rutin and telmisartam on metabolic syndrome X. *International Journal of Phytomedicine*, 5, (2) 233-242.

Rhodes, C.J. & White, M.F. 2002. Molecular insights into insulin action and secretion. *Eur J Clin Invest*., 32, (3) 3-13.

Riccardi, G. & Rivellese, A.A. 2000. Dietary treatment of the metabolic syndrome-the optimal diet. *Br J Nutr*., 83, (1) s143-s148.

Richardson, J.M. & Pessin, J.E. 1993. Identification of a skeletal muscle-specific regulatory domain in the rat GLUT4/muscle-fat gene. *J Biol Chem*., 268, (28) 21021-21027.

Risérus, U. 2008. Fatty acids and insulin sensitivity. *Curr Opin Clin Nutr Metab Care*., 11, (2) 100-105.

Rosen, E.D., Walkey, C.J., Puigserver, P., & Spiegelman, B.M. 2000. Transcriptional regulation of adipogenesis. *Genes Dev*., 14, (11) 1293-1307.

Sajan, M.P., Bandyopadhyay, G., Miura, A., Standaert, M.L., Nimal, S., Longnus, S.L., Van, O.E., Hainault, I., Foufelle, F., Kahn, R., Braun, U., Leitges, M., & Farese, R.V. 2010. AICAR and metformin, but not exercise, increase muscle glucose transport through AMPK, ERK, and PDK1- dependent activation of atypical PKC. *Am J Physiol Endocrinol Metab*., 298, (2) E179-E192.

Sakoda, H., Ogihara, T., Anai, M., Funaki, M., Inukai, K., Katagiri, H., Fukushima, Y., Onishi, Y., Ono, H., Fujishiro, M., Kikuchi, M., Oka, Y., & Asano, T. 2000. Dexamethasone-induced insulin resistance in 3T3-L1 adipocytes is due to inhibition

of glucose transport rather than insulin signal transduction. *Diabetes*, 49, (10) 1700-1708.

Salt, I.P., Connell, J.M., & Gould, G.W. 2000. 5-aminoimidazole-4-carboxamide ribonucleoside (AICAR) inhibits insulin-stimulated glucose transport in 3T3-L1 adipocytes. *Diabetes*, 49, (10) 1649-1656.

Saltiel, A.R. & Kahn, C.R. 2001. Insulin signalling and the regulation of glucose and lipid metabolism. *Nature*, 414, (6865) 799-806.

Sanderson, M., Mazibuko, S.E., Joubert, E., De Beer, D., Johnson, R., Pheiffer, C., Louw, J., & Muller, C.J. 2014. Effects of fermented rooibos (*Aspalathus linearis*) on adipocyte differentiation. *Phytomedicine*, 21, (2) 109-117.

Sarabia, V., Lam, L., Burdett, E., Leiter, L.A., & Klip, A. 1992. Glucose transport in human skeletal muscle cells in culture. Stimulation by insulin and metformin. *J Clin Invest*., 90, (4) 1386-1395.

Sawada, K., Kawabata, K., Yamashita, T., Kawasaki, K., Yamamoto, N., & Ashida, H. 2012. Ameliorative effects of polyunsaturated fatty acids against palmitic acid-induced insulin resistance in L6 skeletal muscle cells. *Lipids Health Dis*., 11, 36.

Schrauwen, P. & Hesselink, M. 2002. UCP2 and UCP3 in muscle controlling body metabolism. *J Exp. Biol*., 205, (Pt 15) 2275-2285.

Sebastián, D., Guitart, M., García-Martínez, C., Mauvezin, C., Orellanà-Gavalda, J.M., Serra, D., Gómez-Foix, A.M., Hegardt, F.G., & Asins, G. 2009. Novel role of FATP1 in mitochondrial fatty acid oxidation in skeletal muscle cells. *J Lipid Res*., 50, (9) 1789-1799.

Senesi, P., Luzi, L., Montesano, A., Mazzocchi, N., & Terruzzi, I. 2013. Betaine supplement enhances skeletal muscle differentiation in murine myoblasts via IGF-1 signalling activation. *J Transl Med*., 11, (1) 174.

Sezik, E., Aslan, M., Yesilada, E., & Ito, S. 2005. Hypoglycaemic activity of *Gentiana olivieri* and isolation of the active constituent through bioassay-directed fractionation

techniques. *Life Sci*., 76, (11) 1223-1238.

Shao, W., Yu, Z., Chiang, Y., Yang, Y., Chai, T., Foltz, W., Lu, H., Fantus, I.G., & Jin, T. 2012. Curcumin prevents high fat diet induced insulin resistance and obesity via attenuating lipogenesis in liver and inflammatory pathway in adipocytes. *PLoS One*, 7, (1) e28784.

Sheng, X., Zhang, Y., Gong, Z., Huang, C., & Zang, Y.Q. 2008. Improved insulin resistance and lipid metabolism by cinnamon extract through activation of peroxisome proliferator-activated receptors. *PPAR Res*., 2008, 581348.

Shi, Y. 2013. Common folds and transport mechanisms of secondary active transporters. *Annu Rev Biophys*., 42, 51-72.

Shimabukuro, M., Zhou, Y.T., Levi, M., & Unger, R.H. 1998. Fatty acid-induced beta cell apoptosis: a link between obesity and diabetes. *Proc Natl Acad Sci USA*, 95, (5) 2498-2502.

Simoneau, J.A., & Kelley, D.E. 1997. Altered glycolytic and oxidative capacities of skeletal muscle contribute to insulin resistance in NIDDM. *J Appl Physiol*. 83, (1) 166-171.

Siriwardhana N., Kalupahana N.S., & Moustaid-Moussa, N. 2013. Health benefits of n-3 polyunsaturated fatty acids. Adv Food Nutr Res., 65:211-222.

Sivitz, W.I., & Yorek, M.A. 2010. Mitochondrial dysfunction in diabetes: from molecular mechanisms to functional significance and therapeutic opportunities. *Antioxid Redox Signal*, 12, (4) 537-577.

Skrobuk, P. 2012. Glucose and lipid metabolism in human skeletal muscle. Academic Dissertation, Helsinki.

Skyler, J.S. 2007. Prediction and prevention of type 1 diabetes: progress, problems, and prospects. *Clin Pharmacol Ther*., 81, (5) 768-771.

Snel, M., Jonker, J.T., Schoones, J., Lamb, H., de, R.A., Pijl, H., Smit, J.W., Meinders, A.E., & Jazet, I.M. 2012. Ectopic fat and insulin resistance: pathophysiology and effect of diet and lifestyle interventions. *Int J Endocrinol*., 2012, 983814.

Soldatow, V.Y., Lecluyse, E.L., Griffith, L.G., & Rusyn, I. 2013. *In vitro* models for liver toxicity testing. *Toxicol Res*., 2, (1) 23-39.

Son, M.J., Minakawa, M., Miura, Y., & Yagasaki, K. 2013. Aspalathin improves hyperglycemia and glucose intolerance in obese diabetic *ob/ob* mice. *Eur J Nutr*., 52, (6) 1607-1619.

Song, Y., Li, J., Zhao, Y., Zhang, Q., Liu, Z., Li, J., Chen, X., Yang, Z., Yu, C., & Xiao, X. 2012. Severe maternal hyperglycemia exacerbates the development of insulin resistance and fatty liver in the offspring on high fat diet. *Exp Diabetes Res*., 2012, 254976.

Staels, B. & Fruchart, J.C. 2005. Therapeutic roles of peroxisome proliferator-activated receptor agonists. *Diabetes*, 54, (8) 2460-2470.

Stalmach, A., Mullen, W., Pecorari, M., Serafini, M., & Crozier, A. 2009. Bioavailability of C-linked dihydrochalcone and flavanone glucosides in humans following ingestion of unfermented and fermented rooibos teas. *J Agric Food Chem*., 57(15):7104-7111

Storlien, L.H., Kraegen, E.W., Chisholm, D.J., Ford, G.L., Bruce, D.G., & Pascoe, W.S. 1987. Fish oil prevents insulin resistance induced by high-fat feeding in rats. *Science*, 237, (4817) 885-888.

Street, R.A., & Prinsloo G. 2013. Commercially important medicinal plants of South Africa: a review. *J of Chem*; article ID 205048.

Stümpel, F., Burcelin, R., Jungermann, K., & Thorens, B. 2001. Normal kinetics of intestinal glucose absorption in the absence of GLUT2: evidence for a transport pathway requiring glucose phosphorylation and transfer into the endoplasmic reticulum. *Proc Natl Acad Sci USA*, 98, (20) 11330-11335.

Su, S.L. 2009.Sodium-glucose transporter. *Form J of Endocrinology and Metabol*, 1, 1-5.

Sugii, S., Olson, P., Sears, D.D., Saberi, M., Atkins, A.R., Barish, G.D., Hong, S.H., Castro, G.L., Yin, Y.Q., Nelson, M.C., Hsiao, G., Greaves, D.R., Downes, M., Yu, R.T., Olefsky, J.M., & Evans, R.M. 2009. PPAR gamma activation in adipocytes is sufficient for systemic insulin sensitization. *ProcNatlAcadSciUSA*, 106, (52) 22504-22509.

Suryawan, A., Nguyen, H.V., Orellana, R.A., Bush, J.A., & Davis, T.A. 2003. Insulin/insulin-like growth factor-I hybrid receptor abundance decreases with development in suckling pigs. *J Nutr*., 133, (9) 2783-2787.

Szewczyk, A. & Wojtczak, L. 2002. Mitochondria as a pharmacological target. *Pharmacol Rev*., 54, (1) 101-127.

Thorens, B. & Mueckler, M. 2010. Glucose transporters in the 21st Century. Am J Physiol *Endocrinol Metab*., 298, (2) E141-E145.

Towler, M.C. & Hardie, D.G. 2007. AMP-activated protein kinase in metabolic control and insulin signalling. *Circ Res*., 100, (3) 328-341.

Tsuchiya, Y., Hatakeyama, H., Emoto, N., Wagatsuma, F., Matsushita, S., & Kanzaki, M. 2010. Palmitate-induced down-regulation of sortilin and impaired GLUT4 trafficking in C2C12 myotubes. *J Biol Chem*., 285, (45) 34371-34381.

Ulicná, O., Greksák, M., Vancová, O., Zlatos, L., Galbavý, S., Bozek, P., & Nakano, M. 2003. Hepatoprotective effect of rooibos tea (*Aspalathus linearis*) on CCl4-induced liver damage in rats. *Physiol Res*., 52, (4) 461-466.

Ulicná, O., Vancová, O., Bozek, P., Cársky, J., Sebeková, K., Boor, P., Nakano, M., & Greksák, M. 2006. Rooibos tea (*Aspalathus linearis*) partially prevents oxidative stress in streptozotocin-induced diabetic rats. *Physiol Res*., 55, (2) 157-164.

Ulicná, O., Vancová, O., Waczulíková, I., Bozek, P., Janega, P., Babál, P., Lísková, S., & Greksák, M. 2008. Does rooibos tea (*Aspalathus linearis*) support regeneration of rat liver after intoxication by carbon tetrachloride? *Gen Physiol Biophys*., 27, (3) 179-186.

Usui, I., Haruta, T., Takata, Y., Iwata, M., Uno, T., Takano, A., Ueno, E., Ishibashi, O., Ishihara, H., Wada, T., Sasaoka, T., & Kobayashi, M. 1999. Differential effects of palmitate on glucose uptake in rat-1 fibroblasts and 3T3-L1 adipocytes. *Horm Metab Res*., 31, (10) 546-552.

Valentine, V. 2012.The role of the kidney and sodium-glucose contransporter-2 inhibition in diabetes management. *Clinical Diabetes*, 30, 4.

Van Belle, T.L., Coppieters, K.T., & von Herrath, M.G. 2011. Type 1 diabetes: etiology,

immunology, and therapeutic strategies. *Physiol Rev*., 91, (1) 79-118.

Viollet, B., Horman, S., Leclerc, J., Lantier, L., Foretz, M., Billaud, M., Giri, S., & Andreelli, F. 2010. AMPK inhibition in health and disease. *Crit Rev Biochem Mol Biol*., 45, (4) 276-295.

Von Wilamowitz-Moellendorff, A., Hunter, R.W., García-Rocha, M., Kang, L., López-Soldado, I., Lantier, L., Patel, K., Peggie, M.W., Martínez-Pons, C., Voss, M., Calbó, J., Cohen, P.T., Wasserman, D.H., Guinovart, J.J., & Sakamoto, K. 2013. Glucose-6-phosphate-mediated activation of liver glycogen synthase plays a key role in hepatic glycogen synthesis. *Diabetes*, 62, (12) 4070-4082.

Vrinda, B., & Uma, D.P. 2001. Radiation protection of human lymphocyte chromosomes in vitro by orientin and vicenin. *Mutat Res*., 498, (1-2) 39-46.

Walgren, R.A., Lin, J.T., Kinne, R.K., & Walle, T. 2000. Cellular uptake of dietary flavonoid quercetin 4'-beta-glucoside by sodium-dependent glucose transporter SGLT1. *J Pharmacol Exp Ther*., 294, (3) 837-843.

Wang, C., Liu, M., Riojas, R.A., Xin, X., Gao, Z., Zeng, R., Wu, J., Dong, L.Q., & Liu, F. 2009. Protein kinase C theta (PKCtheta)-dependent phosphorylation of PDK1 at Ser504 and Ser532 contributes to palmitate-induced insulin resistance. *J Biol Chem*., 284, (4) 2038-2044.

Wang, Q., Somwar, R., Bilan, P.J., Liu, Z., Jin, J., Woodgett, J.R., & Klip, A. 1999. Protein kinase B/Akt participates in GLUT4 translocation by insulin in L6 myoblasts. *Mol Cell Biol*., 19, (6) 4008-4018.

Wang, Y.W., Sun, G.D., Sun, J., Liu, S.J., Wang, J., Xu, X.H., & Miao, L.N. 2013. Spontaneous type 2 diabetic rodent models. *J Diabetes Res*., 2013, 401723.

Watt, M.J., Steinberg, G.R., Chen, Z.P., Kemp, B.E., & Febbraio, M.A. 2006. Fatty acids stimulate AMP-activated protein kinase and enhance fatty acid oxidation in L6 myotubes. *J Physiol*., 574, (Pt 1) 139-147.

Weickert, M.O. 2012. What dietary modification best improves insulin sensitivity and why? *Clin Endocrinol.,* 77, (4) 508-512.

Weickert, M.O., & Pfeiffer, A.F. 2008. Metabolic effects of dietary fiber consumption and prevention of diabetes. *J Nutr*., 138, (3) 439-442.

Weigert, C., Klopfer, K., Kausch, C., Brodbeck, K., Stumvoll, M., Häring, H.U., & Schleicher, E.D. 2003. Palmitate-induced activation of the hexosamine pathway in human myotubes: increased expression of glutamine:fructose-6-phosphate aminotransferase. *Diabetes*, 52, (3) 650-656.

White, M.F. 1997. The insulin signalling system and the IRS proteins. *Diabetologia*, 40, (2) s2-17.

Wilcox, G. 2005. Insulin and insulin resistance. *Clin Biochem Rev*., 26, (2) 19-39.

Wild, S., Roglic, G., Green, A., Sicree, R., & King, H. 2004. Global prevalence of diabetes: estimates for the year 2000 and projections for 2030. *Diabetes Care*, 27, (5) 1047-1053.

Willett, W., Manson, J., & Liu, S. 2002. Glycemic index, glycemic load, and risk of type 2 diabetes. *Am J Clin Nutr*., 76, (1) 274S-280S.

Wu, Q., Ortegon, A.M., Tsang, B., Doege, H., Feingold, K.R., & Stahl, A. 2006. FATP1 is an insulin-sensitive fatty acid transporter involved in diet-induced obesity. *Mol Cell Biol*., 26, (9) 3455-3467.

Wu, X., Motoshima, H., Mahadev, K., Stalker, T.J., Scalia, R., & Goldstein, B.J. 2003. Involvement of AMP-activated protein kinase in glucose uptake stimulated by the globular domain of adiponectin in primary rat adipocytes. *Diabetes*, 52, (6) 1355-1363.

Xie, P., Liu, M.L., Gu, Y.P., Lu, J., Xu, X., Zeng, W.M., & Song, H.P. 2003. Oestrogen improves glucose metabolism and insulin signal transduction in HepG2 cells. *Clin Exp.Pharmacol Physiol*., 30, (9) 643-648.

Yadav, A., Kataria, M.A., Saini, V., & Yadav, A. 2013. Role of leptin and adiponectin in insulin resistance. *Clinica Chimica Acta*., 417, 80-84.

Yang, M., Wei, D., Mo, C., Zhang, J., Wang, X., Han, X., Wang, Z., & Xiao, H. 2013. Saturated fatty acid palmitate-induced insulin resistance is accompanied with myotube loss and the impaired expression of health benefit myokine genes in C2C12 myotubes.

Lipids Health Dis., 12, 104.

Ye, J. 2013. Mechanisms of insulin resistance in obesity. *Front Med*., 7, (1) 14-24.

Yoon, M. 2009. The role of PPARalpha in lipid metabolism and obesity: focusing on the effects of estrogen on PPARalpha actions. *Pharmacol Res*., 60, (3) 151-159.

Youngren, J.F. 2007. Regulation of insulin receptor function. *Cell Mol Life Sci*., 64, (7-8) 873-891.

Yuzefovych, L., Wilson, G., & Rachek, L. 2010. Different effects of oleate vs. palmitate on mitochondrial function, apoptosis, and insulin signalling in L6 skeletal muscle cells: role of oxidative stress. *Am J Physiol Endocrinol Metab*., 299, (6) E1096-E1105.

Zammit, V.A. 2008. Carnitine palmitoyltransferase 1: central to cell function. *IUBMB Life*, 60, (5) 347-354.

Zang, M., Xu, S., Maitland-Toolan, K.A., Zuccollo, A., Hou, X., Jiang, B., Wierzbicki, M., Verbeuren, T.J., & Cohen, R.A. 2006. Polyphenols stimulate AMP-activated protein kinase, lower lipids, and inhibit accelerated atherosclerosis in diabetic LDL receptor-deficient mice. *Diabetes*, 55, (8) 2180-2191.

Zebisch, K., Voigt, V., Wabitsch, M., & Brandsch, M. 2012. Protocol for effective differentiation of 3T3-L1 cells to adipocytes. *Anal Biochem*., 425, (1) 88-90.

Zhang, J., Wu, W., Li, D., Guo, Y., & Ding, H. 2010. Overactivation of NF-kappaB impairs insulin sensitivity and mediates palmitate-induced insulin resistance in C2C12 skeletal muscle cells. *Endocrine*, 37, (1) 157-166.

Zhou, W.L., Medine, C.N., Zhu, L., & Hay, D.C. 2012. Stem cell differentiation and human liver disease. *World J Gastroenterol*., 18, (17) 2018-2025.

.

Appendix 1

List of reagents used in this study

Product name	Catalogue number	Supplier
2-deoxy-[3H]-D-glucose	ART 0200C	American Radiolabeled Chemicals, St Louis, MO, USA
3-(4,5-dimethylthiazol-2-yl)-2,5-diphenyltetrazolium bromide (MTT)	M2003	Sigma-Aldrich , St Louis, MO, USA
3-isobutyl -1-methyl-xanthine (IBMX)	I5879	Sigma-Aldrich , St Louis, MO, USA
5'adenosine monophosphate activated protein kinase (Ampk)	Mm01297600	Applied Biosystems, Foster City, CA, USA
5'adenosine monophosphate activated protein kinase (AMPK)	2532	Cell Signalling Technology, Danvers, MA, USA
5'adenosine monophosphate protein kinase (AMPK)	2603	Cell Signalling Technology, Danvers, MA, USA
Anti-Rabbit IgG (Horseradish peroxidase labeled secondary antibody)	sc-2012	Santa Cruz Biotechnology, Santa Cruz, CA, USA
ATP assay kit	LT27-008	ViaLight, Whitehead Scientific, JHB, SA
Beta actin (ActB)	Sc-47778	Santa Cruz Biotechnology, Santa Cruz, CA, USA
Bio-Rad Bradford protein assay kit	500-0201	Bio-Rad, Hercules, CA, USA
Bio-Rad chemiDoc	170-8265	Bio-Rad, Hercules, CA, USA
Biovision glucose kit	K646	Biovision, Mountain View, CA, USA
Bovine serum albumin (BSA)	100-10SB	Sigma-Aldrich , St Louis, MO, USA
Bovine serum albumin (BSA) fatty acid free	A1302-25G	Separations Scientific, JHB, SA
Carbon dioxide (CO2)	K239C	Air Products, Centurion, SA
Cell counting chamber slides	C10228	Life Technologies Corporation, Carlsbad, CA, USA
Cell extraction lysis Buffer	FNN0011	Life Technologies Corporation, Carlsbad, CA, USA
CELLBIND -24 well plates	3337	Corning, MA, USA
CELLBIND -6 well plates	3335	Corning, MA, USA
CELLBIND -96 well plates	3300	Corning, MA, USA
Centrifuge tubes (15mL; 50mL)	GEN-1860 5810R	Sigma-Aldrich , St Louis, MO, USA
Centrifuge:(Temperature control) Tubes;mL;2.0mL	K82967 3906	Sigma-Aldrich , St Louis, MO, USA
Chloroform	136112-00-0	Sigma-Aldrich , St Louis, MO, USA
Coomasie blue stain	161-0437	Bio-Rad, Hercules, CA, USA

Countess® automated cell counter	C10311	Invitrogen, Carlsbad, CA, USA
Cruz Marker Molecular Weight Standards	sc-2035	Santa Cruz Biotechnology, Santa Cruz, CA, USA
Cryotubes	430659	Corning, MA, USA
Dexamethasone	D4902	Sigma-Aldrich , St Louis, MO, USA
Dimethyl sulfoxide (DMSO)	276855	Sigma-Aldrich , St Louis, MO, USA
Donkey anti-rabbit (IgG-HRP)	sc-2317	Santa Cruz Biotechnology, Santa Cruz, CA, USA
Dulbecco`s modified Eagle`s medium (DMEM without glucose)	51442C	Sigma-Aldrich , St Louis, MO, USA
Dulbecco`s modified Eagle`s medium (DMEM)	12-604Q	Lonza, Walkersville, MD, USA
Dulbecco`s phosphate buffered saline (DPBS)	17-513F	Lonza, Walkersville, MD, USA
Eagle's minimum essential medium (EMEM)	BE12-662F	Lonza, Walkersville, MD, USA
Eppendorf tubes	30123301	Sigma-Aldrich , St Louis, MO, USA
Ethanol	2875	Sigma-Aldrich , St Louis, MO, USA
Ethanol absolute, 200 proof for molecular	E7023-500	Sigma-Aldrich , St Louis, MO, USA
Fetal bovine serum	BC/S0615-HI	Lonza, Walkersville, MD, USA
Filter Pads	23385	Sigma-Aldrich , St Louis, MO, USA
FLX800 Fluorescence microplate reader	Gen5v.1.05	Bio-Tek, Winooski, VT, USA
FOXO1	CST9454S	Cell Signalling Technology, Danvers, MA, USA
Gelatin	9000-70-8	Sigma-Aldrich , St Louis, MO, USA
Glucose powder	D5030	Sigma-Aldrich , St Louis, MO, USA
Glucose transporter 4 (GLUT4)	AB654	Abcam Inc., Cambridge, MA, USA
Glucose transporter 2 (Glut 2)	Mm01245502	Applied Biosystems, Foster City, CA, USA
Glucose transporter 2 (GLUT2)	AB54460	Abcam Inc., Cambridge, MA, USA
Glucose transporter 4 (Glut4)	mM01245502	Applied Biosystems, Foster City, CA, USA
Glyceraldehyde-3-phosphate dehydrogenase (Gapdh)	4352341E	Life Technologies Corporation, Carlsbad, CA, USA
Graphpad Prism ®	Version 5.02	Graphpad Software Inc , CA, USA
High capacity cDNA kit	Am 197	Ambion, Austian, USA
Horse serum	308	Highveld biological, SA
Insulin	I92785	Sigma-Aldrich , St Louis, MO, USA
Insulin powder	10516	Sigma-Aldrich , St Louis, MO, USA
Insulin receptor (INSR)	3025-S	Cell Signalling Technology, Danvers, MA, USA
Insulin receptor substrate (Insr)	Mm01211875	Applied Biosystems, Foster City, CA, USA
Insulin receptor substrate 1(Irs1)	Mm01278327	Applied Biosystems, Foster City, CA, USA

Insulin receptor substrate 2 (Irs2)	Mm03038435	Applied Biosystems, Foster City, CA, USA
Isopropanol	I9516	Sigma-Aldrich , St Louis, MO, USA
Linco rat insulin kit	EZRMI-13K	Millipore, Bellerica, MA, USA
Liquid scintillation analyser (ParkardTricarb series)	2200 CA	Perkin Elmer, CA, USA
Low fat free milk powder	2082054	Clover, JHB, SA
LumiGlo Reserve Chemiluminescent Substate kit	54-71-01	KPL, Gaithersburg, Maryland, USA
Lysis buffer	9803	Cell Signalling Technology, Danvers, MA, USA
Malonly CoA	Ab9594	Abcam,Cambridge, MA,USA
Metformin	1115-70-4	Sigma-Aldrich , St Louis, MO, USA
Methanol	67-56-1	Sigma-Aldrich , St Louis, MO, USA
Newborn Calf Serum (NCS)	BC/S0125-HI	The Scientific Group, JHB, SA
Nuclear factor kappa beta (NFkB)	8242-S	Cell Signalling Technology, Danvers, MA, USA
Nuclease free water	Am9937	Ambion, Austian, USA
Palmitic acid	P5585	Sigma-Aldrich , St Louis, MO, USA
PCR plates	N8010560	Applied Biosystems, Foster City, CA, USA
Peroxisome proliferator-activated receptor alpha (PPARα)	Ab8934	Abcam, Abcam,Cambridge, MA,USA
Peroxisome proliferator-activated receptor gamma (PPARγ)	2430-S	Cell Signalling Technology, Danvers, MA, USA
Phosho threonine kinase B (AKT)	4051-S	Cell Signalling Technology, Danvers, MA, USA
Phosphatidylinositol 3 Kinase (Pi3k)	Mm00803160	Applied Biosystems, Foster City, CA, USA
Phosphatidylinositol 3 kinase (PI3K)	4292	Cell Signalling Technology, Danvers, MA, USA
Phospho FOXO1	CST9461S	Cell Signalling Technology, Danvers, MA, USA
Phospho nuclear factor kappa beta (NFkB)	8242-S	Cell Signalling Technology, Danvers, MA, USA
Phospho phosphatidylinositol 3 kinase (PI3K)	4228-S	Cell Signalling Technology, Danvers, MA, USA
Phosphoprotein kinase PKC thetha (PKCθ)	9376-S	Cell Signalling Technology, Danvers, MA, USA
PKC thetha (PKCθ)	2059-S	Cell Signalling Technology, Danvers, MA, USA
PolyvinylideneFluoridine Membrane (PVDF)	88585	Pierce, Rockford, IL, USA
Ponceau S Stain	p23295	Sigma-Aldrich , St Louis, MO, USA
Protease Inhibitors	11206893001	Roche, Basel, Switzerland
Quantity One Software	170-9600	Bio-Rad, Hercules, CA, USA
Ready gel Ultima Gold	6013329	Merck, Whitehouse Station, NJ, USA
Ready gels	161-0993	Bio-Rad, Hercules, CA, USA

RNase free water	Am9937	Ambion, Austin, TX, USA
RNase Inhibitor	N8080119	Life Technologies Corporation, Carlsbad, CA, USA
RNeasy mini kit	74106	Qiagen, Hilden, Germany
Running buffer SDS	161-0772	Bio-Rad, Hercules, CA, USA
Rutin	5143	Sigma-Aldrich , St Louis, MO, USA
Scintillation vials	80-370-02	CJ Labs, JHB, SA
Sodium dodecyl sulfate	L3771	Sigma-Aldrich , St Louis, MO, USA
Sodium hydroxide (NaOH)	109140	Merck, Whitehouse Station, NJ, USA
Stainless steel beads 5mm	69989	Qiagen, Hilden, Germany
Sterile TC water	59900C	Sigma-Aldrich , St Louis, MO, USA
SYBR Green mix	4385612	Applied Biosystems, Foster City, CA, USA
T75 Flasks	658975	Greiner bio-one, Frickenhausen, Germany
Threonine kinase B (AKT)	4685-S	Cell Signalling Technology, Danvers, MA, USA
Tissue lyser	85600	Qiagen, Hilden, Germany
TRIzol reagent	T3809	Sigma-Aldrich , St Louis, MO, USA
Trypan blue	15050-065	Invitrogen, Carlsbad, CA, USA
Trypsin	2500-056	Millipore, Bellerica, MA, USA
Tubes-15ml	188261	Greiner bio-one, Frickenhausen, Germany
TURBO DNA-free kit	AM 1907	Ambion, Austian, USA
Tween-20	58980C	Sigma-Aldrich , St Louis, MO, USA
Vildagliptin	CAS 274901-16-5	Santa Cruz Biotechnology, Santa Cruz, CA, USA
Whatman3MMChr sheets	3030-931	Sigma-Aldrich , St Louis, MO, USA
β-Actin (C4)	sc-4778-78	Santa Cruz Biotechnology, Santa Cruz, CA, USA
β-mercaptoethanol	60-24-2	Sigma-Aldrich , St Louis, MO, USA

Appendix 2

Buffers and media used in this study

Destaining solution for Western blots

Destaining solution consisted of 15% methanol and 20% acetic acid in distilled water.

Freezing media for cryopreservation of C2C12, 3T3-L1 and C3A cells

- Freezing media for C2C12 muscle cells consisted of DMEM with 10% fetal calf serum (FCS) and 7% (v/v) dimethyl sulfoxide (DMSO)
- Freezing media for 3T3-L1 adipocytes was prepared with DMEM containing10% newborn calf serum (NCS) and 7% (v/v) DMSO.
- C3A cell freezing mediacinsted of Eagle's minimal essential medium (EMEM) containing 10% FCS and 7% (v/v) DMSO.

Preparation of 75 mM palmitate

To prepare a 75 mM stock solution, 19.23 mg palmitic acid (FW 256.43) was dissolved in 1 mL absolute ethanol heated to 90°C. For the working solution, a 1:100 dilution was made in DMEM, yielding a final concentration of 0.75 mM.

Transfer buffer for Western blot

Transfer buffer was prepared by dissolving 3.03 g 2-Amino-2-(hydroxymethyl)-1,3-propanediol (Tris) (MW=121.1) to yield 25 mM and 14.4 g glycine (MW=75.5) to give final concentration of 192 mM in 800 mL of distilled water. Before use the buffer was made up to 1L by adding methanol (200 mL). Transfer buffer was stored at 4° until used. NB. methanol must added on the day of experiment.

10x Tris-buffered saline (10x TBST)

10x TBST buffer was prepared by dissolving 24.22 g 2-Amino-2-(hydroxymethyl)-1,3-propanediol (Tris) (MW=121.1) to yield a concentration of 200 mM and 80.06 g of NaCl (MW = 58.44) to give final concentration of 1.37 M into 1L distilled water.

1x Tris-buffered saline and Tween 20 (1x TBST)

1 X TBST was prepared by diluting 100 mL of 10 x TBST with 900 mL of distilled water (v/v), thereafter 1 mL Tween 20 was added. The buffer was stored at 4°C.

0.1 M sodium hydroxide and 1% SDS lysis buffer

0.1 M NaOH solution was prepared by dissolving (4 g in 1 L distilled water) and adding 1% sodium dodecyl sulphate (SDS).

Sorenson's buffer

Sorenson's buffer was prepared by dissolving 0.751 g glycine and 0.584 g NaCl in 100 mL distilled water. The pH of the buffer was adjusted to pH10.5 with 0.1 mM NaOH.

Appendix 3

Effect of solvents on glucose uptake

The effect of DMSO, an aprotic solvent used throughout the study to dissolve the compounds (aspalathin, orientin, isoorientin and rutin), was assesed by glucose uptake in 3T3-L1 adipocyte and C3A liver cells. For these experiments, DMSO at a concentration of 0.01% was compared against the media control. For the subsequent studies, the DMSO concentration in the media containing the compounds was 0.00004%. DMSO had no effect on glucose uptake (Fig. A 3.1 A and B).

A

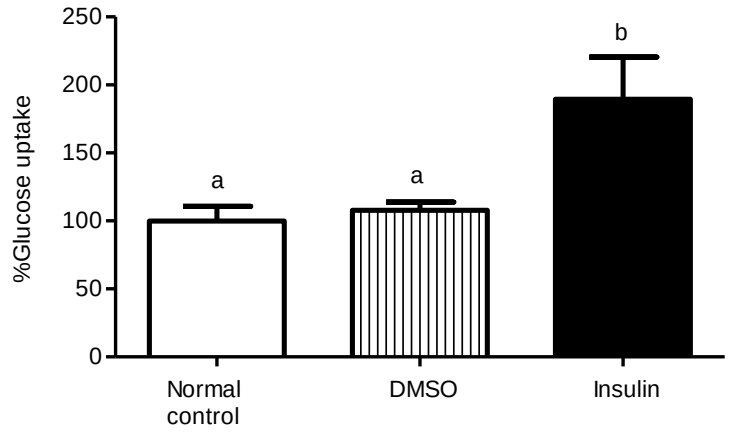

B

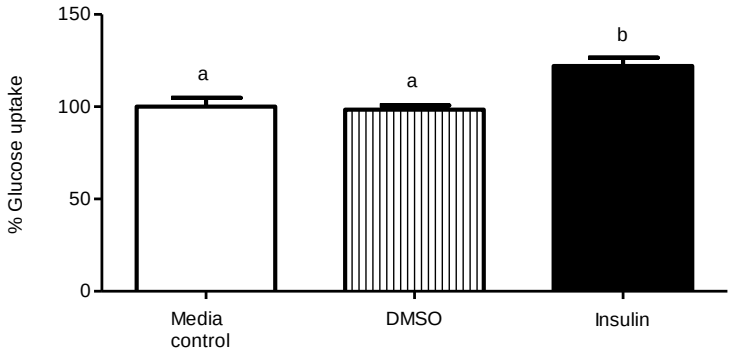

Figure A 3.1. Effect of DMSO on glucose uptake in 3T3-L1 adipocytes (A) and C3A liver cells. 3T3-L1 adipocytes and C3A liver cells were cultured in DMEM with 8 mM glucose with or without 1 µM insulin (15 min) and DMSO (0.001%, v/v) (3 h). Glucose uptake was measured using [^{3}H]-2-deoxy-D-glucose. Results are expressed as the mean of three independent experiments relative to the media control set at 100% ± SEM. Bars with different letters denote statistical differences at $p \leq 0.05$.

Effect of ethanol and palmitate on C2C12 muscle cells

Palmitate stock solution was dissolved in ethanol, heated and diluted in DMEM to yield a final concentration of 0.75 mM palmitate and 1% ethanol.Comparitive results showed that 1% ethanol had no effect on glucose uptake compared to the media control (Fig. A 3.2). The reduction in glucose uptake demonstrated for the palmitate controls is therefore due to palmitate and not ethanol solvent.

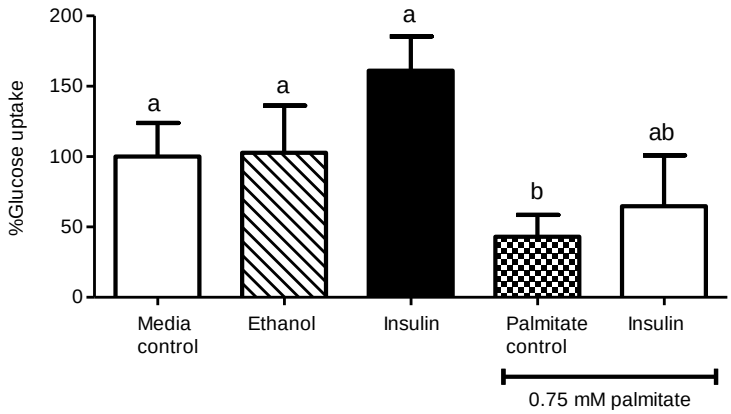

Figure A 3.2. Effect of ethanol and palmitate on glucose uptake in C2C12 muscle cells. C2C12 muscle cells were cultured in DMEM with 5 mM glucose with or without 0.75 mM palmitate for 24 h, then treated with 1 µM insulin. An ethanol (1%, v/v) control was included to establish the effect of the solvent on glucose uptake. Glucose uptake was measured using [^{3}H]-2-deoxy-D-glucose. Results are expressed as the mean of three independent experiments relative to the control set at 100% ± SEM. Bars with different letters denote statistical differences at $p \leq 0.05$.

Appendix 4

Ethical approval

SOUTH AFRICAN MEDICAL RESEARCH COUNCIL

TECHNOLOGY & INNOVATION DIRECTORATE

DIABETES DISCOVERY PLATFORM
PO Box 19070, Tygerberg 7505 Republic of South Africa
Francie van Zijl Drive, Parow Valley, Cape Town
Tel: +27 21 938 0277 Fax: +27 21 938 0456

11 February 2014

To whom it may concern

This letter certifies that Ethical approval for Ms. Mazibuko' s PhD study was granted by the ethics committee at the Medical Research Council of South Africa (ECRA 11/03/H). The study was performed in accordance with the principles and guidelines of the South African Medical Research Council as outlined in Guidelines on Ethics for Medical Research: Use of Animals in Research and Training, 2004 (http://www.mrc.ac.za/ethics/ethicsbook3.pdf).

Yours sincerely

Johan Louw (PhD)
Director: Diabetes Discovery Platform

Appendix 5

Publication